New insights on SepL, the gatekeeper component in Type 3 secretion System of enteropathogenic *E. coli*, though functional interchangeability studies

Bian AlMessiry (PGR)

Submitted for the degree of Doctor of Philosophy
Faculty of Medical Sciences
Newcastle University

January 2022

Abstract

The pathogenesis of many gram-negative bacteria depends on Type Three secretion systems (T3SSs) that deliver subversive effector proteins into the infected host cell. These injectosomes evolved from flagellar export apparatus with significant homology remaining between components that form the T3SS/flagella export channel (which spans the bacterial envelope) and the sorting platform that controls the timing and hierarchy of substrate export. There are distinct T3SS families where high protein homology is a feature within, but not between families. One family is represented by the enteropathogenic *E. coli* (EPEC) T3SS encoded-alongside genes for T3SS substrates (several T3SS components; translocators (link T3SS to host cell); effectors, chaperones (aid stability/export of T3SS substrates), regulators, and intimin surface protein-on a 41-gene region called LEE (Locus of Enterocyte Effacement). Unexpectedly, LEE was found in an *Edwardsiella tarda (E. tarda)* strain with genetic rearrangement linked to gene loss and disruption. However, recent studies support functionality with the discovery of unprecedented divergence indicative of a district T3SS family. Preliminary functional interchangeability studies identified *E. tarda* T3SS proteins that could and, more interestingly, could not functionally substitute their EPEC counterparts. The divergence level did not predict functionality. Studies with support complementation defects for five *E. tarda* T3SS proteins are described here, which revealed unexpectedly novel functions for SepL (the gatekeeper controlling switching from translocator to effector substrates). Further investigation revealed that i) SepL, 3 (CesT, CesAB, CesD2), an effector (EspF), and two T3SS components (EscC, EscD) each control the cellular O127-antigen level; ii) SepL protects Tir from cleavage; and iii) SepL, CesT, CesAB, and CesD2 protect EspF from cleavage. Cleavage event requires EscU; the latter has auto-proteolytic activity linked to regulating substrate export hierarchy. Importantly, these activities were not shared by the *E. tarda* homologs with domain swap experiments linking different SepL functionalities to one or more of its three X-bundling domains.

Acknowledgment

I could not have completed this research without the assistance of the people listed below.

Firstly, I would like to express my deepest appreciation to my supervisor, Prof. Brendan Kenny, for his tremendous guidance, ideas, and unwavering support throughout my PhD studies. I would like to extend my sincere thanks to Dr. Azzeldin Madkour for his extended discussions and valuable suggestions, which have contributed greatly to the improvement of the thesis. I would like to thank my thesis review committee, Dr. Phillip Aldridge and Prof Jeremy Lakey, for their suggestions and encouragement. Thanks to my laboratory colleagues, D.r Manoj Kumar and Bolaji Akanbi, for their kind help and friendship.

I'd like to present my sincere thanks to my dear mother (Sara) and my deceased father (Khalaf), who died last June, for their great role in my life and for looking after my daughter (Shaden) for the past three years.

Much of my appreciation goes to my daughter (Sara). Sorry because I have been busier than normal whilst I wrote this thesis, and to my husband, Saad. Thanks for all your love, patience, and support, without which I would have stopped these studies a long time ago. I also appreciate all the support I received from my sisters, brothers, and niece (Jwana). Thanks to all my friends for the unwavering support and encouragement throughout this process. Finally, thank you to Taibah University and the Saudi Arabian Cultural Bureau (SACB) for funding my studies.

Table of content

List of figures

List of tables

List of Supplementary figures

List of abbreviations

A	
Alkaline phosphatase	AP
Amino acid	aa
Attaching and effacing	A/E
B	
Basal body components	BB
Bundle forming pilus	Bfp
C	
Carbenicillin	Cb
Carbon storage regulator	CsrA
Chloramphenicol	Cm
Citrobacter rodentium	CR
Colanic acid	CA
D	
Diffusely adherent *E. coli*	DAEC
Distilled water	dH2O
Dulbecco's minimal Eagle's medium	DMEM
E	
Edwardsiella tarda	*E. tarda*
enteroaggregative *E. coli*	EAEC
enterohemorrhagic *E. coli*	EHEC
enteroinvasive *E. coli*	EIEC
enteropathogenic *E. coli*	EPEC
enterotoxigenic *E. coli*	ETEC
EPEC secreted/signaling protein F	EspF
EPEC secreted/signaling protein G	EspG
EPEC secreted/signalling protein H	EspH
EPEC secreted/signalling protein Z	EspZ
Escherichia albertii	*E. albertii*
Escherichia coli	*E. coli*
ethylenediamineacetic acid	EDTA
F	
Fetal calf serum	FCS
Forward Primer	FP
fluorescence actin staining	FAS
G	
Guanidine-exchange factor	GEF
H	
Horseradish peroxidase	HRP
Human cervix-derived epithelial-like	HeLa Cells
I	
Integrative elements	IE
Intimin gene	*eae* gene
J	
Japan EPEC	J. EPEC
K	
Kanamycin	Km
L	
Lipopolysaccharide	LPS
Locus Enterocyte Effacement	LEE
Luria Broth	LB

M	
Membrane and supra-membrane	MS
Mitochondrial targeting sequence	MTS
Mitochondrial-associated protein	Map
Molecular Ruler	MR
Molecular switches	MR
Molecular weight	MW
N	
Nalidixic acid	Nal
Needle proteins	NE
Non-LEE-encoded Effectors	Nle Effectors
Nalidixic acid	Nal
Needle proteins	NE
O	
Open reading frames	ORFs
Optical density	OD_{600}
Outer membrane ring	OM ring
P	
Peptidoglycan enzyme	PE
phosphate-buffered saline	PBS
Plasmid-encoded regulator	Per
Polymerase chain reaction	PCR
Proline-rich repeat domains	PRR
Prophages	PP
Peptidoglycan enzyme	PE
Phosphate-buffered saline	PBS
Plasmid-encoded regulator	Per
R	
Rabbit pathogenic E. coli	RPEC
Reverse Primer	RP
S	
Salmonella salamae	SS
SDS-Polyacrylamide gels	SDS-PA gel
Sorting nexin 9	SNX9
Sorting Platform Complex proteins	SPC
Streptomycin	Strep
T	
Tetracycline	Tet
Translocated intimin receptor	Tir
Translocators	TR
Transmembrane domain	TM
Trichloroacetic acid	TCA
Tris-acetate,EDTA	TAE
Type-three secretion system	T3SS
W	
Wiskott Aldrich syndrome protein	N-WASP

Chapter 1: Introduction

1. General Introduction

Escherichia coli (E. coli) is a Gram-negative bacillus that is a member of the microflora of the intestinal digestive tract of most humans and animals (Nataro and Kaper, 1998; Nicolas-Chanoine;Bertrand and Madec, 2014). However, some *E. coli* strains can cause disease, becoming pathogenic in or outside the intestine (Weintraub, 2007), with the name being linked to serological features and/or disease mechanisms. The main strains that cause intestinal disease are enterotoxigenic *E. coli* (ETEC), enteropathogenic *E. coli* (EPEC), enterohemorrhagic *E. coli* (EHEC), enteroaggregative *E. coli* (EAEC), enteroinvasive *E. coli* (EIEC) and diffusely adherent *E. coli* (DAEC) (Nataro and Kaper, 1998; Gruenheid *et al.*, 2001).

EPEC is one of the most common types of bacteria that cause watery diarrhea in new-borns and people worldwide (Levine *et al.*, 1985; Chen and Frankel, 2005; Clements *et al.*, 2012). EPEC is a severe health risk for humans and continues to be a leading cause of new-born mortality in developing countries (Levine *et al.*, 1985; Chen and Frankel, 2005; Clements *et al.*, 2012). EPEC is transmitted through contaminated food and water (Donnenberg and Kaper, 1992). It targets the microvilli surface of absorptive epithelial (enterocytes) and recruits other EPEC, producing characteristic microcolonies via a plasmid-encoded the bundle-forming pilus (BFP) (Giron;Ho and Schoolnik, 1991; Donnenberg and Kaper, 1992; Vallance and Finlay, 2000; Clarke *et al.*, 2003).

EPEC belongs to a family of bacteria called attaching and effacing (A/E) pathogens due to the disease being linked to an ability to cause A/E lesions (Levine *et al.*, 1985). These lesions are characterized by the effacement (loss) of absorptive microvilli and the aggregation of host actin under the bacteria attached to the cell, which form protruding structures called pedestals (Figure 1) (Moon *et al.*, 1983; Knutton *et al.*, 1989). The A/E bacterial family also includes other strains that infect humans – *E. albertii* and EHEC (a zoonotic pathogen) – with others targeting specific animals, such as rabbits (rabbit pathogenic *E. coli* [RPEC]) and mice (*Citrobacter rodentium* [CR]) (Giron;Ho and Schoolnik, 1991; Wong *et al.*, 2011; Clements *et al.*, 2012). The formation of A/E lesions depends on

a type-three secretion system (T3SS) that delivers ‘effector’ proteins into the infected host cells.

Figure 1: EPEC-induced pedestals structure and effacement of microvilli

A) EPEC 2348/69 strains adhere intimately to the intestinal epithelium, leading to microvilli effacement and pedestal formation underneath the adherent bacteria. B) A/E lesion-related bacteria at a greater (x 45000) magnification. Taken an from article by Knutton et al., (Knutton, 1995).

2. Type III secretion system (T3SS)

T3SSs, also known as injectisomes, play an important function in the pathogenicity of many bacteria, by delivering effector proteins into the cytoplasm of eukaryotic cells to subvert host cellular function (Galan and Collmer, 1999; Coburn;Sekirov and Finlay, 2007). This 'injectisome' evolved from the flagella export system and is employed to transport proteins, in an unfolded state, across the bacterial envelop through a channel formed by the T3S/flagellar systems (Lyons and Strynadka, 2019).

The T3SS was initially identified in Yersinia pestis, found to have a common virulence plasmid protein that is transported into host cells via a bacteria–host cell contact-dependent method (Rosqvist;Magnusson and Wolf-Watz, 1994). The acronym T3SS was coined in 1993 and following this, the structure of T3SS was determined in *Salmonella* by examining isolated T3SS under an electron microscope (Salmond and Reeves, 1993; Kubori *et al.*, 1998a).

For EPEC, the T3SS was first identified by Jarvis *et al*. (1995). These authors generated a *cfm* mutant of the EPEC parental strain with two chromosomal TnphoA insertions that created a mutation observed in EscC and SepD, thereby disrupting the structure of the T3SS system. Further analysis of EPEC vs *cfm* A/E lesion formation using the FAS (fluorescence actin staining) test blot confirmed that the ability to cause A/E lesions was lower in the latter case (Jarvis *et al.*, 1995).

The T3SS span the two bacterial membranes and periplasmic space, like the flagella system, but also the eukaryotic plasma membrane. The organelle is composed of four separate parts: the basal body, which traverses the Gram-negative envelope (inner membrane, periplasmic ,space and outer membrane); the cytoplasmic components; the export apparatus; and the extracellular segment (Buttner, 2012). More than 20 proteins are required to form the injectisome organelle, with other proteins coordinating the synthesis, correct assembly and functioning of the T3SS (Figure 2). The synthesis of the proteins that form and/or utilize the T3SS is under a strict hierarchy, leading to an extremely controlled process (Portaliou *et al.*, 2016).

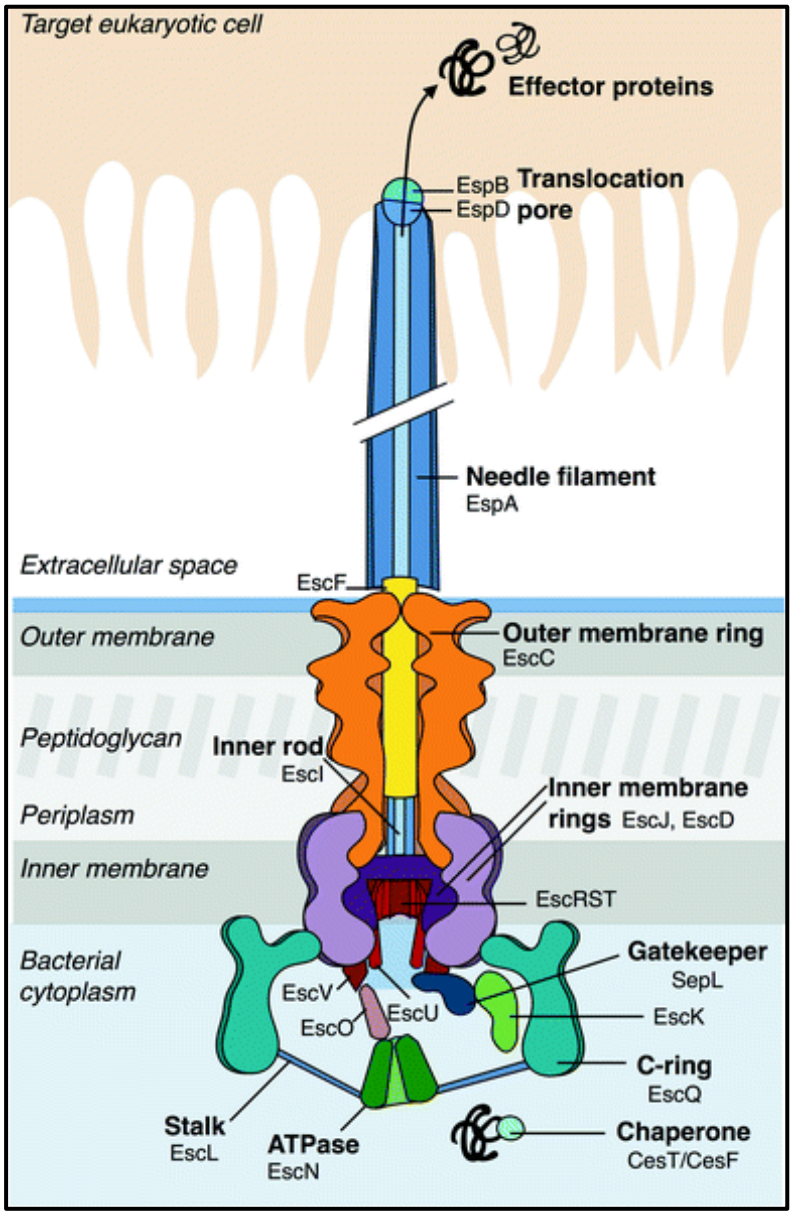

Figure 2: Schematic of T3SS from A/E pathogens

Shown are the names and locations of T3SS-related proteins. Taken from review by Slater et al., (Slater *et al.*, 2018).

The T3SS genes are grouped together on a ~35 kb pathogenicity island called the locus enterocyte effacement (LEE) region (Jarvis *et al.*, 1995). The LEE gene is conserved in all A/E pathogens, but when introduced into the non-pathogenic *E. coli* (K12 strain), EPEC LEE is sufficient for A/E lesion formation, whereas EHEC LEE is insufficient (McDaniel and Kaper, 1997). In 1995, the LEE EPEC strain E2348/6969 has been described (McDaniel *et al.*, 1995). Interestingly, the LEE has 7 operons (LEE1–LEE7) and 4 monocistronic units, as shown in Figure 3 (Elliott *et al.*, 1998; Mellies *et al.*, 1999; Barba *et al.*, 2005; Yerushalmi *et al.*, 2014). EPEC LEE has 41 open reading frames (ORFs) that encode effector proteins, as well as transcription regulators, chaperones (promoting stability and/or the export of T3SS substrates), and an outer membrane protein called Intimin (Figure2+ 3) (Pearson *et al.*, 2013). All genes encoded by the EPEC LEE are present in the same order as in EHEC LEE. They have a high level of homology, presenting an average of 94% identity at the nucleotide level (Perna *et al.*, 1998).

Environmental circumstances, quorum sensing, and transcriptional and post-transcriptional regulation all play a role in the appropriate expression of LEE (Connolly;Finlay and Roe, 2015). LEE encodes three transcription factors, termed Ler, GrlA and GrlR (Mellies *et al.*, 1999). Ler is a 15 kDa protein located in the LEE1 operon and regulates LEE gene expression (Mellies *et al.*, 1999). However, Ler controls its own expression in a negative manner (Berdichevsky *et al.*, 2005; Bhat *et al.*, 2014). Furthermore, the LEE7 operons have *grlA* and *grlR* genes, which work as positive and negative regulators for *Ler* expression respectively (Deng *et al.*, 2004). GrlA binding to the LEE1 promoter has been demonstrated to stimulate LEE gene expression and *Ler* regulates the LEE7 operon, resulting in a positive, feedback regulatory loop (Barba *et al.*, 2005). GrlR suppresses LEE gene expression through a mechanism that is yet unconfirmed (Creasey *et al.*, 2003; Padavannil *et al.*, 2013). However, GrlR is thought to inhibit LEE transcription by sequestering GrlA, preventing it from binding to the LEE1 promoter and thereby suppressing *Ler* expression (Huang;Lesser and Lory, 2008).

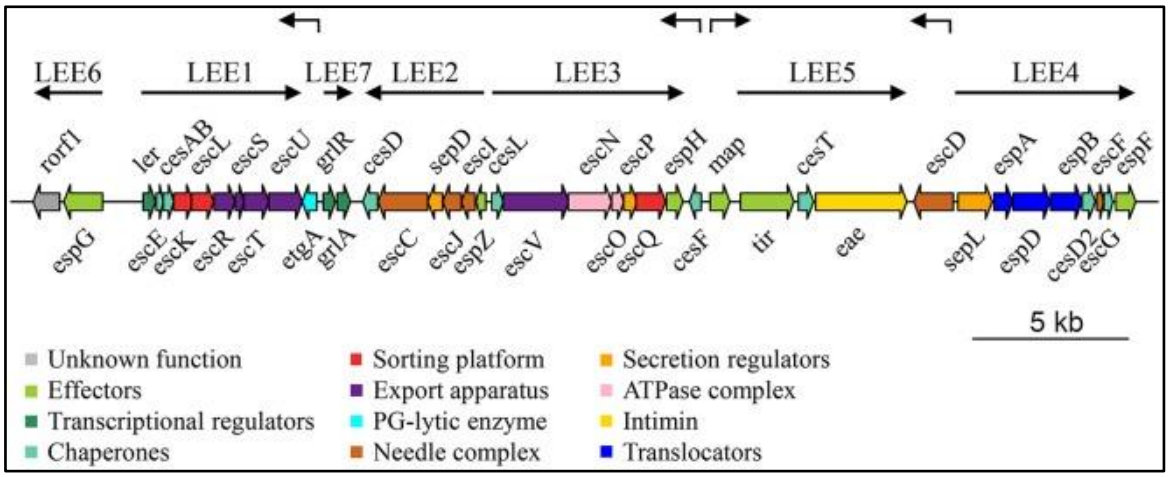

Figure 3: Schematic of the Locus of Enterocyte Effacement (LEE) region

The LEE region has genes encoding the T3SS. Genes are represented as full arrows, with different colours indicating their hypothesized function. Solid black arrows over the LEE genes represent the island's operon arrangement (LEE1–LEE7). Taken from review by Gaytán et colleagues al., (Gaytán *et al.*, 2016).

2.1 T3SS components

2.1.1 Basal body

The basal body structure spans the bacterial envelop and the membrane-spanning rings of inner and outer membranes are connected by the neck structure formed by the inner rod protein, EscI (Kubori *et al.*, 2000) (see Figure 4). Transmission electron microscope (TEM) imaging reveals that the basal body, particularly the inner ring, looks unstable. The cytoplasmic membrane has toroid-shaped ring structures associated with its cytoplasm- and periplasm-facing surfaces formed from 24 mer of a membrane-spanning protein (EscD, which has a single transmembrane domain [TM], spanning residues of 120 to 141) and a lipoprotein (EscJ) respectively (Figure 4) (Kresse *et al.*, 1998; Ogino *et al.*, 2006). This membrane and supra-membrane (MS) structure is vital for the formation of the T3SS (Minamino and Macnab, 1999) and has a central cavity for substrate transport through the injectisome (Galan and Wolf-Watz, 2006). EscJ is exported to the periplasm, where it is anchored to the membrane by the N-terminal lipid modification. The central, EscJ-related, pore contains negative charges and may function as an adapter for anchoring the EscI inner rod protein (Yip;Finlay and Strynadka, 2005) (Figure 4). EscD has a small N-terminal cytoplasmic domain and a large periplasmic C-terminal domain with an oligomerization motif that undergoes self-oligomerization, together with the transmembrane domain (TMD) (Tseytin *et al.*, 2018).

Interestingly, the development of the outer membrane ring with EscC polymerization was confirmed in EPEC using a TEM assay comprising a pure needle complex stained with immunogold-tagged anti-EscC. EscC is a member of the secretin family of proteins that has N- and C-terminal regions located in the periplasmic space and outer membrane respectively (Genin and Boucher, 1994; Gauthier;Puente and Finlay, 2003). Within the crystal structure, the periplasmic part of EscC includes two tiny domains (residues 21–174) associated by a linker region with a fold similar to that of the EscJ. The N-terminal domain interacts with the EscD C-terminal region and is important for EscC oligomerization (Ogino *et al.*, 2006).

It is presumed that the MS and outer membrane rings (OM rings) are connected by the periplasmic inner rod protein, i.e. the EscI protein (Pallen;Beatson and Bailey, 2005).

Under an electron miscroscope, the inner rod appears to have a ring-like structure at the base, 9 nm in width and 20 nm in length (Ogino *et al.*, 2006).

The efficient assembly of the T3SS requires the activity of a periplasm-located lytic transglycosylase (EtgA) that modifies the peptidoglycan layer (Pallen;Beatson and Bailey, 2005; Garcia-Gomez *et al.*, 2011). The active site of the EtgA has similarities with both lytic transglycosylases and lysozymes. EtgA interacts with EscI, promoting its enzymatic activity (Burkinshaw *et al.*, 2015).

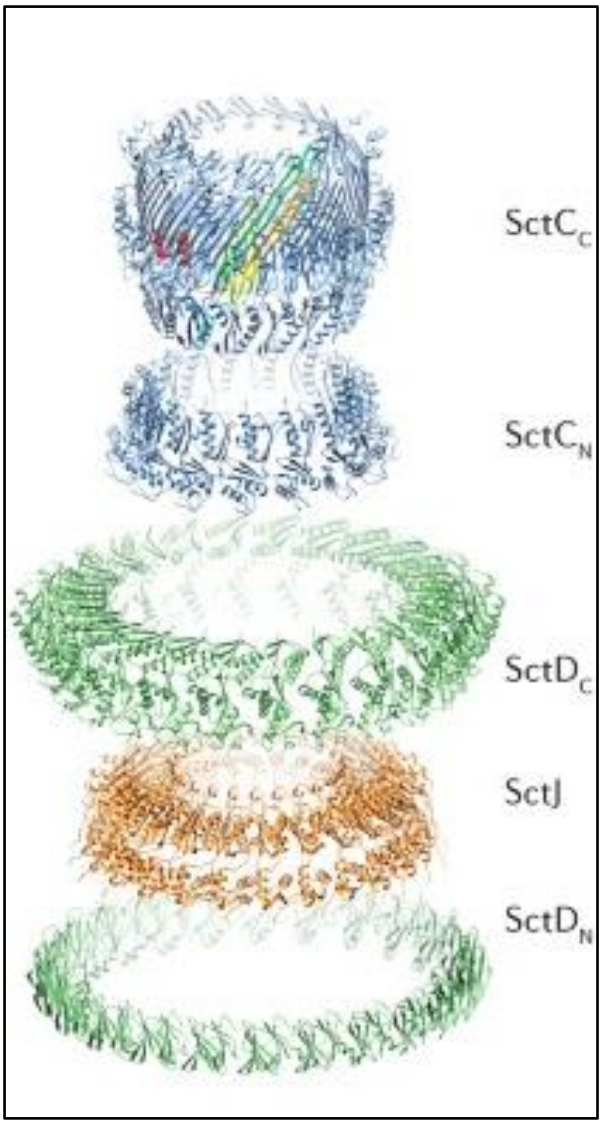

Figure 4: Structure of Basal Body components

Cryo-electron microscopy data reveal the structure of the basal body rings in the A/E pathogen T3SS. The sub-scripts N and C indicate the N- and C-terminal parts of the indicated proteins. The outer membrane ring is coloured blue (SctC; EscC). The inner membrane rings are coloured in green (SctD, EscD) and brown (SctJ, EscJ). Taken from review by Deng et al.,(Deng *et al.*, 2017).

2.1.2 Export Apparatus

The export apparatus is located within the central cavity provided by the basal body structure (Kimbrough and Miller, 2000) and is composed of five proteins, EscRSTUV (Figure 2+5) (Deng *et al.*, 2004; Diepold and Wagner, 2014; Portaliou *et al.*, 2016). These five proteins collectively have up to 104 transmembrane domains that span the inner membrane (Zilkenat *et al.*, 2016). Sequencing analysis shows that both EscU and EscV have large cytoplasmic domains, such that EscU is able to undergo auto-cleavage at a conserved amino acid sequence, which switches substrate secretion from early T3SS substrates (EscI and EscF) to intermediate substrates, i.e. the translocator proteins (EspA, EspB, EspD) (Zarivach *et al.*, 2008; Thomassin;He and Thomas, 2011; Sal-Man;Deng and Finlay, 2012; Monjaras Feria *et al.*, 2015). This event was confirmed in a crystallization study of EscU undertaken by (Zarivach *et al.*, 2008) that assessed EscU auto-cleavage and detected post-auto-cleavage products using the double-tagged recombinant EscU form. The full length of EscU is 39 KDa and the C- terminal cleavage produces 2 polypeptide species comprising 29- and 10-KDa bands (Thomassin;He and Thomas, 2011). The role of this process in the ability of T3SS apparatus to deliver Tir into the target cells and cause A/E lesions was established through fluorescent microscopy images of HeLa cells (Thomassin;He and Thomas, 2011).

It is proposed that all the five export apparatus proteins locate to a membrane patch where they function to select substrates and provide a secretion channel for substrate translocation (Minamino and Macnab, 1999; Ghosh, 2004; Diepold and Wagner, 2014). Recent findings obtained with extreme high resolution scanning electron microscopy (XHR-SEM) suggest that the export apparatus proteins also form part of another organelle – a membranous nanotube appendage that makes direct contact with infected host cells to enable nutrient extraction (Pal *et al.*, 2019) (Figure 5).

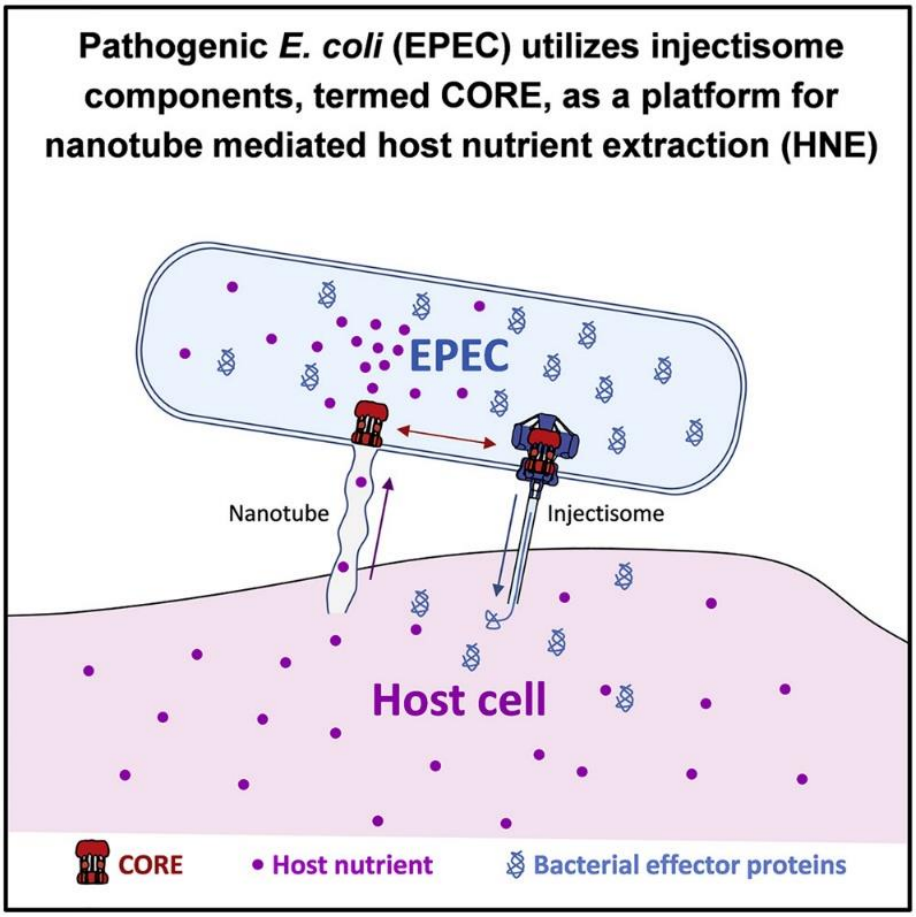

Figure 5: EscRSTUV components in the T3SS and nanotube for extracting nutrients from host cells

Schematic of position of export apparatus components in the T3SS and a novel nanotube use to extract nutrients for host cells. Taken from article by Pal et al., (Pal *et al.*, 2019).

2.1.3 Cytoplasmic components

Examination using the yeast two-hybrid assay indicates that interaction between three cytoplasm-located proteins (EscN, EscL, EscO) forms an ATPase complex (Figure 2). EscN is a peripheral membrane protein situated at the base of the export entry channel where it provides energy that promotes the secretion process (Gauthier;Puente and Finlay, 2003; Deng *et al.*, 2004; Akeda and Galan, 2005; Andrade *et al.*, 2007; Ku *et al.*, 2009; Biemans-Oldehinkel *et al.*, 2011; Romo-Castillo *et al.*, 2014a). The oligomeric state of EscN has a direct impact on enzyme activity, which is further controlled by EscL and EscO, decreasing and increasing ATPase activity respectively (Biemans-Oldehinkel *et al.*, 2011; Romo-Castillo *et al.*, 2014a). EscN–EscL complexes in the cytoplasm have no ATPase activity, with a conformational shift occurring when the EscN/EscL/EscO complex is formed near the export apparatus, where its interaction with EscV leads to EscO-triggering oligomerization and ATPase activity (González-Pedrajo *et al.*, 2006).

The EPEC *escO* gene was named before *escA* was encoded inside the *LEE3*. It was realized that EscO interacts with the EscC OM ring protein in the EPEC periplasm (Sal-Man *et al.*, 2012). EscO also interacts with the chaperones CesA2 and CesL in EHEC (Lin *et al.*, 2014), suggesting that EscO may play mysterious roles that can be discovered.

It has been proposed that the sorting platform – a cytoplasmic ring structure – is formed mainly by the SepQ protein. The C terminal of SepQ in the LEE EPEC has a high level of homology with the FliN protein in the flagella. This was detected by searching in the NCBI conserved-domain database (Marchler-Bauer *et al.*, 2005). In 2011, the SepQ was renamed EscQ. This protein interacts with the ATPase (EscN/EscL/EscO) complex, as confirmed by co-immunoprecipitation experiments (Pallen;Beatson and Bailey, 2005; Biemans-Oldehinkel *et al.*, 2011) (Figure 2).

EscK (a 23.4 kDa protein) is the second sorting platform component. Yeast two-hybrid (Y2H) and pulldown assays revealed that EscK interacts with EscQ and EscL (ATPase complex protein) to form the sorting platform, which ensures the export of the T3SS

components, then the translocators and finally the effector proteins (Lara-Tejero *et al.*, 2011; Soto *et al.*, 2017).

2.1.4 The Extracellular Structure

In EPEC, the extracellular needle-like structure is formed from 4 proteins (Figure 2). One protein (EscF) forms a needle-like structure that connects the inner rod protein (EscI) to the extracellular space (Wilson *et al.*, 2001). EscF was firstly identified using a red blood cell (RBC) infection model. The study observed that a portion of the filament structures was not labelled with the EspA antiserum. This part was important for the connection between the bacteria and target cell (Shaw *et al.*, 2001). Sequencing analysis confirmed that this structure was primarily found in both *Shigella* and *Salmonellae* and built with PrgI and MxiH respectively (Elliott *et al.*, 1998).

A pulldown assay using purified EscF and basal body proteins confirmed that the EscF interacts with EscC, EscD and EscJ to connect the extracellular space and the inner rod structure (Wilson *et al.*, 2001; Ogino *et al.*, 2006) (Figure 2). The needle measures 23 nm in length and 8–9 nm in width (Sekiya *et al.*, 2001; Ogino *et al.*, 2006). Therefore, this channel is too narrow to accommodate folded proteins and effectors must be unfolded before being transported through the T3SS (Feldman and Cornelis, 2003; Akeda and Galan, 2005; Fujii *et al.*, 2012). The successful transportation of unfolded proteins via this structure was demonstrated using cryo-EM (Radics;Konigsmaier and Marlovits, 2014). Interestingly, translocator secretion was found to be inhibited by a mutation in *escF*, as validated by Western blots probing the supernatants of bacterial cultures for EspA, EspB and EspD polyclonal sera (Wilson *et al.*, 2001).

The needle is further extended by up to 800 nm by polymerization of an exported translocator protein (EspA) according to immunofluorescence investigations of EPEC strains stained with the EspA antiserum. The filament is tipped by the EspB and EspD translocator proteins (Knutton *et al.*, 1998; Ide *et al.*, 2001) (Figure 2). The EspA organelle provides a structure 12 nm wide with a 2.5 nm central channel for substrate transport (Knutton *et al.*, 1998; Daniell *et al.*, 2003; Wang *et al.*, 2006). The EspA protein has a coiled-coil domain at the C terminus needed for filament assembly and subunit polymerization (Delahay *et al.*, 1999). Moreover, the filament is thought to play a role in detecting the presence of mammalian cells implicated in bacterial and epithelial cell adhesion (Ebel *et*

al., 1998; Knutton *et al.*, 1998; Cleary *et al.*, 2004). However, six hours following infection, (Knutton *et al.*, 1998) found the expression of *espA* was downregulated.

The EspB and EspD translocator subunits hetero-oligomerize with their insertion into the host plasma membrane, creating a 'translocation' pore which is essential for effector delivery into the host cell (Figure 2). EspB and EspD proteins are thought to have one and two putative transmembrane domains, respectively, critical to their membrane anchoring and insertion functions (Delahay and Frankel, 2002; Dasanayake *et al.*, 2011). The insertion of these proteins in the erythrocyte membrane causes red cell homolysis (Warawa *et al.*, 1999). However, EspB, unlike EspD, produces a partial homolysis, confirming the important role of EspD in pore formation (Shaw *et al.*, 2001). These two hydrophobic translocators, together with the hydrophilic translocator EspA, create the translocon (Luo and Donnenberg, 2011) (Figure 2). Bacteria cannot form A/E lesions when one of translocon proteins is missing as these proteins prevent the translocation protein infecting the cell (Lai *et al.*, 1997; Deng *et al.*, 2004).

Low-resolution atomic force microscopy has confirmed that the size of the pore formed by EspD and EspB is 3–5 nm (Ide *et al.*, 2001). After needle connection and pore formation, the EspB translocates to the host cell and inhabits the myosin actin interaction, leading to microvilli effacement and phagocytosis inhibition (Taylor *et al.*, 1998; Iizumi *et al.*, 2007).

3. LEE-encoded Effector Proteins

3.1 Translocated intimin receptor (Tir)

The translocated intimin receptor (Tir) was initially known as Hp90 and presented as a host protein (Figure 2). A few years later, Hp90 was found not to be a host protein, but rather a LEE-encoded effector known as Tir (Figure 2). This finding was the result of research into the optimal circumstances for injectosome secretion of translocator proteins, which revealed a unique secreted protein with a molecular mass of 78 kDa. The encoding gene of this secreted protein was identified by isolating the protein for N-terminal sequencing and the design of the polyclonal antibody. Tir is the first effector delivering through T3SS to the host cell (translocated intimin) (Kenny *et al.*, 1997b). This was detected by fractionating the infected Hela cell using Triton x100 to isolate soluble components (containing host cytoplasm and membrane proteins plus T3SS effectors) and insoluble components (containing host nuclear and cytoskeletal proteins plus proteins from adherent or remaining bacteria). The soluble fraction was then probed for the presence of Tir utilizing Western blot analysis. This method validated Tir delivery through T3SS.

Tir is inserted into the host plasma membrane in a hairpin-like structure with both N- and C-terminal domains within the host cytoplasm (Kenny *et al.*, 1997b). The extracellular Tir domain (residues 260–352) provides the interaction site for intimin, with binding inducing signalling which produces actin-rich pedestals (Abe *et al.*, 1999; Kenny, 1999; Fairman *et al.*, 2012). Intimin, the outer membrane protein identified in 1991, is essential for EPEC–host cell adhesion (Jerse and Kaper, 1991).

Tir insertion into the plasma membrane is linked to shifts in apparent molecular mass – by 5 and 2 kD – due to phosphorylation of serine and/or threonine residues by host kinases (Kenny and Warawa, 2001). Moreover, Tir undergoes host phosphorylation on tyrosine residues with one modification generating a binding location for the SH2 motif (Campellone *et al.*, 2002) of the Nck adapter protein, which recruits N-WASP (Wiskott Aldrich syndrome protein family members) and the Arp2/3 actin-nucleating machinery to

produce the actin-rich pedestal structure (Lai *et al.*, 2013). Tir and intimin are needed for virulence.

3.2 Mitochondrial-associated protein (Map)

A Mitochondrial-associated protein (Map) is a protein encoded by a gene located upstream of the *tir* gene. Studies have confirmed the delivery of *orf19* by T3SS into the HeLa cell and the generation of the *orf19* mutant using Western blot and epifluorescent microscopy approaches. Moreover, these approaches confirmed the accumulation of Orf19 in mitochondria, leading to Orf19 being renamed Map.

Map targets mitochondria through an N-terminal mitochondrial targeting sequence (MTS), with its import into these organelles linked to dysfunction enabling entry via the classical TOM/Hsp70 import system, while organelle dysfunction has been linked to features between residues 101–152 of this 203-residue protein (Kenny and Jepson, 2000). However, the main activity of Map occurs outside the mitochondria linked to it, activating a small GTPase, Cdc42, as a Cdc42-specific guanidine-exchange factor (GEF) (Kenny *et al.*, 2002; Alto *et al.*, 2006). Activated Cdc42 targets N-WASP to trigger Arp2/3-dependent formation of actin-rich filopodia at the infection site (Miki *et al.*, 1998; Svitkina *et al.*, 2003; Alto *et al.*, 2006). However, these filopodia are transient in nature due to Tir activity (in an intimin-dependent manner), illustrating the concept of effector synergy/cooperativity and demonstrating that Tir can have intimin-dependent functionality (Kenny and Jepson, 2000).

3.3 EPEC secreted/signalling protein F (EspF)

Investigations of the LEE region have discovered a gene producing a polyproline-rich 206 amino acid protein that is likely to be an effector (Elliott *et al.*, 1998). Western blot analysis confirmed the secretion of this protein by T3SS by generating antibodies for several proteins, removing the encoding gene and cloning it onto an expression vector. This protein is known as EspF (Elliott *et al.*, 1998).

Like Map, EspF has an N-terminal MTS linked to its import into mitochondria leading to organelle dysfunction and cell death (Nagai;Abe and Sasakawa, 2005). In addition, EspF has an N-terminal nucleolar targeting sequence, with its presence in this organelle linked to nucleolar factor disruption (Dean *et al.*, 2010). However, most EspF functionality is linked to its presence within the host cytoplasm and 3 proline-rich repeat (PRR) domains within the C-terminal region (residues 74–206). Each PPR has motifs that recruit N-WASP and sorting nexin 9 (SNX9), linked to inducing remodelling of the host plasma membrane (Alto *et al.*, 2007).

3.4 EPEC secreted/signalling protein G (EspG)

The *rorf2* gene produces a protein that has a significant sequencing homology to VirA (effector protein in *Shigella flexneri*/enteroinvasive *E. coli*) (Uchiya *et al.*, 1995). A Western blot assay for the *rorf3* mutant, reintroducing the gene by plasmid, confirmed the secretion and delivery of Rorf3 by T3SS. Remarkably, VirA was functionally replaced by Rorf2, which was renamed EspG. Moreover, there are other VirA homologues named EspG2 in other pathogenicity islands that encode the EspC autotransporter in EPEC. EspG2 can also functionally replace VirA (Uchiya *et al.*, 1995).

3.5 EPEC secreted/signalling protein H (EspH)

Braunstein *et al.* (2003) screened LEE genes for those encoding proteins that could be injected in host cells via T3SS. Their work confirmed that orf18 encoded an effector, EspH, an epitope (Flag)-tagged variation for this protein, detected using Western blot analysis and epifluorescent microscopy (Braunstein *et al.*, 2003).

EspH has identified by its ability to alter the ratio of Tir/intimin-triggered pedestal and Map-induced filopodia structures (Wong *et al.*, 2012). This EspH activity has been linked to binding Rho-specific GEF to prevent Rho small GTPase signalling (Dong;Liu and Shao, 2010).

3.6 EPEC secreted/signalling protein Z (EspZ)

EspZ is considered the smallest LEE-encoded effector. Bioinformatics analysis has found that EspZ, like other effectors in A/E pathogen strains, presents considerable sequencing variation(Hauser, 2009). Like Tir, the 98 amino acid EspZ effector forms a hairpin loop topology in the host plasma membrane, with a short (10 amino acid) extracellular loop flanked by two TMDs (Shames *et al.*, 2010). EspZ promotes host cell survival linked to multiple mechanisms, including signalling through its interaction with a host transmembrane protein (CD98), mitochondria and/or EspD, the latter controlling the level of effector protein delivery (Shames *et al.*, 2010; Berger *et al.*, 2012).

4. Non-LEE-encoded (Nle) Effectors

There are >15 other T3SS effectors encoded on prophages (PP) and integrative elements (IE) located in different positions in the chromosome (Dean and Kenny, 2009; Iguchi *et al.*, 2009). The main role of Nle effectors is the inhibition of transcription factor activity that controls the expression of anti-microbial and inflammatory reagents, as well as proteins regulating cell death. By contrast, the LEE effectors are responsible for diarrhoeal-associated alterations, i.e. A/E lesions, loss of ion/nutrient transporter activity and the disruption of cell–cell interactions; the latter is not inflammatory in human EPEC disease due to Nle effector activity (Dean and Kenny, 2009; Iguchi *et al.*, 2009).

5. Chaperones

The stability and/or export efficiency of T3SS export substrates is often controlled by chaperone proteins, of which there are 8 encoded on the LEE region: EscG, EscE, CesAB, CesF, CesL, CesT, CesD, and CesD2 (Wainwright and Kaper, 1998; Elliott *et al.*, 1999; Creasey *et al.*, 2003; Younis *et al.*, 2010; Ramu *et al.*, 2013; Sal-Man *et al.*, 2013). Substrate specificity has led to the following classifications: Class IA binds just one effector, Class IB (also known as multi-cargo chaperones) binds many effectors, Class II binds translocators, and Class III binds the needle protein. EPEC has one Class 1A chaperone, CesF (binding EspF) and a Class 1B chaperone, CesT (binding many effectors) (Tir, EspZ, EspF, Map, NleA, NleG, NleH, NleH2, EspH, EspG), while a small subset of effectors have no known

chaperone requirement (Elliott *et al.*, 2002; Thomas *et al.*, 2005; Mills *et al.*, 2013; Little and Coombes, 2018). CesL was recently classified as a Class I chaperone for SepL (gatekeeper component; see below), however, it is unique as its substrate is an 'abnormal' effector, not being secreted (Younis *et al.*, 2010).

The Class II chaperones, for translocator proteins, are CesD2 (specific for EspD), CesD (binding EspB and EspD) and CesAB, which is unusual as it has a basic pI and binds both EspA and EspB (Wainwright and Kaper, 1998; Neves *et al.*, 2003; Yip *et al.*, 2005). The Class III chaperones are EscG and EscE, which interact with the EscF needle protein to prevent premature protein polymerization (Sal-Man *et al.*, 2013).

6. Gatekeeper and Ruler proteins

T3SS substrates are divided into three classes according to their timed secretion. Inner rod (EscI) and needle (EscF) proteins comprise early secreted substrate, translocator proteins are medium secreted substrate, and effector proteins are late secreted substrate. Two specific-switching mechanisms control orderly secretion (Deane *et al.*, 2010; Büttner, 2012). Once the needle achieves its proper length, the switch from early to middle to late substrate secretion happens.

Needle length is mostly regulated by EscP protein. EscP protein is secreted, and a lack of these proteins causes unusually long needle/hook structures to form (Hirano *et al.*, 1994; Kubori *et al.*, 1998b; Payne and Straley, 1999; Magdalena *et al.*, 2002; Monjaras Feria *et al.*, 2012). However, in EPEC, deleting the *escP* gene leads to a decrease in translocator secretion and an increase in effector secretion. This finding suggests that EscP is not required for substrate switching, even though it improves switching efficiency (Monjaras Feria *et al.*, 2012).

However, the interaction of EscP protein regulates substrate switching. In EPEC, during needle construction, EscP interacts directly with EscF and assesses needle length. Then, when the structure attains its final length, the needle can be linked by all ruler protein subdomains. This prevents early substrate secretion, allowing EscP to interact with EscU

and causing a conformational shift that alters the secretion from early to middle to late (Monjaras Feria *et al.*, 2012). This model was first proposed in the flagella system (Erhardt;Namba and Hughes, 2010).

The *S. enterica* injectosome presents a unique event in terms of secretion regulation, namely that the substrate switching occurs when the inner rod assembly is complete (Marlovits *et al.*, 2006). However, in EPEC, the interaction between the inner rod and ruler is suggested to control its secretion (Monjaras Feria *et al.*, 2012). EscI has also been shown to interact with autocleavage protein (Sal-Man;Deng and Finlay, 2012).

Mechanisms have evolved to ensure the export of T3SS components precedes that of the translocator protein and to control the order and level of effector proteins. Two gatekeeper proteins (SepL and its partner SepD) govern the molecular switching from translocator (EspA, EspB, and EspD) to effector protein (Diepold and Wagner, 2014). Bacteria lacking SepL or SepD have dramatically reduced levels of translocator secretion linked to unusually high levels of effector secretion, indicating that they play a critical function in regulating substrate translocation into host cells (Deng *et al.*, 2004; O'Connell *et al.*, 2004; Deng *et al.*, 2005; Wang *et al.*, 2008). The SepL–SepD complex interacts with the C-terminal domain of EscV, the export apparatus component that provides the substrate entry pore (Portaliou *et al.*, 2017). This interaction leads to translocator/chaperone complexes binding to EscV and prevents secretion of effector proteins, with the disruption of this SepL–EscV interaction enabling secretion of effector proteins (Portaliou *et al.*, 2017) (Figure 6). The subsequent dissociation of SepD, and later SepL, promotes the secretion of late effectors (Portaliou *et al.*, 2017) (Figure 6).

SepL also interacts with the ruler protein EscP, which limits effector secretion until the translocon (formed by EspA, EspB, and EspD) is complete. When the T3SS spans the bacterial envelop, the detection of high calcium levels in the extracellular media stabilizes SepL/EscP, which inhibits SepL-mediated effector export. However, completion of the T3SS by EspB/EspD insertion into the host plasma membrane results in reduced calcium

levels, leading to SepL–EscP complex dissociation, which enables effector export (Shaulov *et al.*, 2017).

As mentioned, the EscN ATPase-related complex is positioned just beneath the export channel entry point, where it is thought to use ATP catalysis to dissociate chaperones from their substrates to enable an efficient export process (Chen *et al.*, 2013) (Figure 2).

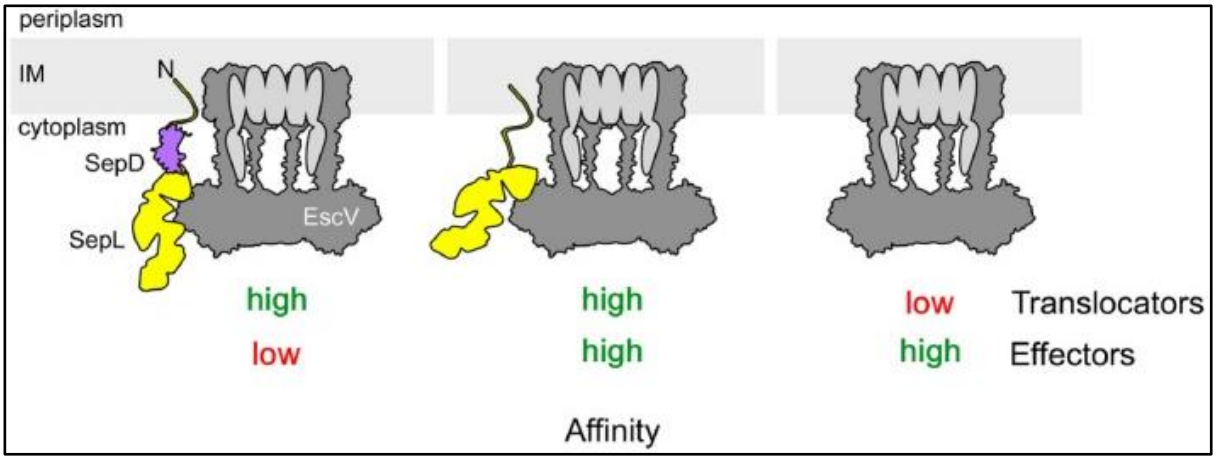

Figure 6: Schematic on how the gatekeeper proteins regulate secretion hierarchy

The molecular switching from middle substrates (EspA, EspB, and EspD) to effectors is controlled by the gatekeepers, SepL and SepD. The SepL–SepD complex binds to the C-terminus of the export apparatus component, EscV, which provides the export channel entry pore and prevents effector proteins from being exported. The subsequent dissociation of SepL enhances export of effector protein (into host cells). Taken from article by Portaliou *et al.*,(Portaliou *et al.*, 2017).

7. Bacteria Outer Membrane

Lipopolysaccharide (LPS) is a polysaccharide that is present only in the outer leaflet of Gram-negative bacteria and has a variety of biological functions. LPS is an endotoxin anchored in the bacterial membrane by a hydrophobic glycolipid (Lipid A). Moreover, LPS is composed of a core oligosaccharide (nonrepeating oligosaccharide containing sugars including heptose and keto-deoxyoctulosonate) and an O antigen (polysaccharide made up of several oligosaccharide repeating units, each with two to seven residues derived from a variety of common and uncommon sugars) (Valvano, 2003; Merino;Gonzalez and Tomás, 2016). Due to differences in the sugars present in the O unit and the connections between O units, the O antigen is one of the most irregular cell parts. The O antigen is located on the cell surface and normally enhances bacterial resistance to phagocytosis and serum killing (Burns and Hull, 1998). The O antigen is also a virulence factor and assists in bacterial pathogenesis (Pluschke *et al.*, 1983; Achtman and Pluschke, 1986). Recently, the O antigen has been found to inhibit bactericidal activity initiated by the lysozyme enzyme (Bao *et al.*, 2018).

Interestingly, the serotyping schemes of several Gram-negative bacteria are based on the heterogeneity in the O antigen structure. The serotyping scheme of *E. coli* was established in 1940 by Fritz Kauffmann and is currently characterized as involving O antigens numbered 1–181. This approach was used to classify strains for epidemiological purposes, as well as being a fundamental tool in disease investigations and surveillance (Liu *et al.*, 2020).

O antigen synthesis genes are normally found in a gene cluster at a particular locus. In O antigen gene clusters, there are three types of genes: genes that make nucleotide sugar precursors, genes encoding glycosyltransferases and genes encoding O unit translocation and polymerization. In addition, the Wzx/Wzy, ABC transporter and synthase pathways are three known pathways for O antigen synthesis, each requiring a cluster of genes for processing the O units (Bronner;Clarke and Whitfield, 1994; Keenleyside and Whitfield, 1996; Daniels;Vindurampulle and Morona, 1998; Linton and Higgins, 1998; Samuel and Reeves, 2003).

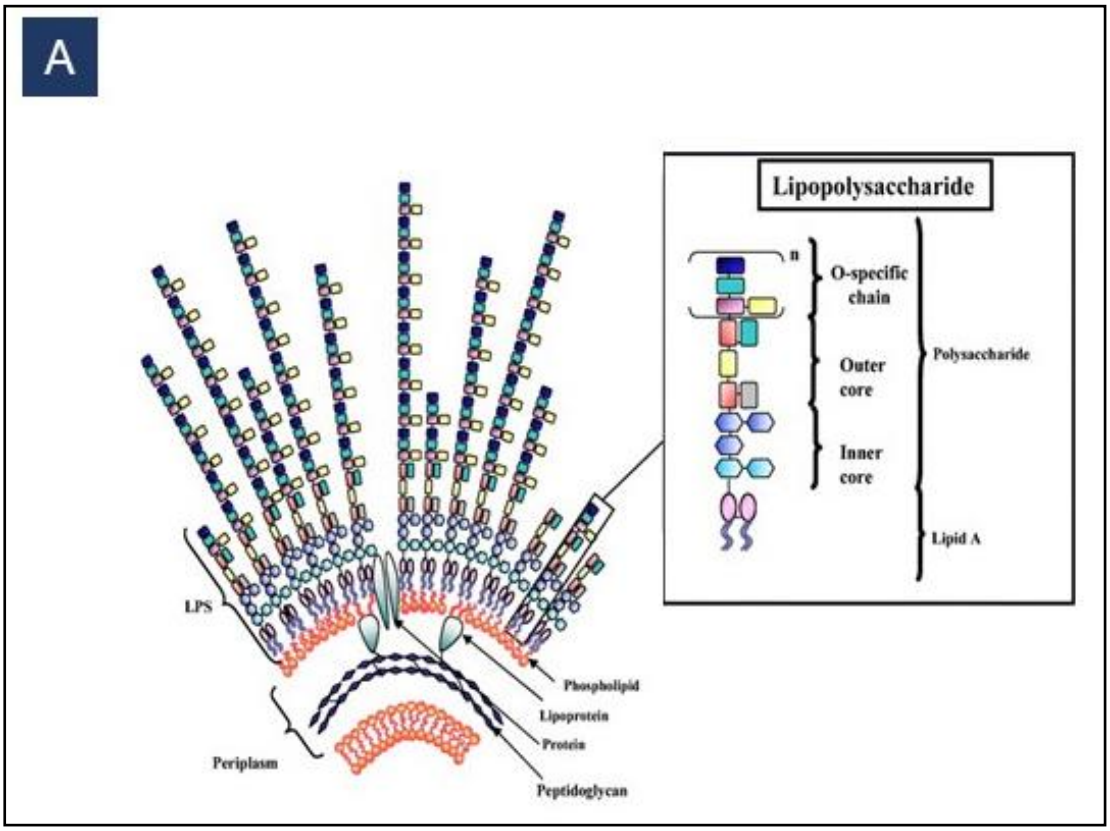

Figure 7: Schematic of how the gatekeeper proteins regulate secretion hierarchy

A) Diagram illustrating the cell wall of Gram-negative bacteria (left) and a lipopolysaccharide structure (right). (Caroff and Karibian, 2003).

8. *Edwardsiella tarda* LEE region

Edwardsiella tarda (E. tarda) is a Gram-negative intracellular pathogen of fish that causes haemorrhagic septicaemia but is also linked to human gastrointestinal infections (Mohanty and Sahoo, 2007). One *E. tarda* strain, FPC503, has been found to have a LEE-like region, with the rearrangement of the main operons linked to the loss, disruption and/or replacement of genes (Nakamura *et al.*, 2013) (Figure 8). However, recent re-interrogation of this region has revealed the presence of genes for all but 8 classical LEE proteins and notably the genes absent from *E. tarda* are not critical for EPEC to produce its T3SS or for virulence (Madkour *et al.*, 2021). More surprisingly, while LEE homologues are highly conserved among A/E pathogens, the *E. tarda* variants display unprecedented levels of divergence, with several proteins produced from 2-orf genes (Madkour *et al.*, 2021). Crucially, some of the *E. tarda* proteins examined that share low, intermediate or high levels of divergence could functionally replace their EPEC counterparts, while others could not, with some functional interchangeability defects linked to divergence (Madkour *et al.*, 2021). Interestingly, some *E. tarda* protein complementation defects are rescued by co-expressing partner proteins suggestive of co-divergence (Madkour *et al.*, 2021). It has been predicted that domain swap experiments between EPEC and *E. tarda* homologues displaying functional interchangeability defects could reveal domains, regions and/or residues critical for EPEC T3SS protein functionality, thus providing novel insights and potentially sought-after therapeutic targets.

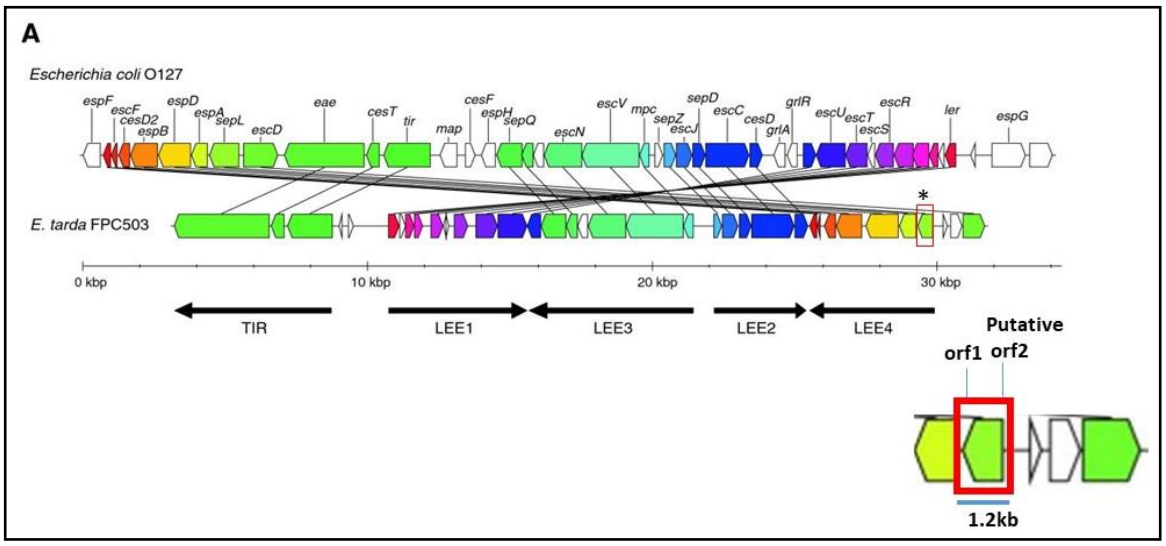

Figure 8: Schematic of LEE regions from EPEC E2348/69 and *E. tarda* FCP503 strains

The homologous genes in both EPEC and *E. tarda* LEE are coloured the same and connected by lines. Note that the location of the *sepL* gene in the *E. tarda* LEE region is underlined (Nakamura *et al.*, 2013). The inset shows the *sepL* orf1, putative orf2 as explained by Azzeldin Madkure and *sepL* gene size in LEE *E. tarda* (Madkour *et al.*, 2021).

Project Aim

The initial aim of the PhD research project was to re-interrogate the functional interchangeability defects of five *E. tarda* proteins to support the earlier, preliminary findings and help decide which protein or proteins to begin domain swap and/or other experiments to provide new insights on their functionality and/or possible therapeutic targets.

Chapter 2: Material and Method

1. Cell culture

1.2 Culturing of bacterial strains

Bacterial strains used in this study are listed in Table 1. Bacteria were retrieved from frozen cultures for inoculation into 2ml Luria Broth (LB) supplemented with, when appropriate, selective antibiotic (s) and incubated overnight (16h) at 37°C without shaking (for infection studies) or with shaking (for molecular biology-related work). Antibiotics were used at final concentration of 12µg/ml for Tetracycline (Tet), 25µg/ml for Kanamycin (Km), Chloramphenicol (Cm) and Streptomycin (Strep), 50µg/ml for Nalidixic acid (Nal) and 100µg/ml for Carbenicillin (Cb). Frozen cultures were generated by adding 50% glycerol (to final 10% v/v concentration) to overnight LB (shaking) culture for storage at -80°C.

1.2.1 Mammalian cell culture

HeLa Cells (human cervix-derived epithelial-like; ATCC_CCL2) were passaged in 75 cm2 tissue culture flasks (Corning) in a Class 2 laminar flow hood (BioMat 2) and kept under antiseptic conditions in a 37°C incubator with 5% CO2. Cells were cultured in Dulbecco's minimal Eagle's medium (DMEM; Sigma Cat No. D5796) containing 10% fetal calf serum (FCS; Sigma Cat No. 7524). Cells were regularly cultured to ~80% confluence before passaging (1:6 dilution) into a new tissue culture flask. To passage cells, they were first washed with phosphate-buffered saline (PBS; Sigma; Cat #SLBK4471V) before adding 2ml of 1 x Trypsin-EDTA [ethylenediamineacetic acid] solution (Sigma; Cat #SLBF3552) at 37°C in 5% CO2 atmosphere until cells observed to have detached. The cells were resuspended in DMEM/FCS for reseeding stock (75 cm2) flasks or other tissue cultured plastics such as 6 well plates (Corning;3506). Cell passage number was recorded with cells passaged up to 30 times before cells were discarded. Frozen stocks were generated by adding DMSO (final 10% v/v) to ~1 x 106 HeLa cells (in DMEM/10% FCS) for slow cooling (overnight) in -80^{o}C before transferring to liquid nitrogen storage.

2. Molecular biology

2.1 Plasmid isolation

Plasmid were extracted from bacteria using the Plasmid Mini Extraction Kit (New England Bio-labs; Cat # T1010L) following the manufacturer instructions. The bacteria were grown overnight (with shaking) in LB media with the appropriate selective antibiotic/s. Plasmid used in this study are listed in Table 2.

2.2 Polymerase chain reaction (PCR)

Genes were amplified from either an appropriate plasmid or from genomic DNA released from bacteria following boiling (100°C, 5 min) in distilled water (dH2O) an oligonucleotide primer pairs specific to the target gene (Table 3). Oligonucleotides were purchased from Sigma-Aldrich-UK following used of their software to design the oligonucleotides. PCR screening procedures used Taq DNA polymerase (New Britain Bio-labs: #M0273L) while cloning and sequencing involved Q5 Hot start high-fidelity DNA polymerase (New Britain Bio-labs; Cat #M0493S). Standard 25µl PCR reactions involved combining the components (New England Bio-labs) and under conditions listed in Table 4 and Table 5. The PCR products were assessed by adding 6x ficoll loading dye (Biolabs; Cat #B70215) to 1x final concentration and loading on 1% or 0.75% TAE (40 mM Tris-acetate, 1 mM EDTA) containing the nucleic acid stain GelRedTM (1:30,000; Biotium). The samples were run alongside 2-log DNA ladder markers (New England Biolabs; Cat # N3200L) in TAE buffer at 100 volts with DNA visualised using a UV transilluminator (Biorad; Molecular Imager Gel Doc™ XR System) for image capturing (Imagelab Software).

2.3 Gibson ligation

The Gibson Assembly kit permits proficient cloning of multiple DNA fragments via recombination across duplicated regions (Gibson *et al.*, 2009). The insertion was obtained by PCR amplification with the gene-specific primers having extensions specific to the target site of the vector or other PCR-generated fragment. The vector (pre-digested with

appropriate restriction enzyme to aid the recombination process) and PCR-generated fragments were resolved on TAE agarose gels with the required bands isolated using a gel extraction kit (New England Bio-labs; Cat #T1020) following the manufactures recommendations. The number of isolated bands were estimated by visualising on TAE agarose gels. The vector and insert fragment were combined (2:1 ratio) in a total 10µl volume with 5µl of the Gibson assembly master mix (New England Bio-labs; Cat #E2621S). The mixture was incubated overnight at 50°C with ligation success assessed by examining 5ul on a 0.75% TAE agarose gel for additional ligation-specific bands. When appropriate 2µl of the ligation product was transformed into chemically competent *E. coli* (NEB turbo-competent cells; Cat #C2984H) as described below.

2.4 Bacterial Transformation

2.4.1 Heat-shock method

An aliquot of NEB turbo-competent E. coli frozen cells (-80^{o}C) were thawed on ice before gently mixing and placing 15µl in a pre-chilled 1.5 ml Eppendorf tube for 10 minutes on ice. Then 2 µl of the ligation mix was added and mixed gently with a pipette. Following 30 minutes on ice, the suspension was placed at 42°C for 30 seconds and then returned to ice for 5 minutes. The cells were then resuspended in 950µl of 37°C SOC media (0.5% Yeast Concentrate, 2% Tryptone, 10mM NaCl, 2.5mM KCl, 10mM MgCl2, 10mM MgSO4 and 20mM Glucose) and incubated for 1 hour at 37°C with shaking (225-250 rpm) before plating 50 and 950µl onto LB agar plates, containing appropriate antibiotics, over ~16-hour incubation at 37°C. Some antibiotic resistant colonies were used for PCR analysis to screen for the cloned target gene.

2.4.2 Electroporation Method

Plasmids were routinely introduced in to EPEC using the electroporation methods. Briefly, the EPEC strain grown overnight at 37°C with shaking were routinely diluted (1:100) into fresh LB and grown (at 37°C with shaking) until obtaining optical density (OD_{600}) of between 0.6-0.8. To measure the OD_{600}, 1ml of bacterial culture was transferred into the plastic cuvette (Greiner Bio-one; Cat #613101) - dilutions if highly dense - and the

absorbance at 600nm measured using a UV 1101 Biotech Photometer. The optical density should be less than 1 with a value of 1 indicating presence of 1 x 10^9 bacteria.
The culture was quickly chilled on ice with gentle shaking before pelleting the bacterial (2800 x g, 15 min, 4°C) in 50 ml tubes (2800 x g, 15 min, 4 °C) (Star lab UK Ltd, #E1450-0200). The pellet was re-suspended in 50ml of ice cold dH_2O before re-pelleting and repeating these steps a final time. The bacterial pellet was re-suspended in 300ul of 10% glycerol and aliquots (40µl) placed into pre-chilled 1.5 ml Eppendorf tubes (Sarstedt; Cat #72.690.001). The aliquots were used immediately or snap frozen (in liquid nitrogen) for storage (-80°C) until needed.

Plasmid DNA was added to a fresh or thawed aliquot of cells and left on ice for 5-10 minutes before transferring to a 2mm electroporation cuvette (Cell project; Cat #EP-102) for used with a Gene Pulser II machine (Bio-Rad) with 2.5kV, 200Ω, 25mF settings. The post-electroporation mixture was rapidly and gently resuspensed in 1ml of pre-warmed (37°C) SOC media for 1-hour incubation at 37°C. Routinely, 100 and 900µl aliquots were plated on LB agar containing appropriate antibiotic/s and incubated 12-16 hours at 37°C. When appropriate PCR reactions were carried out to confirm introduction of the correct DNA fragment carrying plasmid.

2.5 DNA sequencing

PCR amplified fragments – obtained using Q5 high fidelity DNA polymerase (New Britain Bio-labs; Cat #M0493S) - were purified using the GenElute™ PCR Clean-Up Kit (Sigma Cat #NA 1020-1KT). The amount of isolated DNA was estimated by examining a portion on TAE agarose gels. An appropriate amount of DNA fragment and oligonulceotide primer/s were sent to Source Bioscience (Cambridge, UK) for sequencing. The obtained data was compared (http://www.ebi.ac.uk/Devices/psa/emboss_needle/) to the original gene sequence.

2.6 Gene Knockout Procedure

2.6.1 Gene Knockout Procedure

The disruption or deletion of target EPEC genes was carried out using the well-established, recombination-based, allelic exchange procedure as previously described (Donnenberg and Kaper, 1992).Briefly, overnight LB cultures of the recipient EPEC (Nal^R) and donor SM10 λ pir (Km^R) strain– latter contains the pDS132 suicide vector (Cm^R) carrying regions upstream and downstream of the gene targeted for disrupting/deleting – were mixed (1:1 ratio) before plating on LB agar plates for overnight incubation at 37C. The latter facilitates conjugation-mediated transfer of the suicide vector in to EPEC. A small number of bacteria was scraped into LB for growth, at 37°C with shaking, for ~7 hours before plating bacteria - serial dilutions - onto Nal^R/Cm^R plates to select for transconjugants. A resulting colony was inoculated into LB broth containing Nal and cultured, at 37°C with shaking, for ~7 hours before plating – serial dilutions - on LB containing 5% sucrose and Nal at 30°C for ~16 hours. The former provides time for recombination-based deletion of the suicide vector from the genome and the latter selects for strains lacking the suicide vector; encodes protein mediating to sucrose sensitivity. Routinely, ~30 resulting colonies were screened for their ability to grow on Nal, Cm, Km and, lastly, antibiotic free LB plates to identify putative gene deleted strains i.e., grow on Nal but not Cm or Km. PCR screening was carried out to determine if the targeted gene was disrupted/deleted.

3. Bacterial growth and Infection Studies

3.1 Isolating EPEC total cell and secreted protein samples

5.5ml of pre-warmed serum-free DMEM (supplemented, when needed, with antibiotics) was inoculated (1:100 dilution) with overnight LB grown (37°C standing) bacterial cultures. The optical density (OD_{600}) was determined after ~8h at 37°C in 5% CO2 atmosphere with 2ml of bacterial culture centrifuged (16,000 x g, 5 min, 4°C). 1.8ml of the supernatant was transferred to a fresh 2ml tube that contained 200µl of 100% trichloroacetic acid (TCA; BDH Cat #100810.0250) - final 10% (vol/vol) – for overnight incubation at 4°C. The residual supernatant (above bacterial pellet) was removed, and the pellet was resuspended in 80µl

of 1 x SDS-PAGE sample buffer (60 mM Tris-HCl pH 6.8, 1% w/v SDS, 5% v/v glycerol, 5% v/v β-mercaptoethanol & 0.01 % w/v bromophenol blue) per OD_{600} of bacterial cells.

The supernatant containing secreted proteins were pelleted by centrifuging the TCA containing samples (16,000 x g, 15 min, 4°C) and, after removal of all traces of TCA solution, resuspended in 20µl of 1x Laemmli sample buffer per OD_{600} of bacteria from which the sample originated. The sample buffer contained 10% saturated TRIS to neutralize high pH to enable the proteins to dissolve in the buffer. The bacterial total cell and supernatant (SN; contain secreted proteins) samples were heated (100°C, 10 min) before separating by SDS-PA gel electrophoresis (see below) for either Coomassie blue visualization of proteins - 0.1% Coomassie Brilliant Blue (Bio-Rad) in Methanol (50% [v/v]), Glacial acetic acid (10% [v/v]) - and/or Western Blot analyses (see below).

3.2 HeLa cell Infections

Two days prior to infection, HeLa cells (~$5x10^5$) were seeded into 6 well plates to obtain ~80% confluence (~7.2×10^5) on the infection day. Wells were infected with LB grown bacteria (37°C without shaking) at a MOI (multiplicity of infection) of 100:1 (bacteria: host cells) for indicated times before washing twice with ice cold PBS and adding 120µl of ice cold Triton X-100 lysis buffer (PBS containing, at final conc., 1% Triton, 1mM phenylmethylsulphonyl fluoride [v/v; Sigma P7626], 1mM sodium fluoride [NaF; company; Cat#194864], 1mM sodium orthovanadate [NaVO4]; protease inhibitor cocktail (Sigma; P8340 at 1/100 dilution). The cells were detached using a cell scraper (Starstedt; Cat No. 83.183) and the suspension transferred to a 1.5 ml Eppendorf tube for centrifugation (13,000 x g, 5 min, 4°C). The resulting 'soluble' fraction (contains host cytoplasm/membrane proteins and T3SS-delivered effectors) was transferred into a new tube where 5x Laemmli sample buffer (Laemmli, 1970) was added to a final 1x conc. The remaining Triton X-100 'insoluble' pellet (contains host nuclei/cytoskeletal proteins and adherent bacteria) was washed with cold PBS and re-suspended in 1x Laemmli sample buffer. The samples were heated (100°C, 10 min), vortexed and, if not directly used for Western Blot analysis, stored at -20°C.

3.3 Immunoblot analysis

SDS-Polyacrylamide gels (routinely 12% and/or 6%) were prepared as described (Laemmli, 1970) and wells loaded with proteins samples alongside protein molecular mass markers (Biorad; Cat No. 161-0373). The proteins were resolved by electrophoresis in SDS-PA gel running buffer (~1h at 200 Volts) before transferring to nitrocellulose (GE Healthcare Cat No. 15269794) using a Bio-Rad mini-gel wet transfer system containing 1X transfer buffer (25mM Tris, 192mM glycine; pH 8.3) for 1h at 110 Volts. Protein transfer levels was routinely evaluated by adding a reversible stain, Ponceau Red (Sigma, Cat# bP7170). The nitrocellulose membranes were washed in PBS (to remove the stain) and then incubated for 1h (at room temperature) with PBS containing 5% skimmed milk powder (Marvel). These 'blocked' membranes were washed with PBS (5 min x 3) before overnight incubation (40C) with PBS containing the appropriate primary antibody (Table 6). After washing away the antibody with PBS washes (5 min x 3) the membranes were incubated with the appropriate secondary antibody; either alkaline phosphatase (AP) or horseradish peroxidase (HRP)-conjugated (Table 6). After removal of the antibodies and PBS washes, the bound AP-conjugated were detected using NBT/BCIP substrate (Promega-UK Ltd, Cat. No.53771) or for HRP-conjugated antibodies incubated with ECL Buffer (Thermo scientific; Cat No. 34079) with chemo-luminescence signal captured using an imaging machine (Bio-Rad System) and image J gel analysis software.

3.4 Bacterial growth curves

DMEM and LB media that contained 10mM HEPES pH 7 (Sigma; Cat #H4034) was pre-warmed (37^{o}C) before placing 200µl into wells of a 96-well microtiter plate. Overnight LB-grown (37^{o}C without shaking) cultures of the different strains were uses to infect (1:100 dilution) single wells before placing the plate in a microplate reader (BMG LABTECH) set at 37^{o}C and to take OD_{600} readings at 1h post-infection and then 2h intervals for 17hours. The analysis was independently repeated a minimum of 3 times with the mean value and standard deviation calculated for each time point with the growth curves generated using GraphPad Prism 6.

Table 1 :Strains used in this study indicating important characteristics, antibiotic resistance profile and source

Bacterial Strain	Description	Antibiotic Resistance	Source
EPEC E2348/69 (O127:H6)	Wild-Type, Nal variant	Nal	(Levine *et al.*, 1985)
ΔespA	Lacks EspA	Nal/Km	(Kenny *et al.*, 1996)
ΔespD	Lacks EspD	Nal/Km	(Lai *et al.*, 1997)
ΔespAB	Lacks EspA and EspD	Nal/Km	(Madkour *et al.*, 2021)
ΔespDB	Lacks EspB and EspD	Nal/Km	(Madkour *et al.*, 2021)
Δescp	Lacks EscP	Strep	(Monjaras Feria *et al.*, 2012)
ΔescK	Lacks EscK	Strep/Km	(Soto *et al.*, 2017)
ΔsepL	Lacks SepL	Strep	(Gaytan *et al.*, 2016)
ΔespB	Lacks EspB	Nal	(Taylor *et al.*, 1998)
ΔescF	Lacks EscF	Strep/Km	González-Pedrajo Laboratory
ΔetgA	Lacks EtgA	Km	González-Pedrajo Laboratory
ΔescC	Lacks EscC	Nal	(Ogino *et al.*, 2006)
ΔescI	Lacks EscI	Strep/Km	González-Pedrajo Laboratory
ΔescJ	Lacks EscJ	Strep/Km	González-Pedrajo Laboratory
ΔescD	Lacks EscD	Nal	(Madkour *et al.*, 2021)
ΔescRSTU	Lacks EscR, S, T and U proteins	Km	(Yerushalmi *et al.*, 2014)
ΔescU	Lacks EscU	Strep/Km	(Soto *et al.*, 2017)
ΔescV	Lacks EscV	Strep	(Gauthier;Puente and Finlay, 2003)
ΔescN	Lacks EscN	Km	(Donnenberg and Kaper, 1992)
ΔescO	Lacks EscO	Strep/Km	(Romo-Castillo *et al.*, 2014b)
ΔescQ	Lacks EscQ	Strep/Km	(Soto *et al.*, 2017)
ΔescL	Lacks EscL	Strep/Km	(Soto *et al.*, 2017)
ΔsepD	Lacks SepD	Strep	González-Pedrajo Laboratory
ΔescE	Lacks EscF	Nal	(Madkour *et al.*, 2021)
ΔcesD	Lacks CspD	Km	(Nadler *et al.*, 2010)
ΔcesD2	Lacks CspD2	Km	(Neves *et al.*, 2003)
ΔcesT	Lacks CesT	km	(Creasey *et al.*, 2003)
ΔcesAB	Lacks CesAB	Strep/Km	González-Pedrajo Laboratory
ΔcesL	Lacks CesL	Strep/Km	González-Pedrajo Laboratory
ΔcesF	Lacks CesF	Nal/Km	Kenny Lab
ΔescG	Lacks EscG	Nal	(Madkour *et al.*, 2021)
Δtir	Lacks Tir	Nal	(Kenny *et al.*, 1997b)
Δmap	Lacks Map	Nal	(Kenny and Jepson, 2000)
ΔespZ	Lacks EspZ	Nal	(Madkour *et al.*, 2021)
ΔespG/espG2	Lacks EspG and EspG2	Nal	Kenny lab
ΔespH	Lacks EspH	Nal/Km	Kenny lab
ΔgrlA	Lacks GrlA	Km	(Barba *et al.*, 2005)
Δler	Lacks Ler	Km	(Barba *et al.*, 2005)
ΔsepL Δtir	Lacks SepL and Tir	Strep	This study
JPN15	Lack pMar plasmid	Tet	(Jerse and Kaper, 1991)
ΔespC	Lacks EspC	Km	(Stein *et al.*, 1996)
Δeae	Lacks Intimin	Nal	(Donnenberg and Kaper, 1992)
Δfcl	EPEC E2348/69 lacking *fcl* gene	Nal	This study

Bacterial Strain	Description	Antibiotic Resistance	Source
Δfcl ΔCA	EPEC E2348/69 lacking *fcl*, *wcaL, wcaK, wzxC*, *wcaJ* genes	Km	This study
ΔCA	EPEC E2348/69 lacking *wcaL, wcaK, wzxC* and *wcaJ* genes	Nal	This study
ΔsepL full	EPEC E2348/69 lacking *sepL*	Nal	This study
ΔescUΔsepL	EPEC E2348/69 lacking *escU* and *sepL*	Nal	This study
Japan EPEC	Provided EPEC E2348/69	Nal	(Yen *et al.*, 2010)
J. EPEC TOEA7	As above but lack most known non-LEE-encoded (Nle) effectors	Tet	(Yen *et al.*, 2010)
J. EPEC TOEA7 core	J. EPEC TOEA7 but also lacks LEE CesT, CesF, Intimin, Map, EspH, Tir proteins	Tet	(Yen *et al.*, 2010)
SM10λpir	*E. coli* strain with λpir permits replication of R6K ori-based suicide plasmids	Km	(Donnenberg and Kaper, 1992)
K12	Non- pathogenic *E. coli*	NA	Thermo Fisher Scientific

Table 2:Plasmids used in this study indicating what encode, antibiotic (Ab) to select and source

Plasmid	Description	Antibiotic Resistance	References
pACYC	Cloning vector (pACYC)	Cm	(Chang and Cohen, 1978)
pEscP$_{EPEC}$	pTrc expressing EPEC EscP	Cb	(Monjaras Feria *et al.*, 2012)
pEscP$_{E. tarda}$	pACYC expressing *E. tarda* EscP	Cm	(Madkour *et al.*, 2021)
pEspA$_{EPEC}$	Expresses EPEC EspA	Cm	(Kenny *et al.*, 1996)
pEspA$_{E. tarda}$	pACYC expressing *E. tarda* EspA	Cm	(Madkour *et al.*, 2021)
pEspADB$_{E. tarda}$	pACYC expressing *E. tarda* EspA, EspD & EspB	Cm	(Madkour *et al.*, 2021)
pEspD$_{EPEC}$	pACYC expressing EPEC EspD	Cm	Kenny lab
pEspD$_{E. tarda}$	pACYC expressing *E. tarda* EspD	Cm	(Madkour *et al.*, 2021)
pEscK$_{EPEC}$	pET expressing EPEC EscK	Cb	(Soto *et al.*, 2017)
pEscK$_{E. tarda}$	pACYC expressing *E. tarda* EscK	Cm	(Madkour *et al.*, 2021)
pSepL$_{EPEC}$ (pE)	pTrc expressing EPEC SepL	Cb	(Monjaras Feria *et al.*, 2012)
pSepL$_{E. tarda}$ (pT)	pACYC expressing *E. tarda SepL*	Cm	(Madkour *et al.*, 2021)
pEscC$_{EPEC}$	pACYC expressing EPEC EscC	Cm	(Madkour *et al.*, 2021)
pEscC$_{E. tarda}$	pACYC expressing *E. tarda* EscC	Cm	(Madkour *et al.*, 2021)
pEscD$_{EPEC}$	pACYC expressing EPEC EscD	Cm	(Madkour *et al.*, 2021)
pEscD$_{E. tarda}$	pACYC expressing *E. tarda* EscD	Cm	(Madkour *et al.*, 2021)
pCesT$_{EPEC}$	pACYC expressing EPEC CesT	Cm	Kenny lab
pCesT$_{E. tarda}$	pACYC expressing *E.tarda* CesT	Cm	(Madkour *et al.*, 2021)
pCesD2$_{EPEC}$	pACYC expressing EPEC CesD2	Cm	(Madkour *et al.*, 2021)
pCesD2$_{E. tarda}$	pACYC expressing *E. tarda* CesD2	Cm	(Madkour *et al.*, 2021)
pCesAB$_{EPEC}$	pMQ expressing EPEC CesAB:His fusion protein	Cb	(Madkour *et al.*, 2021)
pCesAB$_{E. tarda}$	pACYC expressing *E. tarda* CesAB	Cm	(Madkour *et al.*, 2021)
p*espF*$_{EPEC}$	pACYC expressing EPEC EspF	Cm	(Dean and Kenny, 2004)
pT7*espF*$_{EPEC}$	pACYC expressing T7: EspF fusion protein	Cm	(Dean and Kenny, 2004)
pT7His*espF*$_{EPEC}$	pACYC expressing T7: His:EspF fusion protein	Cm	(Dean and Kenny, 2004)
p*tir*HA	pACYC expressing Tir:HA fusion protein	Cm	This study
pΔ*sepL*$_{full}$	pACYC carrying *escD* and *espA* genes	Cm	This study
pDS-Δ*sepL*$_{full}$	pDS132 vector used to delete *sepL* gene	Cm	This study
pEscU$_{EPEC}$	pACYC expressing EPEC EscU	Cm	(Madkour *et al.*, 2021)
pEscU$_{E. tarda}$	pACYC expressing *E. tarda* EscU	Cm	(Madkour *et al.*, 2021)
pSepL:HA$_{EPEC}$ (pE:HA)	Expresses EPEC SepL:HA fusion protein	Cm	This study
pHA:SepL$_{EPEC}$ (pHA:E)	Expresses EPEC HA:SepL fusion protein	Cm	This study
pSepL:HA$_{E. tarda}$ (pT:HA)	Expresses *E. trade* SepL:HA fusion protein	Cm	(Madkour *et al.*, 2021)
pETT	pACYC expressing SepL EPEC domain1 & *E. tarda* domain2,3	Cm	This study
pETT:HA	C-terminally HA-tagged variant of above	Cm	This study
pTEE	pACYC expressing *E. tarda* domain1 & SepL EPEC domain2,3	Cm	This study
pTEE:HA	C-terminally HA-tagged variant of above	Cm	This study
pETE	pACYC expressing SepL EPEC domain1,3 & *E. tarda* domain2	Cm	This study

Plasmid	Description	Antibiotic Resistance	References
pETE:HA	C-terminally HA-tagged variant of above	Cm	This study
pTET	pACYC expressing SepL EPEC domain2 & *E. tarda* domain1,3	Cm	This study
pTET:HA	C-terminally HA-tagged variant of above	Cm	This study
pTTE	pACYC expressing SepL *E. tarda* domain1,2 & EPEC domain3	Cm	This study
pTTE:HA	C-terminally HA-tagged variant of above	Cm	This study
pEET	pACYC expressing SepL EPEC domain1,2 & *E. tarda* domain3	Cm	This study
pEET: HA	C-terminally HA-tagged variant of above	Cm	This study
pDS132-*ΔPP2*	Used to delete PP2 region in EPEC	Cm	Quitard. Unpublished
pDS132-*Δfcl*	Used to delete *fcl* gene	Cm	This study
pDS132-*ΔCA*	Used to delete *wcaL, wcaK, wzxC* and *wcaJ* genes	Cm	This study
pDS132-*ΔsepL*	Used to delete *sepL* gene	Cm	This study
pCVD442-*Δtir*	Used to delete *tir* gene	Cb	(Warawa;Finlay and Kenny, 1999)

Table 3 :Primers used in this study

Primer	Sequence
EPEC-*tir*-FP	CCGCCACTACCTTCACAAAC
EPEC-*tir*-RP	GCGTTGGTGCGGCATTTACAG
EPEC-*cesT*-FP	GCTCTAGACAACGTTGCAGCATGGGTAA
EPEC-*cesT*-RP	GCGAATTCTCATGTTTGGGCTCCACCAC
EPEC-*gmm*-FP	GGTTAAAAAGGATCGATCCTCATTAATGCTACGCCTATTGTG
EPEC-*gmm*- RP	TTATGCGTTGTCTACTCATGC
EPEC- *gmd*- FP	GCATGAGTAGACAACGCATAAGATGTTTTTACGTCAGGAAGAC
EPEC-*gmd*- RP	GTGGAATTCCCGGGAGAGCTCGTAGTTAATGCCGTAGACCAG
EPEC-*cpsG* –FP	GGTTAAAAAGGATCGATCCTCGCTCGATTTAATTGAAGTG
EPEC-*cpsG*-RP	CGTTGTTCCTGTTATTAGCC
EPEC-*wcaM* –FP	GGCTAATAACAGGAACAACGCTGGTGCCTGAGAACGATG
EPEC-*wcaM* –RP	GTGGAATTCCCGGGAGAGCTCGTCTGGTTGTTACGTAAGAAAC
EPEC-*escD* -FP	GCGACCACACCCGTCCTGTGCTCTCCACCCAATAATTTGAC
EPEC-*escD* -RP	TTATTCAATACCATTAGCCATTG
EPEC-*espA* -FP	TGGCTAATGGTATTGAATAACATGCTAAGAAAGATTATGAAGAGG
EPEC-*espA* -RP	AAGGCTCTCAAGGGCATCGGCCGAGCTCCAGAGGGCGTCACTAATGAG
EPEC-*sepL* HA-FP	GCGACCACACCCGTCCTGTGGGTGAACTTACATCGTCTAAG
EPEC-*sepL* HA- RP1	CTAAGCGTAATCTGGAACATCGTATGGGTACATAACATCCTCCTTATAATCTATCAC
EPEC-*sepL* HA- RP2	AAGGCTCTCAAGGGCATCGGTTAAGCGTAATCTGGAACATCG
HA-EPEC-*sepL* FP1	ATGTACCCATACGATGTTCCAGATTACGCTGCTAATGGTATTGAATTTAATCAAAAC
HA-EPEC-*sepL* FP2	GCGACCACACCCGTCCTGTGATGTACCCATACGATGTTCC
HA-EPEC-*sepL*- RP	AAGGCTCTCAAGGGCATCGGGCACTAGCAACTGATGCTG
pACYC -*sepL*-FP	CTCTTACCAGCCTAACTTCG
E. tarda -*sepL*-D1, D2 RP	AGAAACTATTTCGCTATAATTATTTAATG
EPEC-*sepL* -D3-FP	ATTATAGCGAAATAGTTTCTATCTCCATTAAGAAAGATAAAGATGTC
pACYC -*sepL*-RP	CGAAGTTAGGCTGGTAAGAGGGAAGCGAGAAGAATCATAATG
EPEC -*sepL*-D1, D2 RP	TGCAATAATATCCGTATAG
E. tarda -*sepL* -D3-FP	CTATACGGATATTATTGCATTATCCTTAAAAAAGGATGCTG
EPEC -*sepL*-D1-RP	CCTGGTTTAACTCACCCAC
E. tarda -*sepL*-D2, D3 FP	GTGGGTGAGTTAAACCAGGGTCGGTGGGAAAAAACTAAAG
E. tarda -*sepL* -D1-RP	CTGATCTTTTGCCTTCTGATAG
EPEC -*sepL*-D2,3-FP	CTATCAGAAGGCAAAAGATCAGAGGGGTGGGTGAGTTAAACC
pACYC -*sepL*-FP-2	CCGATGCCCTTGAGAGCCTTC
pACYC- *sepL*- EPEC -RP 2	GAAGGCTCTCAAGGGCATCGGTTACCAAGGGATATTCCTGAAATAG

Table 4: Standard PCR reaction mix, and conditions used with Taq polymerase.

Components	25 µl Reaction	Final Concentration
10X Taq Reaction Buffer	1 µl	1X
10 mM dNTPs	0.5 µl	200 µM
10 µM Forward Primer	0.5 µl	0.2 µM
10 µM Reverse Primer	0.5 µl	0.2 µM
Template DNA	1 µl	Variable
Taq DNA Polymerase	0.125 µl	0.625 units
Water	21.5 µl	

Stage	Temperature	Time (sec)	Cycles
Initial denaturation	95°C	30	1
Denaturation **Annealing** **Extension**	95°C 53°C-68°C 68°C	30 60 60	30
Final Extension	68°C	120	1

Table 5: Standard PCR reaction mix, and conditions used with Q5 polymerase.

Components	25 µl Reaction	Final Concentration
5X Q5 Buffer	5 µl	1X
10 mM dNTPs	0.5 µl	200 µM
10 µM Forward Primer	1.25 µl	0.5 µM
10 µM Reverse Primer	1.25 µl	0.5 µM
Template DNA	1 ul	Variable
Q5 Hot Start High-Fidelity DNA Polymerase	0.25 µl	0.02 U/µl
Water	16 µl	

Stage	Temperature	Time (sec)	Cycles
Initial denaturation	98°C	30	1
Denaturation **Annealing** **Extension**	98°C 53°C-68°C 72°C	10 30 30-60	30
Final Extension	72°C	120	1

Table 6: List of antibodies providing information on type, dilution used and source.

Primary Antibody	Type	Dilution	Source
Anti-Tir	Rabbit (polyclonal)	1/5000	Kenny Lab
Anti-DnaK	Mouse (monoclonal)	1/2000	Cat #SPA-88020009
Anti-EspD	Rabbit (polyclonal)	1/2000	Kenny Lab
Anti-EspB	Rabbit (polyclonal)	1/2000	Kenny Lab
Anti-EspF	Rabbit (polyclonal)	1/2000	Kenny Lab
Anti-EspA	Rabbit (polyclonal)	1/1000	Kenny Lab
Anti-O127	Rabbit (polyclonal)	1/1000	Cat #Oxford Biosystems Ltd-44305
Anti-HA tag	Mouse (monoclonal)	1/1000	Cat #abcam-ab130275

Secondary Antibody	Type	Dilution	Source
Anti-Rabbit IgG-HRP	Goat	1/5000	Jackson Immuno Research; #111-035-003
Anti-Rabbit IgG-AP	Goat	1/5000	Jackson Immuno Research; #111-055-144
Anti-Mouse IgG-HRP	Goat	1/5000	Jackson Immuno Research; #115-035-003
Anti-Mouse IgG-AP	Goat	1/5000	Jackson Immuno Research; #115-055-146

Chapter 3: Interrogating the functional interchangeability of five EPEC and *E. tarda* homologues

3.1 Introduction

Phylogenomic analysis of the *E. tarda* LEE DNA sequence suggested that it may be non-functional as it lacked intact genes for several T3SS and effector proteins needed for functionality (Nakamura *et al.*, 2013). However, studies in the laboratory questioned this idea by revealing gene sequences for all but 8 proteins that are not critical for EPEC T3SS biology or virulence (Madkour *et al.*, 2021). A summary of the findings is given in Table 7, with the 'missing' genes encoding effectors (EspG, EspH, EspF, and Map), an EspF-specific chaperone (CesF), transcriptional regulators (GrlA, GrlR) and a protein of unknown function (rOrf1). However, the analysis revealed that 4 T3SS genes were interrupted by either a 14bp insertion (*escD*), single nonsense (*escK)*, or a single frameshift (*sepL*, *escL)* mutation (Madkour *et al.*, 2021). Notably, work on *E. tarda escD* revealed that it functionally replaced its EPEC homologue while *E. tarda sepL* had some complementation activity with *escK* and *escL* not substituting their EPEC homologues (Madkour *et al.*, 2021). The *E. tarda escD* findings demonstrated that 2-*orf* (open reading frame) genes can be expressed, likely through ribosome-mediated mechanisms (Weiss, 1991; Madkour *et al.*, 2021).

Studies with the *E. tarda* translocator proteins (EspA, EspB, EspD) showed that each had a complementation defect that disappeared when all three were co-expressed together in the EPEC *ΔespA* or *ΔespD* mutant strains (Madkour *et al.*, 2021). This result linked complementation defects to differences in protein sequence between the homologues, suggesting that the *E. tarda* T3SS is functional and acts to deliver the two *E. tarda* LEE-encoded effectors (Tir and EspZ homologues) into infected fish cells (Madkour *et al.*, 2021). Previous preliminary studies investigated the functional interchangeability for 8, of 33, *E. tarda* LEE genes and found that 6 (*escD*, *ler*, *eae* [Intimin] and, when co-expressed, *espA*, *espB*, *espD*) could functionally replace their EPEC variant, 1 (*tir*) could not while 1 (*cesT*) partially substituted (Madkour *et al.*, 2021). Studies by undergraduate final year

students examining another 4 *E. tarda* genes indicated that 2 (*escK*, *escL*) did not functionally substitute while the other two (*sepL*, *escP*) had some activity (unpublished).

The aim of the work presented in this chapter was to confirm the preliminary data suggesting that the *E. tarda* EscP, EspA, EspD, EscK, and SepL proteins, when expressed in EPEC, had complementation defects, in order to then decide which protein (or proteins) would be the subject of further studies.

	Protein	EPEC	*E. tarda*	Identity	similarity	Protein function	Reported
1	rOrf1		Missing			Unknown function	
2	EspG	398aa	Missing			Effector	
3	Ler	129aa	129aa	38.6%	54.5%	LEE encoded the master regulator	✓
4	EscE /Orf2	72aa	76aa	35.1%	51.9%	Class II chaperone for EscF	✓
5	CesAB	107aa	104aa	35.3%	54.6%	Class II chaperone for EspA & EspB	✓
6	EscK /Orf4	199aa	121aa	12.6%	21.4%	A sorting platform protein	✓
7	EscL /Orf5	231aa	215aa	27.3%	53.7%	A negative regulator that inhibits EscN ATPase activity	✓
8	EscR	217aa	218aa	73.4%	88.5%	T3SS core proteins (T3SS export apparatus) contribute to the recruitment and regulation of initial insertion of substrates into the injectisome.	✓
9	EscS	89aa	89aa	63.0%	82.6%		✓
10	EscT	258aa	259aa	56.1%	75.6%		✓
11	EscU	345aa	345aa	58.0%	78.8%		✓
12	EtgA	152aa	158aa	43.2%		A peptidoglycan lytic enzyme	✓
13	grlR		Missing			A negative regulator of LEE gene expression	
14	grlA		Missing			A positive regulator of the *ler* expression	
15	CesD	151aa	153aa	64.3%	79.9%	Class II chaperone for EspD &EspB	✓
16	EscC	512aa	503aa	64.6%	80.3%	T3SS outer membrane ring (IM)	✓
17	SepD	151aa	143aa	39.6%	63.6%	Molecular Switch from translocators to effectors	✓
18	EscJ	190aa	179aa	53.1%	72.9%	T3SS inner membrane ring (IM)	✓
19	EscI /Orf8	142aa	130aa	46.9%	63.3%	The T3SS inner rod that connect OM and IM rings	✓
20	EspZ /SepZ	98aa	129aa	29.9%	38.0%	Effector	
21	CesL/Mpc	117aa	107aa	30.1%	42.3%	A class I chaperone for SepL	✓
22	EscV	675aa	674aa	66.3%	79.9%	T3SS export apparatus	✓
23	EscN	466aa	458aa	62.1%	76.4%	ATPase complex T3SS component	✓
24	EscA/EscO/ Orf15	125aa	122aa	25%	54%	AATPase complex component that stimulates EscN ATPase activity	✓
25	EscP/Orf16	138aa	103aa	21%	39%	Regulate EscI secretion/ Molecular ruler/ Molecular Switch (by interacting with EscU)	✓
26	SepQ/EscQ	305aa	297aa	21%	44.1%	C-ring of T3SS that act as sorting platform	✓
27	EspH	168aa	Missing			Effector	
28	CesF	120aa	Missing			Class IA chaperone that binds EspF	
29	Map	203aa	Missing			Effector	
30	Tir	550aa	529aa	24%	36.3%	Translocate intimin receptor	✓
31	CesT	156aa	156aa	60.3%	80.1%	Class IB chaperone for Tir effector and many LEE/non-LEE effectors	✓
32	Intimin/eae	939aa	1117aa	39.6%	51.6%	Extracellular bacterial protein	✓
33	EscD*	406aa	416aa	43.7%	61.0%	The T3SS inner membrane ring (IM)	✓
34	SepL*	351aa	343aa	49.3%	74.4%	Molecular Switch (gatekeeper)	✓
35	EspA	192aa	199aa	62.0%	74.5%	Translocators	✓
36	EspD	380aa	385aa	50.9%	66.9%		✓
37	EspB	321aa	340aa	37.8%	55.7%		✓
38	CesD2	135aa	136aa	53.7%	66.9 %	Class II chaperone for EspD	✓
39	EscF	73aa	74aa	67.6%	87.8%	T3SS component (needle protein)	✓
40	EscG/Orf29/ CesA2	92aa	89aa	36.8%	56.8%	Class III chaperone of the needle protein EscF and the filament protein EspA	✓
41	EspF	206aa	Missing			Effector	

Table 7: Summary of data from comparing *E. tarda* and EPEC LEE region-encoded proteins

E. tarda LEE encodes 33 proteins in contrast to 41 for EPEC LEE (Madkour *et al.*, 2021), with the absent ones highlighted in green and blue, while the cryptic protein is highlighted in red. The table was taken from Madkour thesis (Madkour, 2017) and shows the key functions of each LEE protein with information on size (amino acid; aa) and percentage (%) of identity/similarity of the homologues.

3.2 Result

3.2.1 *E. tarda* EscP functionally replaces EPEC EscP but recognises Tir more as a translocator, than an effector protein

To determine whether *E. tarda* EscP can functionally replace EscP EPEC, studies first looked at the Δ*escP* secretion profile and the impact of carrying available plasmids encoding the EPEC or *E. tarda escP* gene. Therefore, tissue culture media (DMEM) was inoculated for 8-hours, with the strains before isolating total bacterial cell extracts and secreted (supernatant; SN) proteins (see Materials & Methods). Samples were resolved by SDS-PAGE for visualisation by Coomassie blue staining and processed for western blot analyses to probe for the translocators (EspA, EspD, and EspB) and an effector (Tir) protein (see Materials & Methods).

The Coomassie blue stain data (Figure 9A) revealed a typical total cellular protein profile for each strain with one noticeable difference: the absence of a band of 55KDa linked to *escP* gene inactivation. This protein is unlikely to relate to EscP as the EPEC *escP* gene encodes a 138 residue (~13KDa) protein and the band was also in the plasmid complemented strains (Figure 9A). As expected, EPEC secreted high levels of each translocator (EspA, EspD, EspB) and the EspC autotransporter protein (Figure 9B), with the *ΔescP* mutant secreting low levels of each translocator and an additional protein (>75KDa) shown to be Tir (Monjaras Feria *et al.*, 2012) (Figure 9B). This result supports that EscP is involved in regulating the switching of T3SS substrates from translocator to effector proteins (Monjaras Feria *et al.*, 2012). Interestingly, the *ΔescP* mutant complemented with the plasmid carrying either the *E. tarda* or EPEC *escP* genes rescued the translocator secretion defect, but the *E. tarda* variant did not prevent Tir secretion (Figure 9B).

In western blot analysis probing for EspB and EspD linked loss of *escP* with reduced expression and secretion levels of these proteins (Figure 9C). These defects were rescued fully and partially by introducing the EPEC and *E. tarda escP* genes, respectively (Figure 9C). Failure to get a good anti-EspA signal resulted in another analysis which included an additional control, i.e., cell and supernatant samples from a T3SS-defective mutant (T3SS). This work revealed similar findings to the EspB and EspD proteins (Figure 9C). Probing for

Tir did not reveal a difference within the cellular extracts of the strains but confirmed higher secretion levels by the *ΔescP* mutant carrying no plasmid and the *E. tarda escP* gene carrying plasmid (Figure 9C). Collectively, the findings suggest that EscP influences the expression and secretion levels of the translocator proteins but only the secretion, not expression, of the Tir effector.

To test the strain's ability to deliver effectors in mammalian (Hela) cells, studies examined for shifts in the apparent molecular mass of the Tir effector, as these depend on it being modified by host kinases within the cytoplasm (Kenny *et al.*, 1997b). Therefore, HeLa cells were infected with the different strains before isolating Triton X-100 soluble (contains host cytoplasm and membrane proteins plus T3SS delivered EPEC effectors) and insoluble (contains host nuclei and cytoskeletal proteins and proteins from the adherent bacteria) fractions. Probing for Tir (Figure 9D) revealed a dramatic *escP*-dependent decrease in the kinase-modified Tir (T'') form - noting T^0 is the unmodified form - in the soluble fraction (Figure 9D). This Tir T'' form can interact with the EPEC Intimin surface protein, as revealed by its presence in the insoluble fraction (Figure 9D) which is an Intimin-dependent event (Kenny, 1999). This reduction in Tir delivery levels was rescued by plasmids expressing EPEC *escP*, but to a much lesser level, *E. tarda escP* (Figure 9D; Supplementary Figure 1).

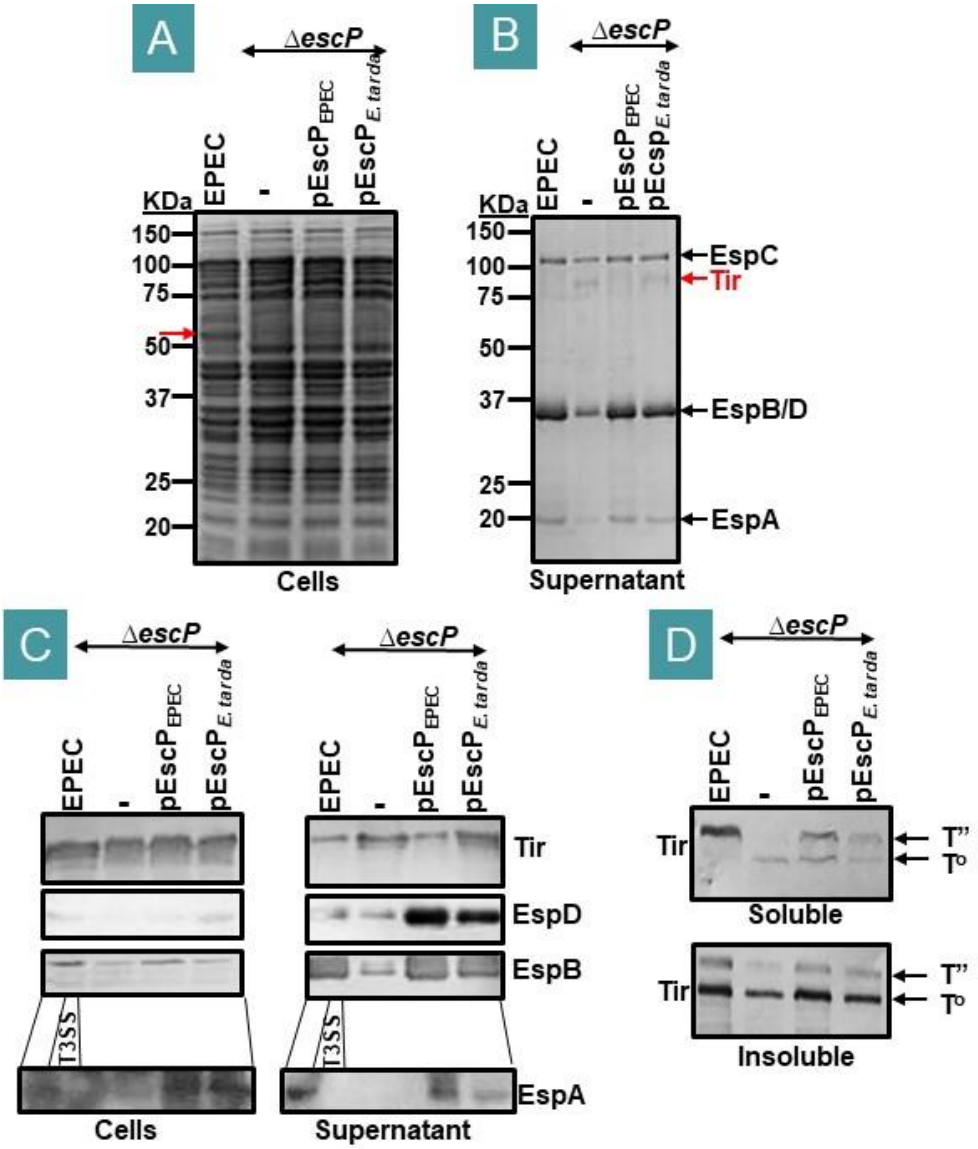

Figure 9:*E. tarda* EscP functionally replaces EPEC EscP but recognises Tir more as a translocator, than an effector protein

Indicated strains were used to infect (A-C) DMEM and (D) HeLa cells. The DMEM was infected (1:100 dilution of bacteria grown overnight in LB) for 8-hours before isolating total bacterial cells and secreted (supernatant) proteins. HeLa cells were infected for 4 hours before isolating Triton X-100 soluble (contains host cytoplasm/membrane proteins and T3SS delivered EPEC effectors) and insoluble (contains host nuclei/cytoskeletal proteins and adherent bacterial proteins) fractions. Samples were resolved on 12% SDS-PA gels for (A-B) Coomassie blue visualisation and for (C-D) western blot analysis to probe for translocators (EspA, EspB, EspD) and an effector (Tir) protein. The positions of the unmodified (T^{o}) and host kinase-modified (T") Tir forms are shown. The position of the molecular weight standards (kDa) is shown (A) with a red arrow indicating the band (~55kDa) whose position differs in the strains. Strains used were EPEC, T3SS-deficient mutant (T3SS) and Δ*escP* mutant; the latter having no introduced plasmids (-) or a plasmid-encoding EPEC EscP ($pEscP_{EPEC}$) or *E. tarda* EscP ($pEscP_{E. tarda}$) proteins.

3.2.2 The *E. tarda* EspA and EspD weakly substitute their EPEC homologues unless co-expressed with the other two *E. tarda* translocator proteins

Earlier T3SS functionality studies suggested that *E. tarda* EspA can partially replace EPEC EspA with the defects rescued by co-expressing all three *E. tarda* translocator proteins (Madkour *et al.*, 2021). Thus, studies first examined the secretion profile of the *ΔespA* and the impact of plasmids carrying EPEC or *E. tarda espA*. The studies also examined the *ΔespAB* secretion profile and impact of introducing a plasmid carrying the *E. tarda espADB* gene operon (Madkour *et al.*, 2021). Coomassie blue staining of isolated bacterial cellular samples, separated on SDS-PA gels, revealed only one difference, i.e., a band of ~23KDa seen in the plasmid-complemented strains (Figure 10A; Supplementary Figure 2). Coomassie blue visualising the secreted proteins confirmed that EPEC secreted high levels of each translocator (EspA, EspD and EspB) and the EspC autotransporter (Figure 10B). By contrast, one secreted protein (EspA) was not secreted by the *ΔespA* mutant, as reported (Kenny *et al.*, 1996; Kenny *et al.*, 1997a), with plasmid re-introducing EPEC *espA* only partially rescued the defect linked to reduced EspB/D secretion (Figure 10B). However, the *ΔespA* mutant complemented with the *E. tarda espA* gene did not restore EspA secretion but secreted another protein, like *E. tarda* EspA (Figure 10B).

Notably, the *ΔespAB* double mutant did not secrete any translocator protein or, surprisingly, EspC (Figure 10B). However, introducing the *E. tarda espADB* gene operon into the double mutant led to secretion of EspC and three novel bands: presumably *E. tarda* EspA, EspB and/or EspD proteins (Figure 10B). However, the apparent molecular weight does not always match predictions, especially for EspA *E.tarda*/EPEC (192/199residues); EspB (321/340 residues); EspD (380/385 residues).

Western blot probing the cellular samples for Tir revealed similar levels in all strains except the *ΔespAB* double mutant (Figure 10C). Interestingly, the double mutant did not express or secrete Tir or any translocator protein with this defect as seen for the complemented strains (Figure 10C). Probing for DnaK illustrated similar loading of the cellular extracts and absence of significant cellular lysis/cellular contamination of

supernatant samples (Figure 10C). Probing for the EspD translocator protein linked EspA loss with reduced cellular, but not secreted levels while plasmid re-introducing EPEC EspA had negatively impacted on EspD expression and secretion levels (Figure 10C; Supplementary Figure 2). Similar results were seen for the *ΔespA* mutant carrying the *E. tarda espA* gene, but the issues were not so prominent (Figure 10C; Supplementary Figure 2). By contrast, loss of EspA was linked to higher cellular, not secreted, levels of EspB with plasmid expressing EPEC or *E. tarda* EspA having little impact (Figure 10C). The anti-EspA western data signal was too weak to interpret (Figure 10C; Supplementary Figure 2). Notably, the antibodies generated against EPEC EspB detected the *E. tarda* variant in the cell and supernatant samples of the *espAB* complemented double mutant strain (Figure 10C).

Studies also examined the ability of the strains to deliver Tir into HeLa cells by western blot probing isolating Triton X-100 soluble and insoluble fractions. This work confirmed that EPEC, but not the *ΔespA* mutant, delivered Tir which interacted with Intimin. The mutant defect rescued by plasmid introducing EPEC *espA* (Figure 10D) (Lai *et al.*, 1997; Kresse *et al.*, 2000). However, the plasmid introducing *E. tarda espA* only weakly restored Tir delivery levels and thus Tir-Intimin interaction (Figure 10D). By contrast, the *ΔespAB* double mutant defect in expressing and delivering Tir was rescued by a plasmid introducing the *E. tarda espADB* gene operon (Figure 10D).

Similar studies were carried out with the EPEC *ΔespD* single and *ΔespDB* double mutants. The Coomassie stain visualising the cellular proteins again revealed the ~25KDa band difference linked to the introduced plasmid (Figure 11A). Examining the *ΔespD* secretion profiles revealed very little EspC or translocator proteins, as reported (Creasey *et al.*, 2003), with little impact of a plasmid introducing EPEC or *E. tarda espD* (Figure 11B). The *ΔespDB* mutant also failed to secrete proteins (Figure 11B). Western blot probing for DnaK confirmed similar gel loading of the cellular extract and absence of cellular proteins from the supernatant samples (Figure 11C). Interestingly, probing for Tir revealed similar levels

in all cellular extracts, including those from the *ΔespDB* double mutant, with EPEC secreting more Tir than the *ΔespD* single mutant while the *ΔespDB* double mutant did not secrete Tir (Figure 11C). Plasmid introducing EPEC, but not *E. tarda espD,* into the *ΔespD* single mutant restored Tir secretion levels as did plasmid introducing the *E. tarda espADB* genes into the *ΔespDB* double mutant (Figure 11C). Probing for the translocator proteins was not very information due to detection/sensitivity issues (Figure 11C). However, analysis of samples from the *ΔespBD* double mutant revealed that the antibodies against EPEC EspD and EspA detected the secreted *E. tarda* homologues (Figure 11C). It was surprising the anti-EPEC EspB antibodies did not detect *E. tarda* EspB (Figure 11C) as they detected an EspB-sized band in the *espAB* double mutant studies (Figure 10C).

The western blot analysis of the Triton X-100 soluble and insoluble HeLa fractions revealed Tir delivery by only EPEC, the *ΔespD* single mutant when carrying the EPEC *espD* or *E. tarda espADB* genes, and the *ΔespBD* double mutant when carrying the *E. tarda espADB* genes (Figure 11D). Tir delivery was linked to Tir-Intimin interaction, though the levels are very weak in this experiment, even for the positive controls (Figure 11D).

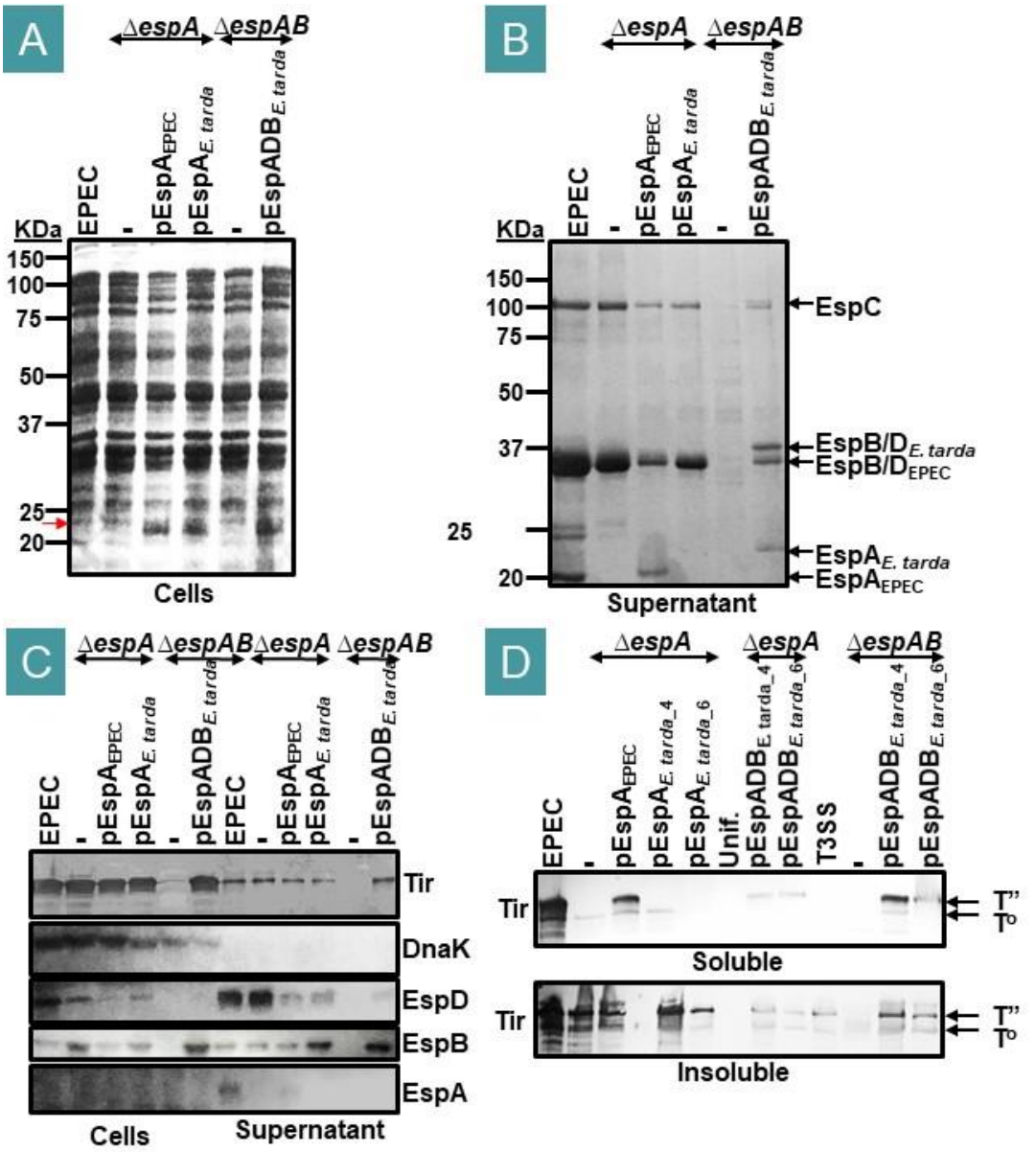

Figure 10: *E. tarda* EspA weakly substitutes EPEC EspA unless co-expressed with the other *E. tarda* translocators

Indicated strains were used to infect (A-C) DMEM and (D) HeLa cells. The DMEM was infected (1:100 dilution of bacteria grown overnight in LB) for 8-hours before isolating total bacterial cells and secreted (supernatant) proteins. HeLa cells were infected for 4, when indicated, 6-hours before isolating Triton X-100 soluble (contains host cytoplasm/membrane proteins and T3SS delivered EPEC effectors) and insoluble (contains host nuclei/cytoskeletal proteins and adherent bacterial proteins) fractions. Samples were resolved on 12% SDS-PA gels for (A-B) Coomassie blue visualisation and for (C-D) western blot analysis to probe for the translocators (EspA, EspB, EspD), Tir (an effector) and DnaK (bacterial cytoplasmic protein as a gel loading control). The positions of the unmodified (T^{o}) and host kinase-modified (T") Tir forms are shown. The position of the molecular weight standards (kDa) is shown (A). Strains used were EPEC, *ΔespA* single mutant and *ΔespAB* double mutant; the latter carrying no introduced plasmids (-) or a plasmid-encoding EPEC EspA ($pEspA_{EPEC}$), *E. tarda* EspA ($pEspA_{E.\ tarda}$) or *E. tarda* EspA/D/B ($pEspADB_{E.\ tarda}$) proteins.

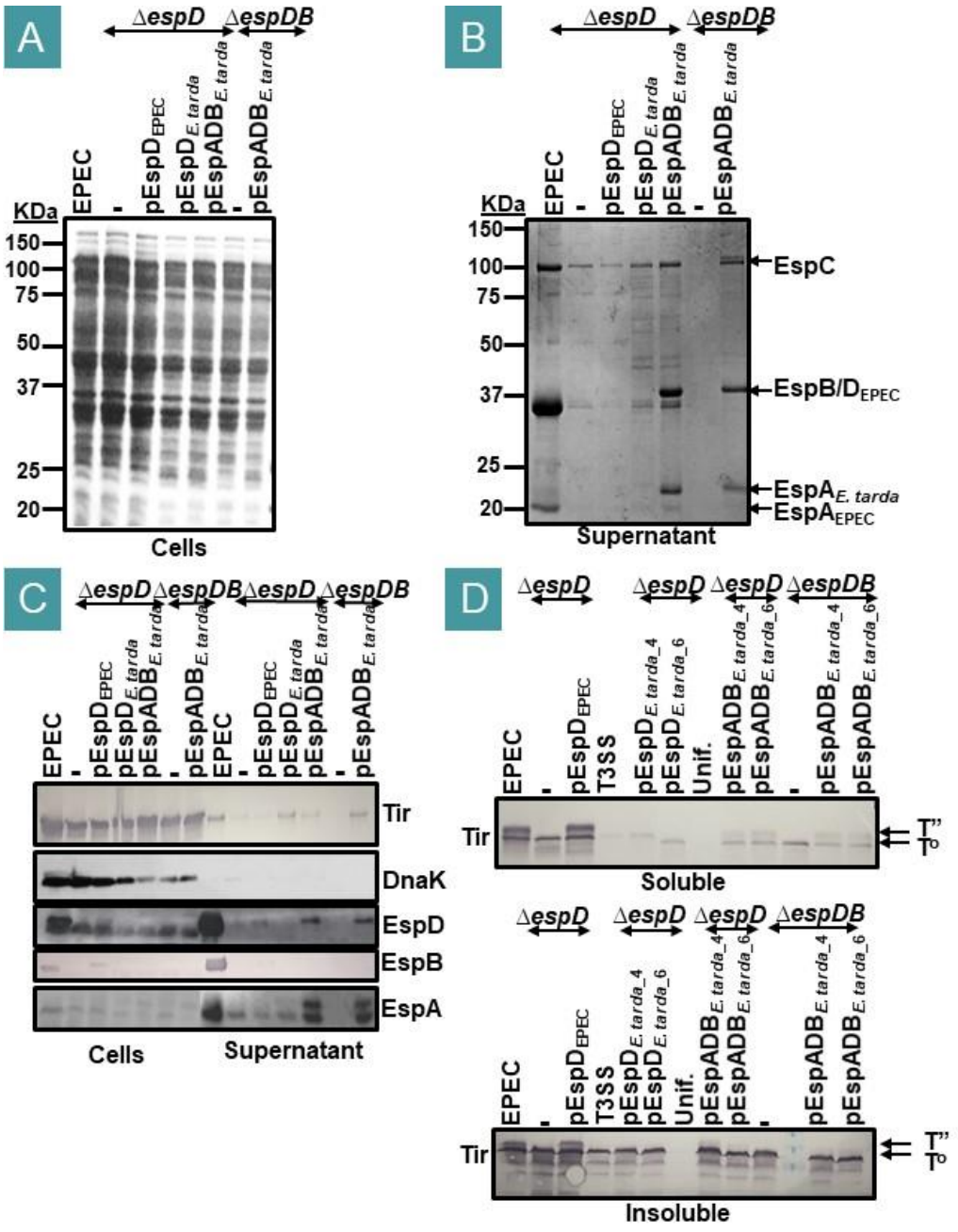

Figure 11: *E. tarda* EspD weakly substitutes EPEC EspD unless co-expressed with the other *E. tarda* translocators

Indicated strains were used to infect (A-C) DMEM and (D) HeLa cells. The DMEM was infected (1:100 dilution of bacteria grown overnight in LB) for 8-hours before isolating total bacterial cells and secreted (supernatant) proteins. HeLa cells were infected for 4, when indicated, 6-hours before isolating Triton X-100 soluble (contains host cytoplasm/membrane proteins and T3SS delivered EPEC effectors) and insoluble (contains host nuclei/cytoskeletal proteins and adherent bacterial proteins) fractions. Samples were resolved on 12% SDS-PA gels for (A-B) Coomassie blue visualisation and for (C-D) western blot analysis to probe for the translocators (EspA, EspB, EspD), Tir (an effector) and DnaK (bacterial cytoplasmic protein as a gel loading control). The positions of the unmodified ((T^{o}) and host kinase-modified (T") Tir forms are shown. The positions of the molecular weight standards (kDa) are shown (A). Strains used were EPEC, *ΔespD* single mutant and *ΔespDB* double mutants; the latter carrying no introduced plasmids (-) or a plasmid-encoding EPEC EspD (pEspD$_{EPEC}$), *E. tarda* EspD (pEspD$_{E. tarda}$) or *E. tarda* EspA, B, D (pEspADB$_{E. tarda}$) proteins.

3.2.3 *E. tarda escK* does not functionally substitute EPEC *escK*

Studies next examined the *ΔescK* mutant to assess, as above, the impact of carrying plasmids encoding EPEC or *E. tarda escK* genes on the translocator secretion and Tir-delivery processes. Coomassie staining of the total cellular proteins revealed similar profiles for all strains, i.e., EPEC, *ΔescK* mutant, and plasmid-complemented *ΔescK* mutant strains (Figure 11A).

Staining the secreted protein samples revealed the standard EPEC profile and confirmed that the *ΔescK* did not secrete translocator proteins with very reduced EspC levels (Figure 12B) (Soto *et al.*, 2017). While plasmid re-introducing EPEC *escK* restored low levels of translocator secretion, plasmid introducing *E. tarda escK* was linked to numerous bands but no obvious EspB/D or EspA secretion (Figure 12B). Western blot probing for DnaK illustrated similar cellular extract loading and the absence of cellular proteins from the supernatant samples (Figure 12C). The latter findings suggest that the secreted bands by the *E. tarda* escK-complemented strains may relate to effector proteins and/or EspC breakdown products. Probing for Tir revealed similar signals in each bacterial extract with EPEC release of some Tir in an EscK-dependent manner (Figure 12C). The Tir secretion defect of the *ΔescK* mutant was rescued by a plasmid expressing EPEC, and to a lesser extent, *E. tarda* escK (Figure 12C). Probing for the translocator proteins revealed EscK dependent secretion with the defect rescued by plasmid re-introducing EPEC but not *E. tarda escK* (Figure 12C). These findings are supported by data from an additional experiment (Supplementary Figure 3). The Western blot probing of fractions isolated from HeLa-infected cells revealed Tir was delivered by 2 strains, EPEC and the *ΔescK* mutant complemented with the EPEC EscK-encoding plasmid (Figure 12D). The Tir delivered by these strains interacted with Intimin (Figure 12D).

Collectively, the work revealed that EscK is required for translocator protein expression/stability and to promote Tir secretion with all these functions, except perhaps the last, rescued by a plasmid introducing the EPEC, but not the *E. tarda escK* gene.

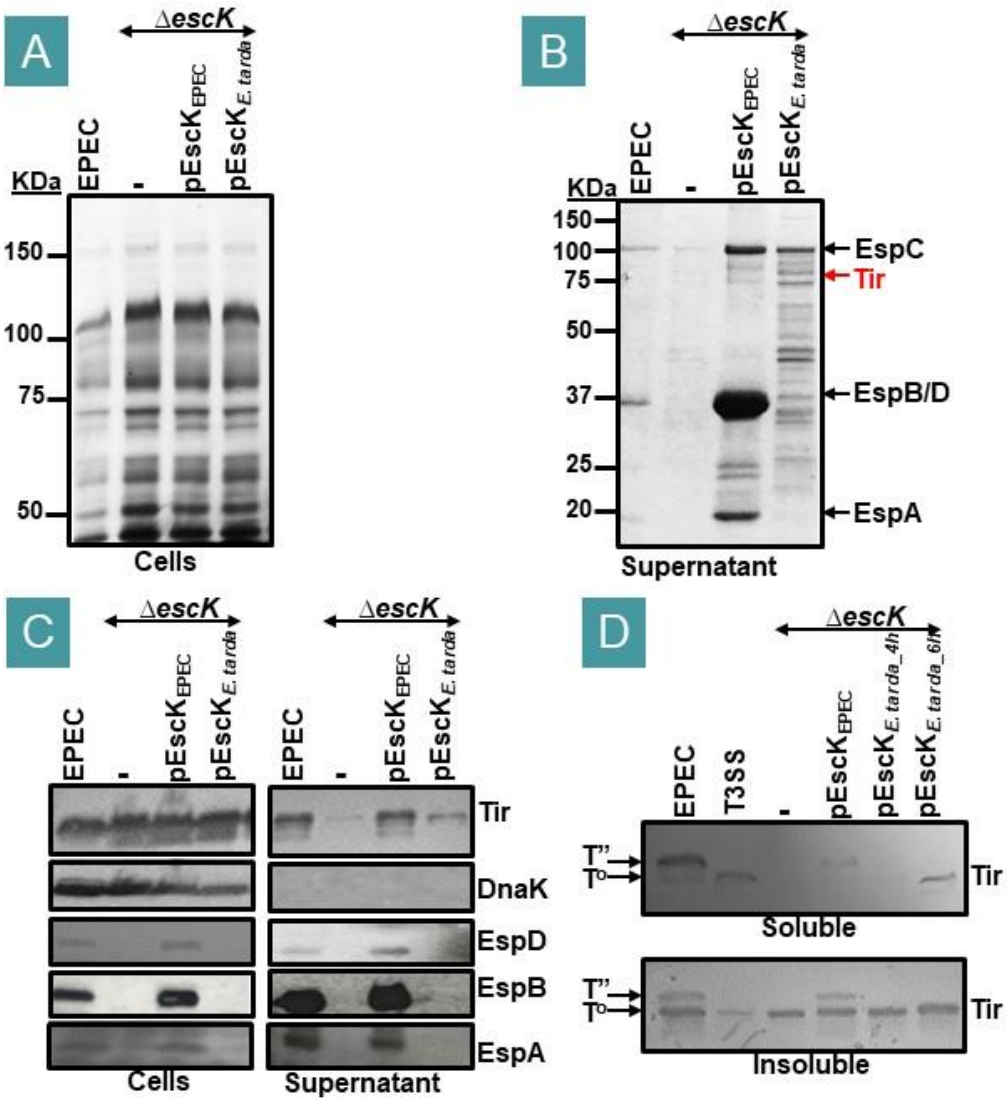

Figure 12: *E. tarda escK* does not functionally substitute EPEC *escK*

Indicated strains were used to infect (A-C) DMEM and (D) HeLa cells. The DMEM was infected (1:100 dilution of bacteria grown overnight in LB) for 8-hours before isolating total bacterial cell and secreted (supernatant) proteins. HeLa cells were infected for 4 and, when indicated, 6-hours before isolating Triton X-100 soluble (contains host cytoplasm/membrane proteins and T3SS-delivered EPEC effectors) and insoluble (contains host nuclei/cytoskeletal proteins and adherent bacterial proteins) fractions. Samples were resolved on 12% SDS-PA gels for (A-B) Coomassie blue visualisation and for (C-D) western blot analysis to probe for the translocators (EspA, EspB, EspD), Tir (an effector) and DnaK (bacterial cytoplasmic protein as a gel loading control). The positions of the unmodified (T^{o}) and host kinase-modified (T") Tir forms are shown. The position of the molecular weight standards (kDa) is shown (A). Strains used were EPEC and the Δ*escK* mutant; the latter carrying no introduced plasmids (-) or a plasmid carrying the EPEC (pEscK $_{EPEC}$) or *E. tarda* (pEscK $_{E.\ tarda}$) genes.

3.2.4 *E. tarda sepL* weakly substitutes EPEC *sepL* to promote secretion of the translocator proteins and Tir delivery into HeLa cells

The final *E. tarda* gene to be assessed in the complementation assays was *sepL*. The Coomassie staining of bacterial cell samples unexpectedly revealed a new phenotype for the *ΔsepL* mutant, i.e., faster migration of proteins >50KDa on SDS-PA gels, most evident for the prominent ~100KDa band (Figure 13A). Importantly, this phenotype was rescued by a plasmid introducing EPEC, but not *E. tarda sepL* (Figure 13A). Staining for secreted proteins confirmed the *ΔsepL* mutant defect, i.e., secreting effectors, most prominently Tir and NleA, but not translocator proteins (O'Connell *et al.*, 2004) (Figure 13B). As expected (Gaytan *et al.*, 2018), plasmid re-introducing the EPEC *sepL* gene into the *ΔsepL* mutant restored translocator secretion and prevented effector secretion (Figure 13B). Plasmid introducing the *E. tarda sepL* gene into the *ΔsepL* mutant was linked to a minor increase in the secretion of the translocator proteins but did not prevent effector secretion (Figure 13B).

Western blot probing for DnaK unexpectedly revealed it to provide an alternative marker for the apparent protein migration phenotype (Figure 13C). In addition, the DnaK supported equal cellular extract loadings and that the supernatant samples were not contaminated with cellular proteins (Figure 13C). Probing for Tir linked loss of SepL activity with reduced levels of this effector but additional bands suggestive of Tir cleavage (Figure 13C). SepL absence was also linked to loss of cellular EspB and EspD signals (no interpretable data for EspA) rescued by introducing the plasmid carrying EPEC, but not *E. tarda sepL* (Figure 13C). Analysis of the supernatant samples revealed SepL-dependent secretion of each translocator protein with plasmid expressing EPEC SepL restored some secretion of each translocator (~5x less than by EPEC). Plasmid expressing *E. tarda* SepL was linked to secretion of just one translocator, EspD, and at very low levels, with no obvious impact on Tir secretion levels or the Tir cleavage phenotype (Figure 13C).

HeLa cell infections were also carried out to examine the impact of deleting *sepL* on the Tir delivery process and the ability to rescue defects by plasmid expressing EPEC or *E. tarda* SepL. As expected, EPEC delivered Tir with the kinase-modified (T'') form evident in the soluble and insoluble fractions (Figure 13D). By contrast, only the unmodified Tir form and, assumed, cleavage product was detected in the *ΔsepL* mutant-infected cells (Figure 13D). As predicted, plasmid re-introducing EPEC *sepL* rescued the Tir delivery defect, i.e., detect T'' form in soluble and insoluble fractions at levels similar to EPEC-infected cells (Figure 13D). However, plasmid introducing *E. tarda sepL* led to minor amounts of the T'' modified Tir form, but increasing infections to 6 hours increased the T'' level in the soluble and insoluble fractions (Figure 13D) consistent with earlier studies (Madkour *et al.*, 2021).

The above findings are supported by data from an additional experiment (Supplementary Figure 4). Collectively, this work supports the suggestion that *E. tarda* SepL, despite being encoded over two adjacent open reading frames, is expressed and can weakly substitute for EPEC SepL. Moreover, the study revealed two new phenotypes (apparent protein migration and Tir cleavage) that are rescued by a plasmid introducing EPEC but not *E. tarda sepL*.

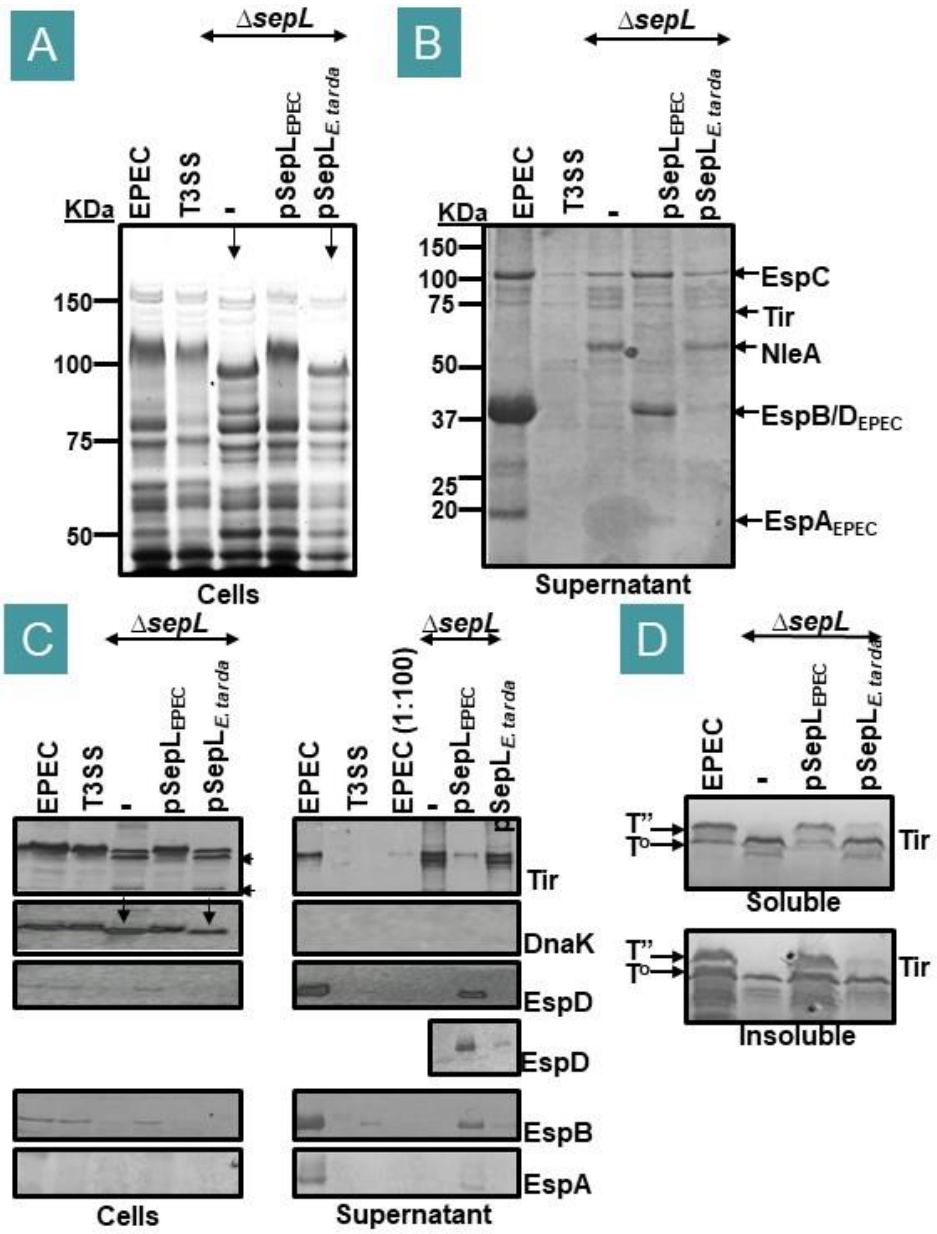

Figure 13: *E. tarda sepL* weakly substitutes EPEC *sepL* to promote translocator secretion and deliver Tir into HeLa cells

Indicated strains were used to infect (A-C) DMEM and (D) HeLa cells. The DMEM was infected (1:100 dilution of bacteria grown overnight in LB) for 8-hours before isolating total bacterial cell and secreted (supernatant) proteins. HeLa cells were infected for 4 and, when indicated, 6-hours before isolating Triton X-100 soluble (contains host cytoplasm/membrane proteins and T3SS-delivered EPEC effectors) and insoluble (contains host nuclei/cytoskeletal proteins and adherent bacterial proteins) fractions. Samples were resolved on 12% SDS-PA gels for (A-B) Coomassie blue visualisation and for (C-D) western blot analysis to probe for the translocators (EspA, EspB, EspD), Tir (an effector) and DnaK (bacterial cytoplasmic protein as a gel loading control). The positions of the unmodified (T^{o}) and host kinase-modified (T") Tir forms are shown. The position of the molecular weight standards (kDa) is shown (A). Strains used were EPEC and the Δ*sepL* mutant; the latter carrying no introduced plasmids (-) or a plasmid carrying the EPEC (pSepL EPEC) or *E. tarda* (pSepL*E. tarda)* genes.

3.2.5 The *ΔsepL* mutant aberrant protein migration phenotype is shared by other T3SS mutants

Identifying this novel *sepL*-specific phenotype led to a screen to determine whether it was shared by other LEE-gene deficient strains. Thirty mutants were available which mostly lacked an individual LEE gene, but one lacked 2 (*espG*/*espG2*; latter a non-LEE homologue) or four (*escR*/*S*/*T*/*U*) genes. Following an 8-h infection, total cellular extracts were isolated and resolved on SDS-PA gels for Coomassie blue staining and Western blot to probe for DnaK. This work confirmed the *ΔsepL* mutant aberrant protein migration profile and revealed a similar phenotype for 6 other mutants: *ΔescC* (lacks the secretin; Figure 14A), *ΔescD* (lacks an inner membrane ring structure protein; Figure 14A), *ΔcesT* (lacks CesT chaperone; Figure 14C), *ΔcesAB* (lacks CesAB chaperone; Figure 14C), *ΔcesD2* (lacks CesD2 chaperone; Figure 14C) and *ΔespF* (lacks EspF effector; Figure 14D). These findings are supported by data from additional experiments (Supplementary Figure 5).

To support these findings, studies examined whether the defects could be rescued by plasmid re-introducing the missing gene, both in the EPEC and the *E. tarda* variant. Initial studies examined the *ΔescC* and *ΔescD* mutants by plasmid-complementing the strains for growth in DMEM (8 hours) to isolate total cell extracts for separation on SDS-PA gels. The resulting Coomassie blue staining and anti-DNA western blot analysis data verified that both single mutants had *ΔsepL* mutant-like phenotypes that were rescued by plasmid re-introducing the EPEC, but not the *E. tarda* variant of the missing gene (Figure 15). Similar studies with the chaperone-deficient mutant strains confirmed *ΔsepL* mutant-like phenotypes that were again rescued by plasmid re-introducing the EPEC, but not the *E. tarda* variant of the missing gene (Figure 16). Finally, complementation studies were done with the *espF* mutant but only the EPEC variant, as *E. tarda* does not have an LEE *espF* gene. These studies included plasmids encoding EspF and variants carrying epitope tags (T7 and/or His) at the N-terminal end. Again, the work verified the phenotype and revealed that it was rescued by all 3-plasmid encoded EspF variants (Figure 17; Supplementary Figure 6). The results (summarised in Table 8) collectively confirm the *ΔsepL* mutant phenotype (aberrant protein migration) and reveal it to be shared by strains

lacking a subset of T3SS chaperones (CesT, CesAB or CesD2), an inner membrane ring protein (EscD), the secretin (EscC) or EspF effector.

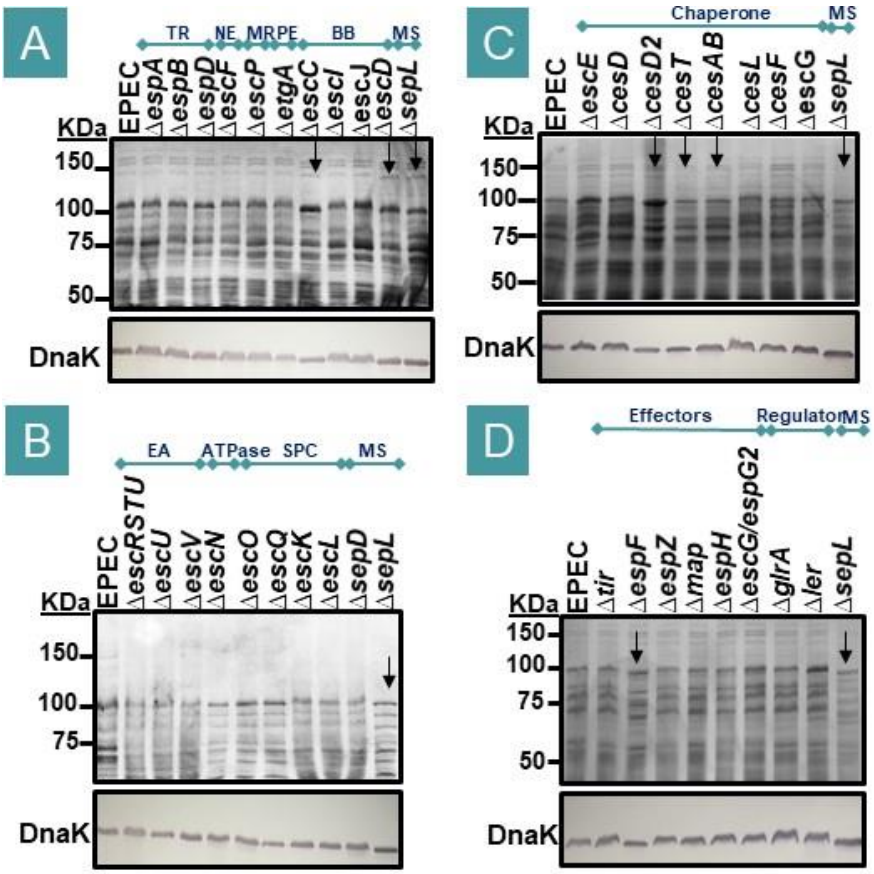

Figure 14: The *ΔsepL* mutant aberrant protein migration phenotype is shared by other T3SS mutants

Indicated strains were used to infect DMEM (1:100 dilution of LB overnight bacteria) for 8-hours before isolating total bacterial cell samples for separation on SDS-PA gels - 6 % for Coomassie blue visualisation and 12% for western blot analysis to probe for DnaK. Molecular standards are shown (KDa) for Coomassie blue stained gels. The strains were analysed in clusters relating to the role of the missing gene in T3SS functionality using the following abbreviations: TR (Translocators), NE (Needle proteins), MR (Molecular Ruler), PE (Peptidoglycan enzyme), BB (Basal body components), MR (Molecular switches), EA (Export Apparatus components), ATPase (ATPase complex components), SPC (Sorting Platform Complex proteins). Other examined genes encoded effectors, transcriptional regulators, and Intimin (surface protein). Downward facing arrows indicate strains with the *ΔsepL* mutant-like phenotype.

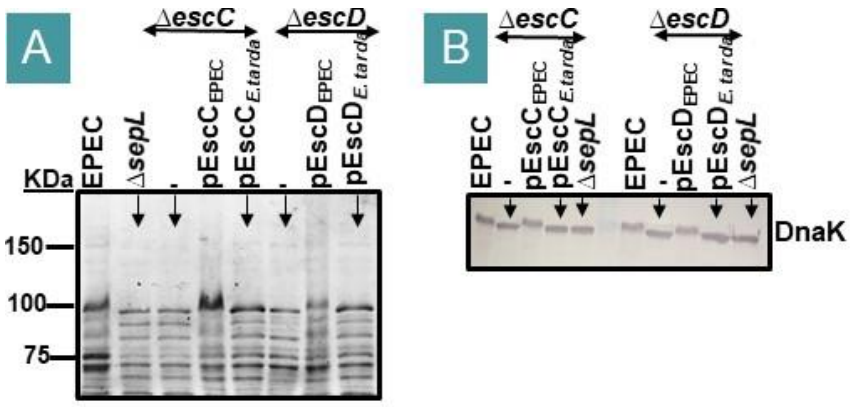

Figure 15: The aberrant protein migration phenotype of the *ΔescD* and *ΔescC* single mutants is rescued by plasmid complementing with the appropriated EPEC, but not the *E. tarda* gene

Indicated strains were used to infect DMEM (1:100 dilution of LB overnight bacteria) for 8-hours before isolating total bacterial cell samples to resolve on 6% SDS-PA gels for Coomassie blue visualisation and 12% SDS-PA gels for western blot analysis to probe for DnaK. Molecular standards are shown (KDa) for Coomassie blue stained gels. Strains used were EPEC, *ΔescD* and *ΔescC* mutants; the latter with no introduced plasmids (-) or a plasmid carrying the EPEC ($pEscD_{EPEC}$ or $pEscC_{EPEC}$) or *E. tarda* ($pEscD_{E\ tarda}$ or $pEscC_{E\ tarda}$) genes. Downward facing arrows indicate a *sepL* mutant-like phenotype.

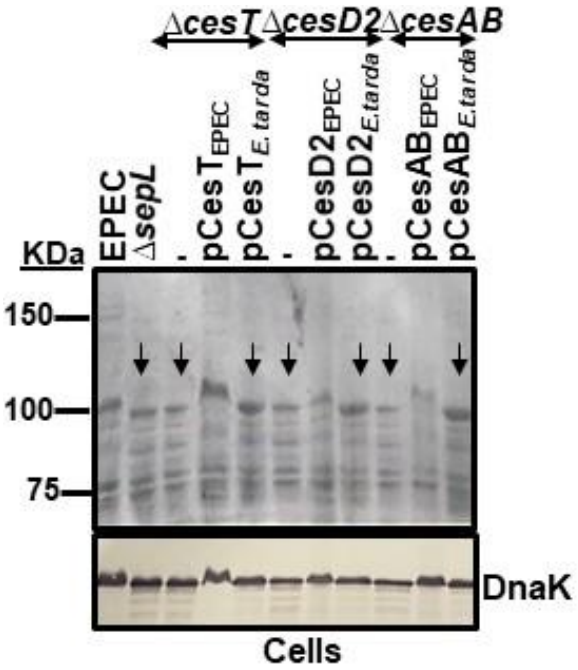

Figure 16: The aberrant protein migration phenotype of *ΔcesT, ΔcesD2* and *ΔcesAB* single mutants is rescued by plasmid complementing with the appropriated EPEC, but not the *E. tarda* gene

Indicated strains were used to infect DMEM (1:100 dilution of LB overnight bacteria) for 8-hours before isolating total bacterial cell samples to resolve on 6% SDS-PA gels for Coomassie blue visualisation and 12% SDS-PA gels for western blot analysis to probe for DnaK. Molecular standards are shown (KDa) for Coomassie blue stained gels. Strains used were EPEC, *ΔcesT, ΔcesD2* and *ΔcesAB* mutants; the latter with no introduced plasmids (-) or a plasmid carrying the EPEC (pCesT$_{EPEC}$ or pCesD2$_{EPEC}$ or pCesAB$_{EPEC}$) or *E. tarda* (pCesT$_{E\ tarda}$ or *p*CesD2$_{E\ tarda}$ or pCesAB$_{E\ tarda}$) genes. Down-ward facing arrows indicate a *sepL* mutant-like phenotype.

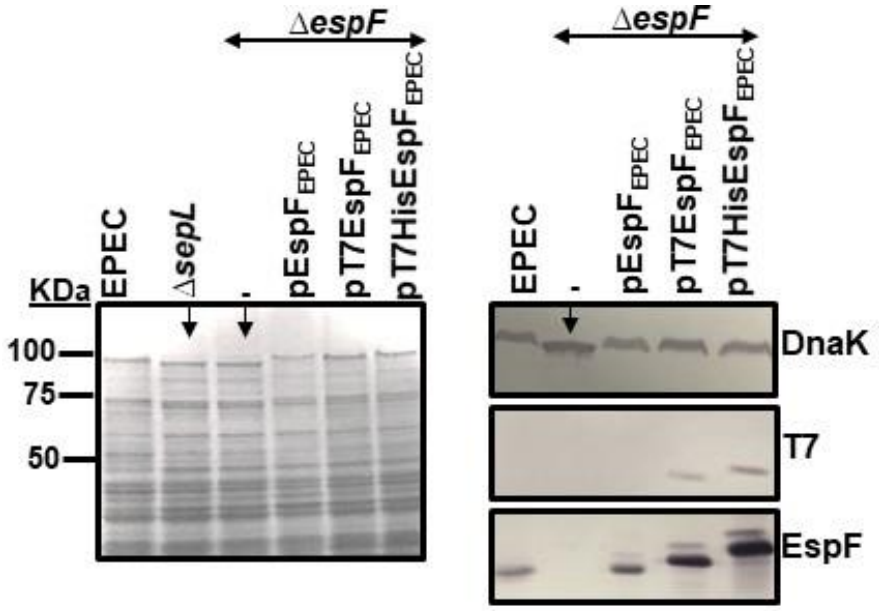

Figure 17: The aberrant protein migration phenotype of *ΔespF* mutant is rescued by plasmid introducing EPEC EspF native and epitope-tagged variants

Indicated strains were used to infect DMEM (1:100 dilution of LB overnight bacteria) for 8-hours before isolating total bacterial cell samples to resolve on 6% SDS-PA gels for Coomassie blue visualisation and 12% SDS-PA gels for western blot analysis to probe for DnaK. Molecular standards are shown (KDa) for Coomassie blue stained gels. Strains used were EPEC and Δ*espF* mutant; the latter with no introduced plasmids (-) or a plasmid encoding EPEC EspF (pEspF$_{EPEC}$) or variants carrying N-terminally-located T7 (pT7EspF$_{EPEC}$) or T7/His (pT7HisEspF$_{EPEC}$) epitope tags. Down-ward facing arrows indicate a *ΔsepL* mutant-like phenotype.

3.2.6 The *ΔsepL* mutant 'Tir cleavage' phenotype is not shared by other T3SS-defective mutants

The cellular extracts were also probed for Tir to determine if the *ΔsepL* mutant-associated 'Tir cleavage' phenotype (see Section 3.2.4) was shared by any of the other 30 LEE gene-deficient mutant strains. This work confirmed the Δ*sepL* phenotype and indicated that it was not shared by any of the other examined mutants (Figure 18A-D). As expected, (Abe *et al.*, 1999; Thomas *et al.*, 2005; Yerushalmi *et al.*, 2008), little or no Tir was evident in the cellular extracts obtained from the *ΔcesT* (Figure 18C), *Δtir* or *Δler* (Figure 18D);- CesT is required for Tir stability while Ler is needed for LEE gene expression. Surprisingly, Tir levels were reduced in the Δ*espG/espG2* and, more dramatically, *ΔespH* mutant strains (Figure 18D). These results are supported by findings from additional experiments (Supplementary Figure 7). This work suggests that SepL, but not other LEE proteins, has a function that protects Tir from being modified or cleaved within EPEC.

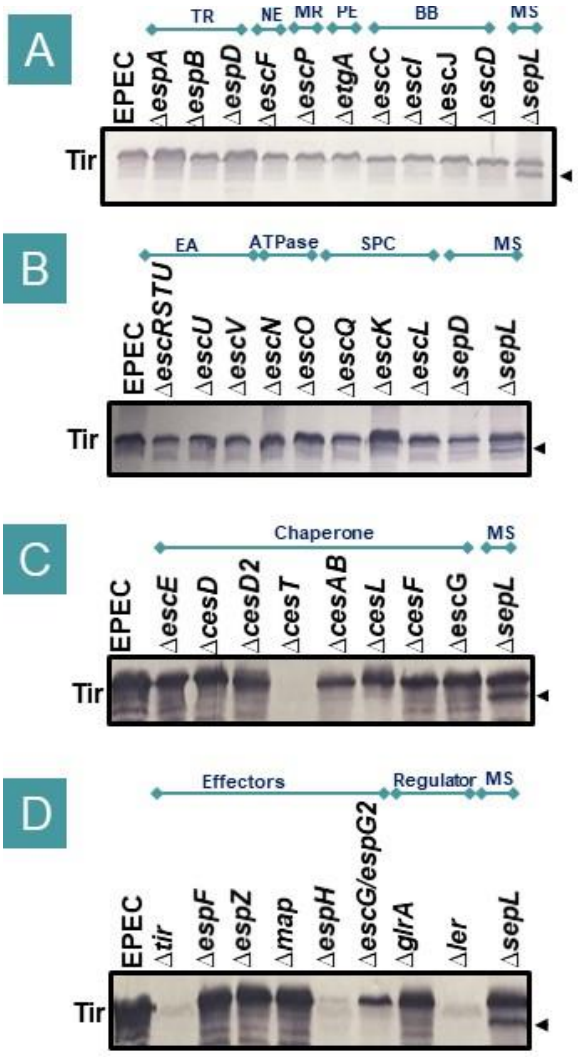

Figure 18: The *ΔsepL* mutant 'Tir cleavage' phenotype is not shared by other T3SS-defective mutants

Previously isolated bacterial cell samples, from 30 LEE-gene deficient strains, were resolved on 12% SDS PA gels for western blot analyses and probed for the Tir effector. The strains were analysed in clusters relating to the role of the missing gene in T3SS functionality using the following abbreviations: TR (Translocators), NE (Needle proteins), MR (Molecular Ruler), PE (Peptidoglycan enzyme), BB (Basal body components), MR (Molecular switches), EA (Export Apparatus components), ATPase (ATPase complex components), SPC (Sorting Platform Complex proteins). Other examined genes encoded effectors, transcriptional regulators, and Intimin (surface protein). Arrowheads indicate the position of the Tir cleavage product only seen in extracts from the *ΔsepL* mutant.

3.2.7 C-terminal cleavage of Tir when SepL is absent

The second Tir form, seen in extracts from SepL-deficient EPEC mutants, was thought to be the result of a C-terminal cleavage event, because the faster migrating (cleaved) form is detected in the supernatant, indicating it has an intact N-terminal secretion signal (Creasey *et al.*, 2003). To determine if Tir was C-terminally cleaved when SepL is absent, a plasmid was generated to express a C-terminally HA-tagged variant (Tir:HA) for studies with a *ΔsepLΔtir* double mutant.

A *tir*:HA gene fusion was available on plasmids adjacent to the LEE gene for the Tir chaperone, CesT (Kenny *et al.*, 1997b). It was decided to subclone the *tir*:HA gene away from the *cesT* gene. Thus, a *tir*:HA *cesT* carrying plasmid (pSK-3'gtHAo), was digested with XbaI (in multiple cloning sites [upstream of *tir* gene]) and BglII (within 5' end of *cesT* gene) restriction enzymes to release the *tirHA* gene (Figure 19A). The isolated *tirHA* gene fragment and vector (pACYC184 pre-digested with XbaI and BamHI restriction enzymes) fragments (Figure 19B) for T4 DNA-mediated, ligation (see Materials and Methods), noting BamHA and BglII have compatible ends for ligation reactions. Agarose gel analysis of some of the ligation products supported success (Figure 19B), leading to some of the ligation mix being transformed (see Materials and Methods) into chemically competent K12 (NEB) *E. coli*. PCR screening of plasmid-carrying clones for *tir* and *cesT* genes supported all five having the *tir*:HA but not the *cesT* genes (Figure 19C), providing pACYC-*tir*:HA.

Next, a *ΔsepLΔtir* double mutant was generated using the Δ*sepL* mutant and an available suicide vector for inactivating the *tir* gene (Kenny *et al.*, 1997b) following the well-established gene knockout (allelic exchange) protocol (see Materials and Methods). PCR screening for disruption of the *tir* gene - large internal fragment exchange for a stop (TAA) codons (Kenny *et al.*, 1997b) - revealed that 1 strain lacked an intact *tir* gene (Figure 19D) to provide an EPEC *ΔsepLΔtir* double mutant.

The pACYC-*tir*:HA plasmid was electroporated (see Materials and Methods) into the Δ*sepL* and Δ*sepL*Δ*tir* mutants and used for an 8-h infection in DMEM before isolating total bacterial cell samples for western blot analysis to probe for Tir and HA-tagged proteins. As expected, no Tir was seen in extracts from the Δ*sepL*Δ*tir* double mutant with two Tir-

related in EPEC (Figure 20A). These bands were also detected in the Δ*sepL* mutant extract along with additional, presumably cleavage-related, bands (Figure 20A). However, the plasmid complemented Δ*sepL* single and Δ*sepL*Δ*tir* double mutant strains had little, if any, of the additional, putative cleavage-related, bands (Figure 20A). These findings imply that deleting the *tir* gene, plasmid over-expression of *tir*, or, more likely, adding the HA tag to the C-terminus compromise the putative Tir cleavage events that occur in the SepL-deficient mutant. Nevertheless, HA-detecting only one Tir band suggests that the faster migrating band lacks the HA-tag (Figure 20B versus 20A) due to cleavage events in the C-terminal domain.

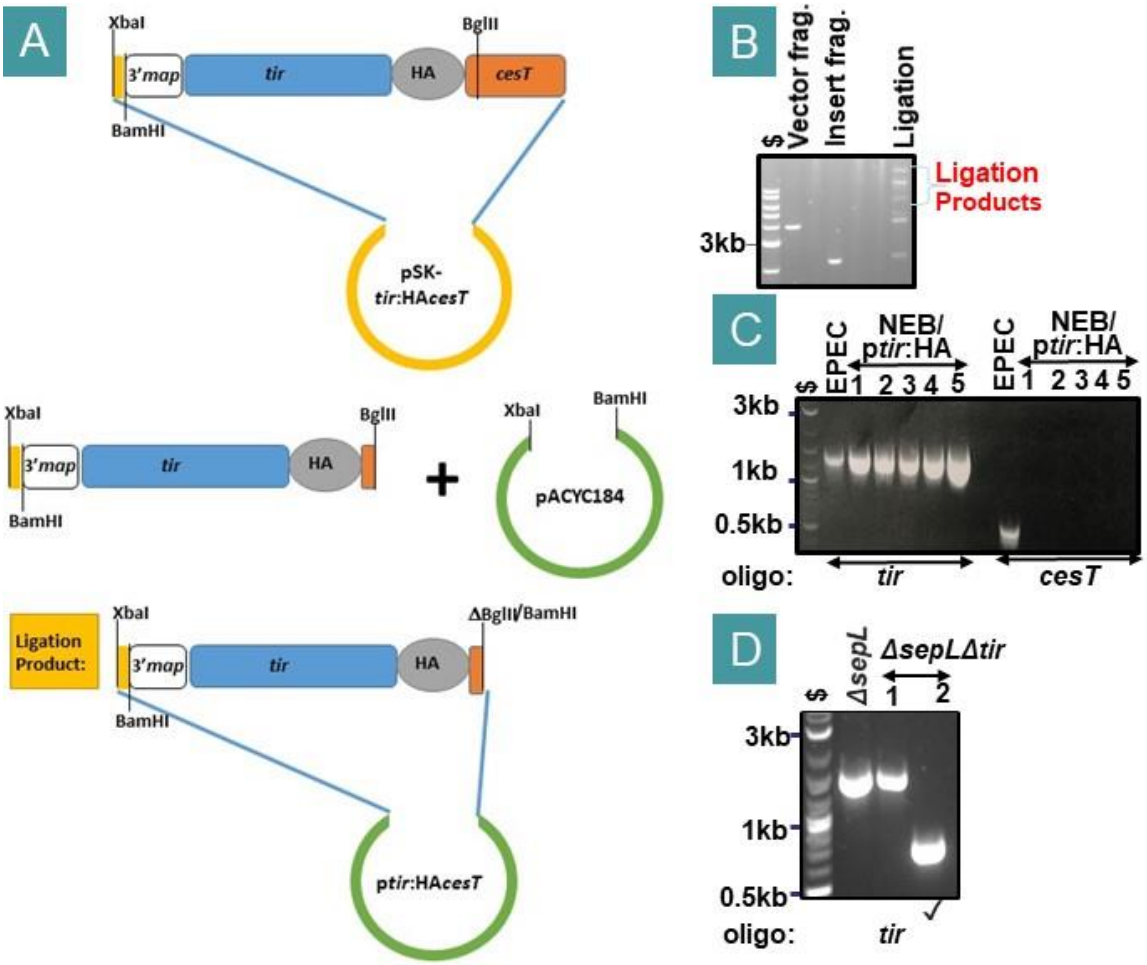

Figure 19: Construction of pACYC-tir: HA and *ΔsepLtir* double mutant strain

Schematic (A) of strategy to generate pACYC-*tir*:HA with agarose gel data (B-D) showing fragments used in T4 DNA-mediated ligation with success indicated by additional, ligation-associated, bands (B), PCR screening of plasmid-carrying K12 (NEB) *E. coli* strain for the presence of *tir* or *cesT* genes (C) and PCD screening for a *ΔsepLΔtir* double mutant (D). The DNA samples were separated on a 1% agarose gel data, alongside 2 log molecular mass markers, with DNA visualized with gel red stain.

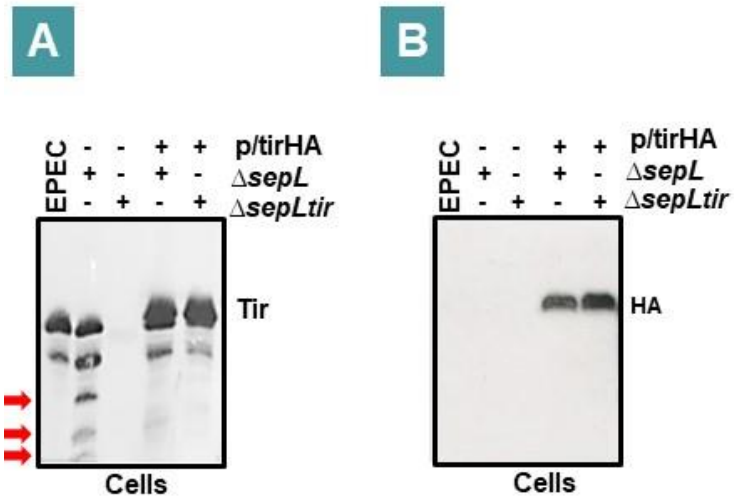

Figure 20: C-terminal cleavage of Tir when SepL is absent

Indicated strains were used to infect DMEM (1:100 dilution of LB overnight bacteria) for 8-hours before isolating total bacterial cell samples to resolve on 6% SDS-PA gels for western blot analysis to probe for Tir (A) or HA-tagged (B) proteins. The red arrows indicate putative Tir cleavage products in the *ΔsepL* mutant. Strains used were EPEC, the *ΔsepL* single and *ΔsepLΔtir* double mutant; the latter strains had either no introduced plasmids (-) or a plasmid carrying the EPEC *tir*:HA gene (p*tir*HA) encoding Tir with a C-terminally-located HA epitope tag. Arrowheads indicate the position of the Tir cleavage product.

3.2.8 EspF cleavage in strains lacking a functional SepL, CesT, CesD2 or CesAB protein

The C-terminus of Tir plays an important role in targeting it to the T3SS and, thus, cleavage in the absence of SepL would provide a mechanism to prevent Tir delivery if the T3SS is not fully functional. Thus, studies investigated whether cleavage in the *ΔsepL* mutant was specific to Tir or was also relevant to other effectors. This work focused, as antibodies were available, on EspF which has its own dedicated chaperone, CesF (Elliott *et al.*, 2002). Thus, the isolated cellular extracts from the *ΔsepL* and bank of other LEE gene-deficient mutants were resolved on 15% SDS-PA gels for western blot analysis to probe for the ~25KDa EspF protein. This analysis revealed a single ~25KDa band in EPEC with a second, presumed, cleavage product in strains lacking SepL (*ΔsepL*; Figure 21C), CesD2 (*ΔcesD2*; Figure 21C), CesT (*ΔcesT*; Figure 21B) or CesAB (*ΔcesAB*; Figure 21C). EspF was missing in the EspF-(Figure 21D), CesF-(Figure 21C), Ler (needed for LEE gene expression; Figure 21D), also in the EspH-(Figure 21D) and EspG/EspG2 (Figure 21D)-deficient strains. In addition, reduced EspF levels were noted for the Δ*escN* and *ΔescU* mutants (Figure 21B). Importantly, plasmids introducing the EPEC, but not *E. tarda,* version of the missing gene led to EPEC-like EspF profiles (Figure 22). The latter findings show that EPEC SepL, CesD2, CesT and CesAB proteins all have functions - not present in their *E. tarda* counterparts - that prevent EspF from being, presumably like Tir, cleaved.

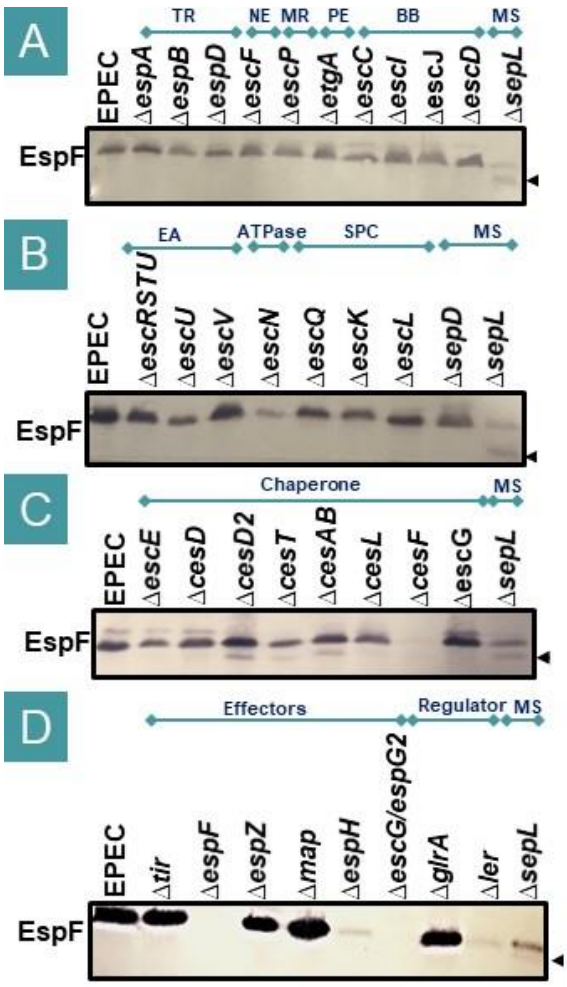

Figure 21: EspF cleavage in strains lacking a functional SepL, CesT, CesD2 or CesAB protein

Previously isolated bacterial cell samples, from 30 LEE-gene deficient strains, were resolved on 12% SDS PA gels for western blot analyses and probed for the EspF effector. The strains were analysed in clusters relating to the role of the missing gene in T3SS functionality using the following abbreviations: TR (Translocators), NE (Needle proteins), MR (Molecular Ruler), PE (Peptidoglycan enzyme), BB (Basal body components), MR (Molecular switches), EA (Export Apparatus components), ATPase (ATPase complex components), SPC (Sorting Platform Complex proteins). Other examined genes encoded effectors, transcriptional regulators, and Intimin (surface protein). Arrowheads indicate the position of the EspF cleavage product seen in extracts from the *ΔsepL, ΔcesD2, ΔcesT* and *ΔcesAB* mutants.

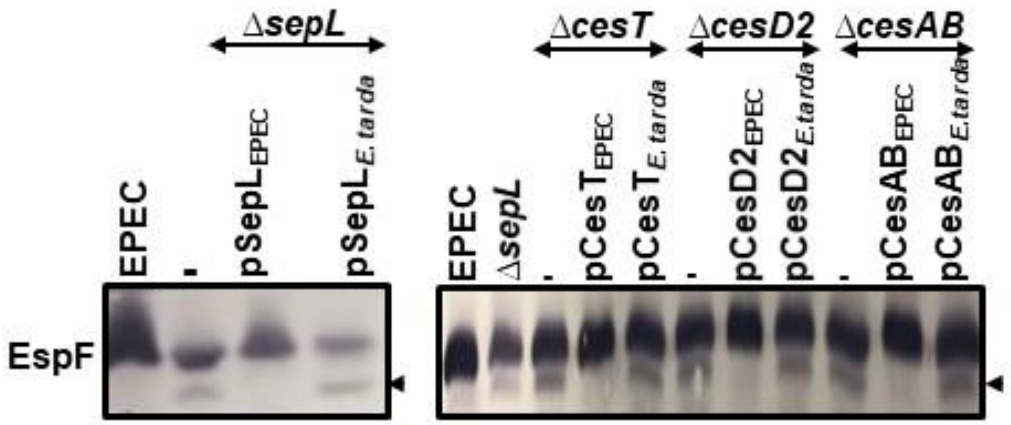

Figure 22: Rescuing the EspF cleavage defect of EPEC *ΔcesT, ΔcesD2* and *ΔcesAB* mutants by plasmid introducing the EPEC but not the *E.tarda* version of the missing gene

Indicated strains were used to infect DMEM (1:100 dilution of LB overnight bacteria) for 8-hours before isolating total bacterial cell samples to resolve on 6% SDS-PA gels for western blot analysis to probe for EspF. Strains used were EPEC, *ΔcesT*, *ΔcesD2* and *ΔcesAB* mutants; the latter mutant strains had either no introduced plasmids (-) or a plasmid carrying the EPEC or *E. tarda version* of the missing gene. Arrowheads indicate the position of the EspF cleavage product.

P	strain	Defect:: Lacks	Commassie detected shift	DnaK detected shift	Tir Predected cleavage	EspF Predected cleavage
1	EPEC E2348/69	Nothing	NO	NO	NO	NO
2	*ΔsepL*	Molecular Switch (gatekeeper).	↓	↓	✔	✔
3	*ΔescC*	T3SS Outer membrane ring (OM).	↓	↓	EPEC	EPEC
4	*ΔescD*	T3SS inner membrane ring (IM).	↓	↓	EPEC	EPEC
5	*ΔcesD2*	EspD's chaperone.	↓	↓	EPEC	✔
6	*ΔcesT*	Many LEE and non-LEE effector's chaperone.	↓	↓	-	✔
7	*ΔcesAB*	EspA's and EspB's chaperone.	↓	↓	EPEC	✔
8	*ΔespF*	EspF effector.	↓	↓	EPEC	-

Table 8: Summary of screening data for LEE gene-deficient mutant that have *ΔsepL* mutant-like phenotypes

The western blot and Coomassie results for eight T3SS-related mutants are shown in the table. Down-ward facing arrows indicate strains with the *sepL* mutant-like phenotype (aberrant protein migration phenotype). A tick symbol revealed the presence of an effector cleavage product in the mutant.

3.3 Discussion

The data presented in this chapter not only supports the previous preliminary studies suggesting that the *E. tarda* EscP, EspA, EspD, EscK and SepL proteins do not substitute their EPEC homologues in one or more of the T3SS functionality assays but, most interestingly, reveals novel phenotypes for SepL, making it the focus of further thesis-related studies.

The EscP has multiple functions – a ruler that controls the length of the EspA needle filament with a role in switching T3SS substrates from translocators to effectors (Monjaras Feria *et al.*, 2012). Remarkably, studying the *E. tarda* LEE sequence identified an *escP* gene that encoded a smaller variant (103 versus 138 residues) (Madkour *et al.*, 2021). Therefore, the needle length in *E. tarda* may be shorter to suit interactions of the bacteria with its fish host cell. However, the T3SS functionality assays used in the described studies do not assess ruler function but do report switching defects. The Δ*espP* mutant is known to secrete reduced amounts of translocator (EspA/B/D) proteins and, unlike EPEC, secretes high levels of effectors, most prominently Tir and NleA (Monjaras Feria *et al.*, 2012). Interestingly, plasmids introducing the EPEC or *E. tarda escP* gene rescued the translocator protein secretion defect, but only the EPEC variant prevented Tir secretion. This failure to prevent Tir secretion was linked to reduced amounts of Tir being delivered into host cells. Before making definitive conclusions, more repeat experiments are needed. Moreover, further research should be undertaken to quantify the protein signal relative to protein loading controls (such as DnaK, for EPEC, and actin, for host cells). Nevertheless, the findings suggest that studies with the EPEC and *E. tarda* EscP homologues could be useful to reveal domains, regions, or residues key to the substrate switch process and also control of needle length.

The complementation studies with *E. tarda* EspA and EspD also supported previous findings, i.e., each had defects in delivering Tir (and, subsequent, Tir-Intimin interaction) that were rescued by a plasmid expressing all 3 *E. tarda* translocator proteins. However, the previous work did not examine the intracellular or secreted levels of the translocator

proteins or Tir effector, unlike the here-in described studies, and all included Δ*espAB* and Δ*espBD* (Δ*espAD* and Δ*espABD* were not available) mutants. This work revealed some differences when the strains were plasmid-complemented with the missing EPEC or *E. tarda* genes, but the most surprising finding related to an unexpected secretion defect by the double mutants. Thus, neither double mutant secreted significant (Coomassie stain detectable) levels of the translocator or EspC (autotransporter) proteins, with this defect rescued by introducing a plasmid encoding all three *E. tarda* translocator proteins. Western blot probing revealed Tir in the cells of the Δ*espAB* but not Δ*espBD* double mutant, suggesting that EspB and EspD have an unknown, cooperative function that controls the expression or intracellular stability of Tir. Future studies could investigate this possibility to perhaps reveal hidden regulatory mechanisms. Similar findings were observed for translocator proteins; that is, plasmid complementation was linked to the secretion of EspC and other, presumably, translocator proteins because their apparent molecular masses were mostly similar to that expected for *E. tarda* variants. the predicted *E. tarda* EspA protein (secreted form recognised by anti-EPEC EspA antibodies) migrated significantly slower than EPEC EspA despite having fewer amino acids (192 versus 199). Unusual molecular mass is a feature of some proteins, including EPEC Tir, that presumably reflects usual amino acid composition or structural features that impact on SDS-binding during PAGE. Further studies (Madkour *et al.*, 2021) using the domain swap approach linked the *E. tarda* EspA and EspD complementation defects to sequence differences in a specific region within the C-terminal domains of each protein. It is proposed that these regions/residues are important for EspA and EspD to function together to enable efficient Tir delivery and subsequent Tir-Intimin interaction and may provide targets for the development of anti-virulence therapies (Madkour *et al.*, 2021). Studies with the EPEC and *E. tarda* EscK-encoding genes confirmed that the *E. tarda* variant had no ability to functionally replace its EPEC counterpart. More recent studies with an HA-epitope tagged variant supported expression of *E. tarda escK* in EPEC where it produces a full length (~12KDa) protein (Madkour *et al.*, 2021). Therefore, future domain swap experiments between the EPEC and *E. tarda* EscK variants could reveal domain/s, region/s or specific residue/s key to its role as a sorting platform protein to provide mechanistic insights on how the platform influences the timing and order of substrate export.

The most unexpected findings came from the *ΔsepL* mutant complementation studies. Thus, while the work confirmed previous preliminary findings that *E. tarda* SepL restores some T3SS functionality - i.e., low levels of Tir delivery and translocator secretion but did not prevent Tir hyper secretion- it revealed novel phenotypes. It should be noted that previous studies (Madkour *et al.*, 2021) with epitope-tagged variants supported expression of the *2-orf E. tarda sepL* gene in EPEC to produce a full-length protein. The *ΔsepL* mutant phenotypes were i) faster migration of proteins (>50KDa) through SDS-PA gels and ii) apparent cleavage of EspF and Tir; the latter in the C-terminal domain. Usefully, the aberrant migration phenotype could also be monitored by western blot probing for bacterial proteins including DnaK (~70KDa cytoplasm protein) and Intimin (~100KDa surface protein). Importantly, the phenotypes were rescued by plasmid introducing the EPEC but not the *E. tarda sepL* gene. The screening of 30 LEE gene-deficient strains revealed that the i) 'aberrant protein migration' phenotype was shared by 6 mutant strains, ii) the 'Tir cleavage' phenotype by none, and iii) the 'EspF cleavage' phenotype by 3 mutant strains. Crucially, these defects were rescued by plasmid re-introducing the EPEC, but not *E. tarda* version of the missing gene, which clearly illustrated a key role for EPEC SepL in each phenotype, with additional important (cooperative) roles for 3-6 EPEC T3SS proteins in 2 phenotypes. These unexpected findings led the thesis studies to focus on these aspects. It should be noted that some of these findings have been included in a currently, available on-line manuscript (Madkour *et al.*, 2021).

A final point worth mentioning is that the screening for mutant strains for Tir and/or EspF cleavage events revealed that the Δ*espH* single and Δ*espG/espG2* double mutants (lack 1 and 2 effectors, respectively) had reduced or no detectable Tir and/or EspF proteins. Future studies should confirm the genotype of these mutants and, if appropriate, examine if the defect relates.

Chapter 4: Studies on novel *ΔsepL* mutant phenotypes

4.1 Introduction

4.1.1 Aberrant protein migration on SDS-PA gels

In biomedical studies, SDS-PAGE is widely used to determine the apparent molecular weight (MW) of proteins (Rath *et al.*, 2009). SDS is a detergent with a powerful protein denaturing effect as it accumulates at hydrophobic sites and initiates "reconstructive denaturation", which involves proteins adopting a conformational mixture of α-helix and random coil (Shirahama;Tsujii and Takagi, 1974). This results in the formation of protein-detergent complexes containing helical SDS-coated polypeptide regions spatially separated by flexible and uncoated linkers called "necklace and bead" structures (Shirahama;Tsujii and Takagi, 1974). The sizes of these micellar "beads" differ based on amino acid sequence (Ibel *et al.*, 1990). Determining protein MW through SDS-PAGE also provides an estimate of the amount of detergent binding among proteins (Reynolds and Tanford, 1970). Typically, maximum SDS-binding levels are 1.4 g SDS/g of protein, with many factors affecting protein mobility in SDS-PAGE. For instance, phosphorylation of proteins can reduce or increase the apparent molecular mass of proteins by a few KDa's, as can substitution of specific residues (Wegener and Jones, 1984). In the case of mammalian -crystallin, a change in hydrophobicity (replacing hydrophobic with hydrophilic residues) affects SDS binding, resulting in increased mobility (de Jong;Zweers and Cohen, 1978). Additionally, increased electrophoretic mobility can also be attributed to increasing negative charge due to more SDS binding (Rath *et al.*, 2009), which is a common feature for membrane proteins. Protein tertiary structures can also influence SDS binding levels and thus gel migration rates. For example, disulfide bonds have been observed to decrease SDS binding to globular proteins by up to 2-fold (Pitt-Rivers and Impiombato, 1968). These bonds have been associated with increased migration of unreduced versus reduced lysozyme, probably due to the intact disulfide bonds imposing a more compact shape on the enzyme (Dunker and Kenyon, 1976). The folded form of the E. coli β-barrel membrane protein OmpA is thought to bind less SDS than the fully denatured protein (Dornmair;Kiefer and Jähnig, 1990; Ohnishi;Kameyama and Takagi, 1998), with migration through SDS-PA gels reflecting structural compactness, with the

folded form having faster migration rates than the fully denatured protein (Kleinschmidt;Wiener and Tamm, 1999).

4.1.2 Proteolysis

Proteolysis, or proteolytic cleavage, is an irregular post-translation modification. This process is initiated by the enzyme which brokes a peptide bond in a protein substrate (Nyathi;Wilkinson and Pool, 2013). *E. coli* has large numbers of proteases distributed in the cytoplasm, inner membrane, and periplasm. However, most of the proteolysis happens in the cytoplasm and is ATP - dependant (Maurizi, 1992). This event is important for regulating protein translocation through the most common secretion mechanism (the sec pathway). In this pathway, a protein called SecB captures the pre-secretion protein and holds it in an unfolded condition to assist secretion through the membrane. The SecB delivers protein to SecA is a structure associated with the SecYEG translocase. The pore in the membrane allows protein translocation. SecA is defined by Randall and Hardy (2002) as an ATPase that is responsible for supplying energy to the conducting channel (Randall and Hardy, 2002). This translocation depends on 20 amino acids in the N- terminus of secreted proteins (Natale;Brüser and Driessen, 2008). The specific protease Lep cleaves off the SecB secretion signal from the exported protein, leading to its release into the periplasm (Mogensen and Otzen, 2005).

Numerous proteins are subjected to rapid proteolysis, including truncated proteins, proteins with abnormal amino acids, or misfolded and mutant proteins (Goldberg and Dice, 1974; Gottesman, 1989). Stress emanating from extreme temperatures or overproduction of specific proteins can result in the aggregation of abnormal or non-functional proteins that are subjected to rapid proteolysis. Also, “proteins without partners” are targets for proteolysis, where they are considered to fall between abnormal proteins and naturally unstable proteins (Gottesman and Maurizi, 1992).

Interestingly, there are several cleavage events linked to EPEC T3SS biology. Some of these events help to regulate the substrate secretion and translocation processes. The T3SS protein, EscN, is an ATPase and potential source of energy that localizes to the inner leaflet of the bacterial cytoplasmic membrane where it is thought to accelerate the dissociation of the secretory protein-chaperone complexes (Biemans-Oldehinkel *et al.*, 2011; Romo-Castillo *et al.*, 2014a). The unfolding of the secretory proteins is essential for transport through the T3SS export apparatus (Biemans-Oldehinkel *et al.*, 2011; Romo-Castillo *et al.*, 2014a). Another example is the auto cleavage protein, EscU, which has two main domains; the N- domain has four putative transmembrane regions while the C-terminal domain undergoes auto-cleavage at a conserved amino acid sequence (NPTH). This self-cleavage event takes part in the switching from early (T3SS components) to intermediate (translocator) substrates (Thomassin;He and Thomas, 2011).

Some T3SS-related cleavage events are linked to bacterial pathogenicity. For example, EspC has protease activity linked to cleaving human haemoglobin, human coagulation factor V, spectrin, and pepsin proteins (Dutta *et al.*, 2002; Drago-Serrano;Parra and Manjarrez-Hernández, 2006). Moreover, EPEC EspC can also cleave fodrin, paxillin, and focal adhesion kinase (FAK) linked to cell rounding and detachment processes (Navarro-Garcia *et al.*, 2014). EspC is a non-LEE-encoded protein (Sanchez-Villamil *et al.*, 2019) that is a type V secretion system (T5SS or autotransporter) protein but also a T3SS substrate (Stein *et al.*, 1996; Mellies *et al.*, 2001).

The goal of the studies described in this section was to provide molecular insights into why the absence of specific EPEC LEE genes results in phenotypes such as 'abnormal protein migration,' 'TIr cleavage,' and/or 'EspF cleavage'.

4.2 Results

4.2.1 Linking the aberrant protein migration phenotype to reduced levels of O-antigen or/and colanic acid

Earlier work (Chapter 3, section 3.2.5) revealed novel *ΔsepL* mutant phenotypes which included aberrant migration of cellular proteins during SDS-PA electrophoresis. Studies were carried out to examine if strains lacking specific EPEC virulence-associated factors shared this phenotype. The initial screen included control strains (EPEC and *ΔsepL* mutant) and strains lacking i) the EspC autotransporter (*ΔespC*), ii) the pMar plasmid, which encodes the Bundle Forming Pilus (BFP) and Plasmid-encoded regulator (Per) systems (JPN15), iii), the Intimin surface protein, encoded by the LEE *eae* gene, iv) all but 4 of the known repertoire of non-LEE-encoded (Nle) effectors (EPEC TOEA7), v) and TOEA7 engineered to lack the LEE genes encoding CesT, CesF, Intimin, Map, EspH and Tir (EPEC TOEA7C). The experiment also included additional controls; non-pathogenic (K12) *E. coli*, the *Δtir* mutant and parental EPEC strain (J. EPEC as from a Japan research group), used to generate TOEA7 (Yen *et al.*, 2010).

These strains were grown, as before, in DMEM for 8 hours before isolating total bacterial cell samples to resolve on 6% SDS-PA gels with aberrant band migration phenotype examined by Coomassie blue staining. As expected, the *ΔsepL* mutant displayed the phenotype, which was shared by K12 and, surprisingly, all three J. EPEC-related strains (Figure 23). This band migration difference was supported by Western blot data using antibodies to detect DnaK (Figure 23) or Intimin (Supplementary Figure 9; noting K12 and J. TOEA7C are Intimin-deficient strains). Previous studies with J. EPEC revealed an unexpected defect in binding enterocyte cells (Kenny lab. unpublished), leading to genome sequencing revealing an undocumented 50Kb deletion that removed many genes from adjacent operons needed for EPEC to produce two polysaccharides: O127 antigen and colanic acid (Figure 24).

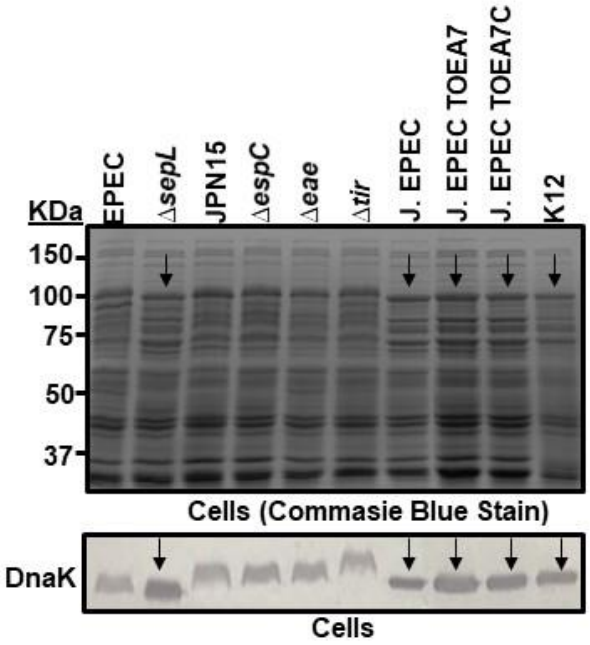

Figure 23: Linking aberrant protein migration phenotype to reduced O-antigen or/and colanic acid levels

Indicated strains were used to infect DMEM (1:100 dilution of bacteria grown in LB overnight without shaking) for 8 hours before isolating total bacterial cell extracts. Samples were resolved on 12% SDS-PA gels for (A) Coomassie blue visualization or (B) western blot analysis probing for DnaK (bacterial cytoplasmic protein). Molecular weight standards are given (A). Strains used were EPEC E2348/69 (EPEC), EPEC E2348/69 from Japan lab. (J. EPEC), *ΔespC* (lacks EspC autotransporter), JPN15 (lacks pMar plasmid encoding Bundle Forming Pilus and Plasmid-encoded regulator; latter promotes LEE gene expression), *Δtir* (lacks Tir effector), *Δeae* (lacks Intimin surface protein), J. EPEC TOEA7 (lacks all but four known non-LEE-encoded T3SS substrates), J. EPEC TOEA7C (TOEA7 also lacking LEE Intimin, CesT, CesF, Tir, Map and EspH proteins) and K12 (non-pathogenic) *E. coli*. Downward facing arrows indicate samples showing aberrant protein migration profile.

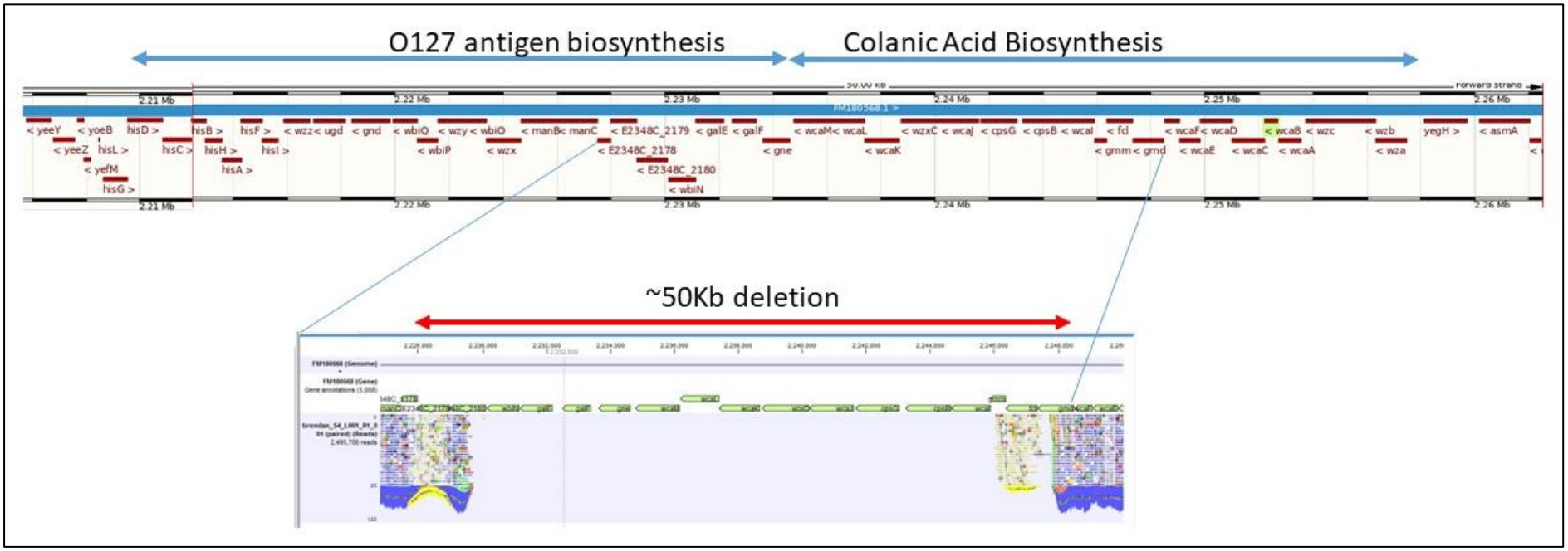

Figure 24: Region absent in J. EPEC strain

EPEC E2348/69 O127 and colanic gene operons – from KEGG genome sequence data (https://bacteria.ensembl.org/Escherichia_coli_o127_h6_str_e2348_69_gca_000026545/Location/View?g=E2348C_2200;r=Chromosome:2172874-2222873;t=CAS09748;db=core) – with position of undocumented deletion in the EPEC E2348/69 strain obtained from research group in Japan (J. EPEC). Note E2348C_2179, E2348C_2178 and E2348C_2180 are synonyms for *fcl, gmm* and *gmd* genes respectively

4.2.2 The aberrant protein migration phenotype is rescued by adding O-antigen

To probe the possibility that the aberrant protein migration phenotype reflects the absence of EPEC specific factors, such as O127 and/or colanic acid, studies examined the ability to rescue the phenotype by mixing cell extracts, prior to SDS-PA analysis, with those from EPEC (1:1 ratio) or commercially purified O127:B8 antigen (L3129; Sigma-Aldrich). Coomassie blue staining of the SDS-PAGE resolved samples revealed that both strategies rescued the phenotype for the K12 (Figure 25A), *ΔsepL* mutant (Figure 25B) and J. EPEC (Figure 25C) strains. Similar findings were obtained in an independent analysis (Supplementary Figure 10). Western blot probing of duplicate samples for O127 antigen revealed a 'background' signal in K12 extracts, in contrast to a strong dark'smeary' signal (from 50KDa to 100KDa) in the EPEC sample with a reduced signal in the sepL mutant extract (Figure 25D). This western blot difference was supported by another analysis, which also included J. EPEC samples, where a K12-like profile was detected (Supplementary Figure 10). Collectively, the work suggests that the aberrant protein migration phenotype reflects reduced levels of O127 antigen and, in K12 and J. EPEC, other factor/s (possibly colanic acid).

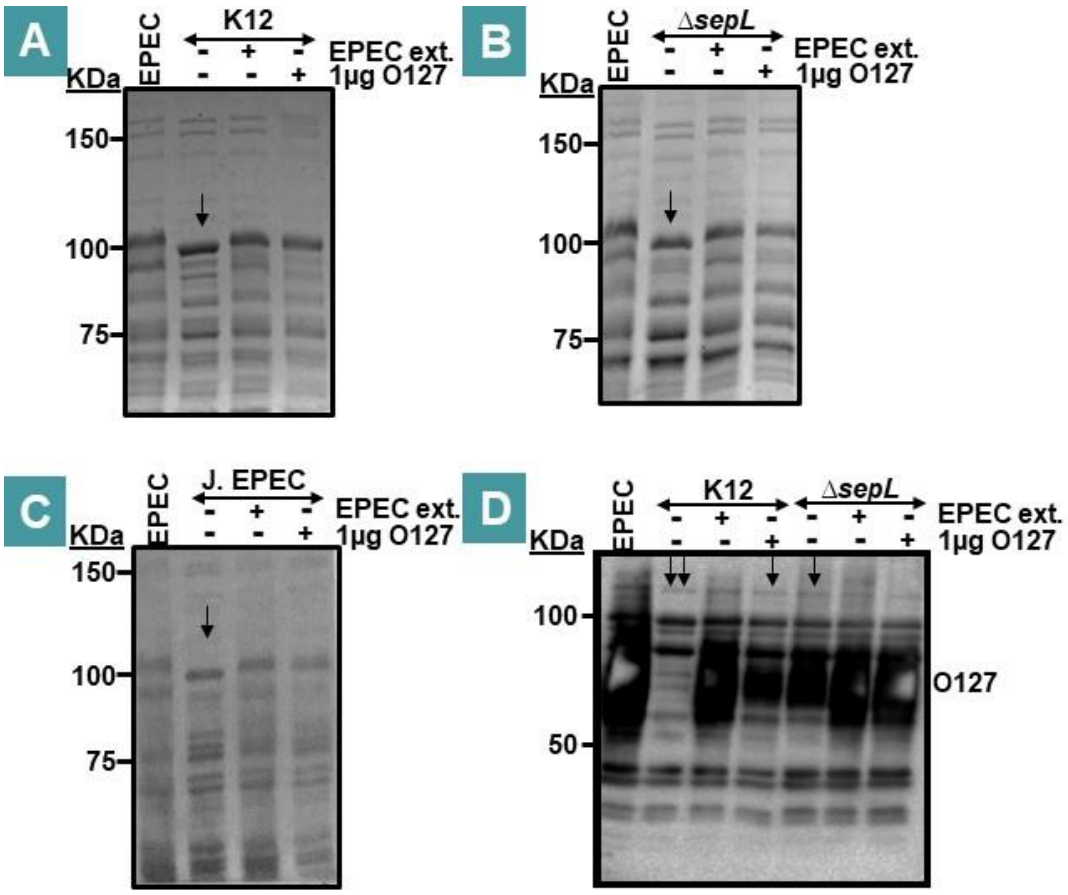

Figure 25: The aberrant protein migration phenotype is rescued be adding O-antigen

Indicated strains were used to infect DMEM (1:100 dilution of bacteria grown in LB overnight without shaking) for 8 hours before isolating total bacterial cell extracts. Samples were mixed (+) or not (-) with EPEC cellular extract (1:1 ratio) or 1µg of O127:B7 antigen (O127) prior to running samples on (A-C) 6% SDS-PA gels for Coomassie blue visualization and (D) a 12% SDS-PA gel for western blot detection of O127 antigen. Strains used were EPEC E2348/69 (EPEC), EPEC E2348/69 from Japan lab. (J. EPEC), *ΔsepL* (lacks SepL gatekeeper) and K12 (non-pathogenic *E. coli*). Downward facing, green arrows indicate samples showing an aberrant protein migration profile.

4.2.3 Linking aberrant protein migration phenotype to reduced O127 antigen levels

Next, it was decided to screen the cellular extracts of the 30 LEE-gene deficient strains to determine if any shared the aberrant protein migration phenotype. Hence, the samples were re-run on 10% SDS-PA gels for western blot analysis. Probing for O127 antigen revealed that, as before, the cell extract from the *ΔsepL* mutant had a relatively weak 'smear' (in ~50 -100 KDa range) compared to EPEC (Figure 26A). A similar relatively weak O-antigen 'smear' was detected in the extracts from mutants previously shown to share the aberrant protein migration phenotype, i.e., *Δ*escC (encode secretin protein)*, ΔescD* (encode basal body protein), *ΔcesT, ΔcesD2, ΔcesAB* (encode chaperones) and *ΔespF* (encodes an effector) mutants (Figure 26A-D).

Studies also assessed the effect of plasmid re-introducing the missing gene (EPEC or *E. tarda* variant) on the O127 antigen profile. Initial studies with the *ΔsepL* revealed the phenotype could be rescued by a plasmid introducing the EPEC but not the *E. tarda sepL* gene (Figure 27). Similar studies were carried out with the other mutant strains, but the *ΔespF* mutant complementation studies only involved the EPEC *espF* variant as *E. tarda* does not have a LEE *espF* gene. Importantly, these complementation studies revealed that the EPEC but not the *E. tarda* variant rescued the O127 antigen defect for the i) *ΔescD* and *ΔescC* (Figure 27A) and ii) *ΔcesT*, *ΔcesD2* and *ΔcesAB* (Figure 27B) mutants. The *ΔespF* mutant phenotype was rescued by a plasmid expressing EPEC EspF or an N-terminally, T7-epitope, tagged variant (Figure 27C).

Collectively, these findings link the aberrant protein migration phenotype to reduced O127 antigen levels due to the absence, individually, of SepL, CesT, CesAB, CesD, EscD, EscC, or EspF and this phenotype can be rescued by plasmid reintroducing the EPEC, but not the *E. tarda* variant.

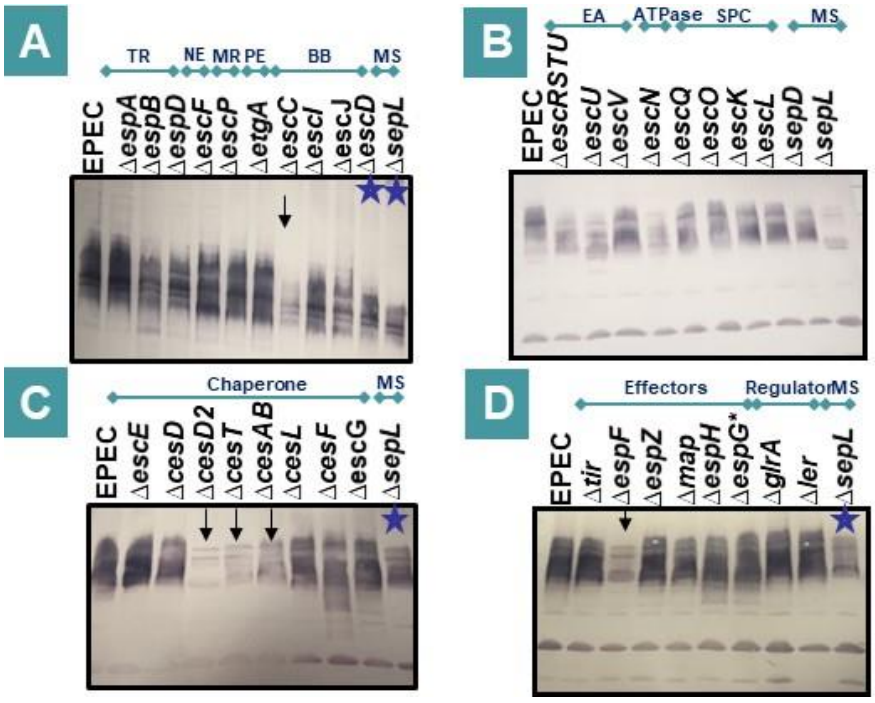

Figure 26: Linking aberrant protein migration phenotype to reduced O127 antigen levels

Available bacterial extracts (see Chapter 3; Figure 14) from indicated T3SS mutant strains were resolved on 10% SDS PA gels for western blot analyses to probe for O127 antigen. The samples were loaded into groups relating to the role of the missing gene in T3SS functionality using the following abbreviations: TR (Translocator), NE (Needle protein), MR (Molecular Ruler), PE (Peptidoglycan enzyme), BB (Basal body component), MR (Molecular switch), EA (Export Apparatus component), ATPase (ATPase complex component) and SPC (Sorting Platform Complex protein) plus effectors, transcriptional regulators, and Intimin (surface protein). Downward facing arrows indicate strains with reduced O127 antigen levels. Stars symbols indicate strains with partially reduced O127 antigen levels.

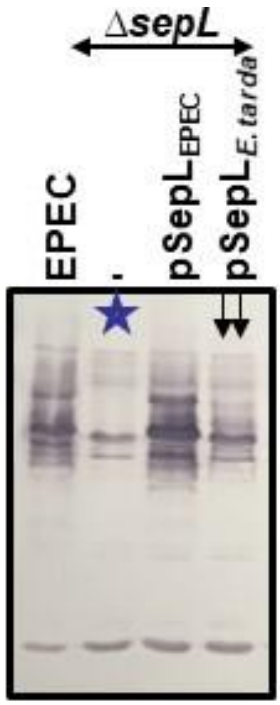

Figure 27: Rescuing *sepL* O-antigen defect by plasmid introducing EPEC, but not *E. tarda sepL*

Available bacterial extracts from indicated strains were resolved on 10% SDS PA gels for western blot analyses to probe for O127 antigen. Samples were from EPEC and the *ΔsepL* mutant with no introduced plasmids (-) or a plasmid carrying the EPEC (pSepL$_{EPEC}$) or *E. tarda* (pSepL$_{E. tarda}$) gene. Downward facing arrows indicate a plasmid-complemented strain with reduced O127 antigen levels. Stars symbols indicate strains with partially reduced O127 antigen levels.

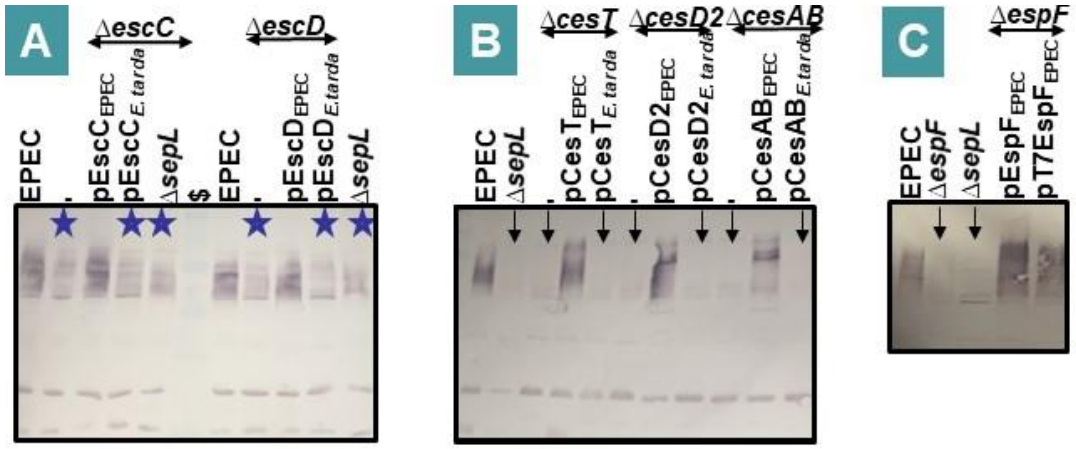

Figure 28: Plasmid complementing the *ΔescD, ΔescC, ΔcesT, ΔcesD2, and ΔcesAB* and *ΔespF* mutant restores O127 antigen defect

Available bacterial extracts (see Chapter 3; Figure 15, 16, 17) from indicated strains were resolved on 10% SDS PA gels for western blot analyses to probe for O127 antigen. Samples were from EPEC, *ΔescD*, ΔescC, *ΔcesT, ΔcesD2, ΔcesAB,* and *ΔespF* mutant strains. The mutant strains carried either no introduced plasmids (-) or a plasmid carrying the indicated EPEC or *E. tarda* genes. *E. tarda* LEE lacks an *espF* gene with complementation studies using plasmids encoding EspF ($pEspF_{EPEC}$) or variants carrying an N-terminally-located T7 epitope tag ($pT7EspF_{EPEC}$). Downward facing arrows indicate a plasmid-complemented strain with reduced O127 antigen levels. Stars symbols indicate strains with partially reduced O127 antigen levels.

4.2.4 Generating EPEC strains lacking O127 antigen and/or colanic acid genes

To examine whether the aberrant protein migration phenotype was due to issues in expressing O127 and/or colanic acid, attempts were made to generate mutants unable to produce one or both of these factors. The J. EPEC strain lacks the first 7 genes of the O127 antigen synthesis operon, which includes *gmd*, *fcl,* and *gmd* (Figure 24). Thus, it was decided to delete the *fcl* gene, which is needed for lipopolysaccharide production and is important for EHEC virulence (Barua *et al.*, 2002).

The strategy for deleting the *fcl* gene is shown schematically (Figure 29A). First, the upstream and downstream regions flanking the *fcl* gene DNA sequence were PCR amplified for ligation into the suicide vector, pDS132 (see Materials & Methods). Briefly, pDS132 carrying an unrelated fragment was digested with XbaI and SacI restriction enzymes to release the unwanted insert, with the vector fragment isolated for ligation with the two PCR-generated insert fragments (Figure 28B). The PCR reaction involved gene-specific oligonucleotides and a proof-reading polymerase to amplify the upstream region (1121bp; has *gmd* gene sequence) and, in a separate reaction, the downstream region (500bp; has *gmm* gene sequence). Some of the oligonucleotides had extension to target the fragments into the vector and to place *gmd* next to the *gmm,* i.e., without the intervening 965bp *fcl* gene (Figure 28A). The PCR-amplified fragments were ligated using the Gibson Assembly kit with the vector fragment, with success indicated by additional ligation-related bands (Figure 28B). Introduction of the ligation, by electroporation (See Materials and Methods), into SY317 (λpir) resulted in plasmid-carrying colonies with PCR screening of 4 colonies supporting generation of the required plasmid, pDS32-Δ*fcl* (Figure 28C). The pDS32-Δ*fcl* plasmid was isolated and introduced, again by electroporation, into SM10 (λpir) for allelic exchange-mediated, as previously described (Donnenberg and Kaper, 1992), removal of the *fcl* gene (Materials and Methods). PCR analysis supported the generation of an *fcl* gene-deficient (*Δfcl*) EPEC strain (Figure 28D).

The J. EPEC strain also lacked the final 13 genes of the colanic acid operon, including *wcaL, wcaK, wzxC,* and *wcaJ* (Figure 24). To examine the role of colanic acid production in the aberrant protein migration phenotype, a suicide vector was generated to delete these four genes from EPEC. Loss of *wcaL* gene activity inhibits colanic acid (CA) production while the *wcaJ* gene product is needed to initiate CA assembly (Stevenson *et al.*, 1996). A similar strategy was used to generate a suicide vector to delete these four genes (Figure 30A). Thus, gene-specific oligonucleotides were used to PCR amplify a region upstream (including the 1394bp *wcaM* gene) of *wcaL* and, in a separate reaction, a region (including the 1370bp *cpsG* gene) downstream of *wcaJ* (Figure 29B). These PCR fragments were mixed with the pDS132 fragment (pre-digested with XbaI and SacI restriction enzymes) for recombination-directed ligation using the Gibson Assembly kit protocol. Some of the oligonucleotides had extension to target PCR fragments with the vector fragment and to place two CA operon-related genes next to each other, i.e., *wcaM* and *cpsG* without the intervening *wcaL, wcaK, wzxC,* and *wcaJ* genes (Figure 29A). The generation of the suicide vector was suggested by agarose gel detecting additional ligation-related bands (Figure 29B). Electroporation of SY317 (λpir) with the ligation mix resulted in plasmid-carrying colonies with PCR screening indicating that both had the required plasmid, pDS-Δ*CA* (not shown). This plasmid was introduced into SM10 (λpir) for allelic exchanged-mediated removal of the four CA operon genes, with PCR analysis supporting generation of the EPEC *ΔCA* mutant (Figure 29C).

Finally, the *CA* mutant was used with the SM10 (λpir) strain containing the pSD-*Δfcl* suicide vector to make a double (*ΔCAfcl*) mutant. PCR screening of 4 potential double mutants revealed that each lacked the *fcl* gene supporting generation of the required *ΔCAfcl* double mutant (data not shown).

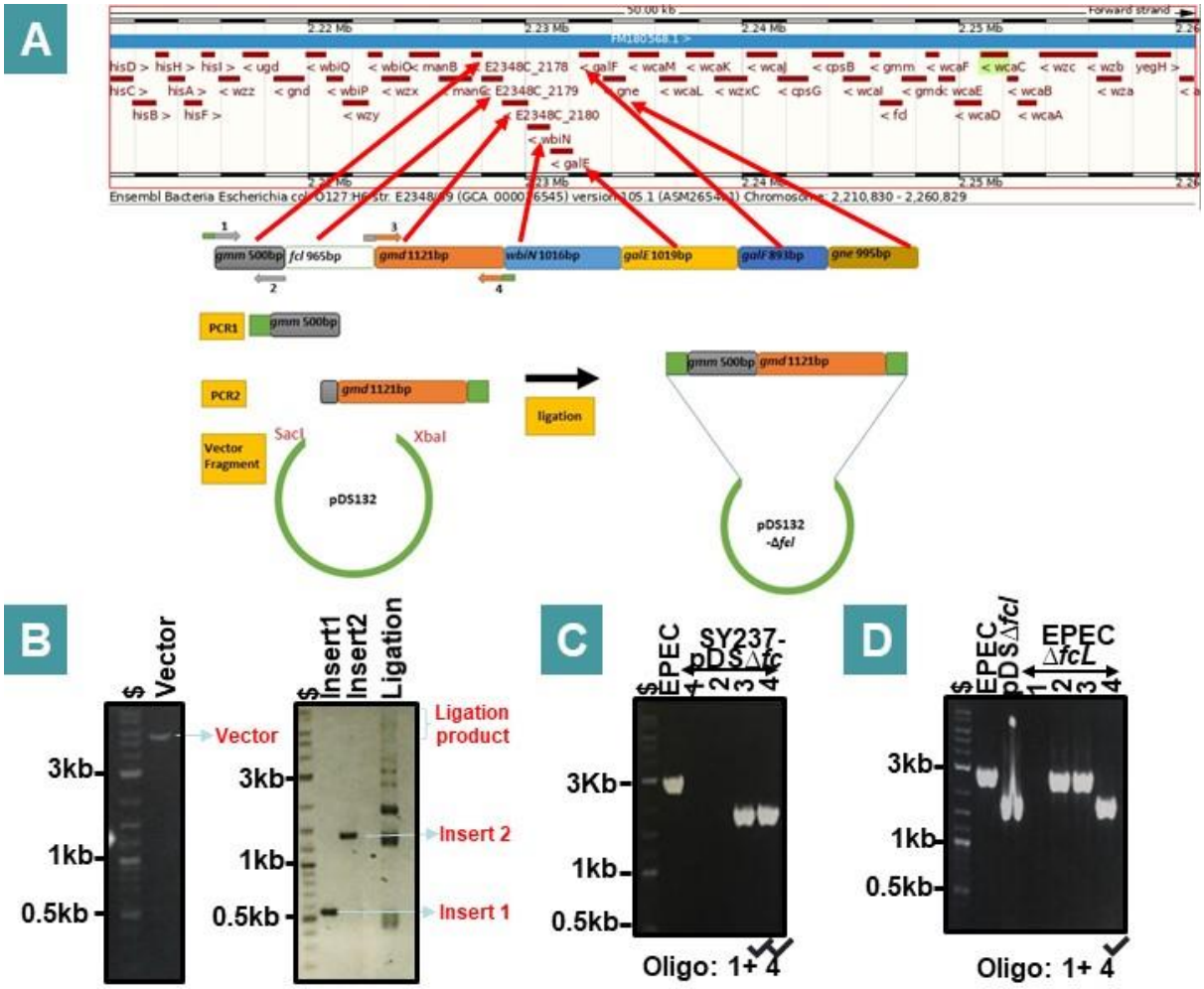

Figure 29: Generation of *Δfcl* mutant

Strategy for generating a pDS132-related suicide vector to delete the *fcl* gene from the EPEC O127 gene operon (A) and agarose gel data (B-D) showing steps in generating pDS-*Δfcl* (B) with PCR support for generating pDS-*Δfcl* (C) and the required EPEC *Δfcl* mutant (D). The samples were run alongside 2 log molecular mass marker ($) with the size of some indicated.

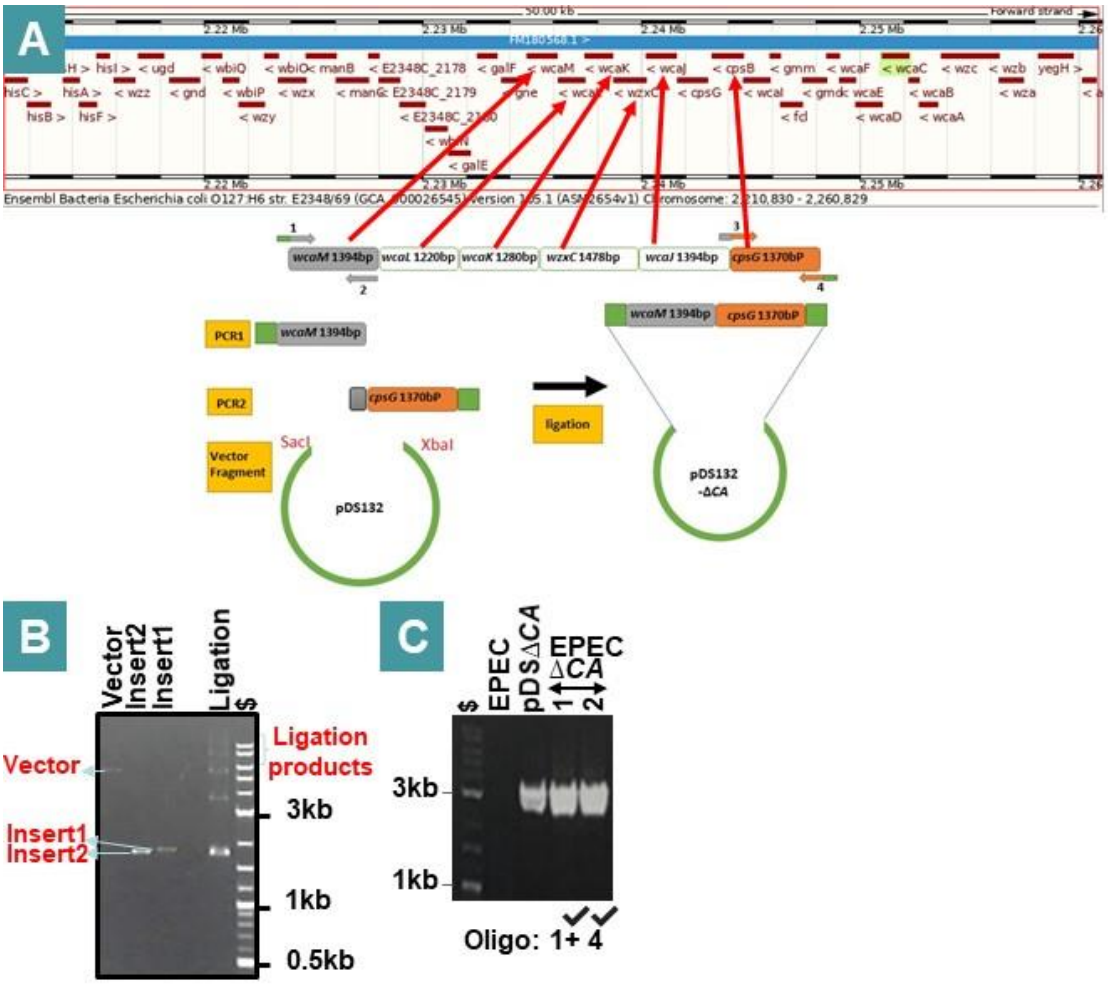

Figure 30: Generation of *ΔCA* and *ΔCAfcl* mutants

Strategy for generating a pDS132-related suicide vector to delete four genes from the EPEC colanic acid (CA) gene operon (A) and agarose gel data (B-C) showing steps in generating pDS-*ΔCA* (B) with PCR support for generating i) pDS-*Δfcl* (C), ii) EPEC *ΔCA* mutant. The samples were run alongside 2 log molecular mass marker ($) with the size of some indicated.

4.2.5 The Δ*fcl*, Δ*CA,* and Δ*CAfcl* mutants do not display the aberrant protein migration phenotype

Once the single and double mutants were generated, they were grown with control strains (EPEC and *ΔsepL*) in DMEM for 8-h prior to isolating total cell extract to examine the protein profiles by Coomassie Blue staining and Western blot probing for O127 antigen. Surprisingly, this work revealed EPEC-like profiles for all but the *ΔsepL* mutant strain, which had the expected reduced O127 antigen signal (Figure 31A) and aberrant protein migration phenotype (Figure 31B).

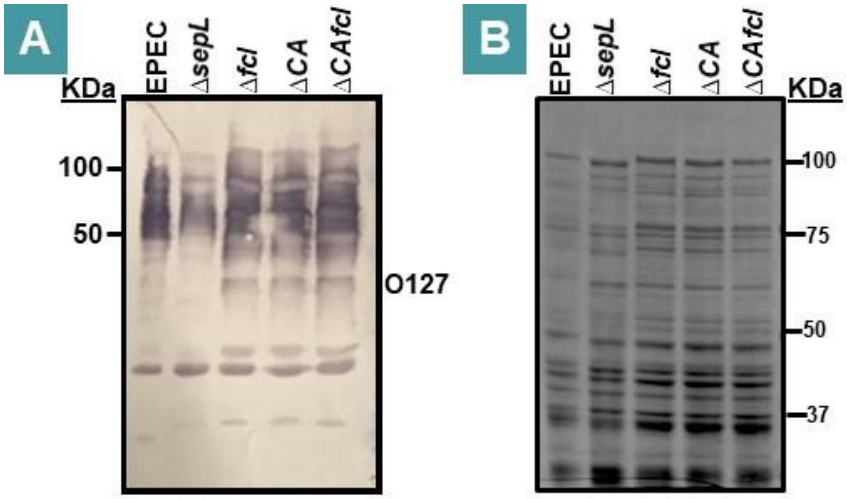

Figure 31: The *fcl, CA,* and *CAfcl* mutants do not have aberrant protein migration phenotype

Indicated strains were used to infect DMEM (1:100 dilution of bacteria grown in LB overnight without shaking) for 8 hours before isolating total bacterial cell extracts. Samples were resolved on 10% SDS-PA for western blot analysis probing for O127 antigen (A) and 6% SDS-PA gel for Coomassie blue staining (B). The position of molecular weight (KDa) standard proteins is shown. Strains used were EPEC, the *ΔsepL* mutant and newly generated *Δfcl*, *ΔCA* single and *Δ*CA*Δfcl* double mutants.

4.2.6 Disrupting O127 and colanic acid gene operons alters EPEC's growth profile

Both O-127 antigen and colanic acid are wall-associated extracellular polysaccharides with important biological roles such as providing resistance to phagocytosis and serum killing (Burns and Hull, 1998). The O-antigen is a well-established virulence factor with recent studies identifying a new function, i.e., inhibiting bactericidal activity by the host lysozyme enzyme. Colanic acid (CA), also known as M antigen, is an exopolysaccharide produced by *E. coli* and other Enterobacteriaceae linked to functions including bacterial adhesion, antibiotic resistance, and biofilm formation (Borgersen *et al.*, 2018). Moreover, CA protects bacteria from harsh environments by forming a protective capsule (Vogeleer *et al.*, 2014).

To provide support for the deletion of O-antigen and/or colanic acid genes, the single and double mutants were assessed for defects relative to control strains; - EPEC, J. EPEC, K12 *E. coli*, and *ΔsepL* mutant. This work involved monitoring bacterial growth over a 17-hour period (at 37^{o}C) in media that promotes (DMEM) or inhibits (LB) T3SS expression (Rosenshine;Ruschkowski and Finlay, 1996). Thus, bacteria from LB-grown overnight cultures (without shaking), were inoculated into 96 well plates and grown at 37^{o}C in a plate reader machine with optical density reading *(*OD_{600}*)* taken 1-hour post-infection and then at 2-hours intervals (See Materials & Methods). The results from three independent experiments when the strains were grown in LB (Figure 32A) and DMEM (Figure 32B) are shown, providing mean $\pm$ standard deviation. Notably, the *ΔsepL* mutant and K12 *E. coli* strains were, in LB, the fastest and slowest growing strains, respectively, with intermediate growth profiles for EPEC, J. EPEC and the single (*Δfcl, ΔCA*) mutants, while the *ΔCAfcl* double mutant behaved like K12 *E. coli* during the final 3h period (Figure 32A).

The data from growth in DMEM revealed the *ΔsepL* to, again, be the fastest growing strain, noting the highest OD_{600} value at 4-hours post-infection followed by reduced values suggestive of bacterial lysis or bacterial aggregation. By contrast, the other strains initially shared a similar, less dramatic growth profile with OD_{600} values, again peaking at ~4-hours

post-infection (Figure 32B). However, while the subsequent OD_{600} values for one strain (J. EPEC) remained stable for the following ~7-hours those of the EPEC and *Δfcl* mutant strains decreased, while the value for the *ΔCA* and *ΔCAfcl* double mutant appeared to increase over the final 4-hours period (Figure 32B). These results link the deletion of *fcl*, *CA,* and both *fcl*/*CA* gene regions to alterations in bacterial growth.

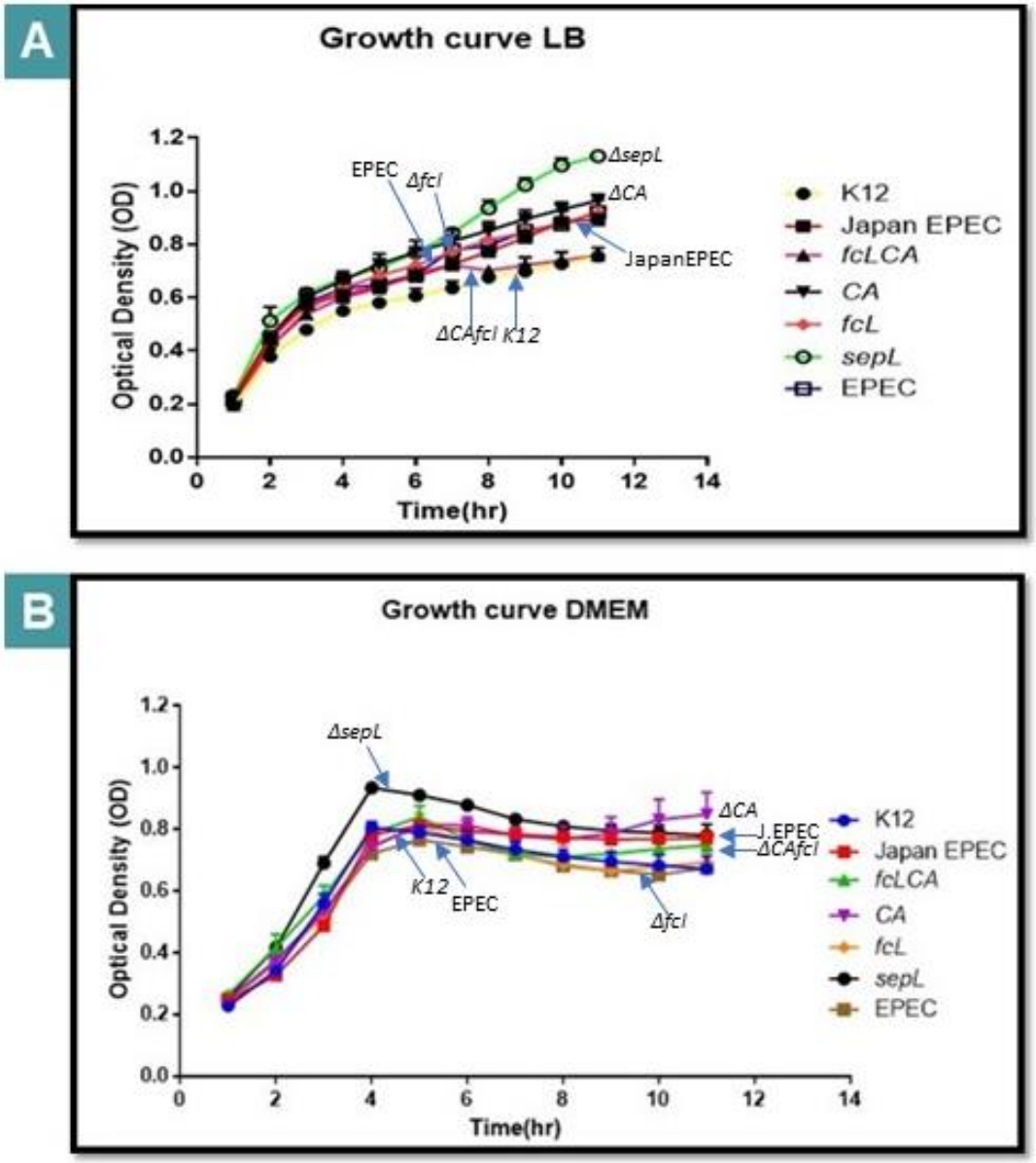

Figure 32: Disrupting EPEC O127 and colanic acid gene operons alters the growth profile

Indicated strains were used to infect 200µl of (A) LB or (B) DMEM in 96 well microtiter plates. Infections involved a 1:100 dilution of bacteria grown overnight at 37°C without shaking. The plates were placed into a plate reader (set at 37°C) with optical density readings taken at 1-hour post-infection and then at 2 hourly intervals. Data from 3 independent experiments is shown as mean ± SD. Strains used were EPEC E2348/69 (EPEC), EPEC E2348/69 from Japan (J. EPEC), K12 (non-pathogenic) *E. coli*, the *ΔsepL* mutant, and newly generated *Δfcl*, *ΔCA* single, and *ΔCAfcl* double mutants.

4.2.7 Linking the Tir and EspF cleavage phenotype to EscU functionality

The second *ΔsepL* mutant phenotype was cleavage of the Tir and EspF effectors (see Chapter 3, Section 3.2.7). It was predicted that this may be mediated by proteases linked to T3SS biology, such as EscU whose autoprotease activity regulates T3SS substrate switching to translocator and effector proteins (Thomassin;He and Thomas, 2011). Autocleavage of EscU is thought to provide a more stable binding interface for substrate/chaperone complexes, which facilitates export (Thomassin;He and Thomas, 2011).

To examine this possible EscU role, it was necessary to inactivate the *escU* in a *ΔsepL* mutant background to determine if the effectors were no longer cleaved. Thus, a suicide vector was generated, using a slightly altered strategy (Figure 33A), where the region immediately upstream and downstream of *sepL* were PCR-cloned into pACYC184 before being transferred into the pDS132 suicide vector. Briefly, the ~1220bp region immediate upstream of *ΔsepL* (includes the *escD* gene) and ~900bp immediate downstream (includes the 578bp *espA* gene) were PCR amplified. The oligonucleotides had extensions to allow recombination-mediated insertion into pACYC184 (pre-digested with SalI and XbaI restriction enzymes) with the *escD* fragment next (upstream) to the *espA* fragment (Figure 33A). The pACYC184 vector and PCR-generated insert fragments were ligated using the Gibson Assembly kit, with success supported by agarose gel detection of ligation-specific bands (Figure 33B). Introducing some of the ligation mix into K12 (NEB) *E. coli* resulted in plasmid-carrying (Cm resistant) colonies with PCR screening supporting the presence of *escD-espA* (Figure 33C), i.e., *escD* and *espA* without the intervening *sepL* gene. Oligonucleotides were used to amplify the *escD-espA* fragment while extensions directed ligation, via the Gibson Assembly kit, with the pDS132 suicide vector; the latter pre-digested with SacI/XbaI (Figure 33A). Ligation success was again supported by agarose gel detection of additional bands (Figure 33D). Introducing some of the ligation product into SY327 (λpir) resulted in plasmid-carrying (Cm resistant) colonies with PCR screening supporting each having the *escD-espA*, not *escD-sepL-espA*, gene region (Figure 33E). The resulting suicide vector, pDS-*ΔsepL*$_{full}$ was isolated and introduced into SM10 (λpir), with PCR supporting its presence in one colony (Figure 33F). The suicide vector containing strain was used with EPEC and the *ΔescU* mutant (Soto *et al.*, 2017) to generate a new SepL-

deficient (*ΔsepL*$_{full}$) and EscU/SepL-deficient double (*ΔescUΔsepL*) mutant strain. PCR studies supported the generation of the *ΔescUΔsepL* double mutant (Figure 33G). Finally, plasmids carrying the EPEC or *E. tarda escU* genes were introduced into the double mutant.

To determine EscU's role in the effector cleavage phenotype, the strains were grown in DMEM for 8-hours before isolating total cell abstracts for Western blot analysis. Probing for Tir and EspF revealed cleavage in the *ΔsepL* and *ΔsepL*$_{full}$ mutant cells (Figure 34A & 34B). Notably, the cleavage event was not evident in the *ΔescU* single or *ΔescUΔsepL*$_{full}$ double mutant strains (Figure 34A & 34B). Crucially, the double mutant defect was rescued by a plasmid introducing the EPEC but not the *E. tarda escU* gene (Figure 34A & B). This finding reveals that the cleavage of the Tir and EspF effector proteins in the *ΔsepL* mutant depends on EscU protein activity.

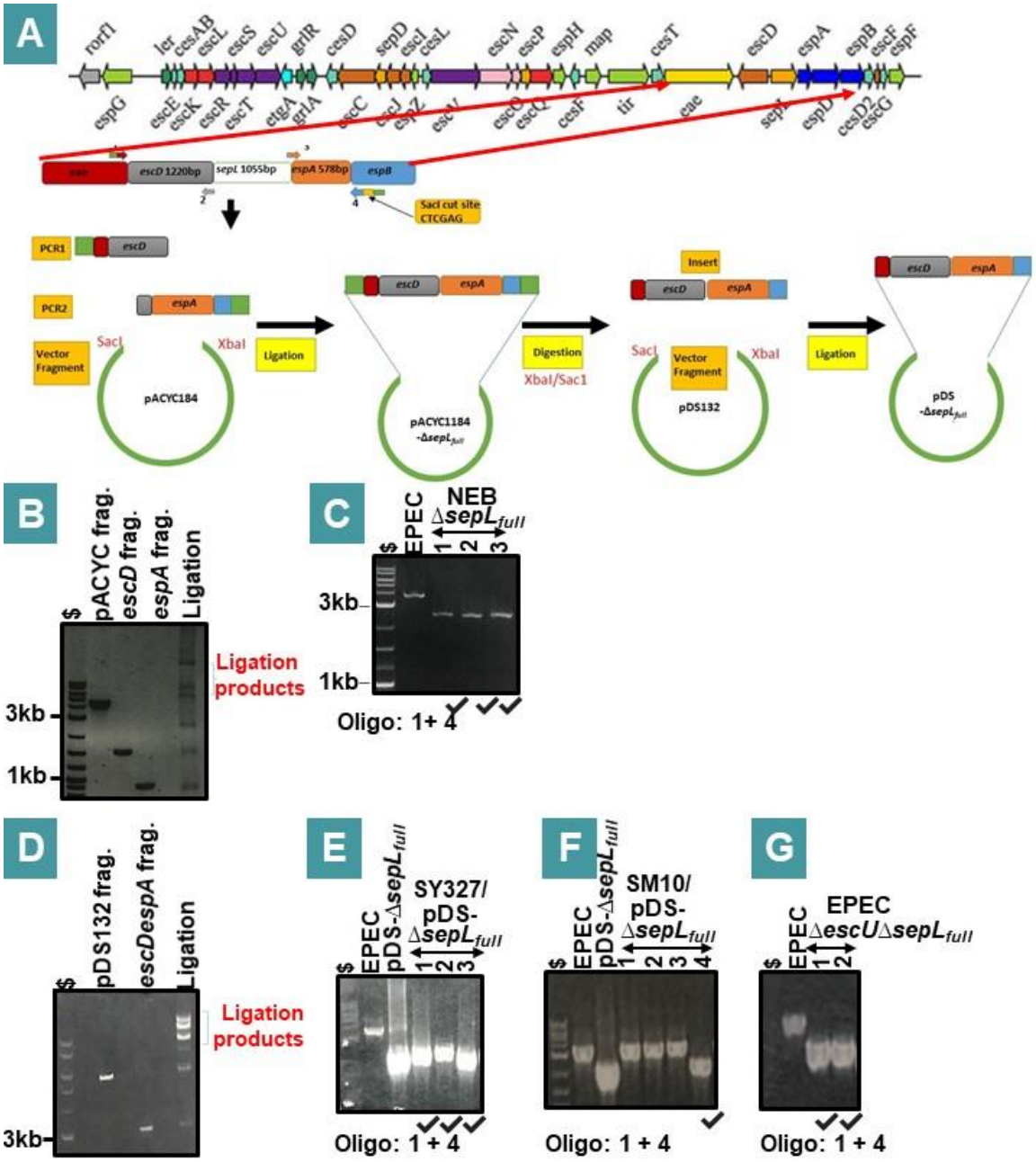

Figure 33: Generation of new *ΔsepL* single and *ΔescUΔsepL* double mutants

Strategy for generating a pDS132-related suicide vector (A) to delete the *sepL* gene from EPEC and an *escU* mutant with agarose gel data (B-G) showing steps in generating pACYC-$\Delta sepL_{full}$(B) and pDS-$\Delta sepL_{full}$ with PCR support for generating (B-C) pACYC-$\Delta sepL_{full}$, (D-F) pDS-$\Delta sepL_{full}$ (G) EPEC $\Delta escU\Delta sepL_{full}$ double mutant. The samples were run alongside 2 log molecular mass marker ($) with the size of some indicated.

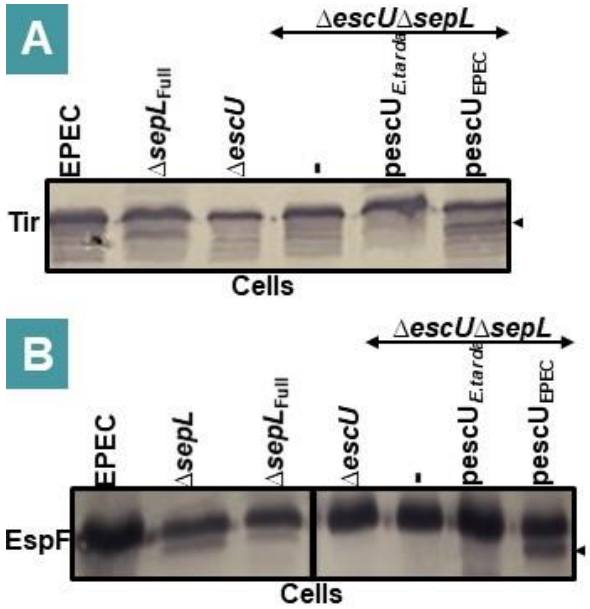

Figure 34: Linking Tir and EspF effector cleavage in the *ΔsepL* to EscU functionality

Indicated strains were used to infect DMEM (1:100 dilution of bacteria grown in LB overnight without shaking) for 8 hours before isolating total bacterial cell extracts. Samples were resolved on 10% SDS-PA for western blot analysis probing for the Tir and EspF effector proteins. The arrowhead indicates the position of the cleaved form of Tir and EspF proteins. Strains used were EPEC, the *ΔsepL* mutant, and newly generated *ΔsepL*$_{full}$ single and *Δ*escU*ΔsepL*$_{full}$ double mutants. When indicated, the double mutant strain carried no introduced plasmids (-) or a plasmid carrying the EPEC (p*escU*$_{EPEC}$) or *E. tarda* (p*escU*$_{E. tarda}$) *escU* gene.

4.3 Discussion

The work described in this chapter suggests that *ΔsepL* phenotype, cryptic protein migration in SDS-Page gel, is related to the absence or weak expression of both O-antigen and colanic acid. However, the study cannot confirm the colanic acid role alone in this phenotype.

The research in this chapter began as a result of an ambiguity in the protein migration way in SDS-Page gel. Therefore, the screening experiments analysed the cryptic migration of the proteins in SDS- page from different strains. Accidentally, the data showed that both non-pathogenic K12 *E. coli* and Japan EPEC strains have *ΔsepL* profiles. In 1922, researchers concluded that non-pathogenic *Escherichia coli* K12 has a gene that makes the exopolysaccharide but cannot produce O-antigen due to a genetic defect (Lederberg and Tatum, 1946; Gottesman, 1989; Liu and Reeves, 1994). Similarly, the Japan EPEC strain does not contain a 50 kb region, including the motif responsible for synthesizing both O127 antigen and colanic acid. As a result, the data point to a direct or indirect relationship between SepL and O-antigen or colonic acid production.

The study set out to detect the O127 antigen for previous strains using western blot analysis, which confirmed the earlier discovery. Additionally, the O127 profile for the cell extract mixed with artificial O-antigen implies a relationship between *ΔsepL* phenotype and the weak (not diminished) production of O127. This data suggests that the exopolysaccharide may compete with proteins for SDS with reduced O-antigen levels, increasing protein SDS interactions and resulting in faster protein migration on SDS-PA gels. Indeed, SDS is known to interact with LPS-composed of lipid A, core oligosaccharides and O-antigen regions-most likely the hydrophilic lipid A region (Jann;Jann and Beyaert, 1973). Alternatively, there could be non-specific protein/O antigen interactions that hinder protein migration through SDS-PA gels. The finding could provide a simple assay for monitoring changes in O-antigen cellular level.

This phenotype is also evident in the cell extracts from *escC, escD, cesT, cesD2, cesAB,* and *espF* mutants. These primary data suggest that the mystery link between some of the T3SS components and O127 production. Some of these proteins are known to interact with SepL, therefore, it is possible these interactions control exopolysaccharide production.

It is worth noting that the LEE region and colonic acid production were regulated by the carbon storage regulator a (CsrA) (Berndt *et al.*, 2019). CsrA is a posttranscriptional inhibitor protein that binds to mRNA and controls various bacterial processes, including motility, cellular respiration, and pathogenicity (Romeo;Vakulskas and Babitzke, 2013). Following Tir transport to the host cell, CsrA interacts with released CesT in the cytoplasm. This interaction suppresses CsrA, binds it to numerous genes mRNAs, and affects the mRNAs' stable function and transformation (Ye *et al.*, 2018). This factor may explain the relatively good correlation between CesT and colanic acid production. It is also possible that the CesT-CsrA influences O127 production. In general, therefore, it seems that the direct or indirect interaction between T3SS components and exopolysaccharide components and this is an important issue for future research.

A complementary study on the *E. tarda* SepL protein slightly rescued the O127 profile of *ΔsepL*. The current findings support the results and conclusions of previous research, which found that SepL *E. tarda* can weakly substitute SepL EPEC to rescue T3SS functionality (Madkour *et al.*, 2021). Thus, the *E. tarda* variant lacks features needed to control EPEC O127 antigen levels, providing an opportunity for domain swap experiments to reveal changes in domains, features, or specific residues that negatively impact on controlling O127 antigen levels.

The variation between *ΔsepL* and the *ΔsepL*, which is complemented with *E. tarda* SepL, is evident in the O127 profile but cannot be detected in the Coomassie and DnaK profiles for both strains. From these results, the protein migration may be sensitive to SDS-page gel percentage, and it may be better to resolve the samples in the lowest percentage gel to see this difference.

The *E. tarda* EscC, EscD, CesT, CesD2, and CesAB proteins failed to rescue the O127 profile of their mutant in EPEC. It also confirms our earlier observations, which showed that all previous *E. tarda* genes could not recover the DnaK and Coomassie profile for their EPEC mutants. However, the current study's findings do not support the previous research as CesAB and EscD *E. tarda* can substitute CesAB and EscD EPEC, respectively, to rescue T3SS functionality

(Madkour *et al.*, 2021). Hence, the study supports previous findings since a LEE homolog has a high level of divergence.

These findings encouraged me to knock out the O127 and colonic acid genes in EPEC by generating suicide vectors to investigate their roles in inhibiting normal protein migration in SDS-page gel. These findings are rather disappointing and contrary to expectations, the deletion of one gene from the O127 operon *fcL* produces the O127 by probing the O127 from *ΔfcL* cell extract. As the *fcl* gene product is required for O-antigen production, with its loss linked to reduce virulence (Dziva *et al.*, 2004). Moreover, the deletion of the same gene completely inhibits O157 production (Barua *et al.*, 2002). In contrast, the current findings are consistent with previous research, which concluded that the *gmd-fcL* mutant in *E. coli* O86 seems to produce semi-rough mutants by creating a lipid A-core structure and a single repeating unit (Yi *et al.*, 2009). This variation encouraged the analysis of the 50KB region associated with Japan EPEC. Unfortunately, the deleted gene is in a region that has a high level of similarity with a specific area in the operon that is responsible to produce the colonic acid. Therefore, there are two expected possibilities. First, this mutation may inhabit the CA instead of O127. It is critical for future work to investigate and confirm the correct mutant generation by using different experimental approaches. For example, studying the colony shape can confirm the O127 production, as an O127 mutant should produce rough, not smooth colonies. Second, there is a big chance that the mutant presumably reduced but did not inhibit the production of O127 (Yi *et al.*, 2009). Therefore, it is crucial to examine the impact of knocking out many O127-related genes and studying the consequences of the bacterial extracellular element.

Next, the findings failed to prove a correlation between the individual roles of colanic acid in this phenotype. The results indicate that this factor did not interfere with the regular protein migration in the indicated mutants on its own. It is likely that the responsible effector is O127 alone or both colonic acid and O127 antigen. Future studies need to verify this prediction by re-generating the O127 mutant then generating the O127 and colonic acid double mutant. Also, the complementary studies on both O127 and colanic acid are necessary to substantiate the cryptic protein migration rescue by introducing a plasmid carrying either colonic acid or the O127 gene.

It is crucial to note that EPEC, J. EPEC, *CA* mutant, and *CAfcl* mutants show the same growth pattern in the LB medium. However, the *fcl* single mutant entered more quickly into the stationary phase, leading to the lowest EPEC related final OD_{600} reading; the latter similar to that for K12 *E. coli*. However, the results indicate that *ΔsepL* likely changes the bacterial physiology since it experienced a faster growth rate and was the last strain to go into stationary phase, resulting in the highest (20% greater) final optical density reading, this finding has not been previously described. In contrast, the experimental results indicate that EPEC, *fcl* mutant, and K12 experienced slower growth in DMEM than the other strains. However, *ΔsepL* likely has a faster growth rate and the entry into the stationary phase is linked to reduce optical density value that may reflect cell lysis or cell clustering. These growth profile differences support the notion that the genomes of the *fcl, CA*, and *CAfcl* mutant strains have been altered during the allelic exchange procedure.

Furthermore, the data analyzed in this chapter suggests the crucial role of EscU in effector (Tir and EspF) cleavage when SepL protein is absent. The secretion of T3SS substrate is controlled by two T3SS switching mechanisms that are commonly referred to as molecular switches (Dean and Kenny, 2004). The first molecular switch, from the needle to the translocator switch, is regulated by EscP and EscU (Monjaras Feria *et al.*, 2012). When the needle reaches the proper length, EscP interacts with the C-terminal domain of EscU, resulting in a switching event from the needle to the translocators (Monjaras Feria *et al.*, 2012). EscU has a C-terminal domain, which undergoes auto-cleavage at an (NPTH) amino acid sequence. This self-cleavage event is required for efficient effector delivery into infected cells (Thomassin;He and Thomas, 2011). It can therefore be assumed that the SepL's new role of protecting the effector from the function of the protease. However, there is no evidence in publications of a relationship between EscU and the SepL protein. Moreover, the bioinformatic analysis showed that both Tir and EspF did not have an NPTH region in their C-terminal, the target region of EscU cleavage. However, it could be the auto protease function of EscU target, not only the NPTH region. It is also possible that the high level of effectors was secreted when SepL's absence caused the upregulation of the system, leading to effector

degradation by EscU. These findings suggest a new and unknown role for the SepL protein. Further studies are required to determine if other LEE or NLE effectors were cleaved, especially the NelA effector, since this effector secreted too much in the *sepL* mutant. Additionally, more studies are required to shed insight into the mechanism and enable future researchers to assess the SepL protein homolog for these phenotypes.

To rule out the interfering of Km cassette in effector cleavage the study aimed to delete SepL gene from start to stop codon. Of note, the findings confirmed the cleavage product on the cell extract from the *ΔsepL ΔsepLΔescU*, which EPEC, not *E. tarda* EscU, complements. Therefore, the study results show that *E. trada* EscU protein did not substitute for their homologs in this phenotype. This conclusion backs up prior research, indicating that EscU *E. tarda* cannot replace EscU EPEC in rescuing T3SS functionality (Madkour *et al.*, 2021).

The last interesting finding is that the EspF did not cleave when some chaperones were absent (CesAB-CesD2 and CesT). Chaperone proteins perform a variety of functions, including preserving intracellular stability, avoiding undesired protein-protein interactions, maintaining proteins in an unfolded state, and supplying substrate to the T3SS (Mills *et al.*, 2008; Ramu *et al.*, 2013). Therefore, keeping the effector from the antiprotease effect could be a new function of these proteins. However, the interaction between CesD2 or CesAB and EspF is unreported, but CesT is known as EspF and other effector chaperones (Creasey *et al.*, 2003).

In conclusion, the studies suggest numerous unknown and cryptic functions of T3SS components. Studies in this chapter suggest that T3SS components can inhibit either O127 or colonic acid production. Moreover, T3SS components can protect the effector from cleavage. The work also allows the future study to investigate other issues, including i) evaluating whether the O127 plays a role in abnormal protein migration on an SDS-page gel and ii) figuring out how SepL and three chaperones stop effectors from cleaving.

Chapter 5: SepL Domain swap experiments

5.1 Introduction

Previous phylogenetic studies identified a LEE region in another non-A/E pathogen called *Salmonella salamae* (SS). The *Salmonella* subspecies *salamae* serovar Sofia is commonly detected in broiler chickens, however, it does not appear to be pathogenic to humans or chickens (Harrington *et al.*, 1991). The LEE region in SS appears with a genetic rearrangement also linked to gene loss: *grlA*, *grlR*, *rorf1*, *cesF*, *espF* (Chandry et al., 2012). These genes are not needed for EPEC T3SS biology or virulence (Ruano-Gallego;Álvarez and Fernández, 2015). Recent examination of the *Salmonella salamae* LEE proteins revealed that they differ significantly in sequences from EPEC and *E. tarda* (Madkour *et al.*, 2021). The *S. salamae* SepL gatekeeper is encoded on a single *orf,* unlike the 2 *orf E. tarda sepL* gene (Madkour *et al.*, 2021), to produce a 346 residue protein that is intermediate in size to that from EPEC (351 residues) and *E. tarda* (343 residues) (Figure 35). The *S. salamae* SepL protein shares 66.7% identity (84.3% similarity) to EPEC SepL but only 47% identity (73.8% similarity) to *E. tarda* SepL i.e., similar to the divergence level between *E. tarda* and EPEC SepL (49.3% identity; 51.9% similarity). Alignment of these proteins reveals that the size differences relate to the absence/addition of residues within the first 30 AA (location of secretion signal and, often, part of the chaperone binding region) and, for *E. tarda*, the absence of the final 2 residues (Figure 35). Divergence relates to 170 residues changed in *E. tarda* and 112 in the *salamae* relative to EPEC SepL (Figure 35).

The structure of EPEC SepL (residues 80-348) has been resolved and revealed three X- bundle domains, each consisting of five helices (Burkinshaw *et al.*, 2015) (Figure 36). Comparison of the predicted secondary structures reveals, apparently, *E. tarda* SepL-specific differences (Figure 35).

SepL regulates, with a partner gatekeeper protein (SepD), the timing of translocator and effector substrate secretion through the T3SS (O'Connell *et al.*, 2004). Deletion of SepL or SepD prevents translocator secretion and leads to effector secretion (Deng *et al.*, 2005).

Moreover, SepL forms a heterotrimeric complex with its chaperone, CesL, and SepD (Younis *et al.*, 2010) which is important for regulating SepL protein stability and thus secretion hierarchy within the bacterial cell. However, each of these proteins can also interact with SepL independently, therefore, it's possible that binding to the gatekeeper doesn't require a pre-existing SepD/CesL chaperone complex (Díaz-Guerrero *et al.*, 2021). SepL activates translocator protein secretion by interacting with the major export apparatus protein, EscV, and this interaction does not depend on calcium level (Portaliou *et al.*, 2017; Gaytan *et al.*, 2018). SepL linked to SepD/CesL diffuses to the membrane, where it attaches to a place near EscV, preventing CesT/Tir from attaching to EscV. However, the translocator/chaperone binds to SepL linked with EscV. The EscN binds to the N-core of the chaperone, leading to dissociation of the translocator chaperone complex and translocator secretion. SepL and SepD affinity for EscV decreases, leading to increased EscV and effector/chaperone interaction. Again, EscN binds to the chaperone, leading to effector secretion(Portaliou *et al.*, 2017). Moreover, T3SS-dependent detection of the extracellular calcium levels leads SepL to interact with the molecular ruler, EscP, which inhibits effector export. Once the translocator pore inserts into the cell membrane, the T3SS detects the lower calcium level within the host cytoplasm, triggering SepL-EscP complex disassociation initiating effector export. The final 48 residues of SepL provide binding sites for Tir and EscD, with the former being important to organise effector secretion (Wang *et al.*, 2008).

As previously mentioned (Chapter 3; Section 3.2.7), 12 *E. tarda* homologues had complementation defects when expressed in EPEC but, surprisingly, the *Salmonella salamae* counterparts, which included SepL, complemented despite similar divergence levels (Madkour *et al.*, 2021). Indeed, domains-swapping experiments with complementation defective variants and their EPEC homologues have linked divergence in domains or features involved in complementation defects, highlighting possible targets to develop anti-virulence strategies (Madkour *et al.*, 2021).

The aim of the work described in this chapter was to use the domain-swapping approach in an attempt to define divergence-related changes responsible for *E. tarda* SepL defects in i) controlling O127 antigen levels, ii) protecting Tir and EspF from cleavage events, and iii) the T3SS-export process.

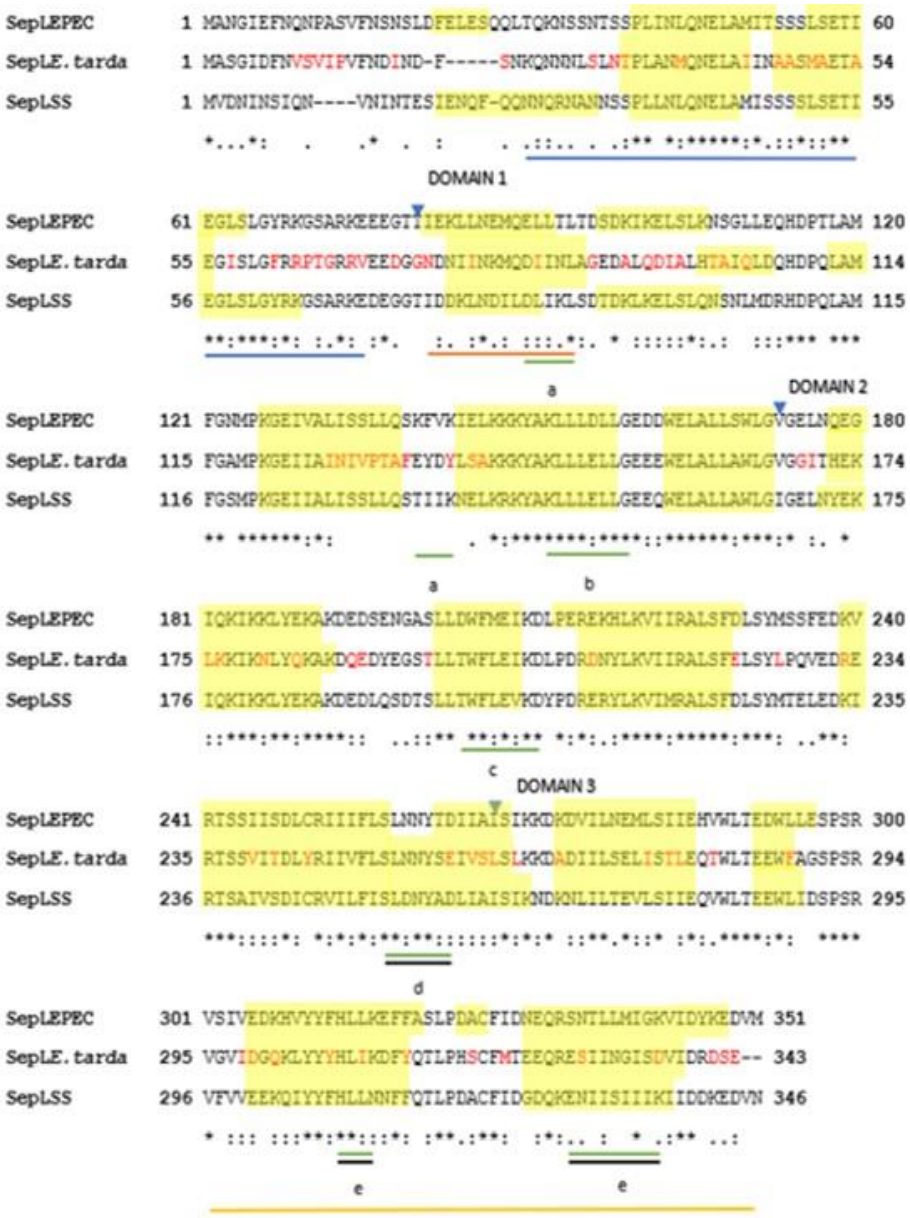

Figure 35: Alignment of EPEC, *E. tarda* and Salmonella salamae SepL sequences

The enteropathogenic *E. coli* (EPEC), *Edwardsiella tarda (E. tarda),* and *Salmonella salamae* (SS) SepL sequences were aligned (https://www.ebi.ac.uk/Tools/msa/clustalo/) with identical, similar, and different residues indicated by stars, double dots, and single dots, respectively, while a dash indicates no corresponding residue. The arrowhead points to the start of the protein visualized in structural studies (see Figure 36). *E. tarda* specific residues are highlighted by red lettering, while the binding region for the SepL chaperone, CesL (Díaz-Guerrero *et al.*, 2021) is underlined (blue colour). Regions linked to the binding of SepD, CesAB/EspA complex (Portaliou *et al.*, 2017), EscV (Portaliou *et al.*, 2017)and Tir (Wang *et al.*, 2008) are indicated by orange, green, black and yellow underlining, respectively. Predicted alpha helices are highlighted by yellow shading.

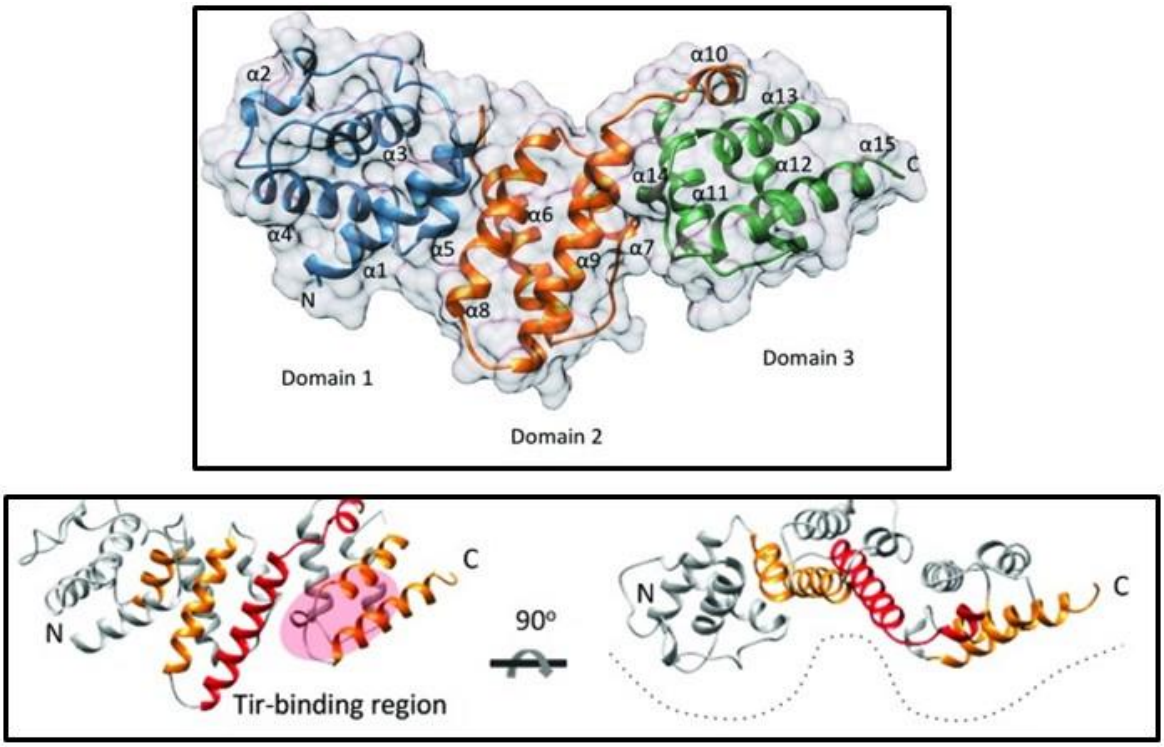

Figure 36: EPEC SepL protein structure

Schematic of EPEC SepL protein structure, taken from Burkinshaw et al., (Burkinshaw *et al.*, 2015), showing three X bundle domains (top panel), with views from other angles also shown (bottom panel) and indicating region that interacts with the N-terminus of Tir.

5.2 Results

5.2.1 C-terminal tagging of EPEC SepL interferes with some of its functions

The *E. tarda sepL* gene weakly substituted for EPEC *sepL* as it allowed low levels of Tir delivery into Hela cells but did not rescue the translocator secretion defect (Chapter 3; section3.2.5). Weak complementation could be caused by a problem with 2-orf gene expression or protein stability. Therefore, plasmids were generated to express variants with an HA-epitope tag at the C-terminal end of EPEC and *E. tarda* SepL, producing plasmids psepL: HA_{EPEC} (Figure 37) and psepL: $HA_{E.\ tarda}$ (not shown) respectively to monitor protein expression levels.

The strategy for generating HA-tagged EPEC SepL is shown (Figure 37A), involving standard molecular biology approaches described in Material and Methods. Briefly, the *sepL* gene was PCR amplified using pACYC-$sepL_{EPEC}$ as a template with oligonucleotides to amplify the *sepL* gene; the reverse primer also served to replace the stop codon with the DNA sequence for the HA epitope tag (Figure 37A). The amplified *sepL*: HA gene fragment was used in another PCR reaction to provide flanking vector-specific regions to enable recombination, via the Gibson assembly kit, with the vector fragment; pACYC184, pre-digested with BamHI and SalI restriction enzymes (Figure 37A). Cloning success was supported by agarose gel analysis of a portion of the ligation product alongside samples of the isolated fragments (Figure 36B). Introduction of some ligation product into non-pathogenic K12 *E. coli* (NEB) resulted in plasmid-containing, Cm resistant, colonies with PCR screening of 4 revealing that 1 had the expected ~1.2Kb fragment (Figure 37C) supporting generation of p*sepL*:HA_{EPEC}. The same approach was used to clone *E. tarda sepL* into pACYC184 to generate p*sepL*:$HA_{E.tarda}$ (not shown).

To determine if the plasmids produced HA-tagged proteins of the expected molecular mass, total cell lysates of the plasmid carrying K12 (NEB) strains, grown ~16-hour in LB, were processed for western blot analysis to probe with anti-HA specific monoclonal antibodies. This analysis revealed HA-tagged proteins in both strains (Figure 38A), with the *E. tarda* variant migrating slightly faster than the EPEC homologue, as expected, as it has fewer residues (343

versus 351). Notably, there was ~2-4 fold more of the *E. tarda* than the EPEC HA-tagged variant (Figure 38A).

Studies then examined the impact of expressing the fusion proteins in the *ΔsepL* mutant on the total cellular (i.e., aberrant migration phenotype) and protein secretion profiles. Thus, bacterial cellular extracts and secreted protein samples were isolated for separation by SDS-PAGE before processing for Coomassie blue staining (Figure 38B & 38C) and western blot (Figure 38D & 38E) analyses. As expected, Coomassie blue staining revealed the *ΔsepL* mutant-associated aberrant migration phenotype that was rescued by plasmid introducing EPEC but not *E. tarda sepL* (Figure 38B). HA-tagged EPEC SepL prevented it from rescuing the phenotype, while HA tagging *E. tarda* SepL had not detectable impact (Figure 38B). This finding was supported by studies probing for DnaK (Figure 38D) to detect the aberrant migration phenotype. Plasmid expression of EPEC SepL:HA (pE:HA) was supported by its presence in the *ΔsepL* mutant, restoring low levels of translocator protein secretion and reducing the amount of secreted effector proteins (Figure 38C). This partial functionality was supported by western blot analysis using antibodies to detect each translocator and two (Tir, EspF) effectors (Figure 38D & 38E).

Of note, HA-tagging EPEC SepL decreased the secretion levels of EspB and, more dramatically, EspA and EspD (Figure 38D & 38E). Moreover, the Tir/EspF cleavage phenotype was rescued by plasmid-expressing EPEC SepL (pE) or its HA-tagged (pE:HA) but not the *E. tarda* (pT or pT:HA) variants (Figure 38D & 38E). These findings indicate an important role for the EPEC SepL C-terminal residues in regulating the T3SS substrate switch from translocator to effector proteins as almost fully blocked by adding the HA tag. Plasmid expressing the HA-tagging *E. tarda* SepL protein (pT:HA) had one detectable impact i.e. absence of detectable secretion of EspB unlike for the strain plasmid expressing untagged *E. tarda* SepL (pT; Figure 38E).

HeLa cells were also infected with the strains for Western blot analysis of isolated Triton X-100 soluble and insoluble fractions. This work revealed a plasmid expressing the EPEC SepL:HA variant (pE:HA) restored Tir delivery levels but, perhaps, less than the untagged (pE) variant

(Figure 38F). As before, plasmid expressing *E. tarda* SepL (pT) restored a low level of Tir delivery, which was not seen with strain plasmid expressing the HA-tagged (pT:HA) variant (Figure 38F). Thus, C-terminal tagging by EPEC SepL appears to impact on its functionality, possibly by interfering with the terminal region binding to T3SS-related partners.

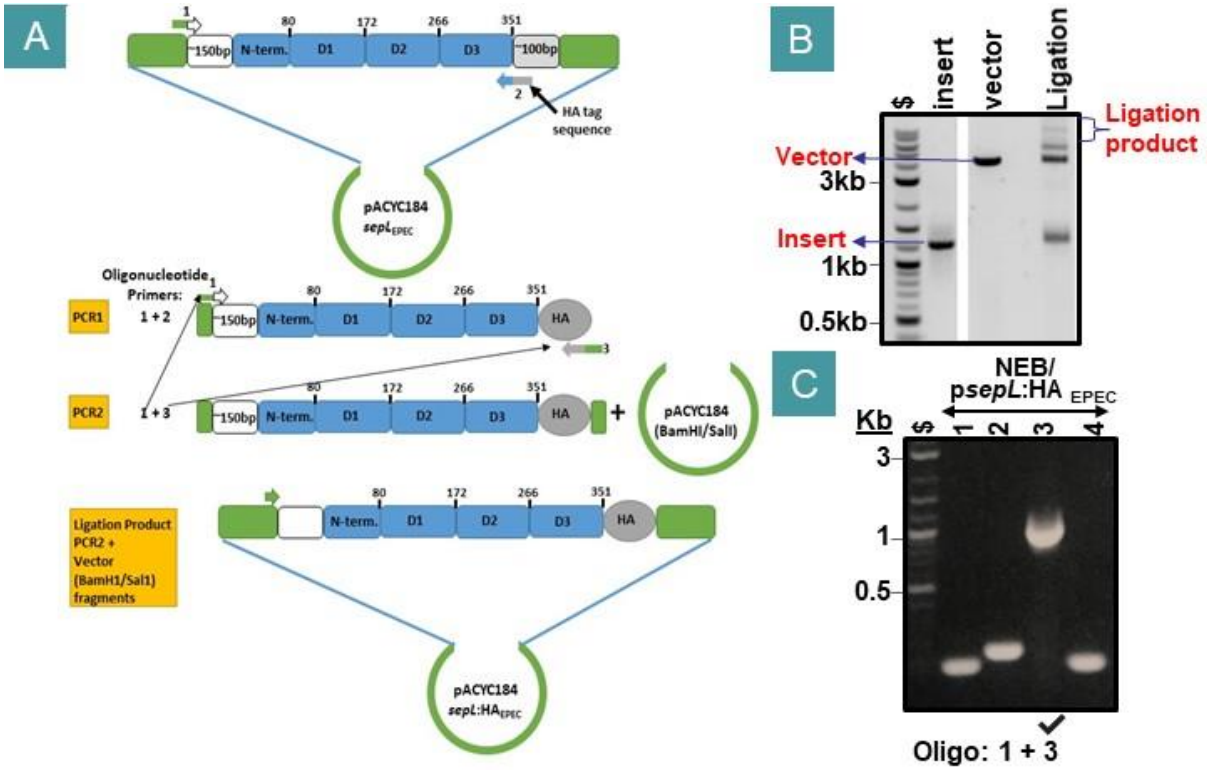

Figure 37: Generating a plasmid encoding EPEC SepL-HA fusion protein

(A) Schematic of the strategy for generating the EPEC SepL-HA tagged fusion protein. The pACYC184-*sepL*$_{EPEC}$ plasmid was used as the template with oligonucleotide primers 1 and 2 to amplify the *sepL* gene with the stop codon replaced by a sequence encoding the HA epitope tag. The resulting PCR product was used in a PCR second reaction, with oligonucleotide primers 1 and 3, to provide both terminal extensions for recombination-mediated insertion into the vector (pACYC184 pre-digested with BamHI and SalI restriction enzymes) fragment. Agarose gels showing (B) vector and insert fragments used for ligation, via Gibson Assembly Kit, with success evidenced by additional ligation-related bands with (C) PCR screening, with total DNA from K12 *E. coli* (NEB) bacteria carrying the putative pACYC184-*sepL*:HA$_{EPEC}$ (p*sepL*:HA$_{EPEC}$) plasmid supporting its presence in one strain. Agarose gels also show 2 log molecular weight markers, with the size of some indicated.

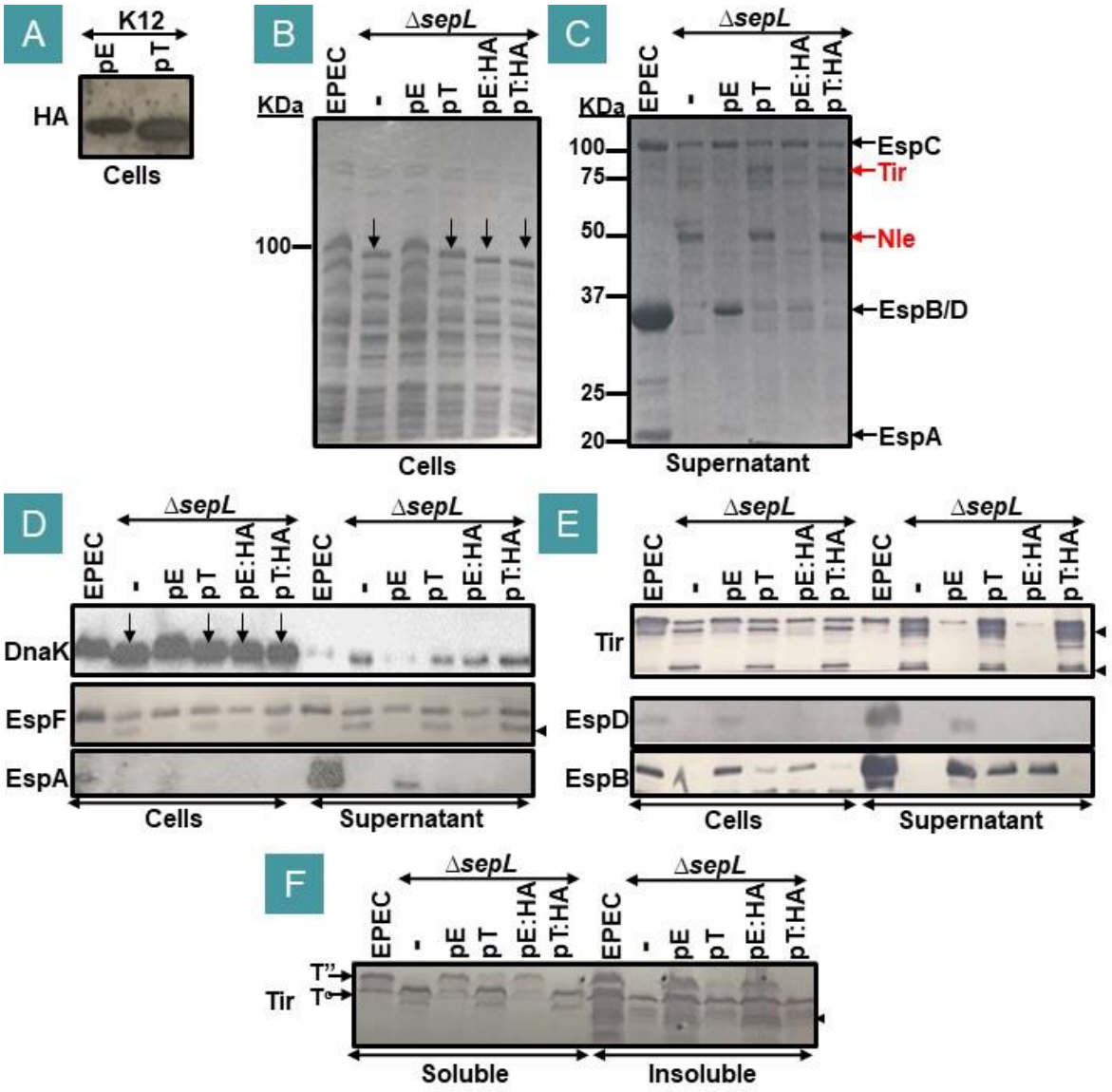

Figure 38: Impact of C-terminal HA-tagging of EPEC and *E. tarda* SepL on protein functionality

Indicated strains were added to (A) LB or (B-E) DMEM or (F) HeLa cells. (A) LB was infected overnight (with shaking) before isolating total cell extract for Western blot analysis. (B-E) DMEM was inoculated (1:100 dilution of bacteria grown in LB overnight without shaking) for 8 hours before isolating total cell extracts and secreted (supernatant) proteins. Samples were resolved on 6% (B) or 12% (A, C-D) SDS-PA gels for Coomassie blue staining (B, C) or western blot analysis (A, D-E). Molecular standards are shown (KDa; B & C). (F) HeLa cells were fractionated, post infection, into Triton X-100 soluble (host cytoplasm/membrane proteins and T3SS delivered EPEC effectors) and insoluble (contains host nuclei/cytoskeletal proteins and adherent bacterial proteins) samples for Western blot analysis on 10% SDS-PA gels. EPEC, non-pathogenic (K12) *E. coli*, and the SepL-deficient mutant (*sepL*) were used; the latter had no (-) plasmids or, when indicated, a plasmid encoding EPEC SepL (pE), *E. tarda* SepL (pT), EPEC SepL: HA fusion protein (pE:HA), or *E. tarda* SepL: HA fusion protein (pT:HA). The positions of the unmodified (T°) and host kinase-modified (T") Tir forms are shown. Down-ward pointing arrows indicate strains with *ΔsepL* mutant-like phenotype with arrowheads indicating putative cleavage-related forms of the EspF and Tir effectors.

5.2.2 N-terminally tagging EPEC SepL also impacts on some of its functions

As C-terminally tagging EPEC SepL negatively impacted on its functionality, studies examined if the issue could be avoided by placing the tag at the other, N-terminal, end. Thus, an EPEC HA:SepL expressing plasmid (pHA:*sepL*$_{EPEC}$) was generated (Figure 39). A similar cloning strategy was used as described for the p*sepL*:HA variant, but with the HA gene sequence encoded on the forward primer in frame with the SepL start codon (Figure 39A). The amplified ~1.2Kb *sepL* related fragment (carries, as before, vector-related extensions) was added to the BamHI/SalI-digested vector fragment for a ligation reaction, using the Gibson assembly kit, with success supported by agarose gel analysis of a portion of the ligation product (Figure 39B). Some of the ligation products were transformed into non-pathogenic K12 (NEB) *E. coli* with PCR screening of 3 colonies supporting all 3 having the insert (Figure 39C) indicating generation of pHA:*sepL*$_{EPEC}$.

To determine whether this fusion protein was functional, the usual experimental protocols were used for post-infection, isolation of total bacterial and secreted proteins, and, from infected Hela cells, Triton X-100 soluble and insoluble fractions. The impact of the fusion protein on the aberrant protein migration phenotype was assessed by probing bacterial extracts for O127 antigen (Figure 40A) and DnaK (Figure 40C) levels. This work revealed that both the N- and C-terminally tagged variants did not rescue the *ΔsepL* mutant defect, unlike the untagged variant. The Coomassie blue stained supernatant samples revealed partial rescuing of the *ΔsepL* mutant secretion defects by the plasmid expressing SepL, but this activity was reduced when the HA tag was added to the C-terminal and, perhaps to a greater extent, the N-terminal end (Figure 40B). Western blot probing for EspB revealed both tagged variants restored some translocator protein secretion but not as much as the untagged variant (Figure 40D). Notably, the SepL:HA but not the HA:SepL variant protected EspF (Figure 40C) and Tir (Figure 40D) from cleavage events revealing an important role for the N-terminal residues. Probing the HeLa cell fractions for Tir revealed that both the N- and C-terminally tagged variants rescued the Tir delivery defect (Figure 40E).

As N-terminally tagging EPEC SepL also impacted on its functionality, it was decided not to make an equivalent *E. tarda* variant but to work with untagged domain swapped variants and, to assess protein expression, C-terminally-tagged variants.

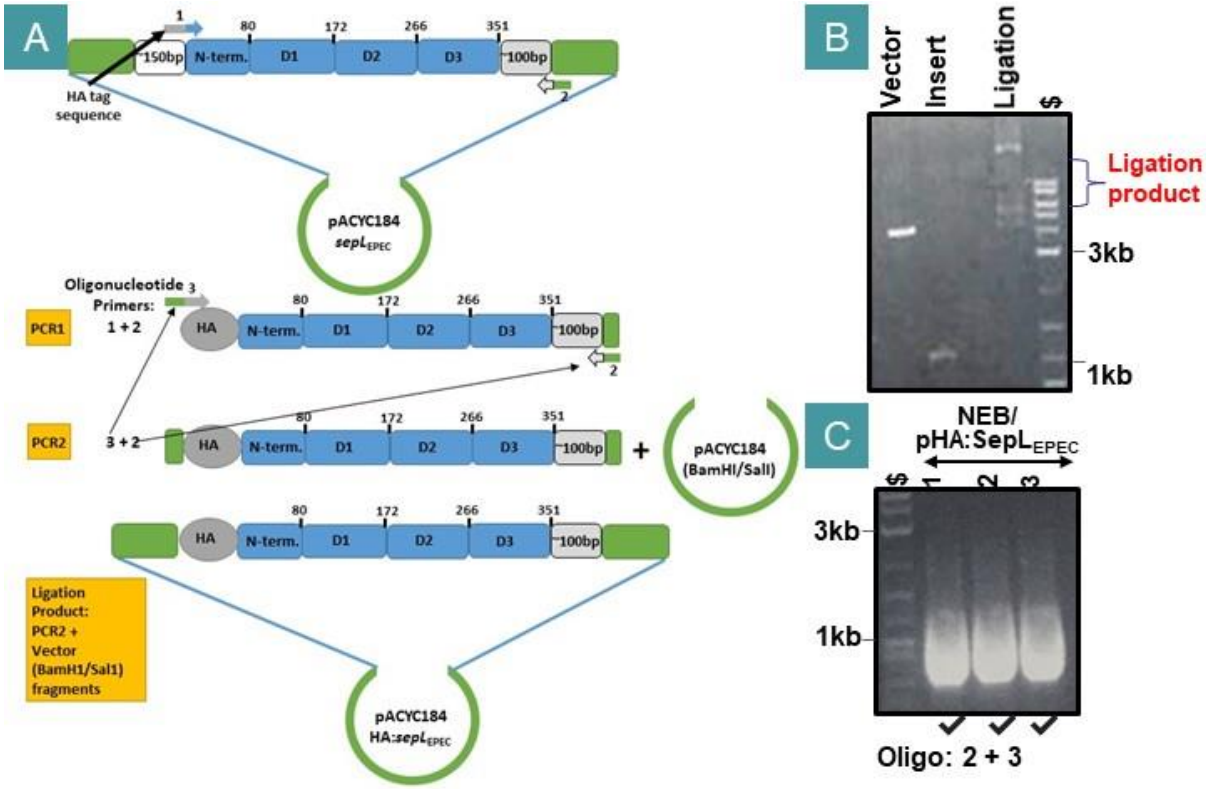

Figure 39: Generating plasmid encoding an EPEC HA-SepL fusion protein

(A) Schematic of the strategy for generating the EPEC HA-SepL tagged fusion protein. The pACYC184-*sepL*$_{EPEC}$ plasmid was used as the template with oligonucleotide primers 1 and 2 to amplify the *sepL* gene with the start codon replaced by a sequence encoding the HA epitope tag. The resulting PCR product was used in a second PCR reaction, with oligonucleotide primers 2 and 3, to provide terminal extensions for recombination-mediated insertion into vector (pACYC184 pre-digested with BamHI and SalI restriction enzymes) fragment. Agarose gels showing (B) vector and insert fragments used for ligation, via Gibson Assembly Kit, with success evidenced by additional ligation-related bands with (C) PCR screening, SDS-PA gels, with total DNA from K12 *E. coli* (NEB) bacteria carrying the putative pACYC184-HA:*sepL*$_{EPEC}$ (pHA:*sepL*$_{EPEC}$) plasmid supporting its presence in all strains. Samples were separated alongside 2 log molecular weight markers with the size of some indicated.

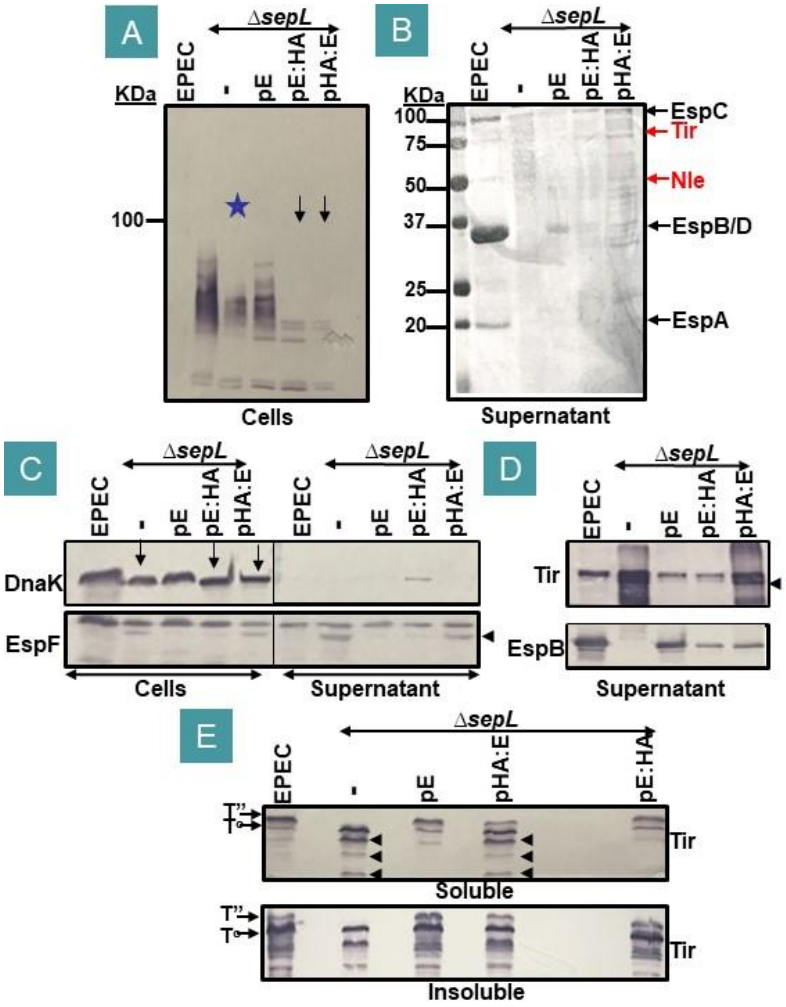

Figure 40: N-terminal HA-tagging EPEC SepL interferes with its ability to regulate T3SS secretion

Indicated strains were added to (A-D) DMEM or (E) HeLa cells. (B-E) DMEM was inoculated (1:100 dilution of bacteria grown in LB overnight without shaking) for 8 hours before isolating total cell extracts and secreted (supernatant) proteins. Samples were resolved on 6% (A) or 12% SDS-PA gels (B-D) for Coomassie blue staining (B) or western blot analysis (A, C & D). Molecular standards are shown (KDa; A & B). (E) HeLa cells were fractionated, post infection, into Triton X-100 soluble (host cytoplasm/membrane proteins and T3SS delivered EPEC effectors) and insoluble (contains host nuclei/cytoskeletal proteins and adherent bacterial proteins) samples for Western blot analysis. Strains used were EPEC and the SepL-deficient mutant (*ΔsepL*); latter with no (-) plasmid or, when indicated, a plasmid encoding EPEC SepL (pE), *E. tarda* SepL (pT), EPEC SepL:HA fusion protein (pE:HA) or EPEC HA:SepL fusion (pHA:E) proteins. The position of unmodified (T°) and host kinase-modified (T") Tir forms are shown. Down-ward pointing arrows indicate strains with *ΔsepL* mutant-like phenotype with arrowheads indicating putative cleavage-related form of the EspF and Tir effectors.

5.2.3 Impact of swapping domain1 on EPEC and *E. tarda* SepL functionality

The domain exchange experiments were restricted to domains 1, 2 and 3, with initial studies focused on domain 1 to develop strategies for generating untagged and C-terminally HA chimera proteins. The strategy is illustrated for generating a chimera of EPEC domain 1 with *E. tarda* domains 2 and 3, i.e., ETT (Figure 41A). Thus, all of EPEC domain 1 (along with its N-terminal and upstream regions) was PCR amplified using specific oligonucleotides – one in the vector upstream of *sepL* and the other within *sepL* at the region encoding end of domain 1. The *E. tarda* domains 2 and 3 were PCR amplified using specific oligonucleotides – one within *sepL* at the region encoding start of domain 2 with extension corresponding to the sequence encoding end of EPEC domain 1, and the other in the *sepL* gene downstream region with extension providing vector sequence (Figure 41A). The isolated PCR amplified bands were used in a ligation, via Gibson Assembly kit, reaction with success, agarose gel detecting additional, ligation specific, products (Figure41B). Introducing some of the ligation reaction into NEB *E. coli* resulted in plasmid-containing (Cm resistant) colonies. PCR screening of 3 clones revealed each had the EPEC domain1 fragment (Figure 41C), supporting generation of the p*sepL*-ETT plasmid encoding the ETT chimera. A similar strategy was used to generate the other three domain1-related swaps: a) TEE (Figure 42), b) TEE:HA (not shown) and c) ETT:HA (not shown). Gene sequencing, using oligonucleotides upstream and downstream of the *sepL* gene, confirmed the successful generation of each plasmid.

The four plasmids were introduced, individually, into the *ΔsepL* mutant for the standard assays with control strains (Figure 43). The isolated total bacterial extracts were resolved on SDS-PA gels and examined for the aberrant migration phenotype by Coomassie blue staining (Figure 43A) and western blot probing for O127 antigen (Figure 43B). These analyses revealed that none of the four chimeras (or HA-tagged SepL variants) rescued the phenotype, unlike the untagged EPEC SepL variant (Figure 43A & 43B). Probing the bacterial cell and supernatant samples for EspB revealed that plasmid expression of the untagged EPEC SepL and all four-chimera restored normal cellular levels, with only the untagged variant restoring secretion levels (Figure 43C). These findings were supported by data from an additional, independent experiment (Supplementary Figure 14). Probing for EspF and Tir revealed that none of the

chimera prevented the cleavage event, unlike the untagged and HA-tagged EPEC SepL variants (Figure 43C).

Probing the isolated Triton X-100 soluble and insoluble fractions for Tir revealed that none of the chimera restored detectable levels of Tir delivery and also supported a failure to protect Tir from cleavage (Figure 43D). Probing the insoluble fractions (contain adherent bacteria) for HA fusion proteins revealed that both HA-tagged chimera were expressed at higher levels than the HA-tagged SepL (native) proteins (Figure 43D).

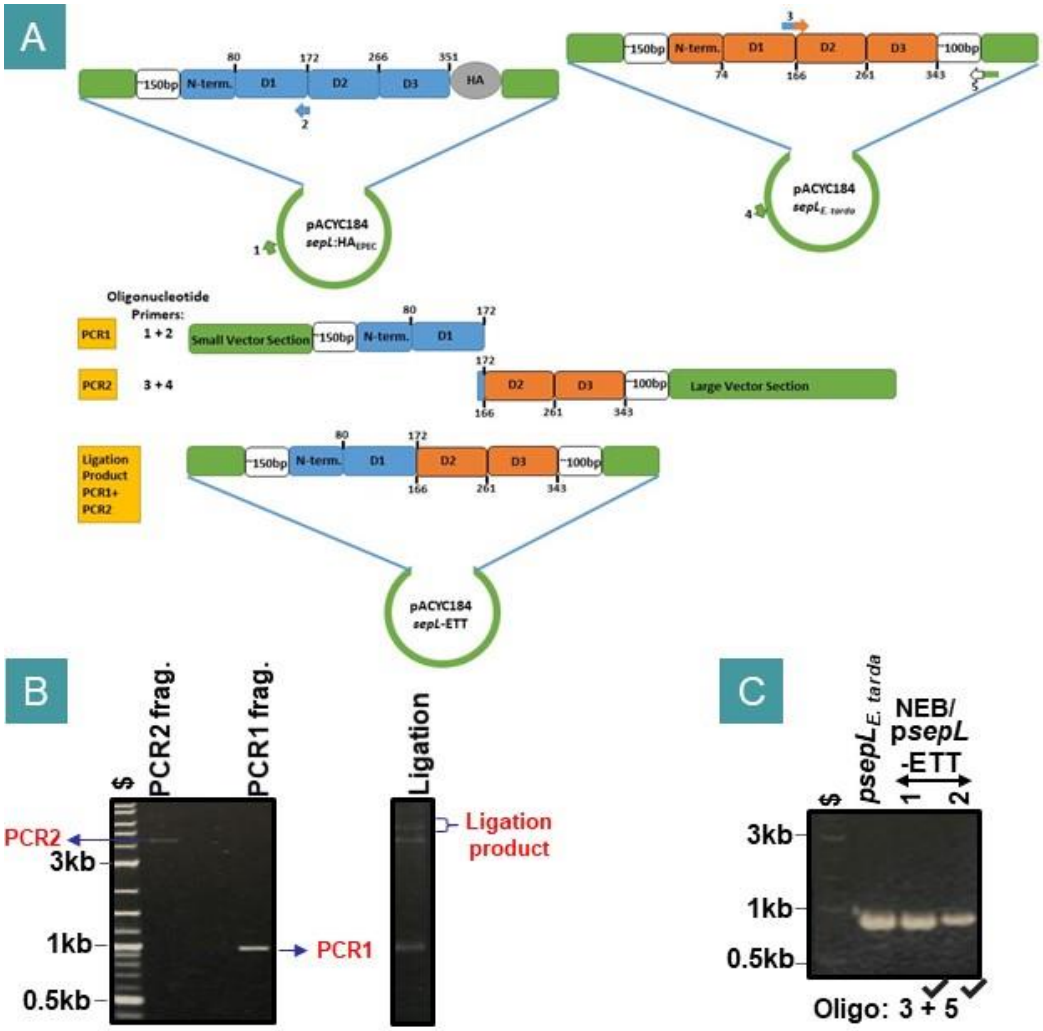

Figure 41: Generating a plasmid with *E. tarda* SepL domain 1 swapped for that from EPEC

(A) Schematic of the strategy for swapping *E. tarda* SepL domain1 for that from EPEC to generate a chimera (SepL-ETT) fusion protein. The pACYC184-*sepL*:HA_{EPEC} plasmid was used as the template, with oligonucleotide primers 1 and 2, to amplify the EPEC *sepL* gene to end of the domain1 sequence with indicated upstream vector region providing the 'PCR1' fragment. The pACYC184-$sepL_{E.\ tarda}$ plasmid was used as the template, with oligonucleotide primers 3 and 4, to amplify the *E. tarda sepL* gene sequence encoding domain 2 and 3 with downstream *sepL* and, indicated, vector regions providing the 'PCR2' fragment. Primer 3 has an extension to direct recombination-mediated ligation between the EPEC and *E. tarda sepL* regions. Agarose gels showing (B) PCR1 and PCR2 fragments used for ligation, via Gibson Assembly Kit, with success evidenced by additional ligation-related bands with (C) PCR screening, using primer 3 and 5, with total DNA from K12 *E. coli* (NEB) bacteria carrying the putative pACYC184*sepL*-ETT (p*sepL*-ETT) plasmid supporting its presence in the two tested strains. Samples were separated alongside 2 log molecular weight markers with the size of some indicated.

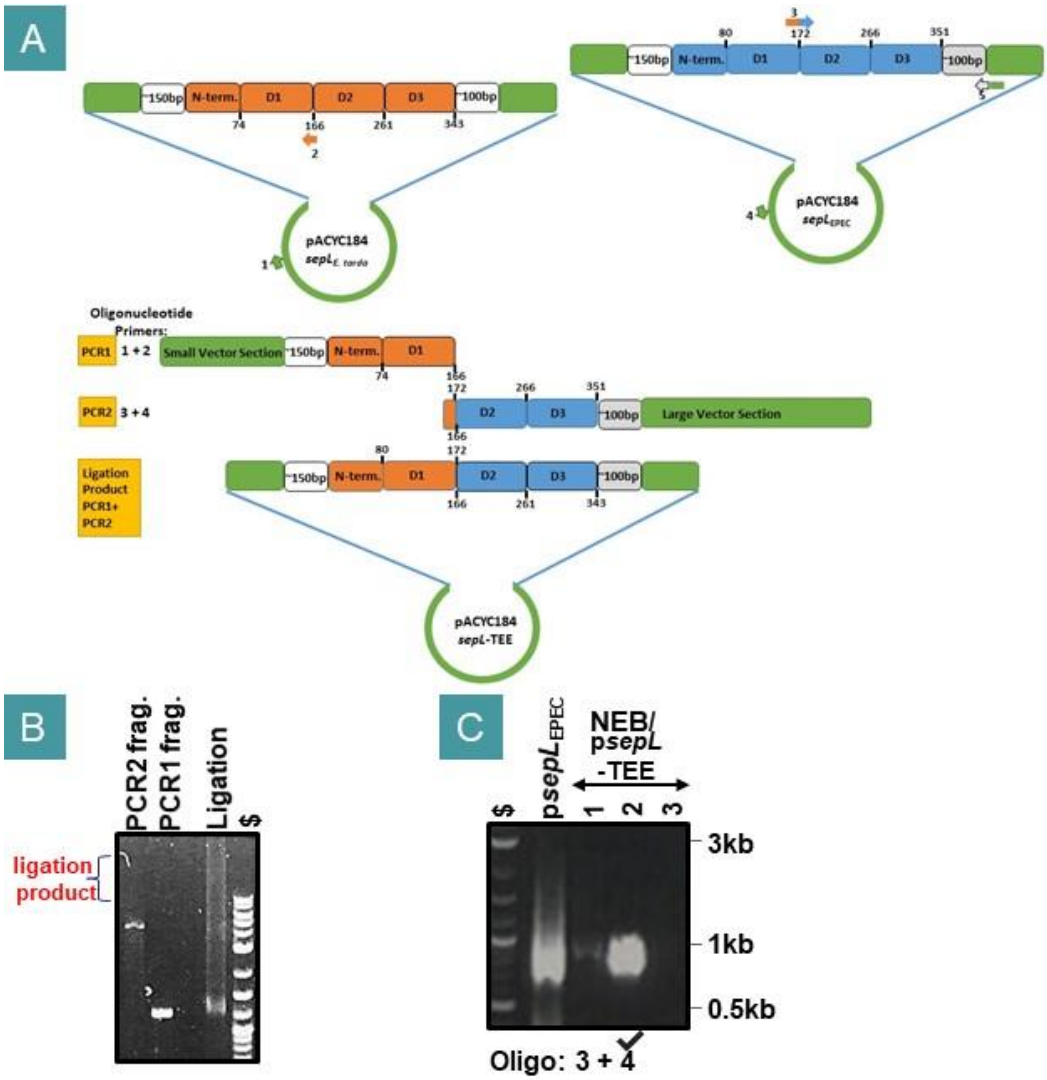

Figure 42: Generating a plasmid with the EPEC SepL domain1 swapped for that from *E. tarda*

Schematic of the strategy for swapping EPEC SepL domain1 for that from *E. tarda* to generate a chimera (SepL-TEE) fusion protein. The pACYC184-*sepL*$_{E.\ tarda}$ plasmid was used as the template, with oligonucleotide primers 1 and 2, to amplify the *E. tarda sepL* gene to end of the domain1 sequence with indicated upstream vector region providing the 'PCR1' fragment. The pACYC184-*sepL*:HA$_{EPEC}$ plasmid was used as the template, with oligonucleotide primers 3 and 4, to amplify the EPEC gene sequence encoding domain 2 and 3 with downstream *sepL* and, indicated, vector regions providing the 'PCR2' fragment. Primer 3 has an extension to direct recombination-mediated ligation between the EPEC and *E. tarda sepL* regions. Agarose gels showing (B) PCR1 and PCR2 fragments used for ligation, via Gibson Assembly Kit, with success evidenced by additional ligation-related bands with (C) PCR screening, using primer 3 and 5, with total DNA from K12 *E. coli* (NEB) bacteria carrying the putative pACYC184*sepL*-ETT (p*sepL*-TEE) plasmid supporting its presence in the two tested strains. Samples were separated alongside 2 log molecular weight markers with the size of some indicated.

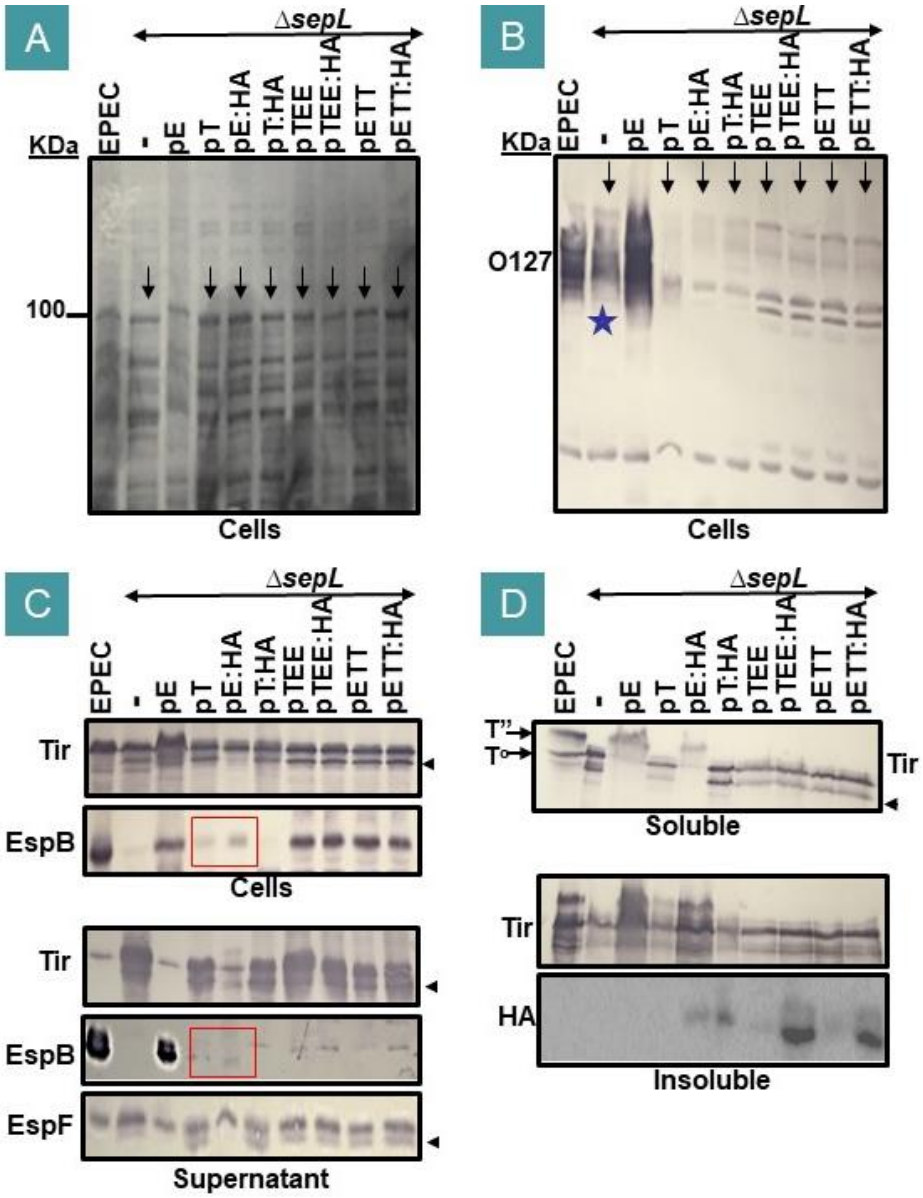

Figure 43: Assessing the impact of swapping domain1 on EPEC and *E. tarda* SepL functionality

Indicated strains were (A-C) added to DMEM (1:100 dilution of bacteria grown in LB overnight without shaking) for 8 hours before isolating total cell extracts and secreted (supernatant) proteins. Samples were resolved on 6% (A) or 12% (B & C) SDS-PA gels for Coomassie blue staining (A) or western blot analysis (B & C). Molecular standards are shown (KDa; A) with blue star (B) indicating weak anti-O127 antigen signal while red rectangle (C) highlights reduced signals. (D) HeLa cells were fractionated, post infection, into Triton X-100 soluble (host cytoplasm and membrane proteins plus T3SS delivered EPEC effectors) and insoluble (contains host nuclei and cytoskeletal proteins plus adherent bacterial proteins) samples for Western blot analysis. Strains used were EPEC and the SepL-deficient mutant (*ΔsepL*) with no (-) plasmid or, when indicated, plasmids encoding EPEC SepL (pE), *E. tarda* SepL (pT), EPEC SepL:HA fusion protein (pE:HA), *E. tarda* SepL:HA fusion protein (pT:HA), SepL-T1E2,3 chimera (pT1E2,3), SepL-T1E2,3:HA chimera (pT1E2,3:HA), SepL-E1T2,3 chimera (pE1T2,3) and SepL-E1T2,3:HA chimera (pE1T2,3:HA). The position of unmodified (T^{o}) and host kinase-modified (T") Tir forms are shown. Downward pointing arrows indicate strains with *ΔsepL* mutant-like phenotype with arrowheads indicating putative cleavage-related form of the EspF and Tir effectors.

5.2.4 Impact of swapping domain2 on EPEC and *E. tarda* SepL functionality

An altered strategy (Figure 45A) was used to make a plasmid encoding EPEC SepL with domain 2 swapped for that from *E. tarda,* i.e., to produce the ETE chimera protein, Briefly, three PCR reactions were designed to amplify 1) all the vector plus the 5'end of EPEC *sepL* to the end of the domain1 encoding sequence, 2) all the domain3 encoding sequence and downstream region that includes a small section of the vector and 3) the *E. tarda sepL* domain 2 encoding sequence with oligonucleotide extension specific to the 3' and 5' ends of the EPEC domain 1 and 3 encoding sequences respectively (Figure 45A). The 3 PCR generated fragments were isolated and used in a ligation reaction, via the Gibson Assembly kit, with success suggested by agarose gel detection of additional ligation-specific bands (Figure 45B). Introducing some of the ligation reaction into NEB *E. coli* resulted in plasmid-containing (Cm resistant) colonies with PCR screening ones that had the expected EPEC and *E. tarda* fragments supporting generation pETE (Figure 45C).

The generation of the other plasmids used the simpler two PCR strategy, making TET, TET:HA, and ETE:HA. The strategy is illustrated for pTET (Figure 46A) and pETE:HA (Figure 47A), with the only change being that all the vector and all but the domain2-encoding sequence of the *E. tarda sepL* region were PCR amplified. The two PCR fragments were isolated and used in a ligation reaction via the Gibson Assembly kit, with success suggested by agarose gel detection of additional ligation-specific bands (Figure 45B & 46B). Introducing some of the ligation reaction into NEB *E. coli* resulted in plasmid-containing (Cm resistant) colonies with PCR screening supporting the generation of pTET (Figure 46C) and pETE:HA (Figure 47C). Gene sequencing, using oligonucleotides upstream and downstream of the *sepL* gene, confirmed the successful generation of each chimera-encoding plasmid (not shown).

The plasmids were introduced into the *ΔsepL* mutant for the standard assays with control strains (Figure 48). The total bacterial extracts were examined for the aberrant migration phenotype by western blot probing for O127 antigen (Figure 48A). This revealed that the

ΔsepL mutant defect was, as expected, rescued by only one of the four of control plasmids i.e. pE (not pE:HA, pT or pT:HA) and one chimera-encoding plasmid, ETE (Figure 48A). Examining the secreted protein profile revealed that only pE and to a lesser extent, as before, pE:HA rescued the *ΔsepL* mutant secretion defects (Figure 47B). Probing the bacterial cell and/or supernatant samples revealed that the Tir and EspF cleavage phenotype was rescued by plasmid-expressing pE, pE:HA or pETE (Figure 48C & 48D). Probing for EspB secretion revealed the *ΔsepL* mutant defect was rescued by pE and, as before, to a lesser extent, pT and pE:HA but not the other plasmids (Figure 48D).

Probing isolated Triton X-100 soluble and insoluble fractions revealed that none of the chimera rescued the Tir delivery defect, with the data supporting Tir not being cleaved for the strains carrying pE, pE:HA or pETE (Figure 48E). These findings are supported by findings from an additional, independent experiment (Supplementary Figure 15), which also includes anti-Tir probing of cellular extracts and anti-HA probing of insoluble fractions that detected expression of both HA-tagged chimera (Figure 47D).

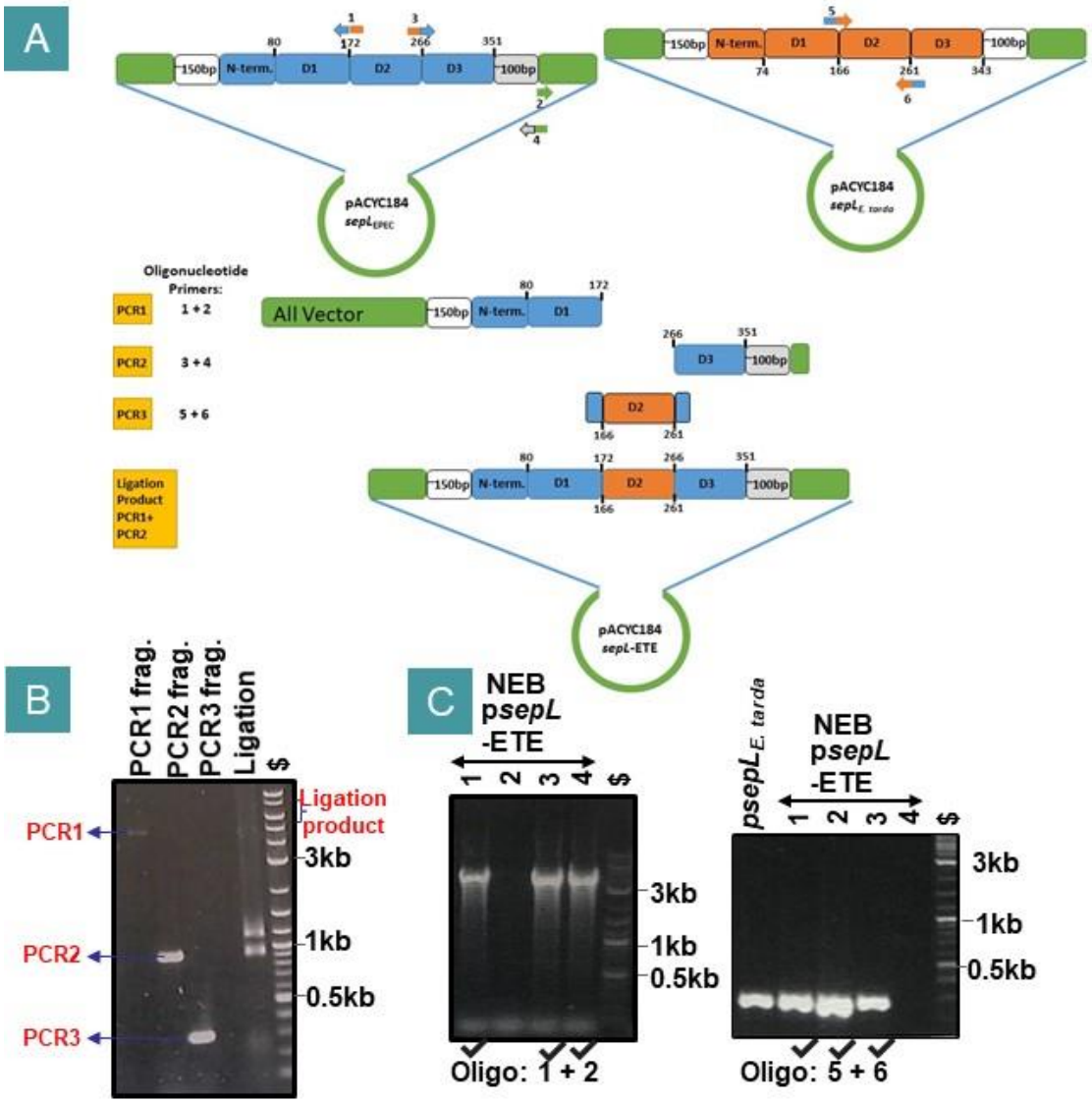

Figure 44: Generating a plasmid with EPEC SepL domain 2 swapped for that from *E. tarda*

(A) Schematic of the strategy for swapping EPEC SepL domain 2 for that from *E. tarda* to generate a chimera (SepL-ETE) fusion protein. The pACYC184-*sepL*$_{EPEC}$ plasmid was used as the template, with oligonucleotide primers 1 and 2 to amplify all the plasmid and the indicated *sepL* region, providing the 'PCR1' fragment. The same plasmid was used as the template, with oligonucleotide primers 3 and 4, to PCR amplify the domain3, and downstream EPEC *sepL* sequences providing the 'PCR2' fragment. The pACYC184-*sepL*$_{E. tarda}$ plasmid was used as the template, with oligonucleotide primers 5 and 6, to amplify the *E. tarda sepL* gene sequence encoding domain2 to provide the 'PCR3' fragment. Primer 5 and 6 have extensions to direct recombination-mediated ligation with the EPEC *sepL* sequences. B) PCR1, PCR2, and PCR3 fragments ligated using the Gibson Assembly Kit, with success evidenced by additional ligation-related bands with (C) PCR screening DNA from K12 E. coli (NEB) bacteria carrying the putative pACYC184sepL-ETE (psepL-ETE) plasmid supporting its presence in two strains. Samples were separated alongside 2 log molecular weight markers with the size of some indicated.

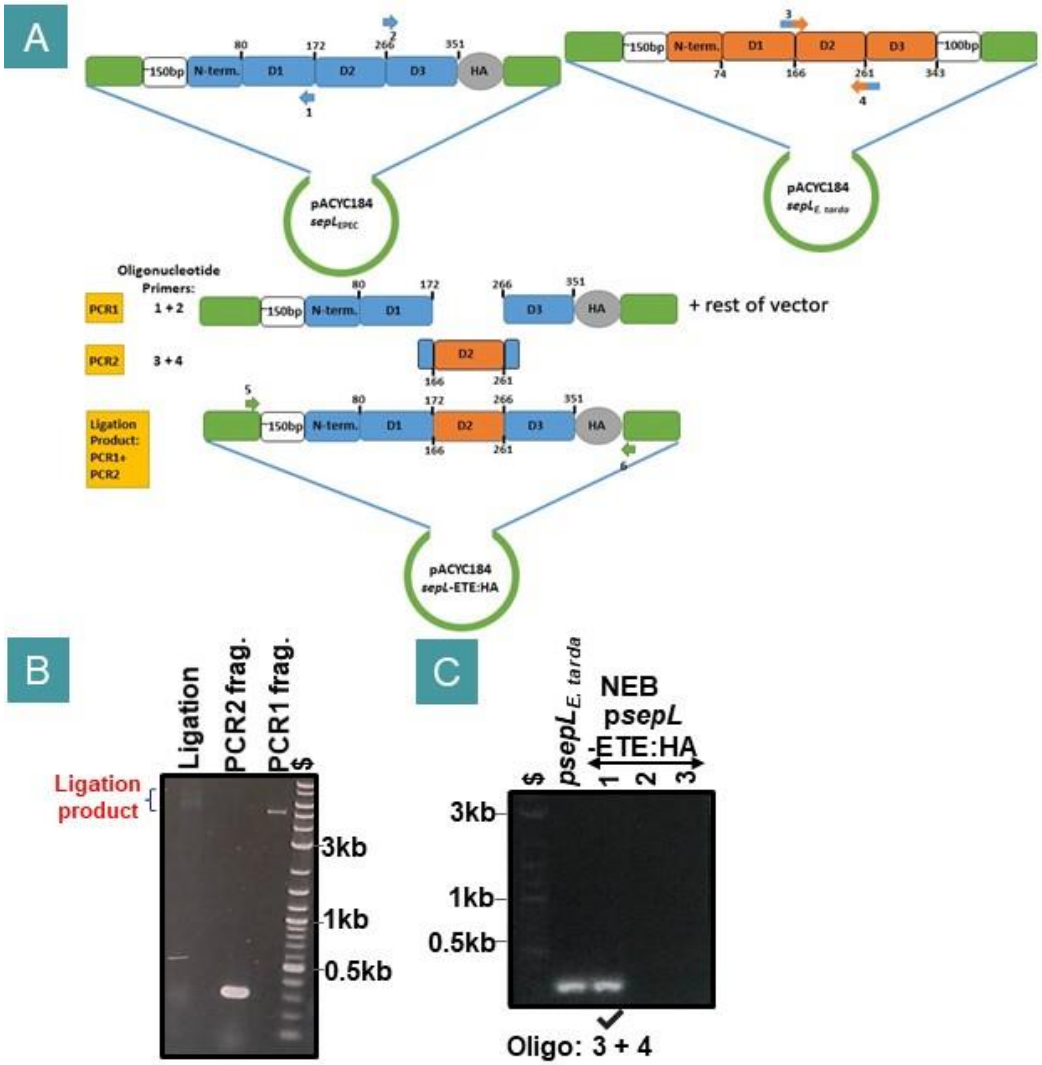

Figure 45: Generating a plasmid with *E. tarda* SepL domain2 swapped for that from EPEC

(A) Schematic of the strategy for swapping *E. tarda* SepL domain2 for that from EPEC to generate a chimera (SepL-TET) fusion protein. The pACYC184-*sepL*$_{E. tarda}$ plasmid was used as the template, with oligonucleotide primers 1 and 2 to amplify all plasmid and all *sepL*, except the domain2 encoding, related sequences to provide the 'PCR1' fragment. The pACYC184-*sepL*$_{EPEC}$ plasmid was used as the template, with oligonucleotide primers 3 and 4 to amplify the EPEC *sepL* domain2 encoding sequence, providing the 'PCR2' fragment. Primer 3 and 4 have extensions to direct recombination-mediated ligation with the *E. tarda sepL*-related sequence. Agarose gels showing (B) PCR1 and PCR2 fragments used for ligation, via Gibson Assembly Kit, with success evidenced by additional ligation-related bands with (C) PCR screening of DNA from K12 *E. coli* (NEB) bacteria carrying the putative pACYC184*sepL*-TET (p*sepL*-TET) plasmid supporting its presence in two strains. Samples were separated alongside 2 log molecular weight markers with the size of some indicated.

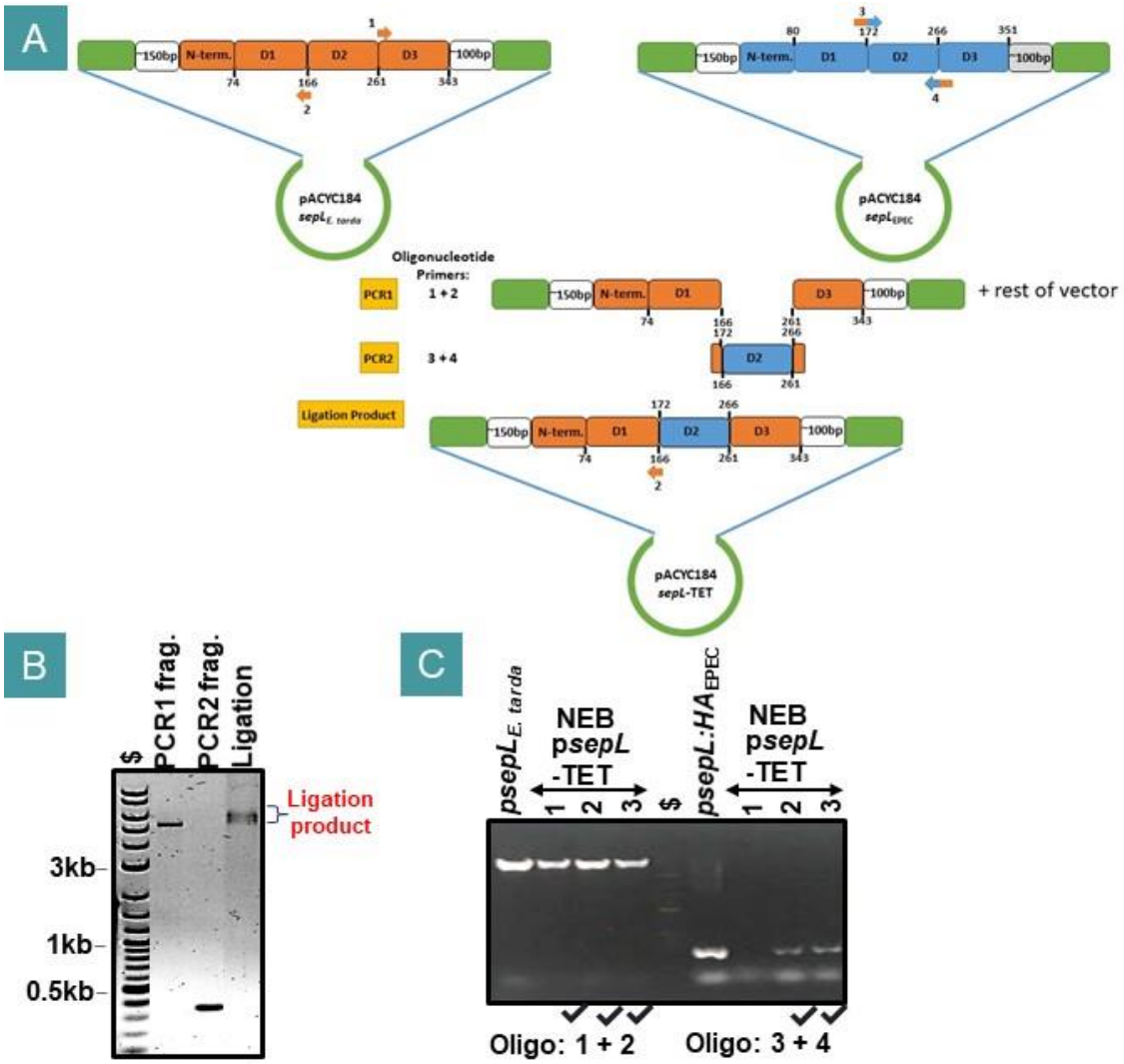

Figure 46: Generating a plasmid with the EPEC SepL domain 2 swapped for that of *E. tarda* to produce a HA-tagged chimera

(A) Schematic of the strategy for swapping EPEC SepL domain 2 for that from *E. tarda* to generate a chimera (SepL-ETE:HA) fusion protein. The pACYC184-*sepL*:HA$_{EPEC}$ plasmid was used as the template, with oligonucleotide primers 1 and 2, , to amplify all plasmid and all *sepL*, except the domain2 encoding, -related sequences to provide the 'PCR1' fragment. The pACYC184-*sepL*$_{E. tarda}$ plasmid was used as the template, with oligonucleotide primers 3 and 4 to amplify the *E. tarda sepL* domain 2 (T2) sequence, providing the 'PCR2' fragment. Primer 3 and 4 have extensions to direct recombination-mediated ligation with the *E. tarda sepL*-related sequences. B) PCR1 and PCR2 fragments used for ligation via Gibson Assembly Kit, with success evidenced by additional ligation-related bands with (C) PCR screening with total DNA from K12 *E. coli* (NEB) bacteria carrying the putative pACYC184sepL-ETE:HA (psepL-ETE:HA) plasmid, supporting its presence in the one tested strain. Samples were separated alongside 2 log molecular weight markers with the size of some indicated.

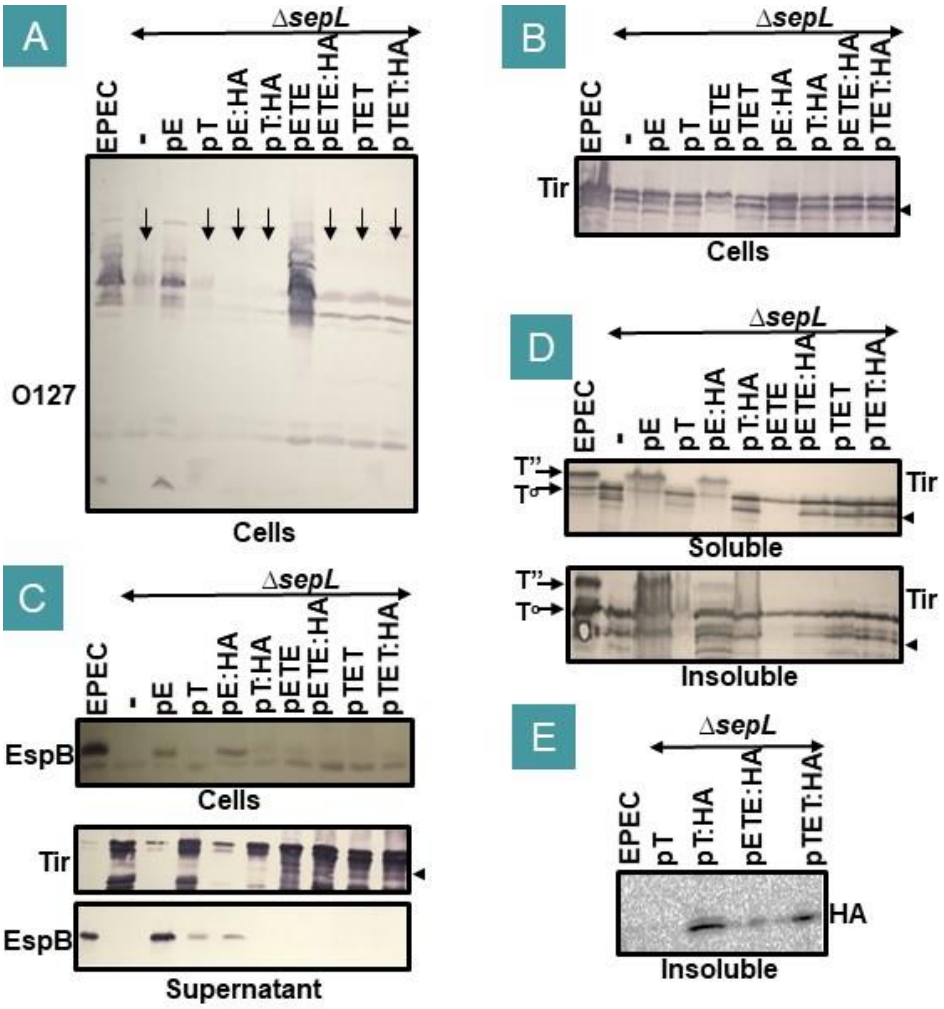

Figure 47: Assessing the impact of swapping domain2 on EPEC and *E. tarda* SepL functionality

Indicated strains were (A-D) added to DMEM (1:100 dilution of bacteria grown in LB overnight without shaking) for 8 hours before isolating total cell extracts and secreted (supernatant) proteins. Samples were resolved on 6% (A) or 12% (B-D) SDS-PA gels for Coomassie blue staining (B) or western blot analysis (A, C & D). Molecular standards are shown (KDa; B). (D) HeLa cells were fractionated, post infection, into Triton X-100 soluble (host cytoplasm/membrane proteins plus T3SS delivered EPEC effectors) and insoluble (contains host nuclei/cytoskeletal proteins plus adherent bacterial proteins) samples for Western blot analysis. Strains used were EPEC and the SepL-deficient mutant (*ΔsepL*); the latter with no (-) plasmid or, when indicated, a plasmid encoding EPEC SepL (pE), *E. tarda* SepL (pT), EPEC SepL:HA fusion protein (pE:HA), *E. tarda* SepL:HA fusion protein (pT:HA), SepL-TET chimera (pTET), SepL-TET:HA chimera (pTET:HA), SepL-ETE chimera (pETE), and SepL-ETE:HA chimera (pETE:HA). The positions of the unmodified (T^{o}) and host kinase-modified (T") Tir forms are shown. Down-ward pointing arrows indicate strains with *ΔsepL* mutant-like phenotype, with arrowheads indicating putative cleavage-related forms of the EspF and Tir effectors.

5.2.5 Impact of swapping domain3 on EPEC and *E. tarda* SepL functionality

The two PCR strategies were used to generate the domain3 swap variants as illustrated for the making of pTTE (Figure 49A) and pEET (Figure 50A). Steps in the generation of these two plasmids (Figure 49B & 50B) and PCR screening (Figure 49C & 50C) are shown. Gene sequencing confirmed the successful generation of these plasmids and those encoding the HA-tagged variants. Again, each plasmid was introduced into the *ΔsepL* mutant for assessment alongside control strains with probing of cellular extracts supporting expression of the HA-tagged chimera (Figure 50A).

Probing the isolated bacterial extracts for O127 antigen to examine the impact of swapping domain3 on the aberrant migration phenotype revealed that each chimera failed to rescue the defect (Figure 50B). Probing these and the supernatant samples for Tir suggested that the hypersecretion phenotype was rescued by each chimera - noting reduced cellular and secreted Tir by the pEET carrying strain (Figure 50C), with the Tir cleavage phenotype rescued by introducing the pTTE plasmid (Figure 50C). Probing for the EspB linked presence of all chimera plasmids, expect pEET, with increased cellular and, although weak, secreted levels (Figure 50C). Data from additional, independent experiments (Supplementary Figure 16 & Supplementary Figure 17).

Finally, examining the Triton X-100 soluble and insoluble fractions for Tir indicated that plasmid introduction of pTTE and, to a lesser extent, pTTE:HA restored Tir delivery (Figure 50D). By contrast, the strain expressing the pEET:HA variant did not deliver Tir, which, notably, was not detected in the fractions from cells infected with the pEET plasmid-complemented strain (Figure 50D).

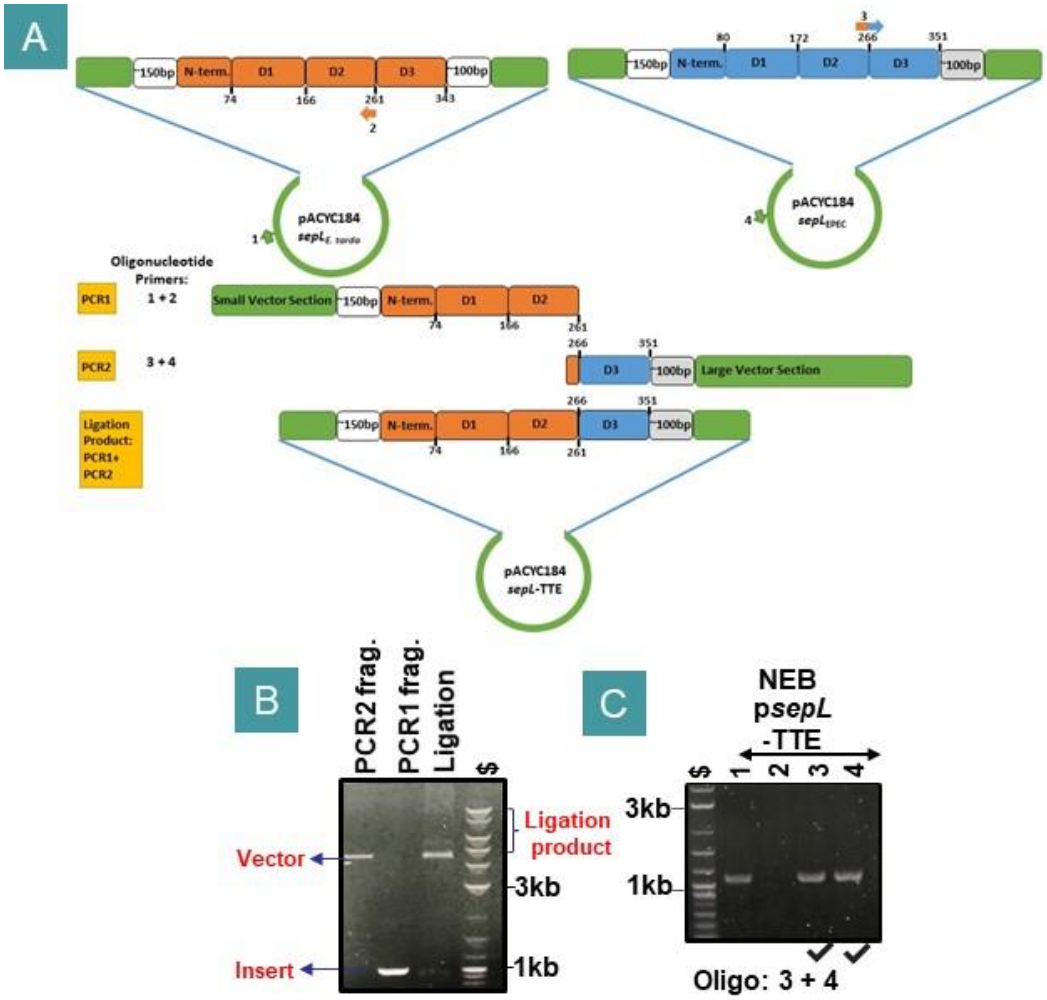

Figure 48: Generating a plasmid with the *E. tarda* SepL domain 3 swapped for that from EPEC

(A) Schematic of the strategy for swapping *E. tarda* SepL domain3 for that from EPEC to generate a chimera (SepL-TTE) fusion protein. The pACYC184-*sepL*:HA$_{E.\ tarda}$ plasmid was used as the template, with oligonucleotide primers 1 and 2, to amplify the *E. tarda sepL* gene to the end of the domain 2 sequence, with the indicated upstream vector region providing the 'PCR1' fragment. The pACYC184-*sepL*$_{EPEC}$ plasmid was used as the template, with oligonucleotide primers 3 and 4, to amplify the EPEC *sepL* gene sequence encoding domain 3 with downstream *sepL* and, as indicated, vector regions providing the 'PCR2' fragment. Primer 3 has an extension to direct recombination-mediated ligation between the EPEC and *E. tarda sepL* regions. Agarose gels showing (B) PCR1 and PCR2 fragments used for ligation, via Gibson Assembly Kit, with success evidenced by additional ligation-related bands with (C) PCR screening, using primer 3 and 5, with total DNA from K12 *E. coli* (NEB) bacteria carrying the putative pACYC184*sepL*-TTE (p*sepL*-TTE) plasmid supporting its presence in the two tested strains. Samples were separated alongside 2 log molecular weight markers with the size of some indicated.

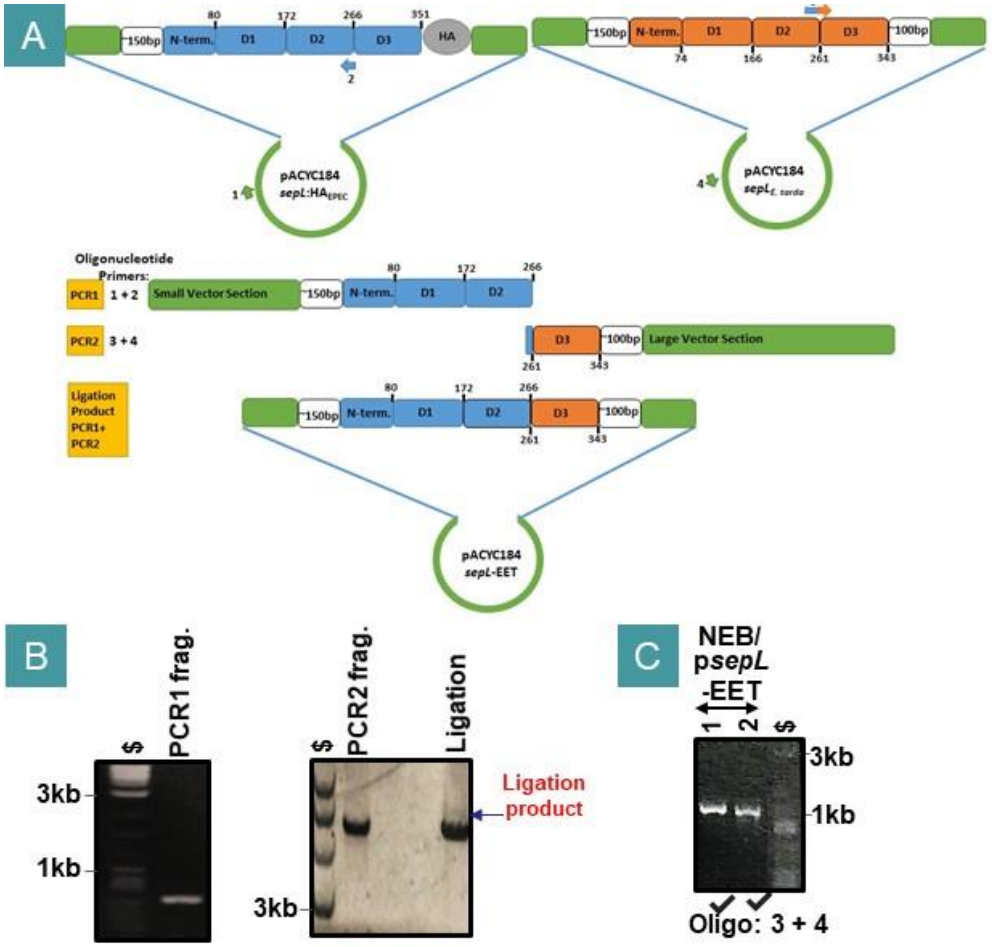

Figure 49: Generating a plasmid with the EPEC SepL domain3 swapped for that from *E. tarda*

(A) Schematic of the strategy for swapping EPEC SepL domain 3 for that from *E. tarda* to generate a chimera (SepL-EET) fusion protein. The pACYC184-*sepL*$_{EPEC}$ plasmid was used as the template, with oligonucleotide primers 1 and 2, to amplify the EPEC *sepL* gene to end of the domain 2 sequence, with the indicated upstream vector region providing the 'PCR1' fragment. The pACYC184-*sepL*:HA$_{E.\ tarda}$ plasmid was used as the template, with oligonucleotide primers 3 and 4, to amplify the *E. tarda* gene sequence encoding domain 3 with downstream *sepL* and, as indicated, vector regions providing the 'PCR2' fragment. Primer 3 has an extension to direct recombination-mediated ligation between the EPEC and *E. tarda sepL* regions. Agarose gels showing (B) PCR1 and PCR2 fragments used for ligation, via Gibson Assembly Kit, with success evidenced by additional ligation-related bands with (C) PCR screening, using primer 3 and 5, with total DNA from K12 *E. coli* (NEB) bacteria carrying the putative pACYC184*sepL*-EET (p*sepL*-EET) plasmid, supporting its presence in the two tested strains. Samples were separated alongside 2 log molecular weight markers with the size of some indicated.

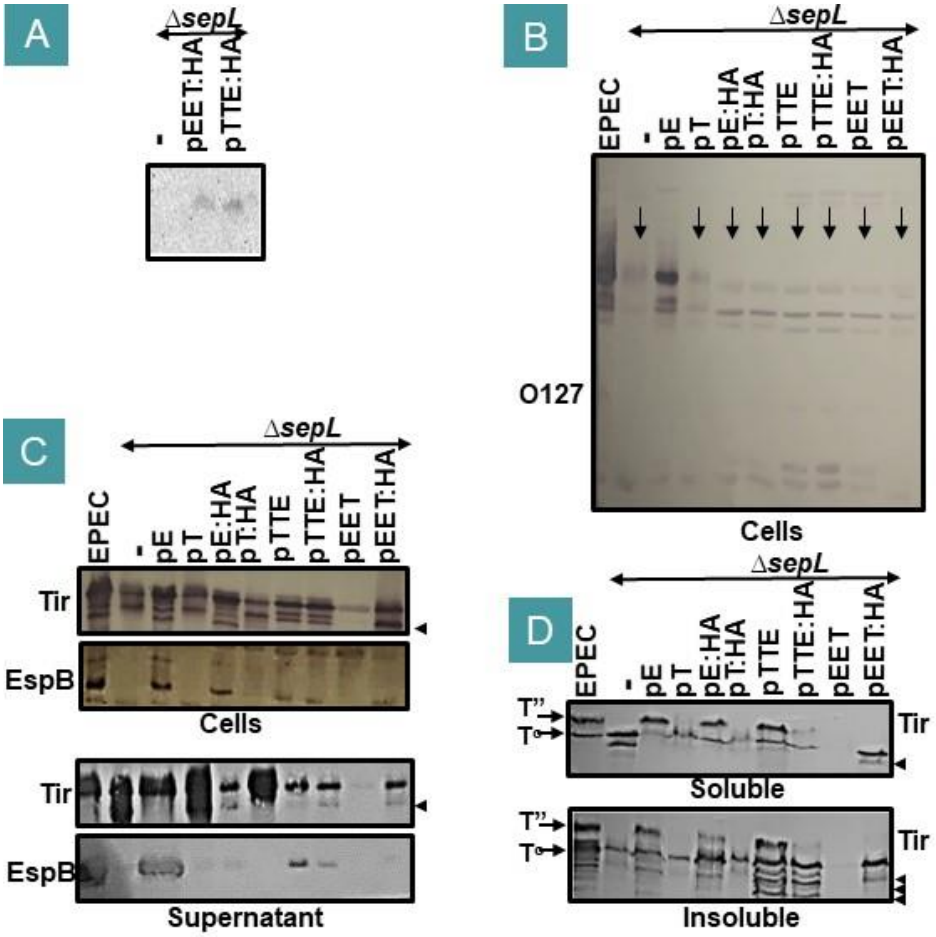

Figure 50: Assessing the impact of swapping domain3 on EPEC and *E. tarda* SepL functionality

Indicated strains were added to (A) LB or (B & C) DMEM or (D) HeLa cells. (A) LB was infected overnight (with shaking) before isolating total cell extract for Western blot analysis on 12% SDS-PA gel. (B & C) DMEM was infected (1:100 dilution of bacteria grown in LB overnight without shaking) for 8 hours before isolating total cell extracts and secreted (supernatant) proteins. Samples were resolved on 6% (B) or 12% (B & C) SDS-PA gels for western blot analysis. (D) HeLa cells were fractionated, post infection, into Triton X-100 soluble (host cytoplasm/membrane proteins plus T3SS delivered EPEC effectors) and insoluble (contains host nuclei/cytoskeletal proteins plus adherent bacterial proteins) samples for Western blot analysis. Strains used were EPEC and the SepL-deficient mutant (*ΔsepL*); latter with no (-) plasmid or, when indicated, a plasmid encoding EPEC SepL (pE), *E. tarda* SepL (pT), EPEC SepL:HA fusion protein (pE:HA), *E. tarda* SepL:HA fusion protein (pT:HA), SepL-TEE chimera (pTEE), SepL-TEE:HA chimera (pTEE:HA), SepL-ETT chimera (pETT) and SepL-ETT:HA chimera (pETT:HA). The positions of the unmodified (T^{o}) and host kinase-modified (T") Tir forms are shown. Down-ward pointing arrows indicate strains with *ΔsepL* mutant-like phenotype, with arrowheads indicating putative cleavage-related forms of the EspF and Tir effectors.

Strain	Plasmid	Shift				Tir cleavage		EspB		EspF cleavage		
		Coomassie	DnaK	O127	Tir hypersecretion	cell	sn	cell	sn	cell	sn	Tir delivery
EPEC		N	N	strong	N	N	N	Y	Y	N	N	Y
ΔsepL		Y	Y	weak	Y	Y	Y	N	N	Y	Y	N
ΔsepL	pE	EPEC	EPEC	EPEC	EPEC	EPEC	EPEC	EPEC	weak	EPEC	EPEC	EPEC
ΔsepL	PT	*ΔsepL*	*ΔsepL*	v weak	*ΔsepL*	*ΔsepL*	*ΔsepL*	weak	v weak	*ΔsepL*	*ΔsepL*	v weak
ΔsepL	pE::HA	*ΔsepL*	*ΔsepL*	no smear	EPEC	EPEC	EPEC	EPEC	v weak	EPEC	EPEC	EPEC
ΔsepL	pT::HA	*ΔsepL*	*ΔsepL*	no smear	*ΔsepL*	*ΔsepL*	*ΔsepL*	*ΔsepL*	*ΔsepL*	*ΔsepL*	*ΔsepL*	*ΔsepL*
ΔsepL	pHA:E	n	*ΔsepL*	no smear	*ΔsepL*	*ΔsepL*	*ΔsepL*	weak	v weak	*ΔsepL*	*ΔsepL*	EPEC
ΔsepL	pTEE	*ΔsepL*	*ΔsepL*	no smear	*ΔsepL*	*ΔsepL*	*ΔsepL*	EPEC	*ΔsepL*	n	*ΔsepL*	*ΔsepL*
ΔsepL	pTEE::HA	*ΔsepL*	*ΔsepL*	no smear	*ΔsepL*	*ΔsepL*	*ΔsepL*	EPEC	*ΔsepL*	n	*ΔsepL*	*ΔsepL*
ΔsepL	pETT	*ΔsepL*	*ΔsepL*	no smear	*ΔsepL*	*ΔsepL*	*ΔsepL*	EPEC	*ΔsepL*	n	*ΔsepL*	*ΔsepL*
ΔsepL	pETT::HA	*ΔsepL*	*ΔsepL*	no smear	*ΔsepL*	*ΔsepL*	*ΔsepL*	EPEC	*ΔsepL*	n	*ΔsepL*	*ΔsepL*
ΔsepL	pETE	n	n	EPEC	EPEC	EPEC	*ΔsepL*	*ΔsepL*	*ΔsepL*	*ΔsepL*	n	*ΔsepL*
ΔsepL	pETE::HA	n	n	no smear	*ΔsepL*	*ΔsepL*	*ΔsepL*	*ΔsepL*	*ΔsepL*	*ΔsepL*	n	*ΔsepL*
ΔsepL	pTET	n	n	no smear	*ΔsepL*	*ΔsepL*	*ΔsepL*	*ΔsepL*	*ΔsepL*	*ΔsepL*	n	*ΔsepL*
ΔsepL	pTET::HA	n	n	no smear	*ΔsepL*	*ΔsepL*	*ΔsepL*	*ΔsepL*	*ΔsepL*	*ΔsepL*	n	*ΔsepL*
ΔsepL	pEET	*ΔsepL*	n	no smear	v weak	EPEC	vv weak	*ΔsepL*	*ΔsepL*	n	n	****
ΔsepL	pEET::HA	*ΔsepL*	n	no smear	EPEC	*ΔsepL*	EPEC	weak	vv weak	n	n	*ΔsepL*
ΔsepL	pTTE	*ΔsepL*	n	no smear	EPEC	EPEC	EPEC	weak	weak	n	n	EPEC
ΔsepL	pTTE::HA	*ΔsepL*	n	no smear	EPEC	EPEC	EPEC	weak	v weak	n	n	v weak

Table 9: Summary table of chimera protein findings

The table summarize the western blot and Coomassie data for 12 chimera proteins; ‘n’ indicates currently none or no clear data, while weak and very weak phenotype are indicated by light and dark grey highlighting respectively.

5.3 Discussion

In this chapter, the generation of HA-tagged and domain-swapped (between EPEC and *E. tarda* homologs) SepL variants are described with functional studies providing some insight on the domain involved in SepL's role in translocator secretion, effector delivery, controlling the O127 antigen cellular level, and preventing the effector cleavage.

Unlike EPEC, SepL *E. tarad* is found to be encoded by two open reading frames that may be linked to partially substituting for its EPEC counterpart. Thus, it was important to examine if the *2-orf* encoded protein was expressed as a single, full-length protein and at a comparable level to the EPEC variant. The study confirmed the expression of similar-sized, full-length EPEC and *E. tarda* SepL. It is also confirmed that the high-level expression of SepL *E. tarda* protein compared to SepL EPEC evident in K12 *E. coli*. Thus, the weak functionality of SepL *E. tarda* is not related to the protein expression problem but to most sequence divergence.

Furthermore, tagging the C-terminus shows that the HA tag interferes with SepL functionality, which is linked to reducing the cellular and secreted level of the translocator with a decreased amount of Tir delivery, resulting in the aberrant protein migration phenotype. These findings reveal a role for the C-terminal end of this gatekeeper in regulating these events, probably due to the HA extension hindering interaction with partner proteins. This data appears to align with the data that confirms the labeling of SepL protein with e-GFP in EHEC O157:H7 rescued the mutant defect from restoring the translocator secretion but not the wild type of profile (Wang *et al.*, 2008). However, this finding contradicts previous studies, which have suggested that the HA did not affect the SepL protein functionality in the mouse pathogen *Citrobacter rodentium* (CR) (Deng *et al.*, 2005). These disagreements could be due to the divergence of the protein sequence between the homologs.

As it would have been very useful to have a fully functional, epitope-tagged, EPEC SepL protein, an HA-SepL variant was generated and assessed. Interestingly, tagging the N-terminal of SepL EPEC restored the T3SS defects but not the new phenotypes (aberrant protein migration and the effector cleavage) of *ΔsepL*. Therefore, the SepL amino terminus must be accessible to restore all the mutant defects. As reported, SepL protein has a T3SS signal in its N-terminal; however, this protein was not secreted. The CesL (SepL chaperone) interaction site on SepL is in N-terminal within residues 30 -75 (Díaz-Guerrero *et al.*, 2021), this complex is vital to regulate the secretion hierarchy and protein stability within the bacterial cell (Díaz-Guerrero *et al.*, 2021). It's possible that SepL partners, particularly CesL (which interacts with SepL's N-terminus), play a role in SepL mutant phenotypes, and that the presence of HA hinders this contact, resulting in abnormal protein migration through the SDS page. Of note, the last observation with CesL protein proves anomalous migration of cell extract from CesL on SDS-PAGE when this protein is tagged N-terminally (Díaz-Guerrero *et al.*, 2021).

The bioinformatics analysis confirmed the presence of a significant divergence across T3SS LEE -encoded homologs, and the weak functionality of T3SS proteins might rely on the sequence differences. The previous work shows the residues replacing technique between EPEC and *E. tarda* homologs highlighted the vital region for T3SS functionality. The study uses the partial complementation translocator protein EspA and found that replacing 10 *E. tarda* with 9 EPEC residues (129-137) rescued the T3SS functionality for EPEC *ΔespA* (Madkour *et al.*, 2021). Therefore, studies in this chapter aimed to use a domain swapping method to identify the domain of SepL proteins, which is essential in SepL biology and functionality. Hence, the aim of reciprocally swapping X-bundle domains 1, 2, and 3 would be generated with and without HA tags; the former would be allowed expression levels to be compared and identify HA-specific differences.

Initial attempts to generate the chimera proteins were hindered by oligonucleotide design and /or domain swap strategy (and Covid 19 lockdown) issues but all 12 chimeras were generated as supported by DNA sequencing. The domain swapping strategy for SepL protein is designed to swap domains and keep the N-terminal stable when replacing any of the *E.*

tarda domains with EPEC, and the opposite is correct. Except for one feature, replacing both *E. tarda* and EPEC domain one with the opposite variant did not rescue the *sepL* defect. All domain one chimeras have an EPEC like EspB level within the strain and, possibly unlike EPEC undetectable levels were secreted. The ETT (EPEC domain 1; *E. tarda* domain 2,3) chimera suggests that the N-terminal/domain 1 region is dependent on a feature in the EPEC SepL domain 2 or domain 3 regions for the majority of its functions. Furthermore, the TEE chimaera defect (EPEC domain 2, 3 plus upstream N-terminal region swapped for *E. tarda*) is predicted to be caused by a change in the 30AA region of the *E. tarda* variant upstream of the CesL binding site (8 substitutions plus deletions).

This domain starts from residue 80 to residue 172 in EPEC (Burkinshaw *et al.*, 2015). However, it starts from residue 74 to residue 166 in *E. tarda*. Moreover, the bioinformatics analysis revealed many critical points. First, this domain seems to be sharing a low level of identity between these two homologs. Second, this domain in SepL EPEC consists of the important region for SepD interaction (14 aa from 81 to 94), and *E. tarda* shares 11 out of 14 of these residues. Finally, another point confirming the importance of this domain is the presence of sits (a, b), which is vital for gatekeeper receptor function (Portaliou *et al.*, 2017). There is a considerable difference between the residues in these patches (especially patches a) in both homologs. Thus, a domain one data swapping may suggest some possibilities, such as replacing patches a and b or the important amino acid for SepD interaction with their EPEC homologous, which may activate SepL E. tarda to rescue EPEC mutant functionality. However, it is more likely that the interaction between the three domains of the SepL protein is required to rescue all of the mutant defects. This is obvious from the bioinformatics analysis of the patches responsible for the translocator-chaperone and SepL interactions, which are divided between the three domains in SepL EPEC (Portaliou *et al.*, 2017).

Replacing domain 2 of SepL EPEC with *E. tarda* suggests the importance of domains 1, 3 of SepL EPEC to rescue the new *ΔsepL* defects (preventing aberrant protein migration and effector cleavage phenotypes). However, the HA-tagged variant (ETE: HA), consistent with EPEC: HA data, had no such activity. These results suggest that the ability of EPEC SepL to

prevent the aberrant protein migration and effector cleavage does not require features in domain 2 or these features are conserved in the *E. tarda* SepL domain 2, as domain 2 of *E. tarda* SepL has a high level of identity with SepL EPEC. To narrow this hypothesis, further research should replace domain 2 with a linker to confirm the crucial role of domains 1, 3 in the new SepL protein phenotypes. This finding raises the opportunity for domains one and three, which are vital for new SepL phenotypes, and domains 1, 2, and 3 which are vital for T3SS functionality, as this construct did not rescue the T3SS functionality to *ΔsepL*. Note, generation of pETE is done by using three regions in ligation, and the plasmid sequencing confirmed the right construct as a first attempt did not succeed. Domain 2 in SepL EPEC starts from residue 173 to residue 266 (Burkinshaw;Souza and Strynadka, 2015), although in *E. tarda,* domain 2 is located between residue 167 and 260. Domain 2 has two important regions in translocator secretion (patches c and d). Patches c seem to be conserved between SepL homologs, and patches d have a high level of similarity between SepL homologs. Although the last region is critical for EscV-SepL crosstalk (Portaliou *et al.*, 2017), replacing it with EPEC in *E. tarda* does not rescue translocator secretion. These findings highlight again that domains one, two, and three of SepL EPEC are important to restore the T3SS functionality to *ΔsepL*.

The most exciting finding comes from swapping domain three between SepL EPEC and *E. tarda*. Indeed, replacing domain 3 of *E. tarda* SepL with its homologs in EPEC rescues all mutant defects except the O127 profile. This chimera prevented the effector cleavage (best seen in Suppl. Figure 16) and delivered Tir into the HeLa cell. However, the presence of HA decreases the amount of Tir delivered to the host cell, inconsistent with SepL EPEC: HA. Surprisingly, replacing domain 3 of EPEC SepL with *E. tarda* seems to express a tiny level of Tir. Further repeat studies are needed to confirm this finding and to interrogate whether it relates to Tir expression (at transcription or translation level) or intracellular stability later linked to CesT activity. In contrast, the presence of HA appears to increase the level of Tir expression. Furthermore, by restoring translocator secretion but not effector delivery to sepL, this construct (EET: HA) can weakly rescue T3SS functionality. A possible explanation for these results may be the HA sequence compensating for the missing residues in *E. tarda* domain 3.

Domain 3 SepL EPEC is situated between 267-351 residue in EPEC (Burkinshaw *et al.*, 2015) and 261-343 in *E. tarda*. The previous report shows that the last 48 amino acids in SepL EPEC are essential in SepL Tir interaction. This interaction is vital in controlling effector secretion (Wang *et al.*, 2008). Moreover, this domain includes the two important regions for EscV and translocator interaction (Portaliou *et al.*, 2017).

In summary, the findings in this chapter suggest the importance of all three domains in SepL EPEC functionality. Moreover, the data is consistent with the finding that many SepL activities depend on partners' proteins interacting with multiple domains. However, the interaction between two domains (domains 1, 3 of SepL EPEC) can restore the normal aberrant migration phenotype to *ΔsepL*. Interestingly, this activity is compromised by HA epitope tag extension at the N-or C-terminal end. Moreover, the ability to protect Tir and EspF from cleavage appears to depend on EPEC specific features in SepL domain 3. However, this interpretation is questioned by the failure of the TEE unlike the ETE and TTE variants to prevent the effector cleavage. By contrast, translocator secretion appears to depend on EPEC specific features in all three SepL domains. Interestingly, Tir delivery into HeLa cells is linked to the EPEC specific features in domain 3, but this interpretation is questioned by the failure of the ETE and TEE variants to enable Tir delivery.

Despite the limited time due to a covid lockdown, 12 different chimeras have been constructed, sequenced, and examined. However, some analyses had a negative impact, such as i) Coomassie staining of cell and supernatant samples for each experiment as well as anti-DnaK data: studies relied upon anti-O127 as a marker for the aberrant migration phenotype. ii) anti- HA analysis on all bacterial cell and Hela insoluble fractions. Moreover, the PCR data using oligonucleotides specific for each chimera should have been carried out on non-adherent bacteria (isolated from Hela infected cells) to confirm that each strain carried the appropriate chimera with anti-HA probing to determine if it is an epitope-tagged variant or not.

Chapter6: Final discussion

The research described in the thesis not only confirmed the weak functionality of five *E. tarda* proteins to restore the T3SS activity of their EPEC counterparts but also discovered novel properties for a gatekeeper protein (SepL), an effector (EspF), two basal body proteins (EscC, EscD) and three chaperone proteins (CesT, CesAB, and CesD2).

Complementation studies on the *ΔsepL* mutant supported earlier findings that T3SS functionality cannot be restored by *E. tarda* SepL. Moreover, this thesis work revealed two novels' functions for the *ΔsepL* mutant: faster migration of proteins through SDS-PA gels and cleavage of at least two effectors (EspF and Tir; latter in its C-terminal domain). This aberrant migration phenotype was originally observed on SDS-PA gels but can also be monitored by western blot probing for the EPEC Intimin surface and DnaK cytoplasmic proteins. Unexpectedly, studies with 30 LEE gene-deficient mutant strains showed that *ΔescD, ΔescC, ΔcesT, ΔcesAB, ΔcesD2,* and *ΔespF* mutant strains shared the aberrant protein migration phenotype, whereas *ΔcesT, ΔcesD2*, and *ΔcesAB* mutant strains shared the EspF cleavage phenotype. By contrast, the Tir cleavage event was unique to the *ΔsepL* mutant. The reintroduction of the EPEC version of these proteins through a plasmid addressed these problems. However, the *E. tarda* version failed to substitute the missing gene. Therefore, the studies in this thesis focused on different aspects of these findings.

Data presented in these studies linked the aberrant protein migration phenotype to the cellular O127 antigen levels. This discovery was based on the finding that an EPEC 2348/69 strain provided by another research group (Yen *et al.*, 2010) shared the *ΔsepL* mutant phenotype and had been found to carry an undocumented 50kb deletion (Madkour *et al.*, 2021). Interestingly, multiple LEE proteins controlling O127 antigen levels support the idea that T3SS proteins have cryptic functions (Katsowich *et al.*, 2017). Notably, a T3SS protein in an EPEC-related strain, EHEC O157, called YgiL was reported to regulate the chains length of O-antigen. Indeed, short O-antigen chain promoted bacteria attachment through increased T3SS effector injection in epithelial cells, leading to enhanced EHEC infectivity (Liu *et al.*,

2021). Further studies are required to determine if SepL, and the other 6 T3SS proteins, impact on O127 antigen levels at the expression or chain-length.

Levels which are detected by altered protein migration on SDS-PA gels. There are likely connections between the SepL protein, O-and M-antigens production as well as other cellular processes that reduce the EPEC's capacity to grow in DMEM and LB. Another evidence that SepL affects cellular processes is the outcome of proteomic analysis conducted through mass spectrometry, which established that EPEC and *ΔsepL* mutants had significant differences. Future studies should remove the O-antigen genes, the M-antigen genes, and the O-and M antigen genes to regenerate the 50 kb deletion. This approach will facilitate exploring how exopolysaccharides contribute to western data profile and aberrant migration phenotype. Studies that investigate different phenotypes can reveal more T3SS crosstalk and pathotype-specific functions that can be used to develop new therapeutic targets.

The EscU protein was shown to be critical for the cleavage phenotype. The EscU protein has the role of a protease that links the T3SS substrate switch to the translocator proteins from the needle component (Liu *et al.*, 2021). In the future, studies should isolate a C-terminal cleavage product and define the cleavage site through mass spectrometry or N-terminal sequencing. Further studies should demonstrate that the cleavage event forms part of the regularity circus, which limits access of the effector to the T3SS.

Studies with epitope-tagged variants show that expression of the 2-orf *E. tarda sepL* gene in EPEC results in the production of the full-length protein (Madkour *et al.*, 2021). The expression of the full-length protein or the functional T3SS protein involves mechanisms mediated by ribosomes (by jumping, read-through, and slippage), which regulate the cellular processes such as T3SSs (Weiss, 1991). Therefore, the defect in *E. tarda* SepL results from divergence of sequences rather than expression issues. Compared to the untagged one, the tagging approach of C-terminal HA affects the SepL protein functionality, resulting in reduced

cellular and secreted levels of translocator proteins with the low level of Tir expression and delivery, also have an aberrant protein migration phenotype. The findings indicate that the C-terminal has a unique expression of the phenotype and the interaction with partner proteins is hindered in the presence of a HA tag.

The SepL *E. tarda* protein lacked the functional capacity to replace its EPEC counterpart. Domain swapping experiments established that SepL EPEC had features in its domain one and N-terminal. However, these features were absent from the corresponding *E. tarda* region, making it difficult for SepL *E. tarda* to have its complete functions. However, the ETT chimaera basically failed to rescue any defects, implying that the N-terminal domain one region requires features in the EPEC SepL domain 2 or domain 3 region for most of its functions. Thus, future research should consider domain swapping experiments and the introduction of specific substitution in *E. tarda*. The latter experiment could be aided by data on the SepL variant from a protein database and compared to other A/E pathogens that have residues changed in the *E. tarda* variant.

According to the domain 2 swapping experiments, SepL EPEC domains 1, 3 can prevent the migration of aberrant protein and cleavage of effector protein. Swapping of domain 3 of *E. tarad* with EPEC demonstrates the importance of domain 3 of SepL EPEC in restoring translocator secretion effector delivery and inhibition of effector cleavage. The phenotype nonetheless failed to be restored in the TEE (domain 2, 3 SepL EPEC) and ETE (domain 1, 3 SepL EPEC), suggesting this restoration appears to be tied to this structure rather than a particular domain. Based on these findings, the domain 3 chimeras should be reanalyzed in future studies to support the data obtained in the present research. Chances of having another domain swap experiment are increased by the re-linking of Tir delivery activity, prevention of aberrant protein migration, and cleavage of Tir/EspF. These findings could also influence studies on residue substitutes, which reintroduce specific changes in *E. tarda* leading to insights on important features or residues of EPEC SepL.

In conclusion, the data has a high consistency with previous findings showing an association between SepL activities and residues interacting with multiple domains (Portaliou *et al.*, 2017). Moreover, the data showed that SepL has not only T3SS functions as a gatekeeper and /or molecular switcher, but there are other unknown functions, where earlier studies had not previously noted, this study emphasized it, and opened the door for more investigation.

Supplementary Data

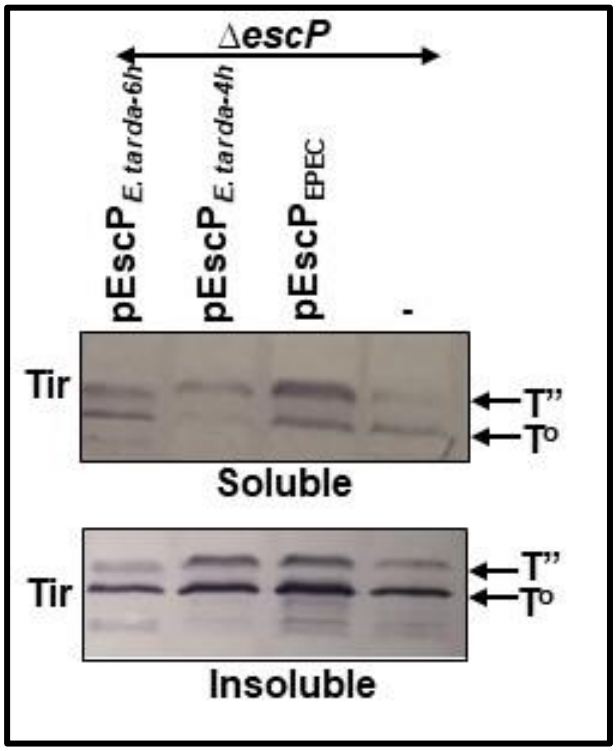

Supplementary Figure 1: *E. tarda* EscP restore Tir delivery

Indicated strains were used to infect HeLa cells. HeLa cells were infected for 4 hours before isolating Triton X-100 soluble (contains host cytoplasm/membrane proteins and T3SS delivered EPEC effectors) and insoluble (contains host nuclei/cytoskeletal proteins and adherent bacterial proteins) fractions. Samples were resolved on 12% SDS-PA gels for western blot analysis to probe for an effector (Tir) protein. The positions of the unmodified (T^{o}) and host kinase-modified (T") Tir forms are shown. Strains used were EPEC, T3SS-deficient mutant (T3SS) and Δ*escP* mutant; latter having no introduced plasmids (-) or a plasmid-encoding EPEC EscP ($pEscP_{EPEC}$) or *E. tarda* EscP ($pEscP_{E.\ tarda}$) proteins.

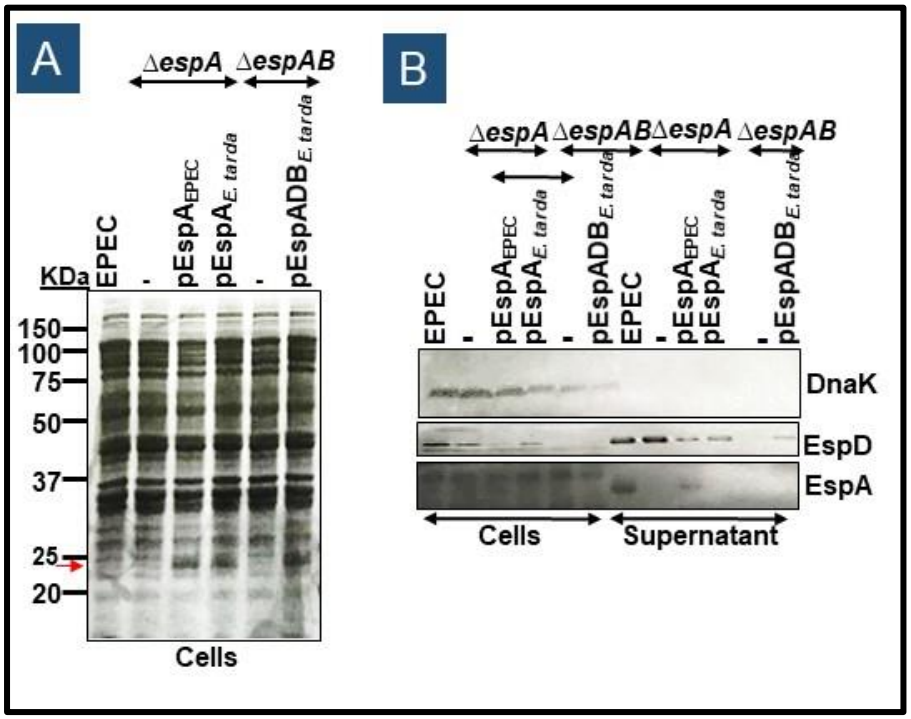

Supplementary Figure 2: *E. tarda* EspA weakly substitutes EPEC EspA unless co-expressed with the other *E. tarda* translocators

The indicated strains were used to infect (A-B) DMEM. The DMEM was infected (1:100 dilution of bacteria grown overnight in LB) for 8-hours before isolating total bacterial cells and secreted (supernatant) proteins. Samples were resolved on 12% SDS-PA gels for (A) Coomassie blue visualisation and for (B) western blot analysis to probe for the translocators (EspA, EspD), and DnaK (bacterial cytoplasmic protein as a gel loading control). The position of the molecular weight standards (kDa) is shown (A). Strains used were EPEC, *ΔespA* single mutant and *ΔespAB* double mutant; the latter carrying no introduced plasmids (-) or a plasmid-encoding EPEC EspA (pEspA$_{EPEC}$), *E. tarda* EspA (pEspA$_{E.\ tarda}$) or *E. tarda* EspA/D/B (pEspADB$_{E.\ tarda}$) proteins.

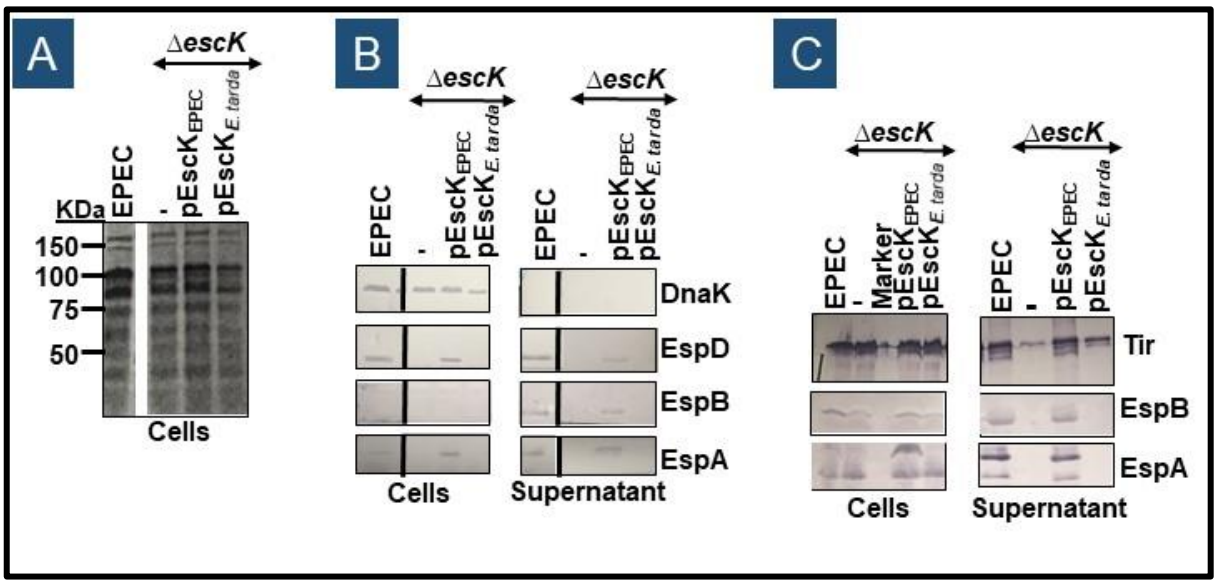

Supplementary Figure 3: *E. tarda escK* does not functionally substitute EPEC *escK*

Indicated strains were used to infect (A-C) DMEM. The DMEM was infected (1:100 dilution of bacteria grown overnight in LB) for 8-hours before isolating total bacterial cells and secreted (supernatant) proteins. Samples were resolved on 12% SDS-PA gels for (A) Coomassie blue visualisation and for (B-C) western blot analysis to probe for the translocators (EspA, EspB, EspD) and DnaK (bacterial cytoplasmic protein as a gel loading control). The position of the molecular weight standards (kDa) is shown (A). Strains used were EPEC and the Δ*escK* mutant; the latter carrying no introduced plasmids (-) or a plasmid carrying the EPEC (pEscK $_{EPEC}$) or *E. tarda* (pEscK $_{E.\ tarda}$) genes.

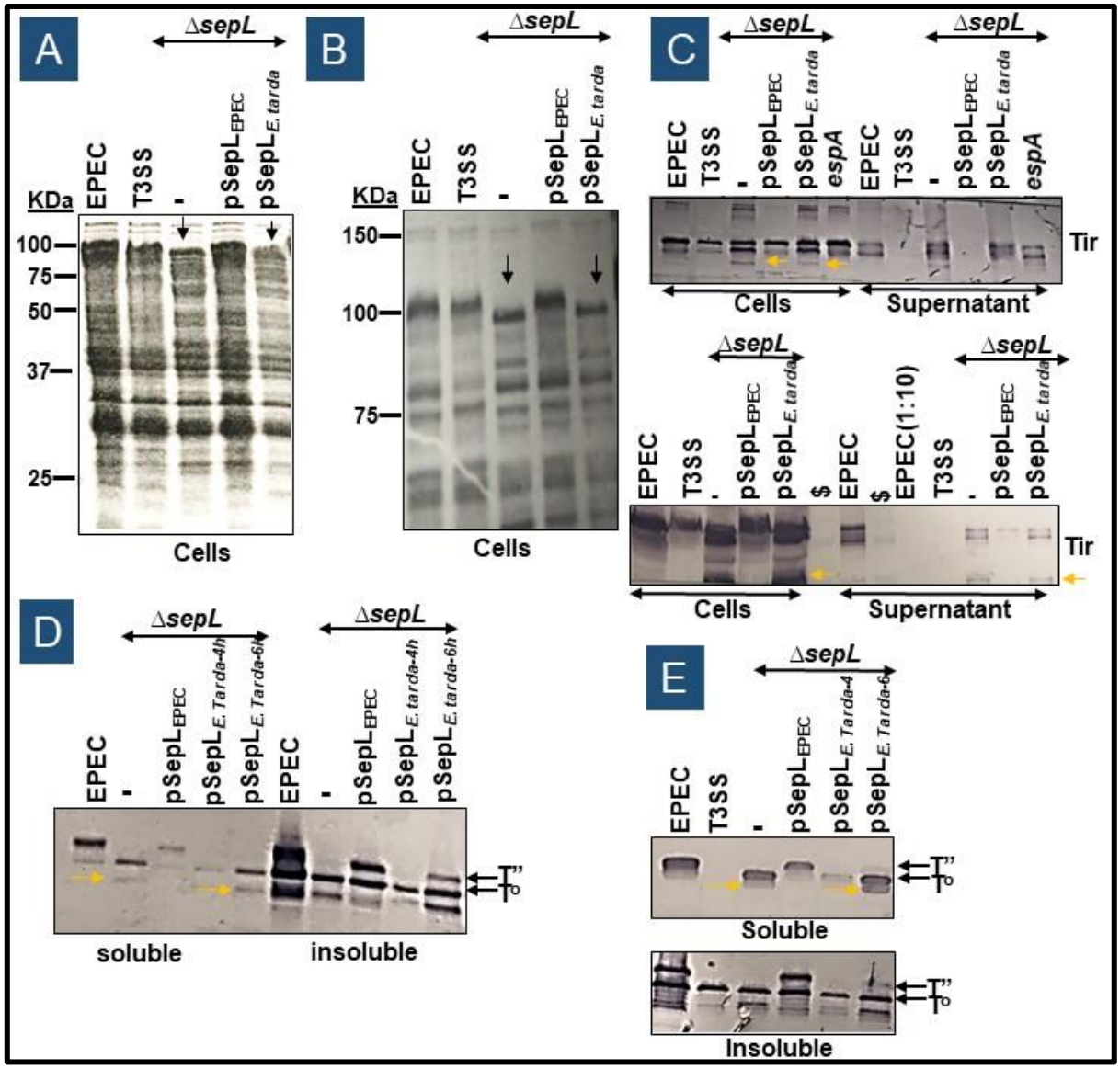

Supplementary Figure 4*: E. tarda* SepL weakly substitutes to promote translocator secretion and delivery of Tir into HeLa cells

Indicated strains were used to infect (A-C) DMEM and (D-E) HeLa cells. The DMEM was infected (1:100 dilution of bacteria grown overnight in LB) for 8-hours before isolating total bacterial cell and secreted (supernatant) proteins. HeLa cells were infected for 4 and, when indicated, 6-hours before isolating Triton X-100 soluble (contains host cytoplasm/membrane proteins and T3SS-delivered EPEC effectors) and insoluble (contains host nuclei/cytoskeletal proteins and adherent bacterial proteins) fractions. Samples were resolved on 12% SDS-PA gels for (A-B) Coomassie blue visualisation and for (C-E) western blot analysis to probe for the Tir (an effector). The positions of the unmodified (T^{o}) and host kinase-modified (T") Tir forms are shown. The position of the molecular weight standards (kDa) is shown (A). Strains used were EPEC and the Δ*sepL* mutant; the latter carrying no introduced plasmids (-) or a plasmid carrying the EPEC (pSepL $_{EPEC}$) or *E. tarda* (pSepL$_{E. tarda}$) genes.

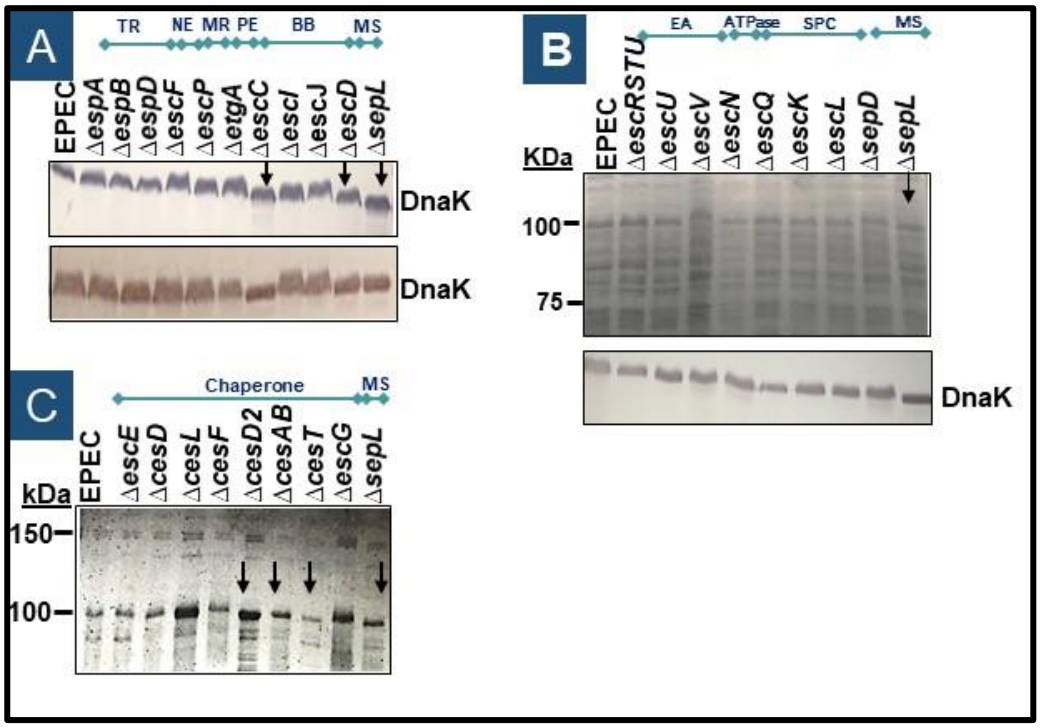

Supplementary Figure 5: *ΔsepL* 'aberrant protein migration' phenotype is shared by other T3SS mutants

Indicated strains were used to infect DMEM (1:100 dilution of LB overnight bacteria) for 8-hours before isolating total bacterial cell samples for separation on SDS-PA gels - 6 % for Coomassie blue visualisation and 12% for western blot analysis to probe for DnaK. Molecular standards are shown (KDa) for Coomassie blue stained gels. The strains were analysed in clusters relating to the role of the missing gene in T3SS functionality using the following abbreviations: TR (Translocators), NE (Needle proteins), MR (Molecular Ruler), PE (Peptidoglycan enzyme), BB (Basal body components), MS (Molecular switches), EA (Export Apparatus components), ATPase (ATPase complex components), SPC (Sorting Platform Complex proteins). Other examined genes encoded chaperone protein. Down-ward facing arrows indicate strains with the *ΔsepL* mutant-like phenotype.

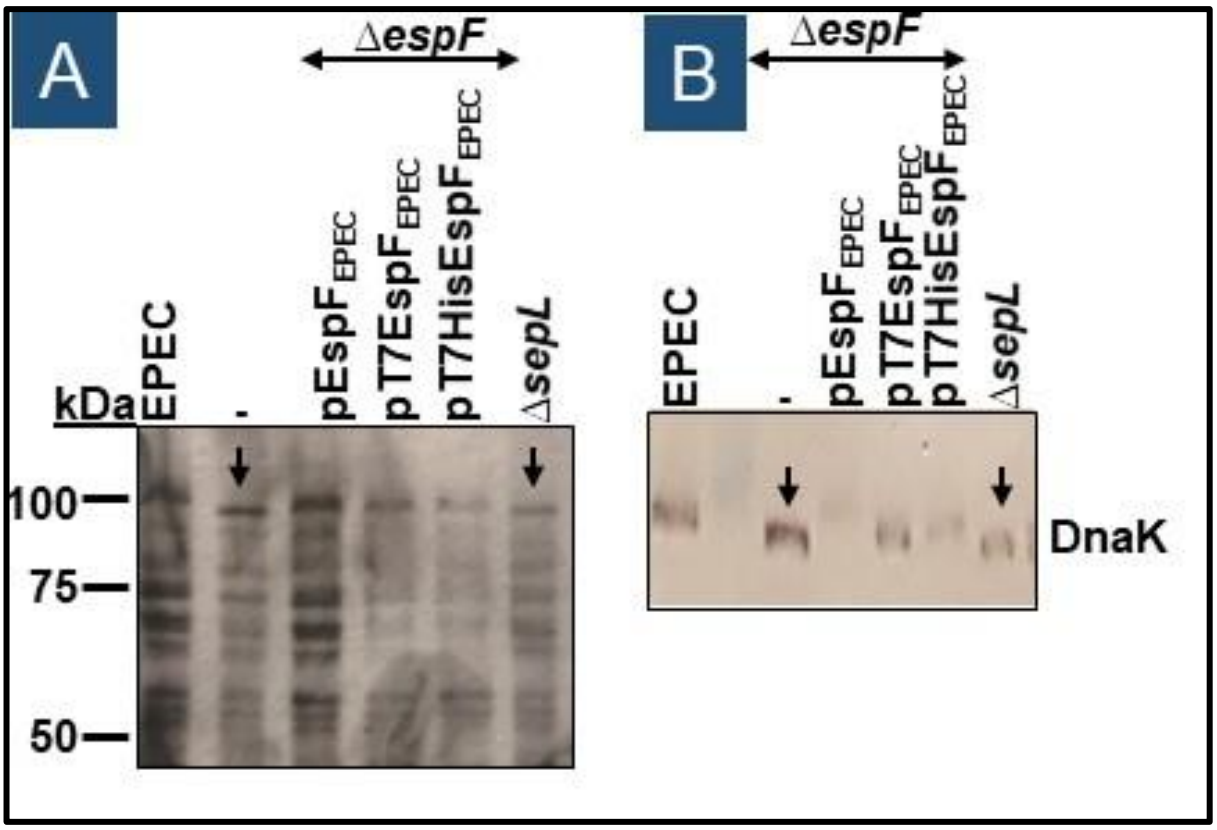

Supplementary Figure 6: The aberrant protein migration' phenotype of *ΔespF* mutant is rescued by a plasmid introducing the EPEC *espF* gene

Indicated strains were used to infect DMEM (1:100 dilution of LB overnight bacteria) for 8 hours before isolating total bacterial cell samples to resolve on 6% SDS-PA gels for Coomassie blue visualisation and 12% SDS-PA gels for western blot analysis to probe for DnaK. Molecular standards are shown (KDa) for Coomassie blue stained gels. Strains used were EPEC and Δ*espF* mutants, the latter with no introduced plasmids (-) or a plasmid encoding EPEC EspF (pEspF$_{EPEC}$) or variants carrying N-terminally-located T7 (pT7EspF$_{EPEC}$) or T7/His (pT7HisEspF$_{EPEC}$) epitope tags. Downward-facing arrows indicate *ΔsepL* mutant-like phenotype.

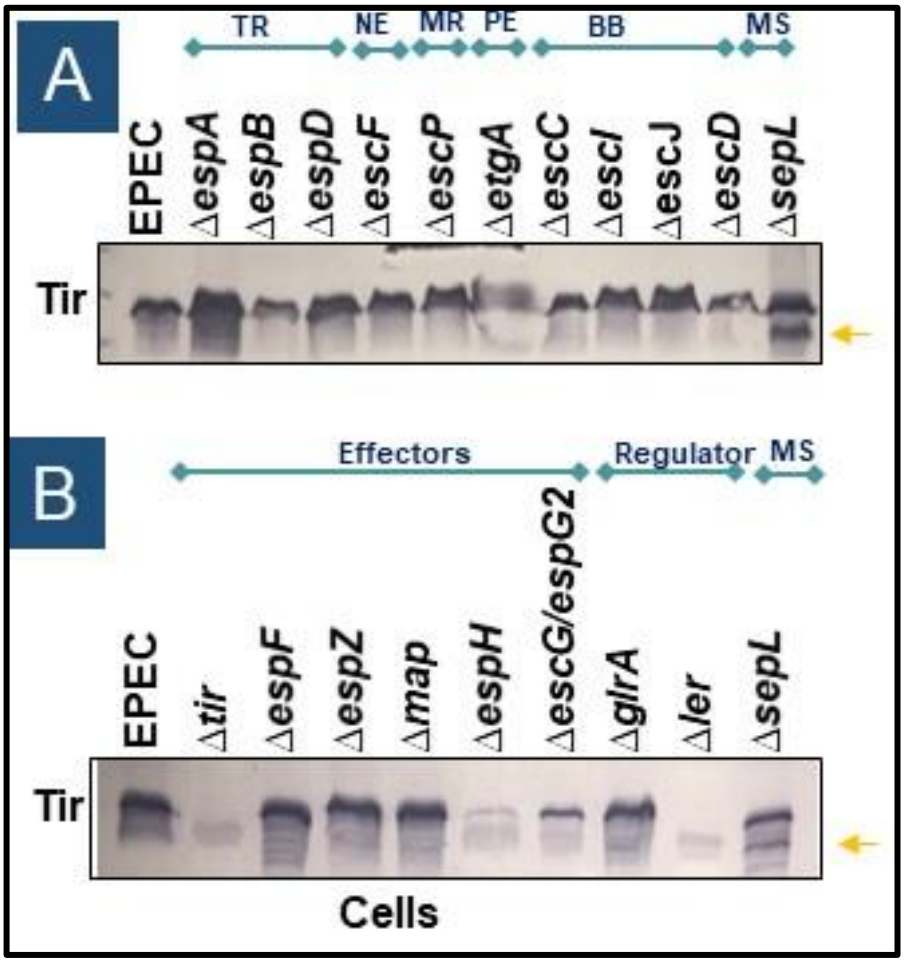

Supplementary Figure 7: *ΔsepL* 'Tir cleavage' phenotype is not shared by other T3SS-defective mutants

Isolated bacterial cell samples from 30 LEE-gene deficient strains, were resolved on 12% SDS-PA gels for western blot analyses and probed for the Tir effector. The strains were analysed in clusters relating to the role of the missing gene in T3SS functionality using the following abbreviations: TR (Translocators), NE (Needle proteins), MR (Molecular Ruler), PE (Peptidoglycan enzyme), BB (Basal body components), MS (Molecular switches). Other examined genes encoded effectors or transcriptional regulators. Arrowheads indicate the position of the Tir cleavage product only seen in extracts from the *ΔsepL* mutant.

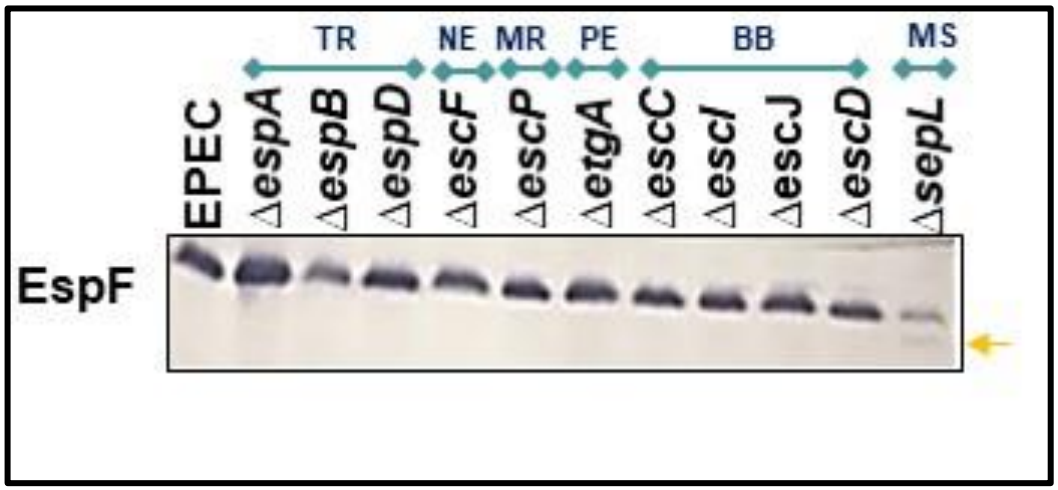

Supplementary Figure 8: *ΔsepL* 'EspF cleavage' phenotype

Isolated bacterial cell samples, LEE-gene deficient strains, were resolved on 12% SDS-PA gels for western blot analyses and probed for the EspF effector. The strains were analysed in clusters relating to the role of the missing gene in T3SS functionality using the following abbreviations: TR (Translocators), NE (Needle proteins), MR (Molecular Ruler), PE (Peptidoglycan enzyme), BB (Basal body components), MS (Molecular switches). Arrowheads indicate the position of the EspF cleavage product seen in extracts from the *ΔsepL* mutant.

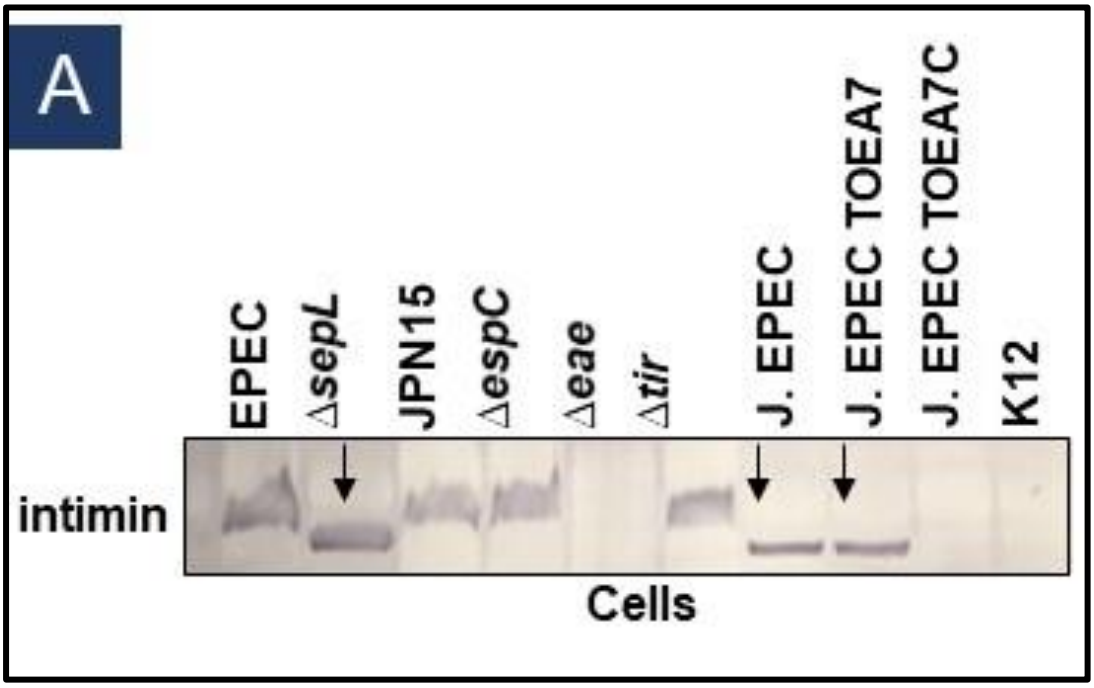

Supplementary Figure 9: Down shift in protein apparent molecular mass in intimin related band

Indicated strains were used to infect DMEM (1:100 dilution of bacteria grown in LB overnight without shaking) for 8 hours before isolating total bacterial cell extracts. Samples were resolved on 12% SDS-PA gels for (A) western blot analysis probing for Intimin. Strains used were EPEC E2348/69 (EPEC), EPEC E2348/69 from Japan lab. (J. EPEC), *ΔespC* (lacks EspC autotransporter), JPN15 (lacks pMar plasmid encoding Bundle Forming Pilus and Plasmid-encoded regulator; latter promotes LEE gene expression), *Δtir* (lacks Tir effector), *Δeae* (lacks Intimin surface protein), J. EPEC TOEA7 (lacks all but four known non-LEE-encoded T3SS substrates), J. EPEC TOEA7C (TOEA7 also lacking LEE Intimin, CesT, CesF, Tir, Map and EspH proteins) and K12 (non-pathogenic) *E. coli*. Downward facing arrows indicate samples showing aberrant protein migration profile.

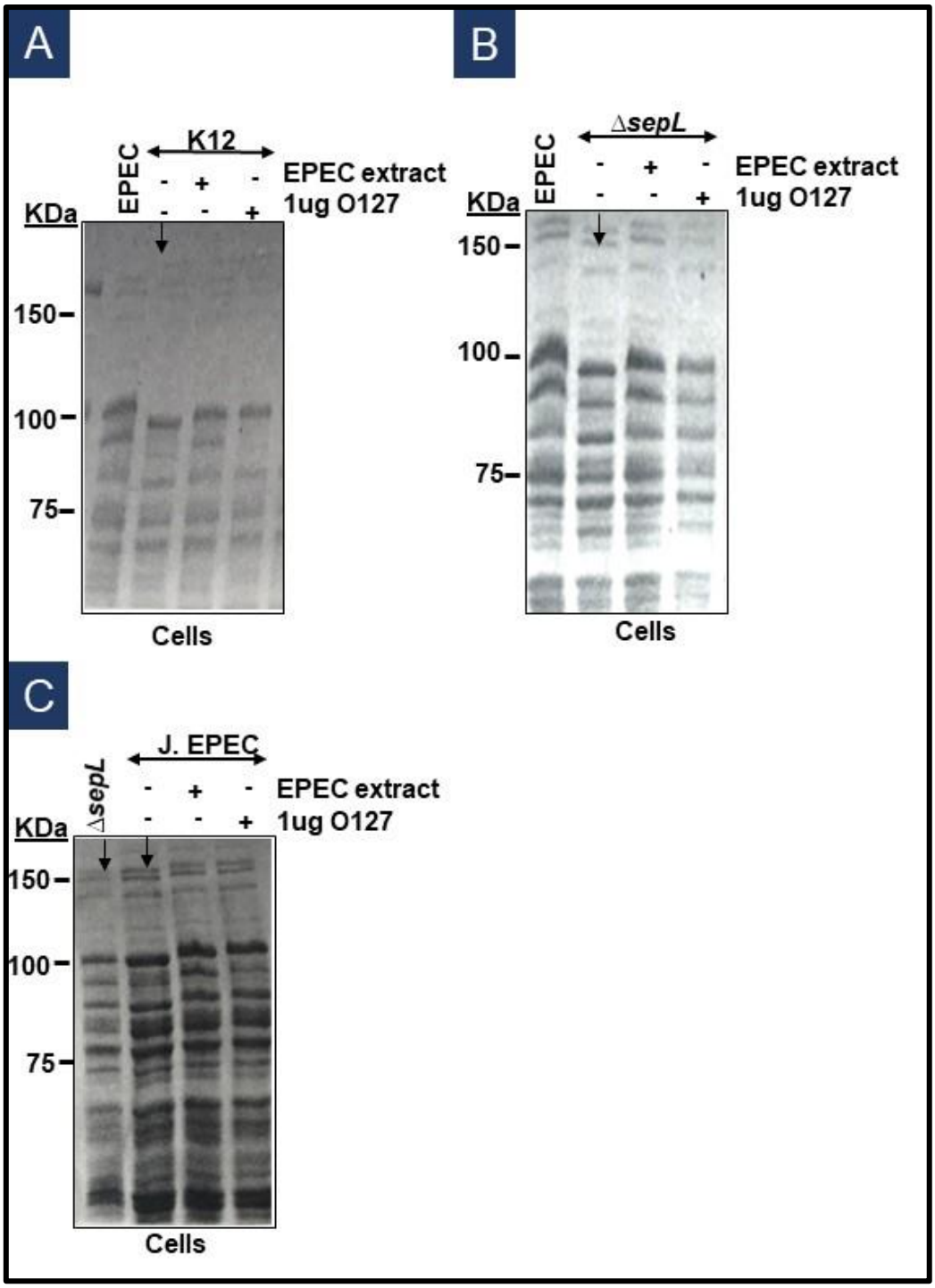

Supplementary Figure 10: A down shift in protein apparent molecular mass is linked to reduced O-antigen levels

Indicated strains were used to infect DMEM (1:100 dilution of bacteria grown in LB overnight without shaking) for 8 hours before isolating total bacterial cell extracts. Samples were mixed (+) or not (-) with EPEC cellular extract (1:1 ratio) or 1µg of O127:B7 antigen (O127) prior to running samples on (A-C) 6% SDS-PA gels for Coomassie blue visualization. Strains used were EPEC E2348/69 (EPEC), EPEC E2348/69 from Japan lab. (J. EPEC), *ΔsepL* (lacks SepL gatekeeper) and K12 (non-pathogenic *E. coli*). Downward facing, green, arrows indicate samples showing an aberrant protein migration profile.

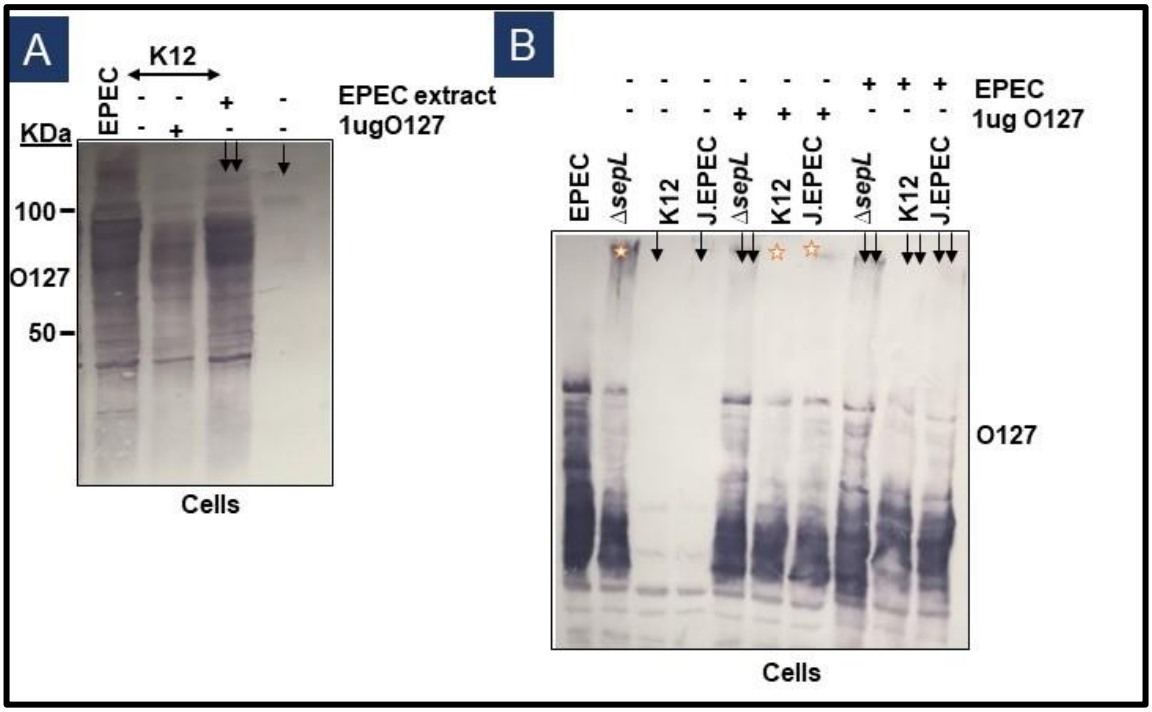

Supplementary Figure 11: A down shift in protein apparent molecular mass linked to reduced O-antigen levels

Indicated strains were used to infect DMEM (1:100 dilution of bacteria grown in LB overnight without shaking) for 8 hours before isolating total bacterial cell extracts. Samples were mixed (+) or not (-) with EPEC cellular extract (1:1 ratio) or 1µg of O127:B7 antigen (O127) prior to running samples on (A-B) 10% SDS-PA gels for western blot detection of O127 antigen. Strains used were EPEC E2348/69 (EPEC), EPEC E2348/69 from Japan lab. (J. EPEC), *ΔsepL* (lacks SepL gatekeeper) and K12 (non-pathogenic *E. coli*). Downward facing, green, arrows indicate samples showing a weak protein smear profile. Stars indicate samples showing no protein smearing.

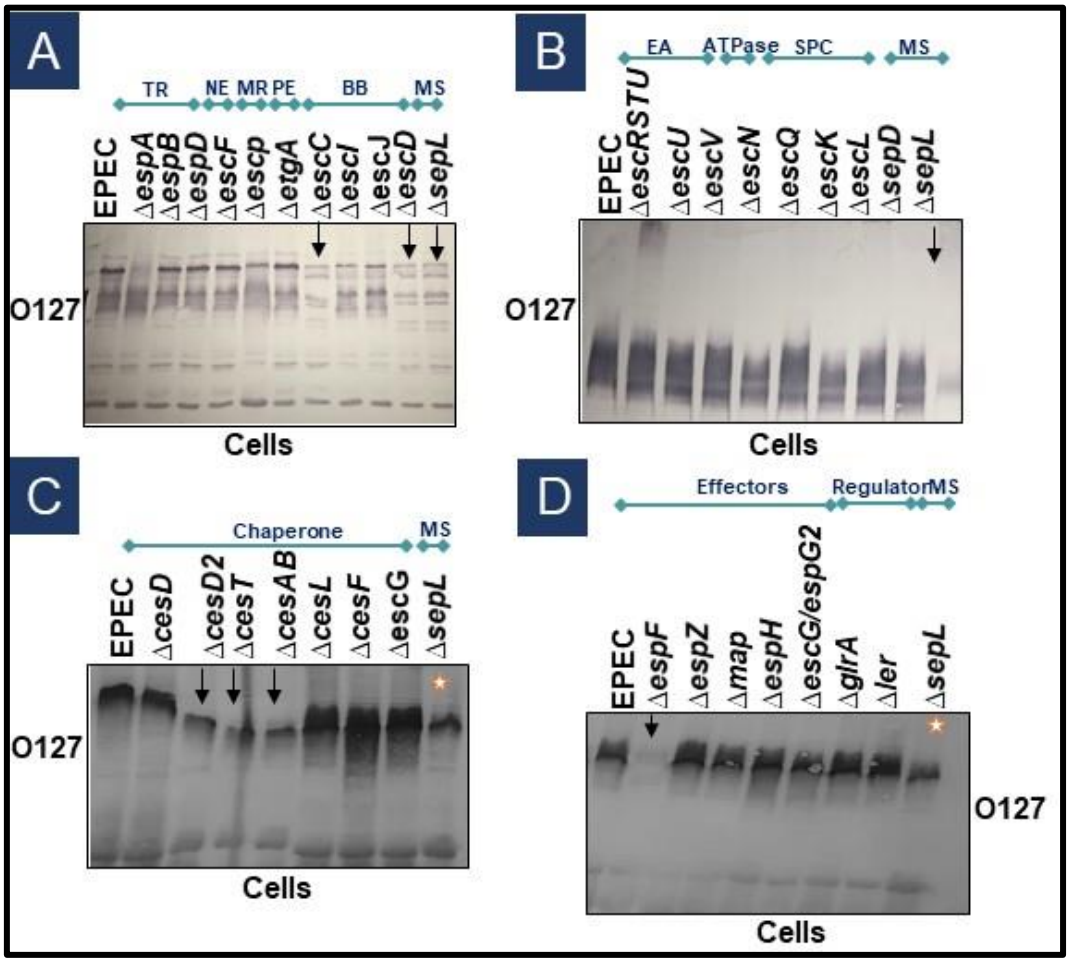

Supplementary Figure 12: Other T3SS mutant share the *sepL* band shift phenotype

Available bacterial extracts from indicated T3SS mutant strains were resolved on 10% SDS PA gels for western blot analyses to probe for O127 antigen. The samples were loaded into groups relating to the role of the missing gene in T3SS functionality using the following abbreviations: TR (Translocator), NE (Needle protein), MR (Molecular Ruler), PE (Peptidoglycan enzyme), BB (Basal body component), MR (Molecular switch), EA (Export Apparatus component), ATPase (ATPase complex component) and SPC (Sorting Platform Complex protein) plus effectors, transcriptional regulators, and Intimin (surface protein). Down-ward facing arrows indicate strains with reduced O127 antigen levels. Stars symbols indicate *sepL* mutant profile.

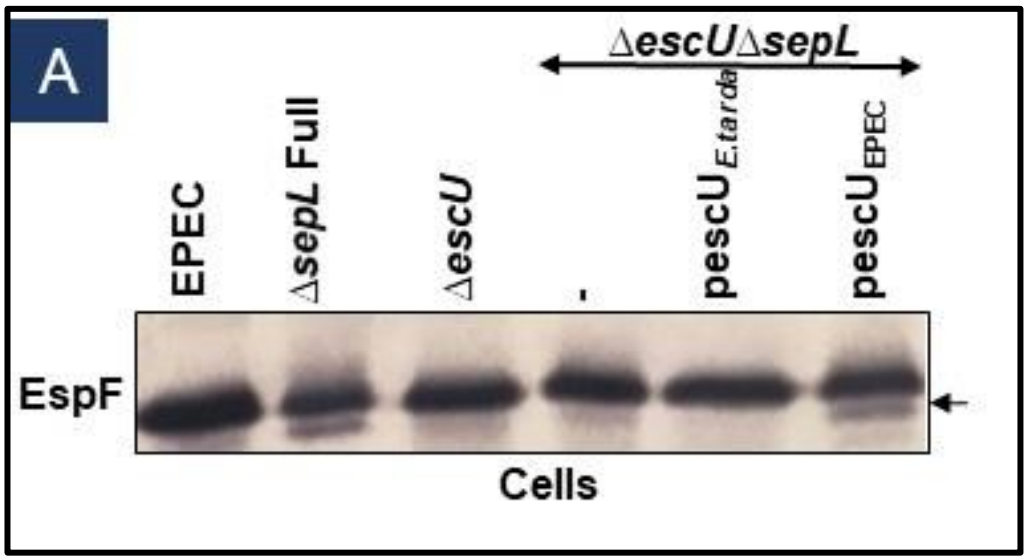

Supplementary Figure 13: The auto-cleavage protein EscU confers effector cleavage when SepL protein is absent

Indicated strains were used to infect DMEM (1:100 dilution of bacteria grown in LB overnight without shaking) for 8 hours before isolating total bacterial cell extracts. Samples were resolved on 10% SDS-PA for western blot analysis probing for the EspF effector protein. Arrowhead indicates the position of the cleaved form of the EspF protein. Strains used were EPEC, the *ΔsepL* mutant, and newly generated *ΔsepL*$_{full}$ single and *Δ*escU*ΔsepL*$_{full}$ double mutants. When indicated, the double mutant strain carried no introduced plasmids (-) or a plasmid carrying the EPEC (p*escU*$_{EPEC}$) or *E. tarda* (p*escU*$_{E. tarda}$) *escU* gene.

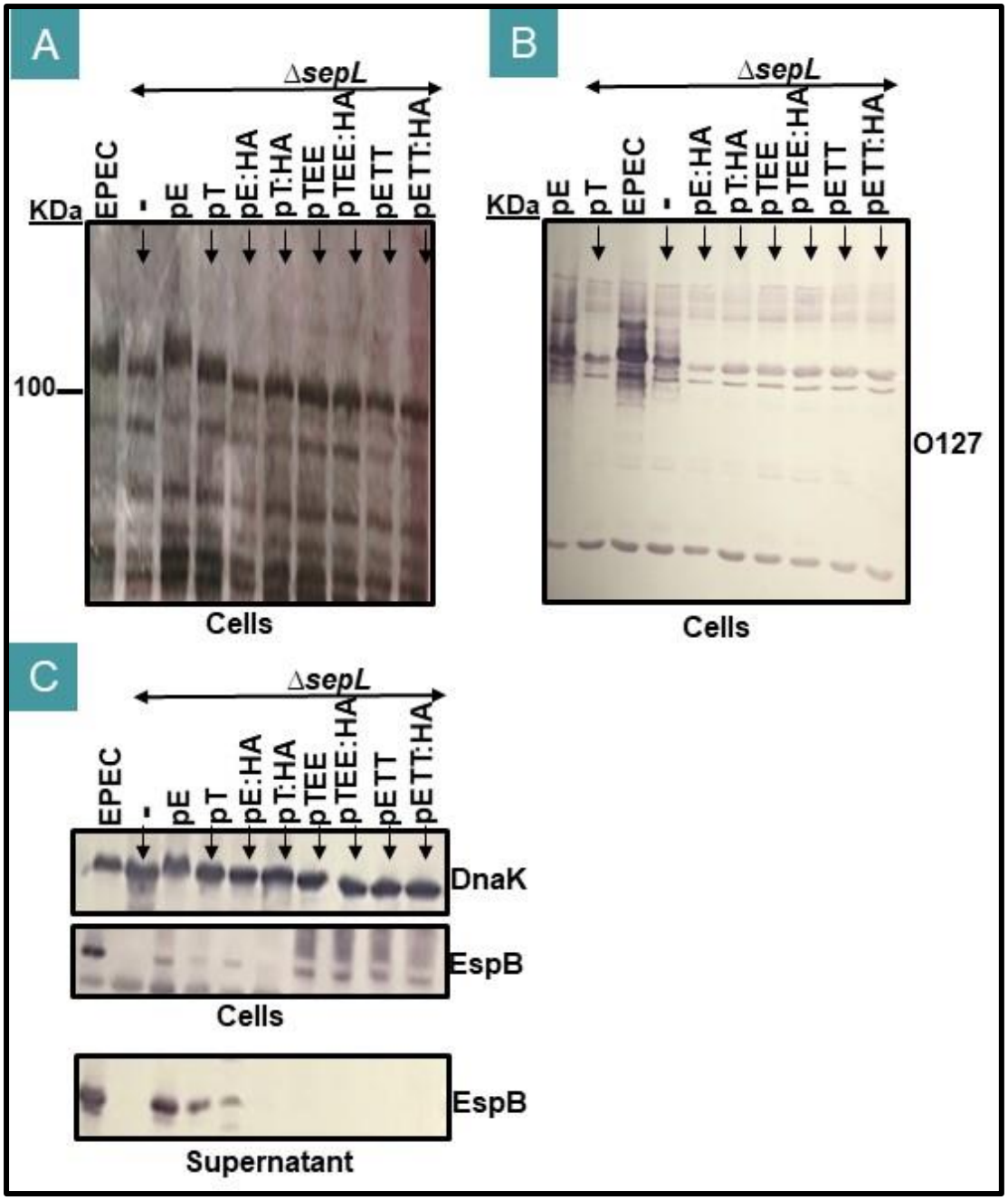

Supplementary Figure 14: Swapping domain one between *E. tarda* and EPEC SepL variants compromises EPEC SepL functionality and does not rescue *E. tarda* SepL defects

Indicated strains were (A-C) added to DMEM (1:100 dilution of bacteria grown in LB overnight without shaking) for 8 hours before isolating total cell extracts and secreted (supernatant) proteins. Samples were resolved at 6% (A) for Coomassie blue staining or 12% (B & C) for western blot analysis. Molecular standards are shown (KDa; A). Strains used were EPEC and the SepL-deficient mutant (*ΔsepL*) with no (-) plasmid or, when indicated, plasmids encoding EPEC SepL (pE), *E. tarda* SepL (pT), EPEC SepL:HA fusion protein (pE:HA), *E. tarda* SepL:HA fusion protein (pT:HA), SepL-T1E2,3 chimera (pT1E2,3), SepL-T1E2,3:HA chimera (pT1E2,3:HA), SepL-E1T2,3 chimera (pE1T2,3) and SepL-E1T2,3:HA chimera (pE1T2,3:HA). Down-ward pointing arrows indicate strains with *ΔsepL* mutant-like phenotype.

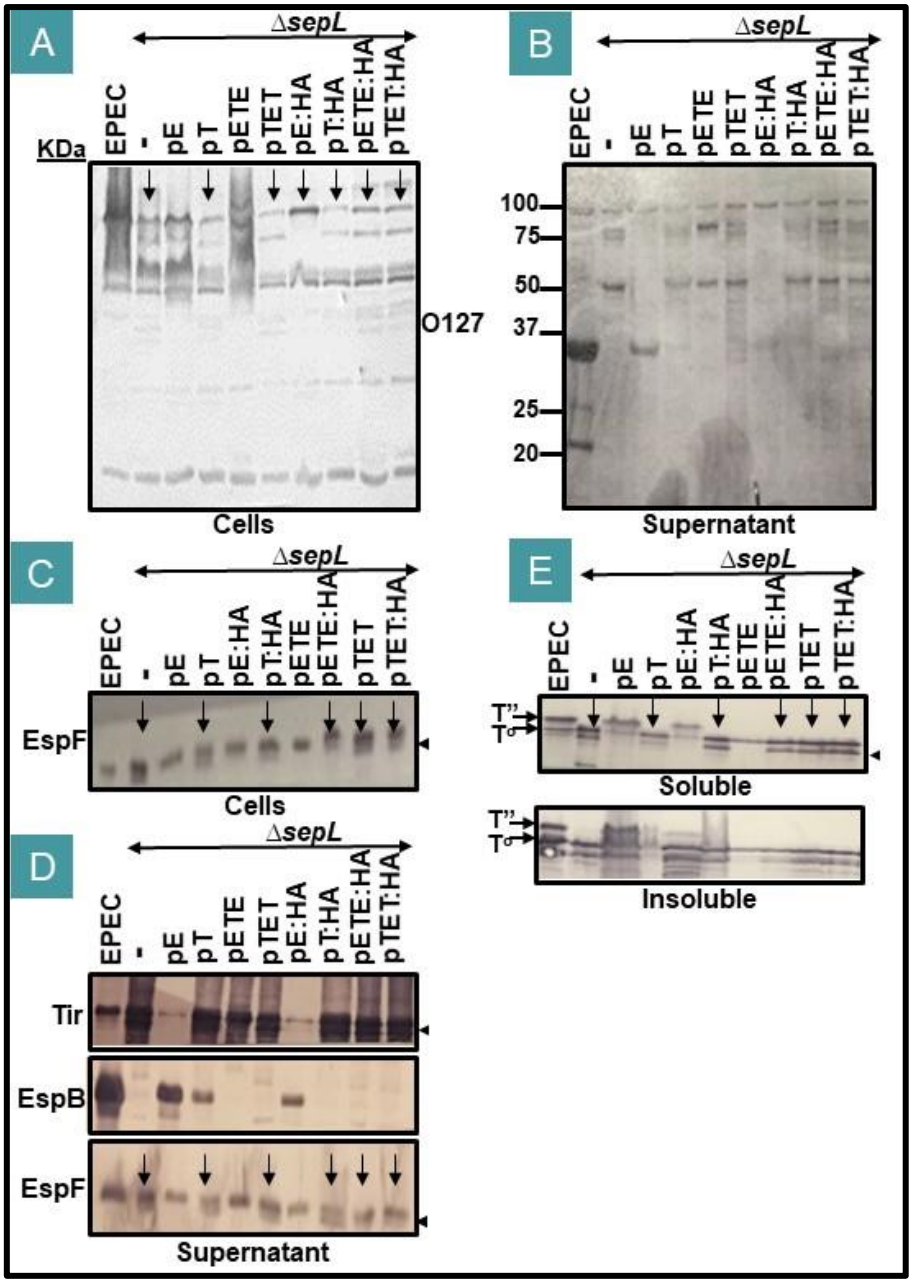

Supplementary Figure 15: Swapping domain 2 between *E. tarda* and EPEC SepL variants compromises nearly all EPEC SepL functions but does not rescue *E. tarda* SepL defects

Indicated strains were (A-D) added to DMEM (1:100 dilution of bacteria grown in LB overnight without shaking) for 8 hours before isolating total cell extracts and secreted (supernatant) proteins. Samples were resolved on 12% (A-D) SDS-PA gels for Coomassie blue staining (B) or western blot analysis (A, C-E). Molecular standards are shown (KDa; B). (E) HeLa cells were fractionated, post infection, into Triton X-100 soluble (host cytoplasm/membrane proteins plus T3SS delivered EPEC effectors) and insoluble (contains host nuclei/cytoskeletal proteins plus adherent bacterial proteins) samples for Western blot analysis. Strains used were EPEC and the SepL-deficient mutant (*ΔsepL*); latter with no (-) plasmid or, when indicated, a plasmid encoding EPEC SepL (pE), *E. tarda* SepL (pT), EPEC SepL:HA fusion protein (pE:HA), *E. tarda* SepL:HA fusion protein (pT:HA), SepL-TET chimera (pTET), SepL-TET:HA chimera (pTET:HA), SepL-ETE chimera (pETE) and SepL-ETE:HA chimera (pETE:HA). The position of unmodified (T°) and host kinase-modified (T") Tir forms are shown. Down-ward pointing arrows indicate strains with *ΔsepL* mutant-like phenotype with arrowheads indicating putative cleavage-related form of the EspF and Tir effectors.

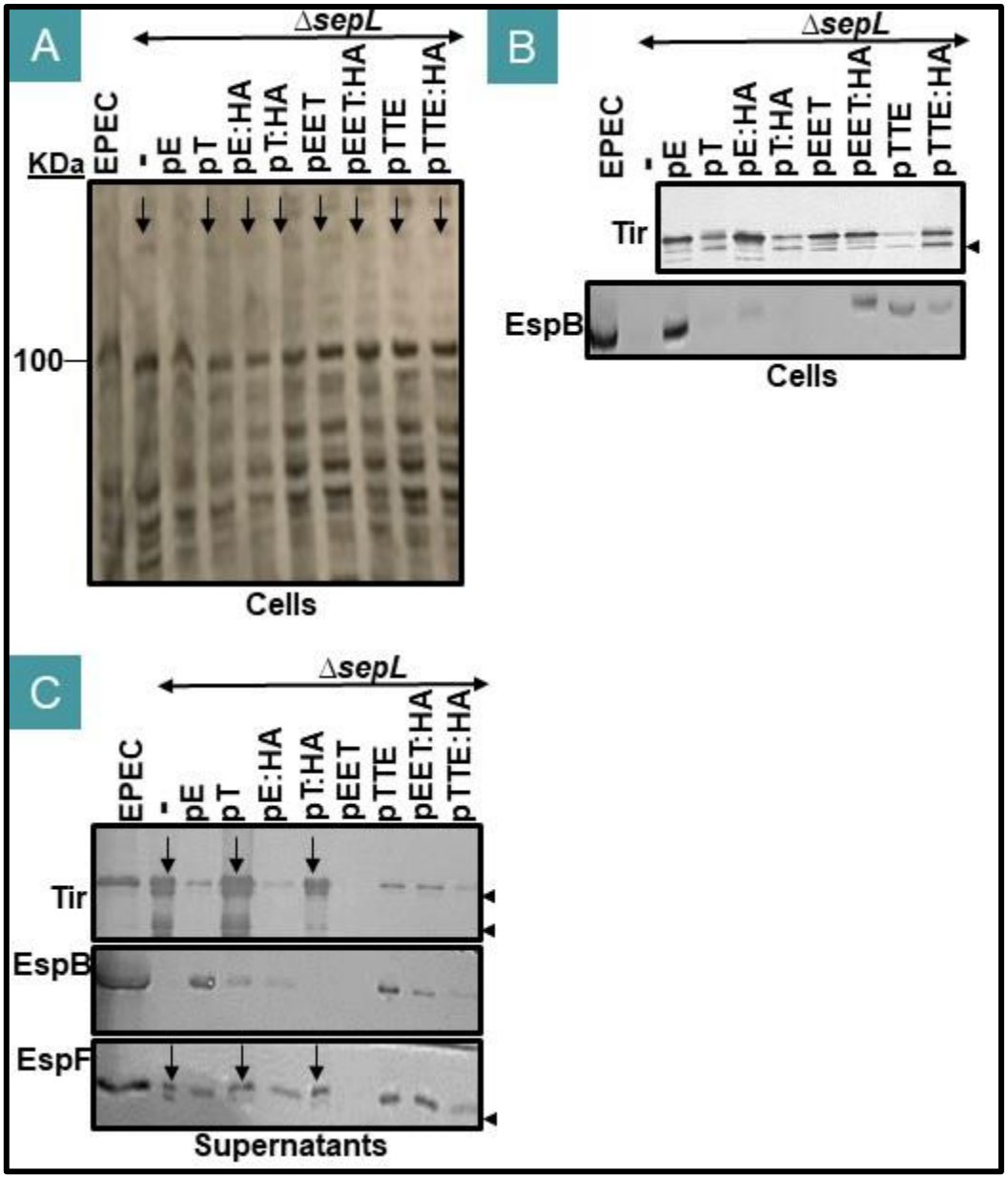

Supplementary Figure 16: Swapping domain 3 between *E. tarda* and EPEC SepL variants compromises nearly all EPEC SepL functions but allows *E. tarda* SepL to deliver Tir into the cell

Indicated strains were added to (A- C) DMEM. (A- C) DMEM was infected (1:100 dilution of bacteria grown in LB overnight without shaking) for 8 hours before isolating total cell extracts and secreted (supernatant) proteins. Samples were resolved at 6% (A) or 12% (B & C) SDS-PA gels for western blot analysis. Strains used were EPEC and the SepL-deficient mutant (*ΔsepL*); the latter with no (-) plasmid or, when indicated, a plasmid encoding EPEC SepL (pE), *E. tarda* SepL (pT), EPEC SepL:HA fusion protein (pE:HA), *E. tarda* SepL:HA fusion protein (pT:HA), SepL-TEE chimera (pTEE), SepL-TEE:HA chimera (pTEE:HA), SepL-ETT chimera (pETT) and SepL-ETT:HA chimera (pETT:HA). The positions of the unmodified (T^{o}) and host kinase-modified (T") Tir forms are shown. Down-ward pointing arrows indicate strains with *ΔsepL* mutant-like phenotype with arrowheads indicating putative cleavage-related forms of the EspF and Tir effectors.

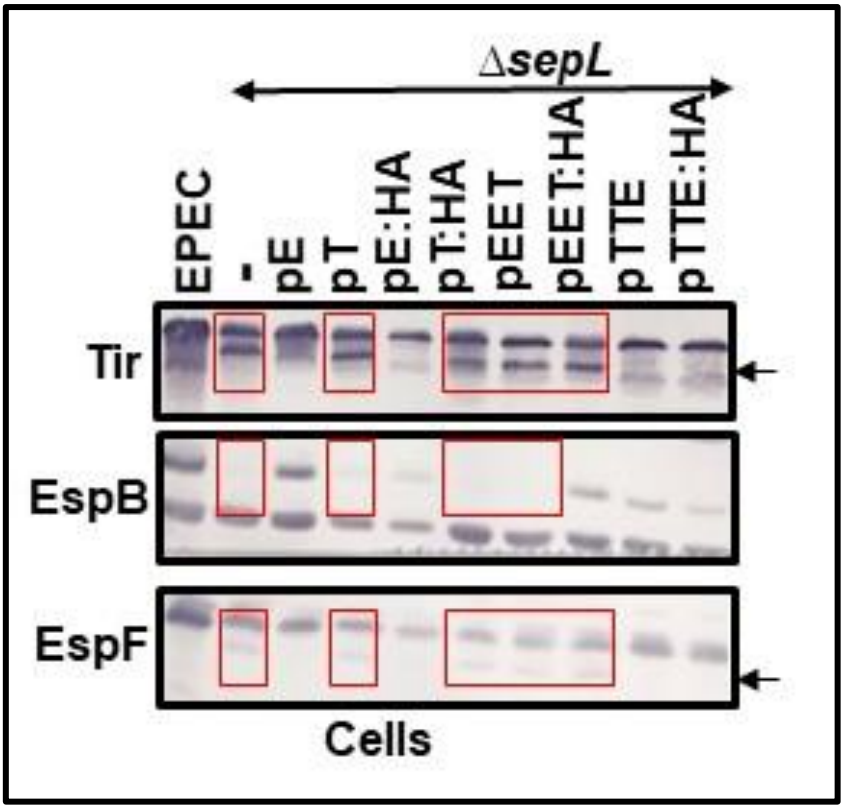

Supplementary Figure 17: Swapping domain 3 between *E. tarda* and EPEC SepL variants compromises nearly all EPEC SepL functions but allows *E. tarda* SepL to deliver Tir into the cell

Indicated strains were added to (A) DMEM. DMEM was infected (1:100 dilution of bacteria grown in LB overnight without shaking) for 8 hours before isolating total cell extracts. Samples were resolved on 12% SDS-PA gels for western blot analysis. Strains used were EPEC and the SepL-deficient mutant (*ΔsepL*); the latter with no (-) plasmid or, when indicated, a plasmid encoding EPEC SepL (pE), *E. tarda* SepL (pT), EPEC SepL:HA fusion protein (pE:HA), *E. tarda* SepL:HA fusion protein (pT:HA), SepL-TEE chimera (pTEE), SepL-TEE:HA chimera (pTEE:HA), SepL-ETT chimera (pETT) and SepL-ETT:HA chimera (pETT:HA). The arrowheads indicating putative cleavage-related forms of the EspF and Tir effectors.

Bibliography

Abe, A., de Grado, M., Pfuetzner, R.A., Sanchez-Sanmartin, C., Devinney, R., Puente, J.L., Strynadka, N.C. and Finlay, B.B. (1999) 'Enteropathogenic Escherichia coli translocated intimin receptor, Tir, requires a specific chaperone for stable secretion', *Mol Microbiol*, 33(6), pp. 1162-75.
Achtman, M. and Pluschke, G. (1986) 'Clonal analysis of descent and virulence among selected Escherichia coli', *Annu Rev Microbiol*, 40, pp. 185-210.
Akeda, Y. and Galan, J.E. (2005) 'Chaperone release and unfolding of substrates in type III secretion', *Nature*, 437(7060), pp. 911-5.
Alto, N.M., Shao, F., Lazar, C.S., Brost, R.L., Chua, G., Mattoo, S., McMahon, S.A., Ghosh, P., Hughes, T.R., Boone, C. and Dixon, J.E. (2006) 'Identification of a bacterial type III effector family with G protein mimicry functions', *Cell*, 124(1), pp. 133-45.
Alto, N.M., Weflen, A.W., Rardin, M.J., Yarar, D., Lazar, C.S., Tonikian, R., Koller, A., Taylor, S.S., Boone, C., Sidhu, S.S., Schmid, S.L., Hecht, G.A. and Dixon, J.E. (2007) 'The type III effector EspF coordinates membrane trafficking by the spatiotemporal activation of two eukaryotic signaling pathways', *J Cell Biol*, 178(7), pp. 1265-78.
Andrade, A., Pardo, J.P., Espinosa, N., Perez-Hernandez, G. and Gonzalez-Pedrajo, B. (2007) 'Enzymatic characterization of the enteropathogenic Escherichia coli type III secretion ATPase EscN', *Arch Biochem Biophys*, 468(1), pp. 121-7.
Bao, Y., Zhang, H., Huang, X., Ma, J., Logue, C.M., Nolan, L.K. and Li, G. (2018) 'O-specific polysaccharide confers lysozyme resistance to extraintestinal pathogenic Escherichia coli', *Virulence*, 9(1), pp. 666-680.
Barba, J., Bustamante, V.H., Flores-Valdez, M.A., Deng, W., Finlay, B.B. and Puente, J.L. (2005) 'A positive regulatory loop controls expression of the locus of enterocyte effacement-encoded regulators Ler and GrlA', *J Bacteriol*, 187(23), pp. 7918-30.
Barua, S., Yamashino, T., Hasegawa, T., Yokoyama, K., Torii, K. and Ohta, M. (2002) 'Involvement of surface polysaccharides in the organic acid resistance of Shiga Toxin-producing Escherichia coli O157:H7', *Mol Microbiol*, 43(3), pp. 629-40.
Berdichevsky, T., Friedberg, D., Nadler, C., Rokney, A., Oppenheim, A. and Rosenshine, I. (2005) 'Ler is a negative autoregulator of the LEE1 operon in enteropathogenic Escherichia coli', *J Bacteriol*, 187(1), pp. 349-57.
Berger, C.N., Crepin, V.F., Baruch, K., Mousnier, A., Rosenshine, I. and Frankel, G. (2012) 'EspZ of enteropathogenic and enterohemorrhagic Escherichia coli regulates type III secretion system protein translocation', *MBio*, 3(5).
Berndt, V., Beckstette, M., Volk, M., Dersch, P. and Brönstrup, M. (2019) 'Metabolome and transcriptome-wide effects of the carbon storage regulator A in enteropathogenic Escherichia coli', *Sci Rep*, 9(1), p. 138.
Bhat, A., Shin, M., Jeong, J.H., Kim, H.J., Lim, H.J., Rhee, J.H., Paik, S.Y., Takeyasu, K., Tobe, T., Yen, H., Lee, G. and Choy, H.E. (2014) 'DNA looping-dependent autorepression of LEE1 P1 promoters by Ler in enteropathogenic Escherichia coli (EPEC)', *Proc Natl Acad Sci U S A*, 111(25), pp. E2586-95.
Biemans-Oldehinkel, E., Sal-Man, N., Deng, W., Foster, L.J. and Finlay, B.B. (2011) 'Quantitative proteomic analysis reveals formation of an EscL-EscQ-EscN type III complex in enteropathogenic Escherichia coli', *J Bacteriol*, 193(19), pp. 5514-9.
Borgersen, Q., Bolick, D.T., Kolling, G.L., Aijuka, M., Ruiz-Perez, F., Guerrant, R.L., Nataro, J.P. and Santiago, A.E. (2018) 'Abundant production of exopolysaccharide by EAEC strains enhances the formation of bacterial biofilms in contaminated sprouts', *Gut Microbes*, 9(3), pp. 264-278.
Braunstein, M., Espinosa, B.J., Chan, J., Belisle, J.T. and Jacobs, W.R., Jr. (2003) 'SecA2 functions in the secretion of superoxide dismutase A and in the virulence of Mycobacterium tuberculosis', *Mol Microbiol*, 48(2), pp. 453-64.
Bronner, D., Clarke, B.R. and Whitfield, C. (1994) 'Identification of an ATP-binding cassette transport system required for translocation of lipopolysaccharide O-antigen side-chains across the cytoplasmic membrane of Klebsiella pneumoniae serotype O1', *Mol Microbiol*, 14(3), pp. 505-19.

Burkinshaw, B.J., Deng, W., Lameignere, E., Wasney, G.A., Zhu, H., Worrall, L.J., Finlay, B.B. and Strynadka, N.C. (2015) 'Structural analysis of a specialized type III secretion system peptidoglycan-cleaving enzyme', *J Biol Chem*, 290(16), pp. 10406-17.
Burkinshaw, B.J., Souza, S.A. and Strynadka, N.C. (2015) 'Structural analysis of SepL, an enteropathogenic Escherichia coli type III secretion-system gatekeeper protein', *Acta Crystallogr F Struct Biol Commun*, 71(Pt 10), pp. 1300-8.
Burns, S.M. and Hull, S.I. (1998) 'Comparison of loss of serum resistance by defined lipopolysaccharide mutants and an acapsular mutant of uropathogenic Escherichia coli O75:K5', *Infect Immun*, 66(9), pp. 4244-53.
Buttner, D. (2012) 'Protein export according to schedule: architecture, assembly, and regulation of type III secretion systems from plant- and animal-pathogenic bacteria', *Microbiol Mol Biol Rev*, 76(2), pp. 262-310.
Büttner, D. (2012) 'Protein export according to schedule: architecture, assembly, and regulation of type III secretion systems from plant- and animal-pathogenic bacteria', *Microbiol Mol Biol Rev*, 76(2), pp. 262-310.
Caroff, M. and Karibian, D. (2003) 'Structure of bacterial lipopolysaccharides', *Carbohydr Res*, 338(23), pp. 2431-47.
Chandry, P.S., Gladman, S., Moore, S.C., Seemann, T., Crandall, K.A. and Fegan, N. (2012) 'A Genomic Island in Salmonella enterica ssp. salamae provides new insights on the genealogy of the locus of enterocyte effacement', *PLoS One*, 7(7), p. e41615.
Chang, A.C. and Cohen, S.N. (1978) 'Construction and characterization of amplifiable multicopy DNA cloning vehicles derived from the P15A cryptic miniplasmid', *J Bacteriol*, 134(3), pp. 1141-56.
Chen, H.D. and Frankel, G. (2005) 'Enteropathogenic Escherichia coli: unravelling pathogenesis', *FEMS Microbiol Rev*, 29(1), pp. 83-98.
Chen, L., Ai, X., Portaliou, A.G., Minetti, C.A., Remeta, D.P., Economou, A. and Kalodimos, C.G. (2013) 'Substrate-activated conformational switch on chaperones encodes a targeting signal in type III secretion', *Cell Rep*, 3(3), pp. 709-15.
Clarke, S.C., Haigh, R.D., Freestone, P.P. and Williams, P.H. (2003) 'Virulence of enteropathogenic Escherichia coli, a global pathogen', *Clin Microbiol Rev*, 16(3), pp. 365-78.
Cleary, J., Lai, L.C., Shaw, R.K., Straatman-Iwanowska, A., Donnenberg, M.S., Frankel, G. and Knutton, S. (2004) 'Enteropathogenic Escherichia coli (EPEC) adhesion to intestinal epithelial cells: role of bundle-forming pili (BFP), EspA filaments and intimin', *Microbiology (Reading)*, 150(Pt 3), pp. 527-538.
Clements, A., Young, J.C., Constantinou, N. and Frankel, G. (2012) 'Infection strategies of enteric pathogenic Escherichia coli', *Gut Microbes*, 3(2), pp. 71-87.
Coburn, B., Sekirov, I. and Finlay, B.B. (2007) 'Type III secretion systems and disease', *Clin Microbiol Rev*, 20(4), pp. 535-49.
Connolly, J.P., Finlay, B.B. and Roe, A.J. (2015) 'From ingestion to colonization: the influence of the host environment on regulation of the LEE encoded type III secretion system in enterohaemorrhagic Escherichia coli', *Front Microbiol*, 6, p. 568.
Creasey, E.A., Friedberg, D., Shaw, R.K., Umanski, T., Knutton, S., Rosenshine, I. and Frankel, G. (2003) 'CesAB is an enteropathogenic Escherichia coli chaperone for the type-III translocator proteins EspA and EspB', *Microbiology*, 149(Pt 12), pp. 3639-47.
Daniell, S.J., Kocsis, E., Morris, E., Knutton, S., Booy, F.P. and Frankel, G. (2003) '3D structure of EspA filaments from enteropathogenic Escherichia coli', *Mol Microbiol*, 49(2), pp. 301-8.
Daniels, C., Vindurampulle, C. and Morona, R. (1998) 'Overexpression and topology of the Shigella flexneri O-antigen polymerase (Rfc/Wzy)', *Mol Microbiol*, 28(6), pp. 1211-22.
Dasanayake, D., Richaud, M., Cyr, N., Caballero-Franco, C., Pittroff, S., Finn, R.M., Ausió, J., Luo, W., Donnenberg, M.S. and Jardim, A. (2011) 'The N-terminal amphipathic region of the Escherichia coli type III secretion system protein EspD is required for membrane insertion and function', *Mol Microbiol*, 81(3), pp. 734-50.

de Jong, W.W., Zweers, A. and Cohen, L.H. (1978) 'Influence of single amino acid substitutions on electrophoretic mobility of sodium dodecyl sulfate-protein complexes', *Biochem Biophys Res Commun*, 82(2), pp. 532-9.
Dean, P. and Kenny, B. (2004) 'Intestinal barrier dysfunction by enteropathogenic Escherichia coli is mediated by two effector molecules and a bacterial surface protein', *Mol Microbiol*, 54(3), pp. 665-75.
Dean, P. and Kenny, B. (2009) 'The effector repertoire of enteropathogenic E. coli: ganging up on the host cell', *Curr Opin Microbiol*, 12(1), pp. 101-9.
Dean, P., Scott, J.A., Knox, A.A., Quitard, S., Watkins, N.J. and Kenny, B. (2010) 'The enteropathogenic E. coli effector EspF targets and disrupts the nucleolus by a process regulated by mitochondrial dysfunction', *PLoS Pathog*, 6(6), p. e1000961.
Deane, J.E., Abrusci, P., Johnson, S. and Lea, S.M. (2010) 'Timing is everything: the regulation of type III secretion', *Cell Mol Life Sci*, 67(7), pp. 1065-75.
Delahay, R.M. and Frankel, G. (2002) 'Coiled-coil proteins associated with type III secretion systems: a versatile domain revisited', *Mol Microbiol*, 45(4), pp. 905-16.
Delahay, R.M., Knutton, S., Shaw, R.K., Hartland, E.L., Pallen, M.J. and Frankel, G. (1999) 'The coiled-coil domain of EspA is essential for the assembly of the type III secretion translocon on the surface of enteropathogenic Escherichia coli', *J Biol Chem*, 274(50), pp. 35969-74.
Deng, W., Li, Y., Hardwidge, P.R., Frey, E.A., Pfuetzner, R.A., Lee, S., Gruenheid, S., Strynakda, N.C., Puente, J.L. and Finlay, B.B. (2005) 'Regulation of type III secretion hierarchy of translocators and effectors in attaching and effacing bacterial pathogens', *Infect Immun*, 73(4), pp. 2135-46.
Deng, W., Marshall, N.C., Rowland, J.L., McCoy, J.M., Worrall, L.J., Santos, A.S., Strynadka, N.C.J. and Finlay, B.B. (2017) 'Assembly, structure, function and regulation of type III secretion systems', *Nat Rev Microbiol*, 15(6), pp. 323-337.
Deng, W., Puente, J.L., Gruenheid, S., Li, Y., Vallance, B.A., Vazquez, A., Barba, J., Ibarra, J.A., O'Donnell, P., Metalnikov, P., Ashman, K., Lee, S., Goode, D., Pawson, T. and Finlay, B.B. (2004) 'Dissecting virulence: systematic and functional analyses of a pathogenicity island', *Proc Natl Acad Sci U S A*, 101(10), pp. 3597-602.
Díaz-Guerrero, M., Gaytán, M.O., Soto, E., Espinosa, N., García-Gómez, E., Marcos-Vilchis, A., Andrade, A. and González-Pedrajo, B. (2021) 'CesL Regulates Type III Secretion Substrate Specificity of the Enteropathogenic E. coli Injectisome', *Microorganisms*, 9(5).
Diepold, A. and Wagner, S. (2014) 'Assembly of the bacterial type III secretion machinery', *FEMS Microbiol Rev*, 38(4), pp. 802-22.
Dong, N., Liu, L. and Shao, F. (2010) 'A bacterial effector targets host DH-PH domain RhoGEFs and antagonizes macrophage phagocytosis', *Embo j*, 29(8), pp. 1363-76.
Donnenberg, M.S. and Kaper, J.B. (1992) 'Enteropathogenic Escherichia coli', *Infect Immun*, 60(10), pp. 3953-61.
Dornmair, K., Kiefer, H. and Jähnig, F. (1990) 'Refolding of an integral membrane protein. OmpA of Escherichia coli', *J Biol Chem*, 265(31), pp. 18907-11.
Drago-Serrano, M.E., Parra, S.G. and Manjarrez-Hernández, H.A. (2006) 'EspC, an autotransporter protein secreted by enteropathogenic Escherichia coli (EPEC), displays protease activity on human hemoglobin', *FEMS Microbiol Lett*, 265(1), pp. 35-40.
Dunker, A.K. and Kenyon, A.J. (1976) 'Mobility of sodium dodecyl sulphate - protein complexes', *Biochem J*, 153(2), pp. 191-7.
Dutta, P.R., Cappello, R., Navarro-García, F. and Nataro, J.P. (2002) 'Functional comparison of serine protease autotransporters of enterobacteriaceae', *Infect Immun*, 70(12), pp. 7105-13.
Dziva, F., van Diemen, P.M., Stevens, M.P., Smith, A.J. and Wallis, T.S. (2004) 'Identification of Escherichia coli O157 : H7 genes influencing colonization of the bovine gastrointestinal tract using signature-tagged mutagenesis', *Microbiology (Reading)*, 150(Pt 11), pp. 3631-3645.
Ebel, F., Podzadel, T., Rohde, M., Kresse, A.U., Krämer, S., Deibel, C., Guzmán, C.A. and Chakraborty, T. (1998) 'Initial binding of Shiga toxin-producing Escherichia coli to host cells and subsequent

induction of actin rearrangements depend on filamentous EspA-containing surface appendages', *Mol Microbiol*, 30(1), pp. 147-61.
Elliott, S.J., Hutcheson, S.W., Dubois, M.S., Mellies, J.L., Wainwright, L.A., Batchelor, M., Frankel, G., Knutton, S. and Kaper, J.B. (1999) 'Identification of CesT, a chaperone for the type III secretion of Tir in enteropathogenic Escherichia coli', *Mol Microbiol*, 33(6), pp. 1176-89.
Elliott, S.J., O'Connell, C.B., Koutsouris, A., Brinkley, C., Donnenberg, M.S., Hecht, G. and Kaper, J.B. (2002) 'A gene from the locus of enterocyte effacement that is required for enteropathogenic Escherichia coli to increase tight-junction permeability encodes a chaperone for EspF', *Infect Immun*, 70(5), pp. 2271-7.
Elliott, S.J., Wainwright, L.A., McDaniel, T.K., Jarvis, K.G., Deng, Y.K., Lai, L.C., McNamara, B.P., Donnenberg, M.S. and Kaper, J.B. (1998) 'The complete sequence of the locus of enterocyte effacement (LEE) from enteropathogenic Escherichia coli E2348/69', *Mol Microbiol*, 28(1), pp. 1-4.
Erhardt, M., Namba, K. and Hughes, K.T. (2010) 'Bacterial nanomachines: the flagellum and type III injectisome', *Cold Spring Harb Perspect Biol*, 2(11), p. a000299.
Fairman, J.W., Dautin, N., Wojtowicz, D., Liu, W., Noinaj, N., Barnard, T.J., Udho, E., Przytycka, T.M., Cherezov, V. and Buchanan, S.K. (2012) 'Crystal structures of the outer membrane domain of intimin and invasin from enterohemorrhagic E. coli and enteropathogenic Y. pseudotuberculosis', *Structure*, 20(7), pp. 1233-43.
Feldman, M.F. and Cornelis, G.R. (2003) 'The multitalented type III chaperones: all you can do with 15 kDa', *FEMS Microbiol Lett*, 219(2), pp. 151-8.
Fujii, T., Cheung, M., Blanco, A., Kato, T., Blocker, A.J. and Namba, K. (2012) 'Structure of a type III secretion needle at 7-A resolution provides insights into its assembly and signaling mechanisms', *Proc Natl Acad Sci U S A*, 109(12), pp. 4461-6.
Galan, J.E. and Collmer, A. (1999) 'Type III secretion machines: bacterial devices for protein delivery into host cells', *Science*, 284(5418), pp. 1322-8.
Galan, J.E. and Wolf-Watz, H. (2006) 'Protein delivery into eukaryotic cells by type III secretion machines', *Nature*, 444(7119), pp. 567-73.
Garcia-Gomez, E., Espinosa, N., de la Mora, J., Dreyfus, G. and Gonzalez-Pedrajo, B. (2011) 'The muramidase EtgA from enteropathogenic Escherichia coli is required for efficient type III secretion', *Microbiology*, 157(Pt 4), pp. 1145-60.
Gauthier, A., Puente, J.L. and Finlay, B.B. (2003) 'Secretin of the enteropathogenic Escherichia coli type III secretion system requires components of the type III apparatus for assembly and localization', *Infect Immun*, 71(6), pp. 3310-9.
Gaytan, M.O., Martinez-Santos, V.I., Soto, E. and Gonzalez-Pedrajo, B. (2016) 'Type Three Secretion System in Attaching and Effacing Pathogens', *Front Cell Infect Microbiol*, 6, p. 129.
Gaytán, M.O., Martínez-Santos, V.I., Soto, E. and González-Pedrajo, B. (2016) 'Type Three Secretion System in Attaching and Effacing Pathogens', *Front Cell Infect Microbiol*, 6, p. 129.
Gaytan, M.O., Monjaras Feria, J., Soto, E., Espinosa, N., Benitez, J.M., Georgellis, D. and Gonzalez-Pedrajo, B. (2018) 'Novel insights into the mechanism of SepL-mediated control of effector secretion in enteropathogenic Escherichia coli', *Microbiologyopen*, 7(3), p. e00571.
Genin, S. and Boucher, C.A. (1994) 'A superfamily of proteins involved in different secretion pathways in gram-negative bacteria: modular structure and specificity of the N-terminal domain', *Mol Gen Genet*, 243(1), pp. 112-8.
Ghosh, P. (2004) 'Process of protein transport by the type III secretion system', *Microbiol Mol Biol Rev*, 68(4), pp. 771-95.
Gibson, D.G., Young, L., Chuang, R.Y., Venter, J.C., Hutchison, C.A., 3rd and Smith, H.O. (2009) 'Enzymatic assembly of DNA molecules up to several hundred kilobases', *Nat Methods*, 6(5), pp. 343-5.
Giron, J.A., Ho, A.S. and Schoolnik, G.K. (1991) 'An inducible bundle-forming pilus of enteropathogenic Escherichia coli', *Science*, 254(5032), pp. 710-3.

Goldberg, A.L. and Dice, J.F. (1974) 'Intracellular protein degradation in mammalian and bacterial cells', *Annu Rev Biochem*, 43(0), pp. 835-69.
González-Pedrajo, B., Minamino, T., Kihara, M. and Namba, K. (2006) 'Interactions between C ring proteins and export apparatus components: a possible mechanism for facilitating type III protein export', *Mol Microbiol*, 60(4), pp. 984-98.
Gottesman, S. (1989) 'Genetics of proteolysis in Escherichia coli*', *Annu Rev Genet*, 23, pp. 163-98.
Gottesman, S. and Maurizi, M.R. (1992) 'Regulation by proteolysis: energy-dependent proteases and their targets', *Microbiol Rev*, 56(4), pp. 592-621.
Gruenheid, S., DeVinney, R., Bladt, F., Goosney, D., Gelkop, S., Gish, G.D., Pawson, T. and Finlay, B.B. (2001) 'Enteropathogenic E. coli Tir binds Nck to initiate actin pedestal formation in host cells', *Nat Cell Biol*, 3(9), pp. 856-9.
Harrington, C.S., Lanser, J.A., Manning, P.A. and Murray, C.J. (1991) 'Epidemiology of Salmonella sofia in Australia', *Appl Environ Microbiol*, 57(1), pp. 223-7.
Hauser, A.R. (2009) 'The type III secretion system of Pseudomonas aeruginosa: infection by injection', *Nat Rev Microbiol*, 7(9), pp. 654-65.
Hirano, T., Yamaguchi, S., Oosawa, K. and Aizawa, S. (1994) 'Roles of FliK and FlhB in determination of flagellar hook length in Salmonella typhimurium', *J Bacteriol*, 176(17), pp. 5439-49.
Huang, J., Lesser, C.F. and Lory, S. (2008) 'The essential role of the CopN protein in Chlamydia pneumoniae intracellular growth', *Nature*, 456(7218), pp. 112-5.
Ibel, K., May, R.P., Kirschner, K., Szadkowski, H., Mascher, E. and Lundahl, P. (1990) 'Protein-decorated micelle structure of sodium-dodecyl-sulfate--protein complexes as determined by neutron scattering', *Eur J Biochem*, 190(2), pp. 311-8.
Ide, T., Laarmann, S., Greune, L., Schillers, H., Oberleithner, H. and Schmidt, M.A. (2001) 'Characterization of translocation pores inserted into plasma membranes by type III-secreted Esp proteins of enteropathogenic Escherichia coli', *Cell Microbiol*, 3(10), pp. 669-79.
Iguchi, A., Thomson, N.R., Ogura, Y., Saunders, D., Ooka, T., Henderson, I.R., Harris, D., Asadulghani, M., Kurokawa, K., Dean, P., Kenny, B., Quail, M.A., Thurston, S., Dougan, G., Hayashi, T., Parkhill, J. and Frankel, G. (2009) 'Complete genome sequence and comparative genome analysis of enteropathogenic Escherichia coli O127:H6 strain E2348/69', *J Bacteriol*, 191(1), pp. 347-54.
Iizumi, Y., Sagara, H., Kabe, Y., Azuma, M., Kume, K., Ogawa, M., Nagai, T., Gillespie, P.G., Sasakawa, C. and Handa, H. (2007) 'The enteropathogenic E. coli effector EspB facilitates microvillus effacing and antiphagocytosis by inhibiting myosin function', *Cell Host Microbe*, 2(6), pp. 383-92.
Jann, B., Jann, K. and Beyaert, G.O. (1973) '2-Amino-2,6-dideoxy-d-glucose (D-quinovosamine): a constituent of the lipopolysaccharides of Vibrio cholerae', *Eur J Biochem*, 37(3), pp. 531-4.
Jarvis, K.G., Giron, J.A., Jerse, A.E., McDaniel, T.K., Donnenberg, M.S. and Kaper, J.B. (1995) 'Enteropathogenic Escherichia coli contains a putative type III secretion system necessary for the export of proteins involved in attaching and effacing lesion formation', *Proc Natl Acad Sci U S A*, 92(17), pp. 7996-8000.
Jerse, A.E. and Kaper, J.B. (1991) 'The eae gene of enteropathogenic Escherichia coli encodes a 94-kilodalton membrane protein, the expression of which is influenced by the EAF plasmid', *Infect Immun*, 59(12), pp. 4302-9.
Katsowich, N., Elbaz, N., Pal, R.R., Mills, E., Kobi, S., Kahan, T. and Rosenshine, I. (2017) 'Host cell attachment elicits posttranscriptional regulation in infecting enteropathogenic bacteria', *Science*, 355(6326), pp. 735-739.
Keenleyside, W.J. and Whitfield, C. (1996) 'A novel pathway for O-polysaccharide biosynthesis in Salmonella enterica serovar Borreze', *J Biol Chem*, 271(45), pp. 28581-92.
Kenny, B. (1999) 'Phosphorylation of tyrosine 474 of the enteropathogenic Escherichia coli (EPEC) Tir receptor molecule is essential for actin nucleating activity and is preceded by additional host modifications', *Mol Microbiol*, 31(4), pp. 1229-41.

Kenny, B., Abe, A., Stein, M. and Finlay, B.B. (1997a) 'Enteropathogenic Escherichia coli protein secretion is induced in response to conditions similar to those in the gastrointestinal tract', *Infect Immun*, 65(7), pp. 2606-12.
Kenny, B., DeVinney, R., Stein, M., Reinscheid, D.J., Frey, E.A. and Finlay, B.B. (1997b) 'Enteropathogenic E. coli (EPEC) transfers its receptor for intimate adherence into mammalian cells', *Cell*, 91(4), pp. 511-20.
Kenny, B., Ellis, S., Leard, A.D., Warawa, J., Mellor, H. and Jepson, M.A. (2002) 'Co-ordinate regulation of distinct host cell signalling pathways by multifunctional enteropathogenic Escherichia coli effector molecules', *Mol Microbiol*, 44(4), pp. 1095-1107.
Kenny, B. and Jepson, M. (2000) 'Targeting of an enteropathogenic Escherichia coli (EPEC) effector protein to host mitochondria', *Cell Microbiol*, 2(6), pp. 579-90.
Kenny, B., Lai, L.C., Finlay, B.B. and Donnenberg, M.S. (1996) 'EspA, a protein secreted by enteropathogenic Escherichia coli, is required to induce signals in epithelial cells', *Mol Microbiol*, 20(2), pp. 313-23.
Kenny, B. and Warawa, J. (2001) 'Enteropathogenic Escherichia coli (EPEC) Tir receptor molecule does not undergo full modification when introduced into host cells by EPEC-independent mechanisms', *Infect Immun*, 69(3), pp. 1444-53.
Kimbrough, T.G. and Miller, S.I. (2000) 'Contribution of Salmonella typhimurium type III secretion components to needle complex formation', *Proc Natl Acad Sci U S A*, 97(20), pp. 11008-13.
Kleinschmidt, J.H., Wiener, M.C. and Tamm, L.K. (1999) 'Outer membrane protein A of E. coli folds into detergent micelles, but not in the presence of monomeric detergent', *Protein Sci*, 8(10), pp. 2065-71.
Knutton, S. (1995) 'Cellular responses to enteropathogenic Escherichia coli infection', *Biosci Rep*, 15(6), pp. 469-79.
Knutton, S., Baldwin, T., Williams, P.H. and McNeish, A.S. (1989) 'Actin accumulation at sites of bacterial adhesion to tissue culture cells: basis of a new diagnostic test for enteropathogenic and enterohemorrhagic Escherichia coli', *Infect Immun*, 57(4), pp. 1290-8.
Knutton, S., Rosenshine, I., Pallen, M.J., Nisan, I., Neves, B.C., Bain, C., Wolff, C., Dougan, G. and Frankel, G. (1998) 'A novel EspA-associated surface organelle of enteropathogenic Escherichia coli involved in protein translocation into epithelial cells', *Embo j*, 17(8), pp. 2166-76.
Kresse, A.U., Beltrametti, F., Muller, A., Ebel, F. and Guzman, C.A. (2000) 'Characterization of SepL of enterohemorrhagic Escherichia coli', *J Bacteriol*, 182(22), pp. 6490-8.
Kresse, A.U., Schulze, K., Deibel, C., Ebel, F., Rohde, M., Chakraborty, T. and Guzmán, C.A. (1998) 'Pas, a novel protein required for protein secretion and attaching and effacing activities of enterohemorrhagic Escherichia coli', *J Bacteriol*, 180(17), pp. 4370-9.
Ku, C.P., Lio, J.C., Wang, S.H., Lin, C.N. and Syu, W.J. (2009) 'Identification of a third EspA-binding protein that forms part of the type III secretion system of enterohemorrhagic Escherichia coli', *J Biol Chem*, 284(3), pp. 1686-93.
Kubori, T., Matsushima, Y., Nakamura, D., Uralil, J., Lara-Tejero, M., Sukhan, A., Galan, J.E. and Aizawa, S.I. (1998a) 'Supramolecular structure of the Salmonella typhimurium type III protein secretion system', *Science*, 280(5363), pp. 602-5.
Kubori, T., Matsushima, Y., Nakamura, D., Uralil, J., Lara-Tejero, M., Sukhan, A., Galán, J.E. and Aizawa, S.I. (1998b) 'Supramolecular structure of the Salmonella typhimurium type III protein secretion system', *Science*, 280(5363), pp. 602-5.
Kubori, T., Sukhan, A., Aizawa, S.I. and Galan, J.E. (2000) 'Molecular characterization and assembly of the needle complex of the Salmonella typhimurium type III protein secretion system', *Proc Natl Acad Sci U S A*, 97(18), pp. 10225-30.
Laemmli, U.K. (1970) 'Cleavage of structural proteins during the assembly of the head of bacteriophage T4', *Nature*, 227(5259), pp. 680-5.

Lai, L.C., Wainwright, L.A., Stone, K.D. and Donnenberg, M.S. (1997) 'A third secreted protein that is encoded by the enteropathogenic Escherichia coli pathogenicity island is required for transduction of signals and for attaching and effacing activities in host cells', *Infect Immun*, 65(6), pp. 2211-7.
Lai, Y., Rosenshine, I., Leong, J.M. and Frankel, G. (2013) 'Intimate host attachment: enteropathogenic and enterohaemorrhagic Escherichia coli', *Cell Microbiol*, 15(11), pp. 1796-808.
Lara-Tejero, M., Kato, J., Wagner, S., Liu, X. and Galan, J.E. (2011) 'A sorting platform determines the order of protein secretion in bacterial type III systems', *Science*, 331(6021), pp. 1188-91.
Lederberg, J. and Tatum, E.L. (1946) 'Gene recombination in Escherichia coli', *Nature*, 158(4016), p. 558.
Levine, M.M., Nataro, J.P., Karch, H., Baldini, M.M., Kaper, J.B., Black, R.E., Clements, M.L. and O'Brien, A.D. (1985) 'The diarrheal response of humans to some classic serotypes of enteropathogenic Escherichia coli is dependent on a plasmid encoding an enteroadhesiveness factor', *J Infect Dis*, 152(3), pp. 550-9.
Lin, C.N., Sun, W.S., Lu, H.Y., Ng, S.C., Liao, Y.S. and Syu, W.J. (2014) 'Protein interactions and regulation of EscA in enterohemorrhagic E. coli', *PLoS One*, 9(1), p. e85354.
Linton, K.J. and Higgins, C.F. (1998) 'The Escherichia coli ATP-binding cassette (ABC) proteins', *Mol Microbiol*, 28(1), pp. 5-13.
Little, D.J. and Coombes, B.K. (2018) 'Molecular basis for CesT recognition of type III secretion effectors in enteropathogenic Escherichia coli', *PLoS Pathog*, 14(8), p. e1007224.
Liu, B., Furevi, A., Perepelov, A.V., Guo, X., Cao, H., Wang, Q., Reeves, P.R., Knirel, Y.A., Wang, L. and Widmalm, G. (2020) 'Structure and genetics of Escherichia coli O antigens', *FEMS Microbiol Rev*, 44(6), pp. 655-683.
Liu, B., Qian, C., Wu, P., Li, X., Liu, Y., Mu, H., Huang, M., Zhang, Y., Jia, T., Wang, Y., Wang, L., Zhang, X., Huang, D., Yang, B., Feng, L. and Wang, L. (2021) 'Attachment of Enterohemorrhagic Escherichia coli to Host Cells Reduces O Antigen Chain Length at the Infection Site That Promotes Infection', *mBio*, 12(6), p. e0269221.
Liu, D. and Reeves, P.R. (1994) 'Escherichia coli K12 regains its O antigen', *Microbiology (Reading)*, 140 (Pt 1), pp. 49-57.
Luo, W. and Donnenberg, M.S. (2011) 'Interactions and predicted host membrane topology of the enteropathogenic Escherichia coli translocator protein EspB', *J Bacteriol*, 193(12), pp. 2972-80.
Lyons, B.J.E. and Strynadka, N.C.J. (2019) 'On the road to structure-based development of anti-virulence therapeutics targeting the type III secretion system injectisome', *Medchemcomm*, 10(8), pp. 1273-1289.
Madkour, A. (2017) *Studies on virulence-critical proteins of enteropathogenic Escherichia coli (EPEC)* Newcastle University (Accessed: 8/1/2108).
Madkour, A., Almessiry, B., González-Pedrajo, B. and Kenny, B. (2021) 'Unprecedented Protein Divergence within a T3SS Family', *bioRxiv*, p. 2021.03.31.437910.
Magdalena, J., Hachani, A., Chamekh, M., Jouihri, N., Gounon, P., Blocker, A. and Allaoui, A. (2002) 'Spa32 regulates a switch in substrate specificity of the type III secreton of Shigella flexneri from needle components to Ipa proteins', *J Bacteriol*, 184(13), pp. 3433-41.
Marchler-Bauer, A., Anderson, J.B., Cherukuri, P.F., DeWeese-Scott, C., Geer, L.Y., Gwadz, M., He, S., Hurwitz, D.I., Jackson, J.D., Ke, Z., Lanczycki, C.J., Liebert, C.A., Liu, C., Lu, F., Marchler, G.H., Mullokandov, M., Shoemaker, B.A., Simonyan, V., Song, J.S., Thiessen, P.A., Yamashita, R.A., Yin, J.J., Zhang, D. and Bryant, S.H. (2005) 'CDD: a Conserved Domain Database for protein classification', *Nucleic Acids Res*, 33(Database issue), pp. D192-6.
Marlovits, T.C., Kubori, T., Lara-Tejero, M., Thomas, D., Unger, V.M. and Galan, J.E. (2006) 'Assembly of the inner rod determines needle length in the type III secretion injectisome', *Nature*, 441(7093), pp. 637-40.
Maurizi, M.R. (1992) 'Proteases and protein degradation in Escherichia coli', *Experientia*, 48(2), pp. 178-201.

McDaniel, T.K., Jarvis, K.G., Donnenberg, M.S. and Kaper, J.B. (1995) 'A genetic locus of enterocyte effacement conserved among diverse enterobacterial pathogens', *Proc Natl Acad Sci U S A*, 92(5), pp. 1664-8.
McDaniel, T.K. and Kaper, J.B. (1997) 'A cloned pathogenicity island from enteropathogenic Escherichia coli confers the attaching and effacing phenotype on E. coli K-12', *Mol Microbiol*, 23(2), pp. 399-407.
Mellies, J.L., Elliott, S.J., Sperandio, V., Donnenberg, M.S. and Kaper, J.B. (1999) 'The Per regulon of enteropathogenic Escherichia coli : identification of a regulatory cascade and a novel transcriptional activator, the locus of enterocyte effacement (LEE)-encoded regulator (Ler)', *Mol Microbiol*, 33(2), pp. 296-306.
Mellies, J.L., Navarro-Garcia, F., Okeke, I., Frederickson, J., Nataro, J.P. and Kaper, J.B. (2001) 'espC pathogenicity island of enteropathogenic Escherichia coli encodes an enterotoxin', *Infect Immun*, 69(1), pp. 315-24.
Merino, S., Gonzalez, V. and Tomás, J.M. (2016) 'The first sugar of the repeat units is essential for the Wzy polymerase activity and elongation of the O-antigen lipopolysaccharide', *Future Microbiol*, 11, pp. 903-18.
Miki, H., Sasaki, T., Takai, Y. and Takenawa, T. (1998) 'Induction of filopodium formation by a WASP-related actin-depolymerizing protein N-WASP', *Nature*, 391(6662), pp. 93-6.
Mills, E., Baruch, K., Aviv, G., Nitzan, M. and Rosenshine, I. (2013) 'Dynamics of the type III secretion system activity of enteropathogenic Escherichia coli', *mBio*, 4(4).
Mills, E., Baruch, K., Charpentier, X., Kobi, S. and Rosenshine, I. (2008) 'Real-time analysis of effector translocation by the type III secretion system of enteropathogenic Escherichia coli', *Cell Host Microbe*, 3(2), pp. 104-13.
Minamino, T. and Macnab, R.M. (1999) 'Components of the Salmonella flagellar export apparatus and classification of export substrates', *J Bacteriol*, 181(5), pp. 1388-94.
Mogensen, J.E. and Otzen, D.E. (2005) 'Interactions between folding factors and bacterial outer membrane proteins', *Mol Microbiol*, 57(2), pp. 326-46.
Mohanty, B.R. and Sahoo, P.K. (2007) 'Edwardsiellosis in fish: a brief review', *J Biosci*, 32(7), pp. 1331-44.
Monjaras Feria, J., Garcia-Gomez, E., Espinosa, N., Minamino, T., Namba, K. and Gonzalez-Pedrajo, B. (2012) 'Role of EscP (Orf16) in injectisome biogenesis and regulation of type III protein secretion in enteropathogenic Escherichia coli', *J Bacteriol*, 194(22), pp. 6029-45.
Monjaras Feria, J.V., Lefebre, M.D., Stierhof, Y.D., Galan, J.E. and Wagner, S. (2015) 'Role of autocleavage in the function of a type III secretion specificity switch protein in Salmonella enterica serovar Typhimurium', *MBio*, 6(5), pp. e01459-15.
Moon, H.W., Whipp, S.C., Argenzio, R.A., Levine, M.M. and Giannella, R.A. (1983) 'Attaching and effacing activities of rabbit and human enteropathogenic Escherichia coli in pig and rabbit intestines', *Infect Immun*, 41(3), pp. 1340-51.
Nadler, C., Baruch, K., Kobi, S., Mills, E., Haviv, G., Farago, M., Alkalay, I., Bartfeld, S., Meyer, T.F., Ben-Neriah, Y. and Rosenshine, I. (2010) 'The type III secretion effector NleE inhibits NF-kappaB activation', *PLoS Pathog*, 6(1), p. e1000743.
Nagai, T., Abe, A. and Sasakawa, C. (2005) 'Targeting of enteropathogenic Escherichia coli EspF to host mitochondria is essential for bacterial pathogenesis: critical role of the 16th leucine residue in EspF', *J Biol Chem*, 280(4), pp. 2998-3011.
Nakamura, Y., Takano, T., Yasuike, M., Sakai, T., Matsuyama, T. and Sano, M. (2013) 'Comparative genomics reveals that a fish pathogenic bacterium Edwardsiella tarda has acquired the locus of enterocyte effacement (LEE) through horizontal gene transfer', *BMC Genomics*, 14, p. 642.
Natale, P., Brüser, T. and Driessen, A.J. (2008) 'Sec- and Tat-mediated protein secretion across the bacterial cytoplasmic membrane--distinct translocases and mechanisms', *Biochim Biophys Acta*, 1778(9), pp. 1735-56.

Nataro, J.P. and Kaper, J.B. (1998) 'Diarrheagenic Escherichia coli', *Clin Microbiol Rev*, 11(1), pp. 142-201.
Navarro-Garcia, F., Serapio-Palacios, A., Vidal, J.E., Salazar, M.I. and Tapia-Pastrana, G. (2014) 'EspC promotes epithelial cell detachment by enteropathogenic Escherichia coli via sequential cleavages of a cytoskeletal protein and then focal adhesion proteins', *Infect Immun*, 82(6), pp. 2255-65.
Neves, B.C., Mundy, R., Petrovska, L., Dougan, G., Knutton, S. and Frankel, G. (2003) 'CesD2 of enteropathogenic Escherichia coli is a second chaperone for the type III secretion translocator protein EspD', *Infect Immun*, 71(4), pp. 2130-41.
Nicolas-Chanoine, M.H., Bertrand, X. and Madec, J.Y. (2014) 'Escherichia coli ST131, an intriguing clonal group', *Clin Microbiol Rev*, 27(3), pp. 543-74.
Nyathi, Y., Wilkinson, B.M. and Pool, M.R. (2013) 'Co-translational targeting and translocation of proteins to the endoplasmic reticulum', *Biochim Biophys Acta*, 1833(11), pp. 2392-402.
O'Connell, C.B., Creasey, E.A., Knutton, S., Elliott, S., Crowther, L.J., Luo, W., Albert, M.J., Kaper, J.B., Frankel, G. and Donnenberg, M.S. (2004) 'SepL, a protein required for enteropathogenic Escherichia coli type III translocation, interacts with secretion component SepD', *Mol Microbiol*, 52(6), pp. 1613-25.
Ogino, T., Ohno, R., Sekiya, K., Kuwae, A., Matsuzawa, T., Nonaka, T., Fukuda, H., Imajoh-Ohmi, S. and Abe, A. (2006) 'Assembly of the type III secretion apparatus of enteropathogenic Escherichia coli', *J Bacteriol*, 188(8), pp. 2801-11.
Ohnishi, S., Kameyama, K. and Takagi, T. (1998) 'Characterization of a heat modifiable protein, Escherichia coli outer membrane protein OmpA in binary surfactant system of sodium dodecyl sulfate and octylglucoside', *Biochim Biophys Acta*, 1375(1-2), pp. 101-9.
Padavannil, A., Jobichen, C., Mills, E., Velazquez-Campoy, A., Li, M., Leung, K.Y., Mok, Y.K., Rosenshine, I. and Sivaraman, J. (2013) 'Structure of GrlR-GrlA complex that prevents GrlA activation of virulence genes', *Nat Commun*, 4, p. 2546.
Pal, R.R., Baidya, A.K., Mamou, G., Bhattacharya, S., Socol, Y., Kobi, S., Katsowich, N., Ben-Yehuda, S. and Rosenshine, I. (2019) 'Pathogenic E. coli Extracts Nutrients from Infected Host Cells Utilizing Injectisome Components', *Cell*, 177(3), pp. 683-696.e18.
Pallen, M.J., Beatson, S.A. and Bailey, C.M. (2005) 'Bioinformatics analysis of the locus for enterocyte effacement provides novel insights into type-III secretion', *BMC Microbiol*, 5, p. 9.
Payne, P.L. and Straley, S.C. (1999) 'YscP of Yersinia pestis is a secreted component of the Yop secretion system', *J Bacteriol*, 181(9), pp. 2852-62.
Pearson, J.S., Giogha, C., Ong, S.Y., Kennedy, C.L., Kelly, M., Robinson, K.S., Lung, T.W., Mansell, A., Riedmaier, P., Oates, C.V., Zaid, A., Mühlen, S., Crepin, V.F., Marches, O., Ang, C.S., Williamson, N.A., O'Reilly, L.A., Bankovacki, A., Nachbur, U., Infusini, G., Webb, A.I., Silke, J., Strasser, A., Frankel, G. and Hartland, E.L. (2013) 'A type III effector antagonizes death receptor signalling during bacterial gut infection', *Nature*, 501(7466), pp. 247-51.
Perna, N.T., Mayhew, G.F., Pósfai, G., Elliott, S., Donnenberg, M.S., Kaper, J.B. and Blattner, F.R. (1998) 'Molecular evolution of a pathogenicity island from enterohemorrhagic Escherichia coli O157:H7', *Infect Immun*, 66(8), pp. 3810-7.
Pitt-Rivers, R. and Impiombato, F.S. (1968) 'The binding of sodium dodecyl sulphate to various proteins', *Biochem J*, 109(5), pp. 825-30.
Pluschke, G., Mayden, J., Achtman, M. and Levine, R.P. (1983) 'Role of the capsule and the O antigen in resistance of O18:K1 Escherichia coli to complement-mediated killing', *Infect Immun*, 42(3), pp. 907-13.
Portaliou, A.G., Tsolis, K.C., Loos, M.S., Balabanidou, V., Rayo, J., Tsirigotaki, A., Crepin, V.F., Frankel, G., Kalodimos, C.G., Karamanou, S. and Economou, A. (2017) 'Hierarchical protein targeting and secretion is controlled by an affinity switch in the type III secretion system of enteropathogenic Escherichia coli', *Embo j*, 36(23), pp. 3517-3531.
Portaliou, A.G., Tsolis, K.C., Loos, M.S., Zorzini, V. and Economou, A. (2016) 'Type III Secretion: Building and Operating a Remarkable Nanomachine', *Trends Biochem Sci*, 41(2), pp. 175-89.

Radics, J., Konigsmaier, L. and Marlovits, T.C. (2014) 'Structure of a pathogenic type 3 secretion system in action', *Nat Struct Mol Biol*, 21(1), pp. 82-7.
Ramu, T., Prasad, M.E., Connors, E., Mishra, A., Thomassin, J.L., Leblanc, J., Rainey, J.K. and Thomas, N.A. (2013) 'A novel C-terminal region within the multicargo type III secretion chaperone CesT contributes to effector secretion', *J Bacteriol*, 195(4), pp. 740-56.
Randall, L.L. and Hardy, S.J. (2002) 'SecB, one small chaperone in the complex milieu of the cell', *Cell Mol Life Sci*, 59(10), pp. 1617-23.
Rath, A., Glibowicka, M., Nadeau, V.G., Chen, G. and Deber, C.M. (2009) 'Detergent binding explains anomalous SDS-PAGE migration of membrane proteins', *Proc Natl Acad Sci U S A*, 106(6), pp. 1760-5.
Reynolds, J.A. and Tanford, C. (1970) 'Binding of dodecyl sulfate to proteins at high binding ratios. Possible implications for the state of proteins in biological membranes', *Proc Natl Acad Sci U S A*, 66(3), pp. 1002-7.
Romeo, T., Vakulskas, C.A. and Babitzke, P. (2013) 'Post-transcriptional regulation on a global scale: form and function of Csr/Rsm systems', *Environ Microbiol*, 15(2), pp. 313-24.
Romo-Castillo, M., Andrade, A., Espinosa, N., Monjaras Feria, J., Soto, E., Diaz-Guerrero, M. and Gonzalez-Pedrajo, B. (2014a) 'EscO, a functional and structural analog of the flagellar FliJ protein, is a positive regulator of EscN ATPase activity of the enteropathogenic Escherichia coli injectisome', *J Bacteriol*, 196(12), pp. 2227-41.
Romo-Castillo, M., Andrade, A., Espinosa, N., Monjarás Feria, J., Soto, E., Díaz-Guerrero, M. and González-Pedrajo, B. (2014b) 'EscO, a functional and structural analog of the flagellar FliJ protein, is a positive regulator of EscN ATPase activity of the enteropathogenic Escherichia coli injectisome', *J Bacteriol*, 196(12), pp. 2227-41.
Rosenshine, I., Ruschkowski, S. and Finlay, B.B. (1996) 'Expression of attaching/effacing activity by enteropathogenic Escherichia coli depends on growth phase, temperature, and protein synthesis upon contact with epithelial cells', *Infect Immun*, 64(3), pp. 966-73.
Rosqvist, R., Magnusson, K.E. and Wolf-Watz, H. (1994) 'Target cell contact triggers expression and polarized transfer of Yersinia YopE cytotoxin into mammalian cells', *Embo j*, 13(4), pp. 964-72.
Ruano-Gallego, D., Álvarez, B. and Fernández, L. (2015) 'Engineering the Controlled Assembly of Filamentous Injectisomes in E. coli K-12 for Protein Translocation into Mammalian Cells', *ACS Synth Biol*, 4(9), pp. 1030-41.
Sal-Man, N., Biemans-Oldehinkel, E., Sharon, D., Croxen, M.A., Scholz, R., Foster, L.J. and Finlay, B.B. (2012) 'EscA is a crucial component of the type III secretion system of enteropathogenic Escherichia coli', *J Bacteriol*, 194(11), pp. 2819-28.
Sal-Man, N., Deng, W. and Finlay, B.B. (2012) 'EscI: a crucial component of the type III secretion system forms the inner rod structure in enteropathogenic Escherichia coli', *Biochem J*, 442(1), pp. 119-25.
Sal-Man, N., Setiaputra, D., Scholz, R., Deng, W., Yu, A.C., Strynadka, N.C. and Finlay, B.B. (2013) 'EscE and EscG are cochaperones for the type III needle protein EscF of enteropathogenic Escherichia coli', *J Bacteriol*, 195(11), pp. 2481-9.
Salmond, G.P. and Reeves, P.J. (1993) 'Membrane traffic wardens and protein secretion in gram-negative bacteria', *Trends Biochem Sci*, 18(1), pp. 7-12.
Samuel, G. and Reeves, P. (2003) 'Biosynthesis of O-antigens: genes and pathways involved in nucleotide sugar precursor synthesis and O-antigen assembly', *Carbohydr Res*, 338(23), pp. 2503-19.
Sanchez-Villamil, J.I., Navarro-Garcia, F., Castillo-Romero, A., Gutierrez-Gutierrez, F., Tapia, D. and Tapia-Pastrana, G. (2019) 'Curcumin Blocks Cytotoxicity of Enteroaggregative and Enteropathogenic Escherichia coli by Blocking Pet and EspC Proteolytic Release From Bacterial Outer Membrane', *Front Cell Infect Microbiol*, 9, p. 334.
Sekiya, K., Ohishi, M., Ogino, T., Tamano, K., Sasakawa, C. and Abe, A. (2001) 'Supermolecular structure of the enteropathogenic Escherichia coli type III secretion system and its direct interaction with the EspA-sheath-like structure', *Proc Natl Acad Sci U S A*, 98(20), pp. 11638-43.

Shames, S.R., Deng, W., Guttman, J.A., de Hoog, C.L., Li, Y., Hardwidge, P.R., Sham, H.P., Vallance, B.A., Foster, L.J. and Finlay, B.B. (2010) 'The pathogenic E. coli type III effector EspZ interacts with host CD98 and facilitates host cell prosurvival signalling', *Cell Microbiol*, 12(9), pp. 1322-39.
Shaulov, L., Gershberg, J., Deng, W., Finlay, B.B. and Sal-Man, N. (2017) 'The Ruler Protein EscP of the Enteropathogenic Escherichia coli Type III Secretion System Is Involved in Calcium Sensing and Secretion Hierarchy Regulation by Interacting with the Gatekeeper Protein SepL', *MBio*, 8(1).
Shaw, R.K., Daniell, S., Ebel, F., Frankel, G. and Knutton, S. (2001) 'EspA filament-mediated protein translocation into red blood cells', *Cell Microbiol*, 3(4), pp. 213-22.
Shirahama, K., Tsujii, K. and Takagi, T. (1974) 'Free-boundary electrophoresis of sodium dodecyl sulfate-protein polypeptide complexes with special reference to SDS-polyacrylamide gel electrophoresis', *J Biochem*, 75(2), pp. 309-19.
Slater, S.L., Sågfors, A.M., Pollard, D.J., Ruano-Gallego, D. and Frankel, G. (2018) 'The Type III Secretion System of Pathogenic Escherichia coli', *Curr Top Microbiol Immunol*, 416, pp. 51-72.
Soto, E., Espinosa, N., Diaz-Guerrero, M., Gaytan, M.O., Puente, J.L. and Gonzalez-Pedrajo, B. (2017) 'Functional Characterization of EscK (Orf4), a Sorting Platform Component of the Enteropathogenic Escherichia coli Injectisome', *J Bacteriol*, 199(1).
Stein, M., Kenny, B., Stein, M.A. and Finlay, B.B. (1996) 'Characterization of EspC, a 110-kilodalton protein secreted by enteropathogenic Escherichia coli which is homologous to members of the immunoglobulin A protease-like family of secreted proteins', *J Bacteriol*, 178(22), pp. 6546-54.
Stevenson, G., Andrianopoulos, K., Hobbs, M. and Reeves, P.R. (1996) 'Organization of the Escherichia coli K-12 gene cluster responsible for production of the extracellular polysaccharide colanic acid', *J Bacteriol*, 178(16), pp. 4885-93.
Svitkina, T.M., Bulanova, E.A., Chaga, O.Y., Vignjevic, D.M., Kojima, S., Vasiliev, J.M. and Borisy, G.G. (2003) 'Mechanism of filopodia initiation by reorganization of a dendritic network', *J Cell Biol*, 160(3), pp. 409-21.
Taylor, K.A., O'Connell, C.B., Luther, P.W. and Donnenberg, M.S. (1998) 'The EspB protein of enteropathogenic Escherichia coli is targeted to the cytoplasm of infected HeLa cells', *Infect Immun*, 66(11), pp. 5501-7.
Thomas, N.A., Deng, W., Puente, J.L., Frey, E.A., Yip, C.K., Strynadka, N.C. and Finlay, B.B. (2005) 'CesT is a multi-effector chaperone and recruitment factor required for the efficient type III secretion of both LEE- and non-LEE-encoded effectors of enteropathogenic Escherichia coli', *Mol Microbiol*, 57(6), pp. 1762-79.
Thomassin, J.L., He, X. and Thomas, N.A. (2011) 'Role of EscU auto-cleavage in promoting type III effector translocation into host cells by enteropathogenic Escherichia coli', *BMC Microbiol*, 11, p. 205.
Tseytin, I., Dagan, A., Oren, S. and Sal-Man, N. (2018) 'The role of EscD in supporting EscC polymerization in the type III secretion system of enteropathogenic Escherichia coli', *Biochim Biophys Acta*, 1860(2), pp. 384-395.
Uchiya, K., Tobe, T., Komatsu, K., Suzuki, T., Watarai, M., Fukuda, I., Yoshikawa, M. and Sasakawa, C. (1995) 'Identification of a novel virulence gene, virA, on the large plasmid of Shigella, involved in invasion and intercellular spreading', *Mol Microbiol*, 17(2), pp. 241-50.
Vallance, B.A. and Finlay, B.B. (2000) 'Exploitation of host cells by enteropathogenic Escherichia coli', *Proc Natl Acad Sci U S A*, 97(16), pp. 8799-806.
Valvano, M.A. (2003) 'Export of O-specific lipopolysaccharide', *Front Biosci*, 8, pp. s452-71.
Vogeleer, P., Tremblay, Y.D., Mafu, A.A., Jacques, M. and Harel, J. (2014) 'Life on the outside: role of biofilms in environmental persistence of Shiga-toxin producing Escherichia coli', *Front Microbiol*, 5, p. 317.
Wainwright, L.A. and Kaper, J.B. (1998) 'EspB and EspD require a specific chaperone for proper secretion from enteropathogenic Escherichia coli', *Mol Microbiol*, 27(6), pp. 1247-60.

Wang, D., Roe, A.J., McAteer, S., Shipston, M.J. and Gally, D.L. (2008) 'Hierarchal type III secretion of translocators and effectors from Escherichia coli O157:H7 requires the carboxy terminus of SepL that binds to Tir', *Mol Microbiol*, 69(6), pp. 1499-512.
Wang, Y.A., Yu, X., Yip, C., Strynadka, N.C. and Egelman, E.H. (2006) 'Structural polymorphism in bacterial EspA filaments revealed by cryo-EM and an improved approach to helical reconstruction', *Structure*, 14(7), pp. 1189-96.
Warawa, J., Finlay, B.B. and Kenny, B. (1999) 'Type III secretion-dependent hemolytic activity of enteropathogenic Escherichia coli', *Infect Immun*, 67(10), pp. 5538-40.
Wegener, A.D. and Jones, L.R. (1984) 'Phosphorylation-induced mobility shift in phospholamban in sodium dodecyl sulfate-polyacrylamide gels. Evidence for a protein structure consisting of multiple identical phosphorylatable subunits', *J Biol Chem*, 259(3), pp. 1834-41.
Weintraub, A. (2007) 'Enteroaggregative Escherichia coli: epidemiology, virulence and detection', *J Med Microbiol*, 56(Pt 1), pp. 4-8.
Weiss, R.B. (1991) 'Ribosomal frameshifting, jumping and readthrough', *Curr Opin Cell Biol*, 3(6), pp. 1051-5.
Wilson, R.K., Shaw, R.K., Daniell, S., Knutton, S. and Frankel, G. (2001) 'Role of EscF, a putative needle complex protein, in the type III protein translocation system of enteropathogenic Escherichia coli', *Cell Microbiol*, 3(11), pp. 753-62.
Wong, A.R., Pearson, J.S., Bright, M.D., Munera, D., Robinson, K.S., Lee, S.F., Frankel, G. and Hartland, E.L. (2011) 'Enteropathogenic and enterohaemorrhagic Escherichia coli: even more subversive elements', *Mol Microbiol*, 80(6), pp. 1420-38.
Wong, A.R., Raymond, B., Collins, J.W., Crepin, V.F. and Frankel, G. (2012) 'The enteropathogenic E. coli effector EspH promotes actin pedestal formation and elongation via WASP-interacting protein (WIP)', *Cell Microbiol*, 14(7), pp. 1051-70.
Ye, F., Yang, F., Yu, R., Lin, X., Qi, J., Chen, Z., Cao, Y., Wei, Y., Gao, G.F. and Lu, G. (2018) 'Molecular basis of binding between the global post-transcriptional regulator CsrA and the T3SS chaperone CesT', *Nat Commun*, 9(1), p. 1196.
Yen, H., Ooka, T., Iguchi, A., Hayashi, T., Sugimoto, N. and Tobe, T. (2010) 'NleC, a type III secretion protease, compromises NF-kappaB activation by targeting p65/RelA', *PLoS Pathog*, 6(12), p. e1001231.
Yerushalmi, G., Litvak, Y., Gur-Arie, L. and Rosenshine, I. (2014) 'Dynamics of expression and maturation of the type III secretion system of enteropathogenic Escherichia coli', *J Bacteriol*, 196(15), pp. 2798-806.
Yerushalmi, G., Nadler, C., Berdichevski, T. and Rosenshine, I. (2008) 'Mutational analysis of the locus of enterocyte effacement-encoded regulator (Ler) of enteropathogenic Escherichia coli', *J Bacteriol*, 190(23), pp. 7808-18.
Yi, W., Liu, X., Li, Y., Li, J., Xia, C., Zhou, G., Zhang, W., Zhao, W., Chen, X. and Wang, P.G. (2009) 'Remodeling bacterial polysaccharides by metabolic pathway engineering', *Proc Natl Acad Sci U S A*, 106(11), pp. 4207-12.
Yip, C.K., Finlay, B.B. and Strynadka, N.C. (2005) 'Structural characterization of a type III secretion system filament protein in complex with its chaperone', *Nat Struct Mol Biol*, 12(1), pp. 75-81.
Yip, C.K., Kimbrough, T.G., Felise, H.B., Vuckovic, M., Thomas, N.A., Pfuetzner, R.A., Frey, E.A., Finlay, B.B., Miller, S.I. and Strynadka, N.C. (2005) 'Structural characterization of the molecular platform for type III secretion system assembly', *Nature*, 435(7042), pp. 702-7.
Younis, R., Bingle, L.E., Rollauer, S., Munera, D., Busby, S.J., Johnson, S., Deane, J.E., Lea, S.M., Frankel, G. and Pallen, M.J. (2010) 'SepL resembles an aberrant effector in binding to a class 1 type III secretion chaperone and carrying an N-terminal secretion signal', *J Bacteriol*, 192(22), pp. 6093-8.
Zarivach, R., Deng, W., Vuckovic, M., Felise, H.B., Nguyen, H.V., Miller, S.I., Finlay, B.B. and Strynadka, N.C. (2008) 'Structural analysis of the essential self-cleaving type III secretion proteins EscU and SpaS', *Nature*, 453(7191), pp. 124-7.

Zilkenat, S., Franz-Wachtel, M., Stierhof, Y.D., Galan, J.E., Macek, B. and Wagner, S. (2016) 'Determination of the Stoichiometry of the Complete Bacterial Type III Secretion Needle Complex Using a Combined Quantitative Proteomic Approach', *Mol Cell Proteomics*, 15(5), pp. 1598-609.